School of Physical and Chemical Sciences, University of Canterbury, Christchurch, New Zealand

PHYS 690 MSc Thesis

submitted in partial fulfilment of the requirements for

The Degree of Master of Science in Physics

Perturbation Theory and Averages in Inhomogeneous Cosmologies

---

by

Rudeep Gaur

Supervisor: Prof. David Wiltshire

2021

Abstract

The standard model of cosmology, Λ Cold Dark Matter (ΛCDM), assumes that the Universe can be modelled by an exact solution to Einstein's equations — the isotropic and homogeneous Friedmann-Lemaître-Robertson-Walker spacetime. The structure we observe in the Universe formed from small initial density perturbations in the early Universe, which the standard model treats by perturbation theory. We investigate two versions of perturbation theory: standard linear perturbation theory and the more recent, non-linear post-Newtonian perturbation theory. Linear perturbation theory involves gauge choices, and it was shown recently by Clifton et al. [1] that many of the common gauges are non-viable in the post-Newtonian expansion. We investigate further gauge choices, introduced by Bičák et al. [2].

If one does not assume that the average evolution of the Universe by an exact solution to Einstein's equations, then in the context of an inhomogeneous cosmology one finds extra terms contributing to the dynamics of the average spacetime — the backreaction terms. We review the most recent and general averaging formalism of Buchert [3], referred to as the "extrinsic averaging approach" and discuss the challenges faced by other constructions of the same formalism. We then also investigate the updated version of the "intrinsic averaging approach" — first introduced by Buchert in 2000 [4].

We show that backreaction can be constructed in the post-Newtonian expansion by using the extrinsic averaging approach. The standard Buchert formalism (the intrinsic averaging approach) cannot be used as it is effectively a 'non-viable gauge' when the post-Newtonian expansion is considered.

Finally, we investigate the magnitude of backreaction terms in an inhomogeneous exact solution to Einstein's equations — the Szekeres model. We consider a particular model containing an underdensity and overdensity on small cosmological scales ($< 100\,\mathrm{Mpc}$), while asymptotically approaching a standard ΛCDM model on larger spatial scales. The magnitude of the backreaction correction to the average evolution equations is found to correlate with the spatial gradient of the density. It reaches 2.3% in the overdense region but is negligible otherwise. These results are compared with a similar analysis undertaken by Bolejko in 2017 [5].

Acknowledgements

Firstly, I would like to thank Professor David Wiltshire for his support and time as my supervisor on this thesis. Thanks are due to him for selecting a project broad enough such that I was able to investigate many aspects of cosmology, some of which did not make it into this thesis. I would also like to thank David for the many conversations over the year which provided insight into many aspects of cosmology and the world of academia. Finally, David, thank you, for making me aware of my *thing*, for commas.

Secondly, I would also like to thank my parents, Ruchir and Deepa, who have always supported me throughout my academic career and have pushed me to always be better. I should also thank my Auntie, Shikha for no particular reason except the fact that she would probably like to be thanked.

I must also thank my partner, Jess. With the pandemic, a broken rib, broken nose, mild concussion, and torn hamstring...it was a wild year and you were there through it all. Thank you for your time, patience, and above all thank you for putting up with me waving my hands around trying to explain general relativity to you.

Finally, I would like to thank all of "The Row" — Joseph, Morag, Alex, Fletcher, Ashton, and Michael. I will remember all of the entertaining and mostly distracting conversations we had over the last year — the majority of which was about a chair and some friction. Thanks go to Morag especially for deciphering code and providing partial data for the analysis in Chapter 7. Special thanks go to Joseph for always engaging my brain in deep discussions regarding mathematics — even when I was unwilling.

Contents

Chapter 1

Introduction

In 1915 Einstein published his theory of general relativity (GR), a theory in which gravity is no longer a force – as in Newton's theory – rather, gravity is an emergent property of the geometry of spacetime [6]. In Einstein's theory, "*matter tells spacetime how to curve and spacetime tells matter how to move*". During the first few years after GR was developed, it successfully explained the precession of the perihelion of Mercury [7] and the curving of light around the sun [8]. In recent times, the detection of gravitational waves with the Laser Interferometer Gravitational-Wave Observatory (LIGO) [9] was another confirmation of GR being the correct theory of gravity. While GR has provided a description of gravity to high precision on small scales (when compared to the size of the Universe), its applicability on large scales is not thoroughly tested and is a point of debate.

Early astronomers were limited to observing and collecting data from stars within our own galaxy. These stars have small velocities compared to the speed of light, which prompted astronomers to believe that the Universe was not expanding, nor contracting — it was static. The first application of GR to cosmology was by Einstein[1] himself, who added a cosmological constant, Λ, to his field equations to counteract the expansion they suggested [10]. Within the next ten years, Aleksandr Friedmann and Georges Lemaître independently derived solutions to Einstein's equations which featured an expanding Universe with no cosmological constant [11–13]. These results did not gain much attention until 1929 when the first piece of observational evidence that the Universe was expanding came to light. This evidence came from Edwin Hubble's observations of extragalactic nebulae, which showed a positive trend between the distance of these nebulae and their radial velocities — suggesting the Universe is expanding [14]. In 1931, Einstein accepted this piece of evidence and that the Universe was indeed expanding, stating that the cosmological constant was no longer needed [15–17].

[1]Einstein did not believe that there was a beginning to time and an expanding Universe would have suggested this. Therefore, it was not only early astrophysical data that led him to add the cosmological constant.

The current standard model of cosmology is based on the Friedmann-Lemaître-Roberston-Walker (FLRW) solution to the Einstein equations, describing a expanding spacetime that is isotropic and homogeneous. The idea of isotropy and homogeneity has its roots in the *Copernican principle*, which is the notion that, we, on Earth, do not occupy a 'privileged' place in the Universe. Thus, from observations implying that the Universe is isotropic, one can use the Copernican principle to formulate the *cosmological principle* which states: "on sufficiently large scales the spatial distribution of matter is isotropic *and* homogeneous".

In 1998 Riess et al. [18] followed by Perlmutter et al. in 1999 [19], fit astrophysical data to the FLRW model and found something unexpected — the Universe was not only expanding, the expansion was also accelerating. The surveys which 'proved' this were observing type 1a supernovae (SNe1a), the SNe1a observed appeared to be fainter than predicted by the FLRW model (without a cosmological constant). The return of the cosmological constant seemingly explained these observations and thus became part of the standard model. The cosmological constant in modern times, is associated with "dark energy" — a repulsive negative pressure, opposing gravity, that drives the expansion of the Universe at late times.

The standard model continued to add various constraints and constituents to form what we know today to be the Λ Cold Dark Matter (ΛCDM) model. Early measurements of the afterglow of the big bang — the Cosmic Microwave Background (CMB) radiation — indicated that within the class of FLRW models the Universe (globally) was very close to spatially flat [20]. Constraints from the CMB also suggested that matter only accounted for $\sim 27\%$ of the total energy density of the Universe [21], requiring a smoothly-distributed energy to reconcile this constraint with a spatially flat geometry. The ΛCDM model evolved further to include dark matter[2] — a type of invisible matter that only interacts gravitationally. Modern measurements[3] of weak gravitational lensing such as in [26] and measurements of CMB anisotropies have strengthened the 'requirement' of dark matter [21, 27] (see [28] for a history and review).

To date, the ΛCDM model — with the addition of standard perturbation theory and Newtonian N-body numerical simulations — has explained most of our cosmological observations. Notable successes include: matching the power spectrum of temperature fluctuations in the CMB [29], the location of the peak separation of large-scale structures in galaxy surveys (the baryon acoustic oscillation (BAO) peak) [30], and the matter power spectrum of large-scale structure at low redshifts [31].

There have been, however, a growing number of tensions in the past two decades between the predictions of the ΛCDM model and observations. These

[2]In the standard model, dark matter must be 'cold' as we require it to be slow-moving

[3]Dark matter was actually first hypothesised by Lord Kelvin and presented in lectures in 1884 [22] and was later inferred from the rotation curves of galaxies in the 1970s [23–25].

tensions include the 'lack of power' at the largest scales in the CMB power spectrum, and the recent 3.7σ tension between local measurements of the Hubble parameter [32, 33] compared to the inferred value from the CMB [29]. Furthermore, there is a growing tension with the lack of 'direct observation' of the 'dark sector' of the Universe. These tensions may be — as most would lead one to believe — due to of insufficient precision, or systematic errors.

There is, however, preexisting physics that is neglected in the standard model that may explain some of these tensions [3, 4, 34–37]. The basis of the ΛCDM model is the assumption of a isotropic and homogeneous expanding background[4] described by the FLRW model. These assumptions are violated on scales smaller than 'the statistical scale of homogeneity' (SSH) (see [38–41] for details and reviews), yet the ΛCDM model is in general, applied on any scale. Current state-of-the-art cosmological simulations model the evolution of structures in the Universe using Newtonian gravity on top of an assumed background spacetime for example, [42, 43]. Newtonian gravity has been shown to be a 'good approximation' for GR on small scales, however, it's applicability on cosmological scales remains a point of debate.

The main argument of why isotropy and homogeneity remain as guiding principles in cosmology is because — as mentioned — the Universe 'is isotropic and homogeneous' on large scales past the SSH. The Universe, however, is clearly inhomogeneous on small scales, and it is not 'clear' whether 'smoothing out' this small-scale structure has an effect on large-scale dynamics. In 2000, Buchert showed that the evolution of general averages of an inhomogeneous Universe is not the same as the evolution of a homogeneous Universe [4]. This is due to the fact that averaging procedures and time evolution do not commute in non-linear GR. Buchert showed that when averaging an inhomogeneous spacetime, extra terms arise that may contribute to the apparently accelerated expansion of spacetime, the extra terms being coined *backreaction*. Buchert has also developed the theory of Lagrangian perturbation theory [44–48] which is a 'background free' approach to perturbation theory in cosmology which has also evolved to include backreaction terms. The significance of backreaction has been the subject of much debate in recent years, see [49–54].

One contribution to this debate, Wiltshire's timescape model [35, 36], claims that the expansion is not actually accelerating and is more of a fundamental issue associated with how one calibrates time parameters in the presence of backreaction. There are also attempts to deviate from the ΛCDM model and standard perturbation theory, for instance, post-Newtonian theory, which is explored by Clifton et al. [1]. The treatment of post-Newtonian gravity by Clifton et al. is an attempt to model the evolution of non-linear structures, though the problem of using an FLRW background remains.

[4]The assumption of homogeneity implies that the background expands at the same rate, everywhere.

New surveys using 'state-of-the-art' telescopes such as Euclid, the Large Synoptic Survey Telescope, and the Square Kilometre Array are expected to greatly tighten the constraints on the various parameters that define our Universe. These surveys are expected to reach percent level precision over a range of redshifts [55, 56], where the differences between the FLRW expansion history and more generic expansion histories will be measurable [57, 58]. Furthermore, drawing the *correct* conclusions from observations require accurate cosmological simulations — simulations that use full GR. These simulations would potentially be able to encapsulate the full effects of backreaction on the large-scale dynamics of the Universe. Examples of such simulations can be seen in [59–61].

This thesis will discuss the standard model of cosmology, ΛCDM, along with standard perturbation theory. We will thereafter, explore alternatives to ΛCDM. In Chapter 2 we shall discuss a brief history of the development of GR and introduce the standard model of cosmology. We will also discuss various pieces of observational evidence that support ΛCDM and those that ΛCDM struggles to explain. Finally, we will introduce inhomogeneous cosmologies and the basis of backreaction.

In Chapter 3 we introduce the 3+1 and 1+3 formalisms. The 3+1 formalism in particular is the basis for numerical relativity (NR) and averaging procedures that Buchert uses to develop his theory of backreaction. In particular, we will introduce the notion of 3–dimensional hypersurfaces in a 4–dimensional spacetime, different types of curvature, and the various projections of the Einstein equations from a 4–dimension manifold to the 3–dimensional hypersurfaces.

In Chapter 4 we introduce how the standard model of cosmology accounts for inhomogeneities in the CMB and models the evolution of structure — standard perturbation theory. We will discuss the mathematical basis of perturbation theory, the solutions to the perturbed Einstein equations, and the problem of gauges, with examples of various gauges.

In Chapter 5 we present the latest form of the Buchert formalism [3] with additional derivations and details. We will discuss the 3+1 formalism in the context of the Buchert formalism with three timelike congruences, introduce the fluid-extrinsic averaging formalism, and the fluid-intrinsic averaging formalism. We shall make contact with various parts of the literature and discuss challenges that the Buchert formalism overcomes/improves on.

In Chapter 6 we present the post-Newtonian formalism which goes beyond standard linear perturbation theory with the aim of modelling the formation of non-linear structures. We will also investigate the various gauges used in simulations to determine their viability in the post-Newtonian expansion, going beyond the gauges explored in [1], such as those found in [2]. We also conduct and original investigation extending the Buchert averaging scheme to the post-Newtonian expansion with an example of how the averaged evolution equations of Buchert may be used in simulations.

In Chapter 7 we perform an original investigation of backreaction effects in a particular Szekeres model. To do so we will introduce the *cosmic quartet* [62] and the pseudo cosmic quartet. A similar investigation was undertaken by Bolejko [5], however, we use different parameters, a different density profile, and the aforementioned pseudo cosmic quartet. We will discuss our results and then compare them with Bolejko's results.

Chapter 2

General Relativity and Cosmology

2.1 From Newton to Einstein

Before general relativity, there was Newtonian gravity and before explaining Einstein's field equations, we will present the history of how our understanding of gravity changed. In 1686, Sir Issac Newton developed his equation for the force of gravity between two objects of mass m_1 and m_2, separated by distance, r:

$$F = G\frac{m_1 m_2}{r^2}, \tag{2.1}$$

where G is a proportionality constant known as the universal gravitational constant. Newton's theory itself was based on the assumption of a reference frame with an absolute space and an absolute time passing at the same rate everywhere in space. For nearly two centuries Newton's equation for the gravitational force was unchallenged. To this day, bridges, buildings, and other feats of engineering only require Newtonian gravity due to its remarkable accuracy within Earth's gravitational field. Newton's theory, however, began to face problems in 1859 as it could not explain the perihelion precession of Mercury, first noticed by Urbain Le Verrier [7].

In 1785 a strikingly similar equation was developed by Charles–Augustin de Coulomb for the electrostatic force between two charged particles with charge q_1 and q_2, separated by distance r [63]:

$$F = \frac{1}{4\pi\epsilon_0}\frac{q_1 q_2}{r^2}. \tag{2.2}$$

One will notice that both the gravitational force and electrostatic force equations were essentially identical. Both forces did not depend on *time*, which to physicists, caused problems as these forces were mediated instantaneously. Instantaneous processes violated the natural notion of "causality" that we all posses — "actions take time to make an effect". The conclusion reached due

to this 'unnatural' behaviour was that there must some 'unknown' physical medium that allows the propagation of the electrostatic force. This medium was named the 'electric field'. In 1862, James Clerk Maxwell published his unified theory of electricity and magnetism, electromagnetism in the form of Maxwell's equations[1]:

$$\begin{aligned}
\nabla \cdot \mathbf{E} &= \frac{\rho}{\epsilon_0}, \\
\nabla \cdot \mathbf{B} &= 0, \\
\nabla \times \mathbf{E} &= -\frac{\partial \mathbf{B}}{\partial t}, \\
\nabla \times \mathbf{B} &= \mu_0 \left(\mathbf{J} + \epsilon_0 \frac{\partial \mathbf{E}}{\partial t} \right).
\end{aligned} \tag{2.3}$$

Maxwell's equations were revolutionary as they explained the entire classical dynamics of electromagnetism. The problem of electromagnetism having no time dependence was resolved and the action was no longer instantaneous. Maxwell's equations were also invariant under coordinate transformations. This was an important quality of Maxwell's equations as most physicists would prefer their physical theories to be true regardless, of a choice of coordinates. The underlying idea being that coordinates do not exist *a priori* in nature. The objective was now clear for gravitation. Any attempt to re-imagine how gravity worked would involve a gravitational field which would determine the motion of objects within it, making the force not instantaneous.

Einstein did not believe the Newtonian idea of an absolute space; he thought only relative motions were physically meaningful. Newton's bucket experiment can be used to illustrate this: when the water inside a bucket rotates, the surface of the water becomes concave. However, if the water rotated with respect to the rotating bucket, the surface of the water would be flat. According to Newton, the water rotates with respect to an absolute space, whereas Einstein postulated the water rotates with respect to a physical entity: the gravitational field.

Galileo Galilei had proved in the 1590s that gravitational and inertial mass were the same for all bodies. This is often referred to as the weak equivalence principle. Einstein knew of this and reasoned that it contained something deep as it meant there was something fundamentally different about gravity and electromagnetism. The interaction between charged particles and an electric field were certainly different if the charges of the particles were changed.

Einstein had, therefore, a few guiding principles: general covariance which he had already proposed for special relativity in a limited sense (Lorentz invariance), motions being relative to some gravitational field, and the weak equiv-

[1]The form of Maxwell's equations presented here are actually not the original form. Maxwell's original equations were reformulated using vector calculus by Oliver Heaviside in 1884.

alence principle. During the process of developing general relativity, Einstein developed the strong equivalence principle which had the following ideas:

- *The principle of uniqueness of free fall* (the weak equivalence principle): All bodies (subject to no forces other than gravity) will follow the same paths given the same initial position and velocity.
- All experiments produce results of special relativity in "small" regions of spacetime.
- *Principle of Equivalence of gravitation and inertia:* All motions in an external static homogeneous gravitational field are identical to those in no gravitational field if referred to a uniformly accelerated coordinate system.
- For *inhomogeneous* gravitational fields we reformulate the Strong Equivalence Principle as: at any event, always and everywhere, it is possible to choose a local inertial frame such that in a 'local' spacetime neighbourhood all non-gravitational laws of nature take on their familiar forms appropriate to the absence of gravity.

Einstein's great insight after developing the weak equivalence principle further was that the gravitational field was built into spacetime itself. The strong equivalence principle seemingly demanded this geometric description of the gravitational field — of spacetime— as locally, the 'usual' laws of motion had to be recovered. A naïve description of a manifold is that it is 'locally' Euclidean at each point, therefore, not a far-fetched description for a notion of spacetime. Einstein postulated that masses altered spacetime and that objects moved in straight lines known as "geodesics" in this 'curved' spacetime. The more these geodesics deviate, the stronger the gravitational field or *curvature*.

2.2 Einstein's Field Equations

Einstein's theory of general relativity was a conceptual leap in the way gravity was understood. He abandoned the idea of a gravitational force and an absolute reference frame. Newtonian ideas of particles moving under the influence of a force were replaced by particles moving on geodesics in a curved spacetime. The mathematical interpretation of spacetime is that it is a four dimensional manifold, $\mathcal{M}$ on which a metric, a bilinear form $\boldsymbol{g}$, with signature $(-,+,+,+)$ acts. The matter and energy content of a spacetime is encoded in the stress-energy symmetric tensor, $\boldsymbol{T}$. The dynamics of $(\mathcal{M}, \boldsymbol{g})$ is linked to the matter and energy content of the spacetime, $\boldsymbol{T}$ via the field equations:

$$\boldsymbol{G} = \boldsymbol{R} - \frac{1}{2}R\boldsymbol{g} + \Lambda\boldsymbol{g} = 8\pi G\boldsymbol{T}. \tag{2.4}$$

Here $\boldsymbol{G}$ is the Einstein tensor, $\boldsymbol{R}$ is the Ricci tensor, and R is the Ricci scalar. The projection of the tensor quantities on a coordinate basis gives us,

$$G_{\mu\nu} = R_{\mu\nu} - \frac{1}{2}Rg_{\mu\nu} + \Lambda g_{\mu\nu} = 8\pi G T_{\mu\nu}. \tag{2.5}$$

In terms of a coordinate basis we have,

$$R_{\mu\nu} = R^{\alpha}{}_{\mu\alpha\nu}, \tag{2.6}$$

and,

$$R = g^{\mu\nu}R_{\mu\nu}. \tag{2.7}$$

Here $R^{\alpha}{}_{\mu\beta\nu}$ is the Riemann curvature tensor and is defined as,

$$R^{\alpha}{}_{\mu\beta\nu} \equiv \partial_\beta \Gamma^{\alpha}{}_{\mu\nu} - \partial_\nu \Gamma^{\alpha}{}_{\mu\beta} + \Gamma^{\alpha}{}_{\sigma\beta}\Gamma^{\sigma}{}_{\mu\nu} - \Gamma^{\alpha}{}_{\sigma\nu}\Gamma^{\sigma}{}_{\mu\beta}, \tag{2.8}$$

where $\Gamma^{\alpha}{}_{\mu\nu}$ are the Christoffel symbols describing the metric connection on the tangent bundle of $\mathcal{M}$ and in a coordinate basis are defined as,

$$\Gamma^{\alpha}{}_{\mu\nu} \equiv \frac{1}{2}g^{\alpha\lambda}(\partial_\mu g_{\nu\lambda} + \partial_\nu g_{\mu\lambda} - \partial_\lambda g_{\mu\nu}). \tag{2.9}$$

The left-hand side of Einstein's equation encodes the curvature in the Einstein tensor[2], $G_{\mu\nu}$. More specifically, the left-hand side consists of:

- Indirectly, the Riemann tensor: $R^{\alpha}{}_{\beta\mu\nu}$. There are a number of ways to interpret the Riemann tensor. The most common one is associated with deviations of geodesics [64]. If one starts with a vector $\mathbf{X}$ and parallel transports it around a small parallelogram on a manifold $\mathcal{M}$ defined by vectors $\mathbf{a}$ and $\mathbf{b}$ the deviation of $\mathbf{X}$ is

  $$\delta X^{\mu} = -R^{\mu}{}_{\nu\alpha\beta}X^{\nu}a^{\alpha}b^{\beta}. \tag{2.10}$$

  This notion carries over to the equation of geodesic deviation in general relativity where two objects moving along geodesics in a spacetime will deviate from each other according to the curvature of that spacetime.

- The Ricci tensor, $R_{\mu\nu}$ which is a contraction of the Riemann tensor. Perhaps one of the most intuitive ways to interpret the Ricci tensor is associating it to volume deformations. If one interprets the Riemann tensor as governing how the evolution of vectors parallel propagated along geodesics then the Ricci tensor governs the evolution of volumes parallel propagated along geodesics[3].

[2]As discussed, $G_{\mu\nu}$, only contains Ricci curvature, which encodes information about distortions of volumes. For a full description of curvature, one also requires information of the Weyl curvature which describes distortion in shape.

[3]We must, however, be careful here because volumes can change in flat space. For a true description then, one must subtract off any volume change that may occur in flat space.

- The Ricci scalar; R which is a contraction of the Ricci tensor. The Ricci scalar, in a sense characterises how the volume measured in a curved spacetime differs from that in flat spacetime.

- Λ, the cosmological constant. When Einstein first published his field equations, he did not consider the cosmological term. This only came into consideration through Einstein's efforts to model the Universe and fit his model to observations.

The right-hand side of Einstein's field equations is the source term, the stress-energy tensor. In cosmology we assume that the matter stress-energy tensor can be approximated as a fluid. In the early Universe with both matter and radiation present such an approximation is well justified. At later epochs when the energy density of radiation becomes negligible, we approximate the stress-energy tensor by particles of a pressureless (non-interacting) dust. Obviously, as structures form the nature of the dust particles changes.

If one prescribes a 4–velocity for the fluid, u^μ then the most general stress-energy tensor takes the form [65]:

$$T_{\mu\nu} = \rho\, u_\mu u_\nu + p\, h_{\mu\nu} + \pi_{\mu\nu} + 2q_{(\mu}u_{\nu)}. \tag{2.11}$$

Here $h_{\mu\nu} = g_{\mu\nu} + u_\mu u_\nu$ is the projection tensor (discussed in Chapter 3), ρ is the energy density, p the isotropic pressure, $\pi_{\mu\nu}$ the spacelike tracefree anisotropic pressure which satisfies $\pi_{\mu\nu}\, u^\mu = 0$, hence providing 5 independent components, and q_μ is the spacelike heat transfer vector, satisfying $q_\mu u^\mu = 0$, thus contributing 3 independent components. This stress-energy tensor is sometimes referred to as describing an 'imperfect fluid'.

The Einstein equations (2.5) embody the contracted Bianchi identity,

$$\nabla_\mu G^{\mu\nu} = 0, \tag{2.12}$$

on the left-hand side and the covariant conservation of stress-energy,

$$\nabla_\mu T^{\mu\nu} = 0, \tag{2.13}$$

on the right-hand side. Here, ∇_μ is the covariant derivative associated with the metric, $g_{\mu\nu}$.

2.3 The Friedmann-Lemaître-Robertson-Walker Spacetime

As with any spacetime in general relativity, the dynamics can be fully determined by specifying a metric tensor and a stress-energy tensor. We begin with the *line element*, $\mathrm{d}s^2$, which is determined by the metric tensor,

$$\mathrm{d}s^2 = g_{\mu\nu}\, \mathrm{d}x^\mu \mathrm{d}x^\nu. \tag{2.14}$$

The line element provides the infinitesimal length between two points in spacetime. We will demonstrate how one obtains the Friedmann-Lemaître-Robertson-Walker (FLRW) line element by first considering only the spatial part,

$$\mathrm{d}l^2 = g_{ij}\,\mathrm{d}x^i \mathrm{d}x^j. \tag{2.15}$$

In this case we consider the line element to be the proper distance between points, $\mathbf{x}$ and $\mathbf{x}+\mathrm{d}\mathbf{x}$. The FLRW spacetime relies on the assumption of isotropy and homogeneity. An example of a isotropic and homogeneous 3-dimensional space is flat space, which has the line element,

$$\mathrm{d}l^2 = \mathrm{d}\mathbf{x}^2. \tag{2.16}$$

This metric is left invariant under spatial translations and rotations. Another example of such a surface is a spherical surface in four-dimensional Euclidean space with radius a, with the line element,

$$\mathrm{d}l^2 = \mathrm{d}\mathbf{x}^2 + \mathrm{d}z^2, \tag{2.17}$$

where $z^2 + \mathbf{x}^2 = a^2$. Another possibility for such a space — the only other one as shown by Weinberg [66] – is,

$$\mathrm{d}l^2 = \mathrm{d}\mathbf{x}^2 - \mathrm{d}z^2, \tag{2.18}$$

where $z^2 - \mathbf{x}^2 = a^2$. The coordinate transformations that leave this line element invariant are four-dimensional pseudo-rotations (much like Lorentz transformations but instead of time here, we use z). We can now rescale these coordinates:

$$\mathbf{x} = a\mathbf{q}, \quad z = aw. \tag{2.19}$$

The two line elements above can then be written as,

$$\mathrm{d}l^2 = a^2\,[\,\mathrm{d}\mathbf{q} \pm \mathrm{d}w^2\,], \tag{2.20}$$

where $w^2 + \mathbf{q}^2 = 1$. The total derivative of this constraint equation gives us,

$$w\,\mathrm{d}w = \mp\,\mathbf{q}\,\mathrm{d}\mathbf{q}, \tag{2.21}$$

which allows one to rewrite (2.20) as,

$$\mathrm{d}l^2 = a^2\left[\mathrm{d}\mathbf{q}^2 \pm \frac{(\mathbf{q}\,\mathrm{d}\mathbf{q})^2}{1 \mp \mathbf{q}^2}\right]. \tag{2.22}$$

One can further simplify the above and also include the flat Euclidean case. To do this, we rewrite the above slightly as

$$\mathrm{d}l^2 = a^2\left[\mathrm{d}\mathbf{q}^2 + k\frac{(\mathbf{q}\,\mathrm{d}\mathbf{q})^2}{1 - k\,\mathbf{q}^2}\right], \tag{2.23}$$

where,

$$k = \begin{cases} +1 & \text{spherical (positive curvature)} \\ 0 & \text{Euclidean (flat)} \\ -1 & \text{hyperspherical (negative curvature)} \, . \end{cases}$$

We note that $a^2 > 0$ as we require $\mathrm{d}s^2 > 0$ at $\mathbf{q} = 0$ because it is a physical length.

To extend this metric to (an expanding) spacetime, we can simply include time in the line element to obtain

$$-g_{\mu\nu}\,\mathrm{d}x^\mu \mathrm{d}x^\nu = \mathrm{d}t^2 - a(t)^2 \left[\mathrm{d}\mathbf{q}^2 + k\frac{(\mathbf{q}\,\mathrm{d}\mathbf{q})^2}{1-k\mathbf{q}^2} \right]. \tag{2.24}$$

Note that a depends only on time, because of the assumption of isotropy and homogeneity. This ensures that at every point in space the Universe is expanding at the same rate in all directions. Therefore, one can assume that this expansion factor, $a(t)$, known as the *scale factor* [65, 67] need only depend on time and not on spatial location.

Finally, instead of using Cartesian coordinates, x^i, we can use spherical polar coordinates where,

$$\mathrm{d}\mathbf{q}^2 = \mathrm{d}r^2 + r^2\mathrm{d}\theta^2 + r^2\sin^2\theta\,\mathrm{d}\phi^2. \tag{2.25}$$

Performing a coordinate transform we find,

$$g_{\mu\nu}\mathrm{d}x^\mu \mathrm{d}x^\nu = -\mathrm{d}t^2 + a^2(t)\left[\frac{\mathrm{d}r^2}{1-kr^2} + r^2\,\mathrm{d}\theta^2 + r^2\sin^2\theta\,\mathrm{d}\phi^2 \right], \tag{2.26}$$

which is the standard form of the FLRW line element. In the present standard model for cosmology, one sets $k = 0$ as on large scales the Universe is assumed to be "spatially flat". In this case, the line element reduces to

$$\mathrm{d}s^2 = g_{\mu\nu}\mathrm{d}x^\mu \mathrm{d}x^\nu = -\mathrm{d}t^2 + a(t)^2 \left[\mathrm{d}r^2 + r^2\mathrm{d}\theta^2 + r^2\sin^2\theta\,\mathrm{d}\phi^2 \right]. \tag{2.27}$$

The distance we would measure here is named the *comoving distance* and the coordinates are referred to as *comoving coordinates*. A comoving distance allows the distance between two points to remain constant as the Universe expands even though the physical distance will change [67]. We can also rewrite the line element as a proper time interval,

$$\mathrm{d}\tau^2 = \mathrm{d}t^2 - a(t)^2 \left[\mathrm{d}r^2 + r^2\mathrm{d}\theta^2 + r^2\sin^2\theta\,\mathrm{d}\phi^2 \right]. \tag{2.28}$$

Note that one may determine the convention used in this thesis from the derivation in this section. I.e., we will use units where $c = 1$ and our metric signature is $(-,+,+,+)$ unless stated otherwise.

2.3.1 About Time and Dimensions

Defining a notion of 'global time' is difficult. This is because clocks tick at different rates in the Universe. In an effective model of the Universe, there would ideally be some notion of averaging over all of these clocks.

In cosmology, there can be multiple notions of time, one of these is the coordinate time, t, also known as *cosmic time*. The cosmic time is the proper time of a comoving observer, as can be seen from (2.27). In cosmology we also often use — in fact, more often than not — *conformal time*. Conformal time is defined as,

$$\eta - \eta_i \equiv \int_{t_i}^{t} \frac{\mathrm{d}t'}{a(t')}, \tag{2.29}$$

where t is the cosmic time. As long as the cosmic time is considered to be a physically relevant proper time, then the conformal time should not be considered a "physically meaningful" time. However, the conformal time is useful for describing the *particle horizon*, defined[4] as $c\eta$, this measures the maximum distance information — such as photons or gravitational waves — could have propagated since the big bang. The particle horizon sets a limit to causal contact between different regions in the Universe, usually leading to the "horizon problem"[65].

The conformal time allows one to rewrite the FLRW line element as

$$\mathrm{d}s^2 = a(\eta)^2 \left(-\mathrm{d}\eta^2 + \frac{\mathrm{d}r^2}{1 - k\,r^2} + r^2\,\mathrm{d}\theta^2 + r^2 \sin^2\theta\,\mathrm{d}\phi^2 \right). \tag{2.30}$$

Hence, the scale factor has become a *conformal factor*, explaining the name for η. The line element (2.30) is a conformal scaling of Minkowski space if $k = 0$, an Einstein static Universe with spatial sections of topology S^3 if $k = 1$, or similarly of a Universe with hyperbolic spatial section if $k = -1$.

Note that when using the line element (2.30), any derivatives with respect to conformal time will be denoted by a prime, $'$. The introduction of the conformal time allows for some freedom of where the 'dimensions of the line element live'. This will be relevant to the interpretation of post-Newtonian cosmology in Chapter 6. Consider the following:

$$[\,\mathrm{d}s^2\,] = \mathrm{L}^2, \tag{2.31}$$

where [.] indicates the dimensions of the object and L is the dimension of length. From the definition of the conformal time we know

$$\frac{\mathrm{d}t}{\mathrm{d}\eta} = a,$$

[4] In (2.29), we have assumed $c = 1$ as per usual, however, the distinction is made in the discussion to provide insight into what the conformal time is.

which gives rise to two choices for allocating dimensions. In units $c = 1$, $[\,t\,] = [\,ct\,] = L$. This gives two natural choices depending on whether a factor of c is implicit in the definition or not.

$$\begin{aligned} &\text{I}: \quad [\,a\,] = \text{L} \implies [\,\eta\,] = 1, \\ &\text{II}: \quad [\,a\,] = 1 \implies [\,\eta\,] = [\,t\,] = \text{L}\,. \end{aligned} \tag{2.32}$$

The spatial FLRW line element which we shall refer to as γ_{ij} will have the corresponding dimensions

$$\begin{aligned} &\text{I}: \quad [\,\gamma_{ij}\,\mathrm{d}x^i\mathrm{d}x^j\,] = 1 \implies [\,\gamma_{ij}\,] = 1, \quad [\,x^i\,] = 1\,, \\ &\text{II}: \quad [\,\gamma_{ij}\,\mathrm{d}x^i\mathrm{d}x^j\,] = \text{L}^2 \implies [\,\gamma_{ij}\,] = 1, \quad [\,x^i\,] = \text{L}\,. \end{aligned} \tag{2.33}$$

2.3.2 Hubble Law

In 1929 Edwin Hubble published a study which showed that the redshift of galaxies was proportional to their distance. This study consisted of 18 galaxies in which Cepheids[5] could be seen. The study analysed the redshift of these galaxies and found the redshift was increasing as a function of distance. This became known as the Hubble law[6]. Hubble's law could be mathematically expressed as

$$z = \frac{H_0\, d}{c}, \tag{2.34}$$

where z is the redshift, d is the distance to the galaxy, and H_0 is the proportionality constant known at the Hubble constant. Hubble interpreted the redshift as a non-relativistic radial Doppler shift, $z = v/c$, writing $v = H_0\, d$, where v is the separation velocity of the galaxy from us.

The Hubble parameter can be defined straightforwardly using the FLRW metric as

$$H(t) = \frac{\dot{a}(t)}{a(t)}, \tag{2.35}$$

where the dot refers to a derivative with respect to the time coordinate, t. The value of the Hubble constant today is H evaluated at t_0,

$$H_0 = \left.\frac{\dot{a}(t)}{a(t)}\right|_{t=t_0}. \tag{2.36}$$

It should be noted that cosmologists often move the ambiguity of the value of the Hubble constant today to a dimensionless Hubble constant, h, and write $H_0 = 100\,h^{-1}\,\mathrm{km s^{-1} Mpc^{-1}}$. Furthermore, it is also common to use the *conformal*

[5]Cepheids are a type of star that pulsate radially, varying in diameter and temperature and produce change in brightness with well defined stable periods and amplitudes.

[6]In 2018 the International Astronomical Union declared that this should be know as the Hubble–Lemaître Law, since Lemaître obtained the relation (2.34) using the same data two years prior to Hubble. [13].

Hubble parameter, which is the Hubble parameter with respect to conformal time. The conformal Hubble parameter is denoted by $\mathcal{H}$ and is defined as

$$\mathcal{H} = \frac{a'(\eta)}{a(\eta)}, \tag{2.37}$$

which can be related to the usual Hubble parameter via

$$\mathcal{H} = aH. \tag{2.38}$$

2.3.3 Friedmann equations

Thus far we have discussed the metric of the standard model of cosmology, the FLRW metric. To fully describe the standard model, we must also describe the matter content as Einstein's field equations couple geometry to the matter content of a spacetime. In the standard model, one assumes that all the matter in the Universe can be smoothed into a perfect fluid with an stress-energy tensor that takes the form [65]:

$$T^{\mu\nu} = (\rho + p)\, u^\mu u^\nu + p\, g^{\mu\nu}. \tag{2.39}$$

Here, u^μ are the components of the 4−velocity of the fluid defined as

$$u^\mu = \frac{\mathrm{d}x^\mu}{\mathrm{d}\tau}, \tag{2.40}$$

ρ is the energy density, and p is the pressure.

In the rest-frame of the fluid[7], the components of the 4–velocity are

$$u^{\bar{\mu}} = (1,0,0,0), \quad \text{or} \quad u^\mu = \frac{1}{a}\,(1,0,0,0), \tag{2.41}$$

i.e., the spatial velocity of the fluid is zero. If the spatial velocity of the fluid were non-zero then one would violate the assumption of spatial homogeneity. Furthermore, the assumption of isotropy and homogeneity imply that the pressure and energy density can only be functions of time. The stress-energy tensor with respect to (2.30) has the following matrix representation:

$$T^\mu{}_\nu = \begin{pmatrix} -\rho & 0 & 0 & 0 \\ 0 & p & 0 & 0 \\ 0 & 0 & p & 0 \\ 0 & 0 & 0 & p \end{pmatrix}. \tag{2.42}$$

The Friedmann equations follow when one computes the relevant terms in the field equations, which can be rewritten in the trace-reversed form:

$$R_{\mu\nu} - \Lambda g_{\mu\nu} = 8\pi G\,(T_{\mu\nu} - \frac{1}{2} T\, g_{\mu\nu}). \tag{2.43}$$

[7]In what follows, when specifying particular coordinate frames we will use barred indices for the standard comoving frame and unbarred for the conformal frame.

For the FLRW metric, the components of the Ricci tensor are:

$$\begin{aligned}
&R_{\bar{0}\bar{0}} = -3\frac{\ddot{a}}{a^2}, \quad \text{or} \quad R_{00} = 3\left(\frac{a'^{\,2}}{a^2} - \frac{a''}{a}\right), \\
&R_{0i} = 0, \\
&R_{\bar{i}\bar{j}} = \left(2\frac{\dot{a}^2}{a^2} + \frac{\ddot{a}}{a} + 2\frac{k}{a^2}\right) g_{\bar{i}\bar{j}}, \quad \text{or} \quad R_{ij} = \left(2\frac{a'^{\,2}}{a^4} + \frac{a''}{a^3} + 2\frac{k}{a^2}\right) g_{ij}.
\end{aligned} \tag{2.44}$$

The Ricci scalar is,

$$R = 6\left(\frac{\dot{a}^2}{a^2} + \frac{\ddot{a}}{a} + \frac{k}{a^2}\right) \quad \equiv \quad R = 6\left(\frac{k}{a^2} + \frac{a''}{a^3}\right). \tag{2.45}$$

The components of the Einstein tensor are:

$$\begin{aligned}
&G_{\bar{0}\bar{0}} = 3\left(\frac{\dot{a}^2}{a^2} + \frac{k}{a^2}\right) - \Lambda, \quad \text{or} \quad G_{00} = 3\,\frac{a'^{\,2}}{a^2} + 3k - \Lambda\, a^2\,, \\
&G_{\bar{0}\bar{i}} = G_{0i} = 0, \\
&G_{\bar{i}\bar{j}} = -\left(2\frac{\ddot{a}}{a} + \frac{\dot{a}^2}{a^2} - \Lambda + \frac{k}{a^2}\right) g_{\bar{i}\bar{j}}, \quad \text{or} \quad G_{ij} = -\left(2\frac{a''}{a^3} - \frac{a'^{\,2}}{a^4} - \Lambda + \frac{k}{a^2}\right) g_{ij},
\end{aligned} \tag{2.46}$$

and finally, the components of the stress-energy tensor are

$$\begin{aligned}
&T_{\bar{0}\bar{0}} = \rho, \quad \text{or} \quad T_{00} = a^2\rho\,, \\
&T_{\bar{0}\bar{i}} = T_{0i} = 0, \\
&T_{\bar{i}\bar{j}} = T_{ij} = p\, g_{ij}.
\end{aligned} \tag{2.47}$$

From the standard form of the field equations, (2.5) we obtain the first Friedmann equation:

$$\frac{\dot{a}^2 + k}{a^2} = \frac{8\pi G\rho + \Lambda}{3}, \quad \text{or} \quad \mathcal{H}^2 + k = a^2\frac{8\pi G\rho + \Lambda}{3} \tag{2.48}$$

and from the trace-reversed equations (2.43) we obtain the second Friedmann equation:

$$\frac{\ddot{a}}{a} = -\frac{4\pi G}{3}\Big(\rho + 3p\Big) + \frac{\Lambda}{3}, \quad \text{or} \quad \mathcal{H}' = -\frac{4\pi G}{3}\Big(\rho + 3p\Big)\, a^2 + a^2\,\frac{\Lambda}{3}. \tag{2.49}$$

Note that if $\Lambda = 0$ then for any matter that obeys the strong energy condition, $\rho + 3p > 0$, the expansion is always decelerating. Generically a perfect fluid with pressure will obey an equation of state

$$p = w\rho, \tag{2.50}$$

where w is restricted by energy conditions. In particular, the dominant energy condition requires that $-1 \leq w \leq 1$ so that the speed of sound does not exceed

the speed of light. The strong energy condition is violated if $-1 \leq w < -1/3$, corresponding to matter which does not clump gravitationally and is therefore called "dark energy". The cosmological constant, which was first introduced as a geometric quantity can also be interpreted as a dark energy with $w = -1$, with pressure

$$p_\Lambda = -\frac{\Lambda}{8\pi G}, \tag{2.51}$$

and density,

$$\rho_\Lambda = \frac{\Lambda}{8\pi G}. \tag{2.52}$$

Following an initial phase which is phenomenologically well described by a period of inflation, the Universe can be considered to pass through a series of epochs in which one component of the energy dominates over the others. Very roughly, if we take the energy conservation equation

$$u_\nu \nabla_\mu T^{\mu\nu} = 0 \quad \text{or} \quad \dot{\rho} = -3\frac{\dot{a}}{a}(\rho + p), \tag{2.53}$$

then for a fluid with a single equation of state, $p = w\rho$, we find $\rho \propto a^{-3(1+w)}$.

For radiation, $w = 1/3$, and $\rho_R \propto a^{-4}$; and for non-relativistic matter (including dark matter) $w = 0$ and $\rho_M \propto a^{-3}$. The mass-energy of the Universe is then

$$\begin{aligned} \rho &= \rho_r + \rho_m + \rho_\Lambda \\ &= \rho_{r0}\left(\frac{a_0}{a}\right)^4 + \rho_{m0}\left(\frac{a_0}{a}\right)^3 + \frac{\Lambda}{8\pi G}. \end{aligned} \tag{2.54}$$

Here ρ_r includes both neutrinos and photons, and $\rho_m = \rho_b + \rho_c$ both baryonic and Cold Dark Matter.

In the early radiation dominated epoch, before matter radiation equality, $a \ll a_{eq} = a_0\,\rho_{r0}/\rho_{m0}$, we find $a \propto t^{1/2}$. Later, following decoupling there is an epoch when $\rho_m \gg \rho_r$, and $\rho_m \gg \rho_\Lambda$ and we find $a \propto t^{2/3}$, as in an Einstein–de Sitter Universe. One can also write an analytic solution with $\Lambda = 0$ which interpolates between the radiation dominated and matter dominated regimes. At decoupling, for example, the energy density of radiation and matter is $\sim 25\%$ and $\sim 75\%$ respectively leading to $a_0/a_{decoupling} \sim 1100$. At very late times, dark energy dominates the energy density of the Universe and the scale factor takes the form $a(t) \propto \exp\left[\frac{1}{2}\sqrt{\Lambda/3}t\right]$.

In the current epoch, we find ourselves at a time when the energy density of matter and dark energy are of a similar order of magnitude, $\rho_m \sim \rho_\Lambda$. Cosmic acceleration appears to have begun only relatively recently, so that at present $\ddot{a} > 0$ but $\dot{H} = (\ddot{a}a - \dot{a}^2/a^2) < 0$. Since this appears to involve a degree of fine-tuning it begs the question of why this occurs at the present epoch.

This is known as the "cosmic coincidence problem". Answering this question could involve the anthropic principle [68], or dynamical dark energy, or alternatively abandoning the FLRW models. Models which involve backreaction of

inhomogeneities — discussed in Chapter 5 — provide a potential alternative resolution in terms of a related coincidence. In particular, the epoch of onset of cosmic acceleration coincides with the first growth of large inhomogeneities.

2.4 The Lambda Cold Dark Matter Model

After the discovery of the apparently accelerated expansion of the Universe in the 1990s by [18, 19] the Lambda Cold Dark Matter model (ΛCDM) became the prevalent model to describe the Universe. The model adapts the FLRW metric and consequently the Friedmann equations to describe our Universe on *any* scale. It is predicated on the cosmological principle — the notion that the average spatial distribution of matter in the Universe is exactly isotropic and homogeneous.

To this day, ΛCDM is the most tested model of cosmology and is supported by many cosmological observations[8]. A particular set of FLRW cosmological parameters agree with independent observations, and have been designated the "concordance model". In terms of the parameters (2.55) defined below, at the present epoch we find negligible spatial curvature, a substantial cosmological constant, and a matter density with an order of four times as many dark matter[9], particles as ordinary baryonic matter. This particulate matter is called "dark matter", as the relative velocities are small, i.e., non-relativistic. Cold Dark Matter is 'well approximated' as dust since it is pressureless and assumed to only interact gravitationally.

2.4.1 Cosmological parameters

Often in cosmology instead of using a dimensionful density, ρ, we define dimensionless density parameters, $\Omega_i = \rho_i/\rho_{\rm cr}$, for each component contributing to the energy density. Here $\rho_{\rm cr} = 3H^2/8\pi G$ is the critical density of a spatially flat matter dominated model. In particular we define:

$$\begin{aligned}
\Omega_m(t) &:= \frac{8\pi G}{3H^2(t)}\rho_m(t), \\
\Omega_r(t) &:= \frac{8\pi G}{3H^2(t)}\rho_r(t), \\
\Omega_\Lambda(t) &:= \frac{\Lambda}{3H^2(t)}, \\
\Omega_k(t) &:= -\frac{k^2}{a^2(t)H^2(t)},
\end{aligned} \tag{2.55}$$

[8]This is *true*, however, in recent years many aspects of the model have come into question with the development of 'precision cosmology'.

[9]While many candidates exist for dark matter, none have been directly observed to date.

where, as before, M, r, Λ, and k refer to matter, radiation, the cosmological constant, and curvature constant respectively. With these parameters, one can rewrite the first Friedmann equation as

$$\Omega_M + \Omega_r + \Omega_\Lambda + \Omega_k = 1. \tag{2.56}$$

We evaluate the parameters at the present epoch to obtain standard cosmological parameters. These have been constrained by many independent tests, including the Planck collaboration in 2015 and 2018 [29, 69] by the temperature fluctuations in the cosmic microwave background (CMB). The present epoch values are given with a 68% confidence level:

$$\begin{aligned} &\Omega_{c\,0} = 0.264 \pm 0.002, \\ &\Omega_{b\,0} = 0.0493 \pm 0.0002, \\ &\Omega_{\Lambda 0} = 0.6911 \pm 0.0062, \\ &|\Omega_{k\,0}| < 0.001 \pm 0.002, \\ &\Omega_0 \approx 1 \times 10^{-5}, \end{aligned} \tag{2.57}$$

where the subscript c refers to cold dark matter, the subscript b refers to ordinary baryonic matter, and the subscript 0 refers to evaluation at the present epoch.

2.4.2 Observations

While this thesis does not delve into how the theory we discuss may be tested, it is nevertheless important to understand the observational side of cosmology. After all, early work constraining $\Omega_{m0} < 1$ [70–73] and the discovery of the accelerated expansion of the Universe marked the beginning of the current standard model and the alternate formalisms we investigate in this thesis.

Cosmic Microwave Background

In 1964 the CMB, the afterglow of the big bang, was discovered [74]. The CMB is isotropic to a high degree, and is the largest piece of evidence supporting a big bang cosmology [75]. Advancements in instruments and data processing led to the realisation that the CMB radiation was actually *anisotropic* [76]. In the years following the discovery of the CMB, it was found to have a dipole temperature anisotropy [77, 78] to an estimated 1 part in 10^{-3}. This dipole has been assumed to be purely kinematic, and can be removed by a local boost. After accounting for this local boost, the temperature anisotropies of the CMB have been observed at the order of a few parts in 10^{-5}, beginning with the observations of the COBE satellite [79, 80], then continuing with the Wilkinson Microwave Anisotropy Probe (WMAP) and the Planck satellite missions. These

have constrained the temperature anisotropy to be parts in 10^{-5} relative to the mean temperature, $\bar{T} \approx 2.725\text{K}$ [69, 81].

The early Universe was dense, and opaque, containing a photon-baryon plasma, and dark matter. The initial conditions of the big bang created a spectrum of density perturbations about the background which were 'scale free'. These density perturbations lead to gravitational collapse of the primordial plasma and dark matter. The baryons, however, experienced a radiation pressure that opposed gravitational collapse, creating pressure perturbations. This interplay between competing effects of radiation pressure and gravitational collapse resulted in acoustic waves in the plasma known as the Baryon Acoustic Oscillations (BAOs), with sound speed $v_{\text{sound}} = \sqrt{\mathrm{d}p/\mathrm{d}\rho}$, where $\mathrm{d}\rho$ is the density perturbation and $\mathrm{d}p$ is the pressure perturbation. The dark matter particles are understood to be pressureless and thus they continued to experience gravitational collapse during this epoch.

As the photon-baryon plasma cooled, free electrons bound with protons to form neutral hydrogen, decreasing the electron density significantly — this epoch is known as *recombination* and occurs near the epoch of photon-electron decoupling [67]. Recombination released photons which travelled freely through the Universe (forming the CMB) meaning the radiation pressure on the baryons vanished, ending the BAOs. The last baryon acoustic waves 'froze' in place, leading to baryon overdensities at the distance the last sound wave travelled — the sound horizon and its harmonics on smaller scales [82, 83]. Due to the continuous gravitational collapse of dark matter before recombination, the relative density of the dark matter particles was greater than that of the baryons — $\delta\rho_c/\bar{\rho} \approx 10^{-4}$ for dark matter and $\delta\rho_b/\bar{\rho} \approx 10^{-5}$ for the baryons, where $\delta\rho$ is the density perturbation and $\bar{\rho}$, the background density. After recombination the relatively larger density perturbations from the dark matter acted as 'gravitational wells' for the baryons to 'fall into'. This was on the scale of small protogalaxies, forming the first structures in the Universe.

The small-scale anisotropies measured in the CMB are dominated by the BAOs. Measuring the location and amplitude of the peaks in the angular power spectrum leads to constraints on the cosmological parameters, (2.4.1) [84]. The BAO is detected principally by two methods. Firstly, the angular power spectrum is measured by determining the temperature fluctuations in the CMB as a function of angular scale. The largest first peak in the power spectrum corresponds to an angular scale in which overdensities and underdensities have had time to undergo only one compression or rarefaction by the decoupling epoch. The scale is observed at an angle $\sim 0.6^\circ$ — corresponding to distance scales on which inhomogeneities are still expanding today as close to linear perturbations in the framework of the standard model. Consequently, we expect an echo of the excess power in galaxy clustering statistics. Secondly, the first BAO peak was detected in 2005 by examining the 2-point galaxy-galaxy correlation function of

thousands of galaxies [85, 86]. The distance determined matched the predicted sound horizon. Over the last decade, it has become an important test as new data sets becomes available.

Type Ia Supernovae

To determine the expansion history of the Universe requires that we observe independent values of the distances and redshifts. While redshifts are 'simple' to measure, estimating the distances is full of systematic errors as well as statistical biases. Ideally, astronomers seek "standard candles", objects of fixed absolute bolometric luminosity, $\mathcal{L}$, which at a distance, d_L — the "luminosity distance" — lead to an observable bolometric flux,

$$\mathcal{F} = \frac{\mathcal{L}}{4\pi {d_L}^2}. \tag{2.58}$$

Measurements of the flux then enable the observed luminosity distances, $d_L = \sqrt{\mathcal{L}(4\pi\mathcal{F})}$, to be compared to different model predictions as a function of redshift.

In reality, there are no perfect standard candles, and the best we have are "standardizable" candles. In 1993, a breakthrough was made by Phillips, [87], who discovered an empirical relation between the peak of the supernova light curve in the rest frame B-band and its decay over 15 days — allowing SNe1a to be standardizable.

The High-z Supernova Search Team [18, 88] and the Supernova Cosmology Project [19] used SNe1a data to plot the Hubble diagram to about $z \sim 0.8$. The results of this showed that SNe1a farthest away from Earth were $\sim 15\%$ dimmer than previously expected for a matter dominated FLRW cosmology with $\Lambda = 0$. The conclusion from this was that the expansion of the Universe was accelerating which was explained well by implementing $\Lambda > 0$ in the context of a FLRW cosmology. One should note that only an FLRW model was used in the data analysis. One may then ask whether the cosmological constant actually exists or whether it is an emergent feature of model fitting. SNe1a at $z > 1$ were also investigated in later years suggesting the Universe underwent *deceleration* at earlier epochs, implying that the Universe was not always dominated by a repulsive 'vacuum energy' [89–91].

In the last two decades numerous SNe1a surveys have been conducted to reinforce the original measurements of Riess et al. [18] and Perlmutter et al. [19]. These SNe1a have been amalgamated into various catalogues and beyond measuring the acceleration of the Universe, they are often used to determine the local Hubble constant.

2.5 Challenges for the Standard Model

The ΛCDM model has had many successes and has been able to explain many of our cosmological observations. There are, however, several tensions which have developed due to the standard model. In addition, the nature of dark energy and dark matter — the most dominant constituents of the Universe — constitute major challenges for fundamental physics. Dark energy is the greater problem, since unlike dark matter, it would not appear to have a "simple" resolution in particle physics. Some general relativists, including Buchert and Wiltshire [4, 36, 44–48] have sought alternatives for dark energy at a fundamental level.

2.5.1 Fundamentals

There are numerous fundamentals in the theory of general relativity which are overlooked or ignored because of complications that arise. One such problem is the largest scale on which Einstein's equations can be applied with a coarse-grained stress-energy tensor. General relativity has only been well tested on 'small scales' explaining phenomena including the precession of the perihelion of Mercury, the bending of light from distant stars around our sun, gravitational lensing, and gravitational wave production from black hole mergers in the strong field regime [92]. Nonetheless, one should be careful when applying general relativity to large scales where it has not been directly tested, such as galaxies, galaxy clusters, the local neighbourhood, and even the entire Universe.

Perhaps the leading challenge to the assumptions of the standard model is the foundation of the cosmological principle. The cosmological principle is based on the Copernican principle. Our galaxy is in a thin filament [93] inside the local void. The filament connects us to the nearest rich cluster of galaxies, the Virgo cluster, of order 20 Mpc away. On larger scales, surveys indicate that 40 to 50% of the volume of the present epoch Universe is contained in voids that have a diameter of $30\,h^{-1}$Mpc on average [94, 95]. These voids have a density contrast of $\delta_\rho \sim -0.95$, where $\delta_\rho = \delta\rho/\bar{\rho} = (\rho - \bar{\rho})/\bar{\rho}$. While we still find ourselves in a galaxy which might be deemed 'typical', the Copernican principle may require refinement [35]. This is because our observations indicate all galaxies constitute a mass-biased view of the Universe and are not representative of typical locations by volume, which are void regions where structures never formed.

The dust approximation also gives rise to fundamental issues [96]. In particular, particles of dust are usually understood as 'discrete masses' which do not change over the timescale of evolution of the problem in question. However, over the life time of the Universe the nature of the dust *must* change as particle geodesics cross — from ions, to stars and planets, to galaxies and galaxy clusters. If we require the mass of a dust particle not to change over the age of the Universe we must coarse-grain on scales larger than the largest typical

non-linear structures. I.e., at scales a few times larger than the most typical voids or $\sim 100\,h^{-1}$Mpc.

We are therefore dealing with fluid elements, rather than isolated dust particles, and we are averaging over geometrical quantities involving small scale structure and the dynamical gravitational energy implicit in solutions of Einstein's equations on small scales. On account of the strong equivalence principle, gravitational energy cannot be localised at a point. Gravitational energy is non-local. It can at best be integrated over regions, giving rise to various quasilocal definitions [97]. However, such definitions are not unique and represent an open frontier for theorists in the mathematical relativity community.

Associated with the problem of averaging is the problem of patching spacetimes. It is known that there are many different gravitational fields in the Universe and, therefore, the most accurate description of the Universe would patch all of these spacetimes together. This is a complicated problem involving fundamental problems of physical interpretation over and above the mathematical issues of the "fitting problem" [98]. The fitting problem leads one to other fundamental questions in cosmology — for instance, "what is the actual scale beyond which bound systems can no longer be influenced by the rest of the Universe?" in the current epoch. This led Wiltshire to define a notion of[10] "finite infinity" [35, 99] to embody a concept suggested originally by Ellis [100].

A similar scale has been called the "matter horizon" by Ellis and Stoeger [101], and is much smaller than the particle horizon. The particle horizon is an absolute limit set by the finite propagation speed of light. However, at the present epoch the energy density of electromagnetic and gravitational waves is negligible in comparison to the local matter density. Variations in the local matter density on scales larger than those of bound structures were primarily determined by the finite speed of sound before decoupling.

This effectively creates new considerations about causality in cosmological averages and leads to the idea that given any two (or more) matter horizons, they will develop separately — as separate Universes. The question then arises, "how much do these separate Universes differ". Rough estimates by Wiltshire [36] based on this idea suggest that on any scale of averaging above $100\,h^{-1}$ Mpc, density differences of $\sim 6\%$ should be expected. In the FLRW model, one expects $\delta_\rho \to 0$ as the scale of averaging is increased. With a nearly scale invariant spectrum of initial density perturbations, and the separate Universe idea, the SSH is one at which δ_ρ becomes bounded. By contrast, the SSH is defined for a scale beyond which δ_ρ monotonically decreases for larger averages in the standard model.

In scenarios in which we seek to explain apparent cosmic acceleration as an effect of inhomogeneities, the basic effect comes about from the differential

[10]Wiltshire [35] defines finite infinity as the timelike boundaries which define the boundary between bound systems and unbound systems.

growth of voids as opposed to walls and filaments – the denser but still expanding regions that contain bound and collapsing structures. The volume of voids is initially negligible. However, considered as "separate universes", locally they decelerate much less than the denser walls. Cosmological distances are measured on scales on which light traverses a significant number of both voids and walls. Early in cosmic history the void volume fraction is tiny and the amount of deceleration appears homogeneous when projected along a light ray. However, in the late universe there is a transition to void dominance. Therefore, consider an observer who tries to interpret cosmological distances in terms of a single deceleration parameter. It may appear that the expansion starts to "accelerate" when the fraction of the distance travelled through the less rapidly decelerating – and hence rapidly growing – voids increases.

Whether the transition to void dominance is significant enough to be interpreted as apparent "acceleration" or not depends crucially on the calibration of the global average expansion rate as compared to local clocks and rulers. The key ingredient in Wiltshire's timescape model is a cumulative "drift" of the canonical clocks "at infinity" for observers in bound structures [35]. This is compared to the time parameter of the normals to the spatial hypersurfaces which describe average evolution, via Buchert averages, on cosmological scales. Such a phenomenology goes beyond the framework of Buchert's scheme, which we develop in Chapter 5.

2.5.2 Observational Challenges

The ΛCDM model is broadly supported by numerous independent observations. There are, however, a number of challenges for the ΛCDM model which are persistent and growing in significance as observational precision increases. A number of these challenges were reviewed by Buchert et al. [102] five years ago. Here we will briefly discuss and update some of the key issues.

Hubble Constant

The value of the Hubble constant has been a matter of debate among astronomers over many decades, dominated by a history in which systematic uncertainties have led to some large differences in estimates values of H_0. Some fifty years ago, competing estimates differed by a factor of two. By comparison, present estimates are much closer. Nonetheless as precision increases, there appears to be a persistent tension which continues to receive a lot of attention from the community at present.

Higher values of H_0 are obtained largely from low redshift measurements, and somewhat lower values are obtained from parameter fits to the ΛCDM model at larger distances. These values are represented by the SH0ES collab-

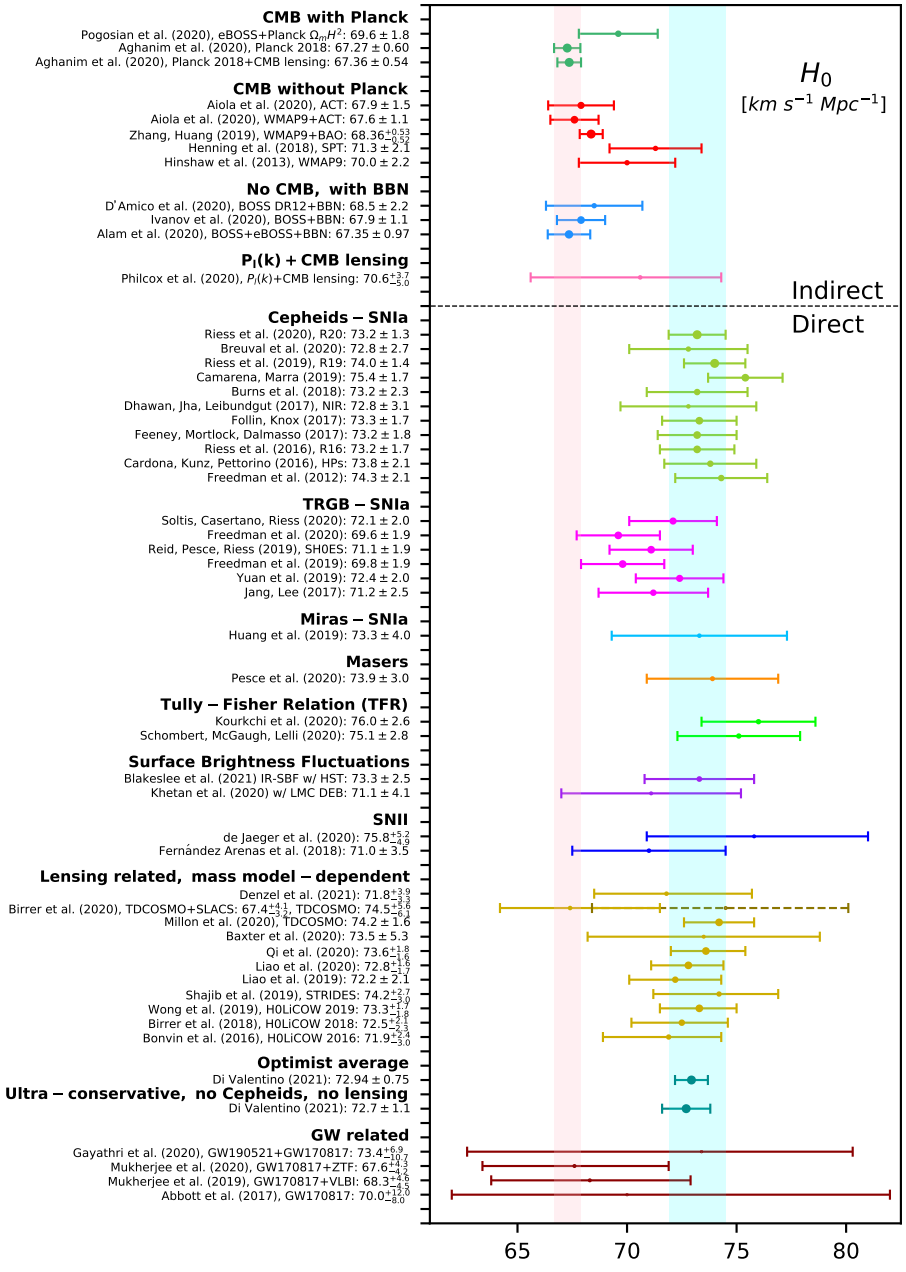

Figure 2.1: Whisker plot with 68% confidence limit constraints on the Hubble constant H_0 from [103], through direct and indirect measurements by different astronomical missions over the years. The cyan vertical band corresponds to the 2020 value from the SH0ES collaboration [104] ($H_0 = 73.2 \pm 1.3$) km s^{-1} Mpc^{-1} and the light pink vertical band corresponds to the 2018 value $H_0 = (67.4 \pm 0.5)$ km s^{-1} Mpc^{-1} from the Planck collaboration [29] from the ΛCDM model.

oration 2018 estimate[11], $H_0 = (73.45 \pm 1.66 \text{kms}^{-1}\text{Mpc}^{-1})$ [33] and the Planck collaboration estimate $H_0 = (67.4 \pm 0.5)\text{kms}^{-1}\text{Mpc}^{-1}$ [29]. These values are obtained by using Cepheid variables and SNe1a and by fitting the angular diameter distance of the sound horizon in the CMB anisotropy data respectively. The tension between these two values is $3.7\,\sigma$.

The situation is significantly more complicated, however. For example, in 2019 using a method based on selecting galaxies with stars at the tip of the red giant branch (TRGB) in the Hertzsprung–Russell diagram, the Carnegie–Chicago collaboration published a value $H_0 = (69.8 \pm 0.8)\text{kms}^{-1}\text{Mpc}^{-1}$. This value sits between the Planck satellite and SH0ES values, being $1.2\,\sigma$ from the former and $1.7\,\sigma$ from the latter. While the TRGB method yields some of the lowest values of H_0 obtained by direct measurements, there are a number of methods which tend to give higher values, as summarised in Figure 2.1. Additional methods include: gravitational lensing estimates, angular diameter distances to masers in accretion disks around supermassive black holes, and the empirical Tully-Fisher relation. Gravitational wave estimates from neutron star binary mergers are a promising independent estimator for the future. However, to date only one event (GW170817) has yielded an independent redshift as well as a distance [105].

Numerous ideas have been put forward to explain the Hubble tension, which usually invoke exotic new physics without changing the Friedmann equation [103]. Inhomogeneous models, however, offer many potential avenues of solution, as they naturally give rise to a scale dependence of the Hubble parameter. For example, Bolejko [37] showed that an emerging globally negative curvature of the Universe can resolve the Hubble tension, while also reducing the amount of dark energy. This was done under the "silent Universe" approximation[12]. Other ideas have been discussed in the context of backreaction and averaging [106]. Examination of the effect of of 'local' structure could also play a significant role in measurements which will be one of the many aims of upcoming 'precision' surveys [107, 108].

Systematic Problems in Type Ia Supernova Data Fitting

In a previous project [109], we used the JLA [110] and Pantheon [111] SNe1a catalogues consisting of 740 and 1048 SNe1a respectively to compare Wiltshire's timescape model [36] to the ΛCDM model. This built on an earlier analysis by Dam et al. [112] using the JLA catalogue. By Bayesian model compasion Dam

[11] This has very recently updated to $H_0 = (73.2 \pm 1.3 \text{kms}^{-1}\text{Mpc}^{-1})$ [104]. Over time individual values of each group have not changed significantly, rather the uncertainties have tightened.

[12] The silent Universe is based on numerical solutions of the field equations in a 1+3 formalism (see Chapter 3) with restricted gravitational degrees of freedom. The Einstein equations are sourced solely by irrotational dust and a cosmological constant, with vanishing magnetic parts of the Weyl tensor and diagonalisable shear.

et al. had found a log Bayes factor of $\ln B = 1.43$ which indicated a slight preference for timescape relative to ΛCDM.

Subsequently, after the Pantheon catalogue [111] was released we first attempted to analyse that data set. However, that proved impossible given the manner in which the data had been reduced before publication. Nonetheless, we were able to reanalyse a subsample consisting of 646 SNe1a common to both Pantheon and JLA, using the data from the JLA catalogue. Surprisingly, we found a log Bayes factor of $\ln B = -1.62$, indicating the ΛCDM was now slightly preferred to the timescape model.

The publication of the Pantheon survey gave no statement as to why 94 supernovae from the earlier JLA catalogue had been omitted. Indeed, the very fact that 94 supernovae were omitted was not stated anywhere, and was something that could only be determined from the data files that were made publicly available[13]. Furthermore, the Pantheon survey also provided new SNe1a already reduced with added systematic uncertainties for example, that incorporate peculiar-velocity modelling based on N-body simulations on a FLRW background. With an increasing tendency of observers to fit the data to the FLRW in order to increase "precision" it is becoming difficult to actually test frameworks that fall outside the FLRW paradigm.

Large-Angle CMB Anomalies

There are several observations concerning the large angle multipoles of the CMB anisotropy spectrum, which may be considered anomalous to varying degrees of statistical significance [115]. These include:

(i) the power asymmetry between the northern and southern hemispheres [116–120];

(ii) the low quadrupole power [116, 121];

(iii) the alignment of the quadrupole and octupole [121–124];

(iv) the parity asymmetry [125] between odd and even multipoles;

(v) a large unusually cold spot [126, 127].

The power asymmetry was observed in the first COsmic microwave background explorer (COBE) sky maps (of the CMB), and was also detected by WMAP with increased significance [116–119]. The significance of this and a number of the other anomalies further increased with the release of Planck satellite data [128–130].

[13]Other concerns have been raised by Rameez and Sarkar [113, 114].

Anisotropies in the Galaxy Distribution

The CMB anisotropies are determined after the CMB dipole has been subtracted, assuming it is purely kinematic, due entirely to a local Lorentz boost between our telescopes and the "CMB rest frame". To fully resolve the observed $3.353 \pm 0.034\,\mathrm{mK}$ CMB dipole [131, 132] as a local boost requires two things. The first being the motion of the sun within the galaxy and of our galaxy within the Local Group (LG) of galaxies. The second being the LG itself must have a boost $v_{\mathrm{LG-CMB}} = 635 \pm 38\,\mathrm{km\,s^{-1}}$ toward galactic coordinates $(\ell, b) = (276.4^\circ, 29.3^\circ) \pm 3.2^\circ$ in the constellation Hydra. However, in generic inhomogeneous cosmologies we can expect differential expansion which cannot be reduced to uniform expansion plus pure local boosts [133, 134].

Any significant nonkinematic local expansion will impact directly on our interpretation of the CMB. This gives rise to corrections at the level of the CMB quadrupole and higher multipoles which do not match an expansion of the Lorentz boost factor in powers of v/c [134]. The Planck team claim to have verified the kinematic nature of the CMB dipole by measuring the higher order effects of modulation and aberration on the anisotropy spectrum [135, 136]. However, this conclusion only holds for the small angle multipoles $l_{\mathrm{min}} = 500 < l < l_{\mathrm{max}} = 2000$. If large angle multipoles are included and l_{max} is reduced to $l_{\mathrm{max}} < 100$, then the inferred boost direction moves across the sky to coincide with the modulation dipole anomaly direction [119], $(\ell, b) = (224^\circ, -22^\circ) \pm 24^\circ$.

Such an angular scale dependence of the results based on the kinematic interpretation are not at all surprising if nonkinematic differential expansion is at play on $\lesssim 100h^{-1}\,\mathrm{Mpc}$ scales [133, 134]. If correct, differential expansion should manifest itself in other ways. Independent tests of the special relativistic modulation effect on number counts of radio galaxies, quasars and mid-infra red active galactic nuclei reveal a dipole whose direction is consistent with the CMB dipole. The amplitude of this, however, is too large to be explained kinematically [137–143]. In 2013, for example, Rubart and Schwarz ruled out a kinematic dipole in radio galaxies at the 99.5% confidence level [138]. There have been numerous debates about systematic uncertainties. However, observational characteristics such as frequency dependence have been examined [142] which mitigate against simple observational explanations for the 'anomaly'. Furthermore, there has been a recent observation of a dipole in a sample of quasars at large redshifts [141]. The amplitude of which rejects the kinematic hypothesis at the level $4.9\,\sigma$. Therefore, ruling out many possible systematic uncertainties that are potentially invoked in nearby radio galaxy samples.

Primordial Lithium Abundance

In the first few minutes after the big bang, big bang nucleosynthesis (BBN) occurred. This process converted about 25% of primordial protons – i.e., hydrogen

nuclei – into helium–4 nuclei (alpha particles) with traces of deuterium, helium–3, and lithium–7. All heavier elements are synthesized in stars. Thus the BBN predictions determine nuclear abundances in the oldest baryonic matter we observe in the Universe, from which all stars formed. Big bang nucleosynthesis uses standard nuclear reactions which are well–understood. One basic parameter, $\eta_{B\gamma}$, the ratio of the densities of primordial baryons to photons tightly constrains the isotopic mass ratios ^{4}He/H, ^{3}He/H, D/H, and ^{7}Li/H of the nuclear end products. The fact that the predictions broadly agree with observation has long been one of the key pieces of evidence supporting the big bang [144, 145].

There have long been weak (1–2σ) intrinsic tensions in astronomical observations of the relative abundances of primordial D/H versus ^{7}Li/H [144], given BBN predictions using a broad constraint on $\eta_{B\gamma}$ from just the CMB temperature and the distance to the last scattering surface. However, the constraint on $\eta_{B\gamma}$ tightened significantly with WMAP's first measurement of the ratio of the heights of the third to first acoustic peaks [145]. This ratio greatly constrains both the densities of baryons and cold dark matter relative to the CMB photons. Such constraints can only be made within a cosmological model, in this case the ΛCDM model. A result of this is that the prediction for the Li/H abundance became seriously discrepant with observations [145] and the significance of the discrepancy has increased with time [146]. The lack of ^{7}Li/H in metal-poor halo field stars in our galaxy is inconsistent with the ΛCDM expectation from the CMB anisotropy spectrum at about 4σ–5σ. This may be resolved with existence of new exotic particles [147, 148].

The primordial Li/H abundance is viewed as a particle physics problem by most of the community. The fact remains, however, that it is largely due to the ΛCDM fit of the heights of the first and third acoustic peaks in the CMB. Any alternative cosmological model which changes the ratio of baryonic matter to dark matter, as is generally the case in Wiltshire's timescape cosmology [36], requires a reexamination of the entire problem.

2.6 Backreaction and Inhomogeneous Cosmology

We have thus far discussed the challenges the standard model faces, both fundamental and observational. We have also discussed various ideas that have been put forward in the field to attempt to reconcile these problems, most of them involving inhomogeneous models of some description. We have also implied that the FLRW metric is overly simplified with the cosmological constant simply being a fine-tuning parameter. One potential solution to the dark energy problem is to *properly* consider the role of small-scale inhomogeneities on the average

large-scale cosmological dynamics, this is the approach taken by Buchert [3, 4, 34]. This approach is a more theoretically 'conservative' (but socially more radical) approach to addressing the dark energy problem. This is because many other theories invoke new physics from the introduction of fundamental fields or modifications to the gravitational action. The idea of how small-scale structure impacts large-scale behaviour is known as *backreaction*.

2.6.1 First look at Backreaction from Inhomogeneities

Let us consider a 'physical spacetime' which is described by $(\mathcal{M}, \boldsymbol{g})$ and an averaged spacetime $\Big(\langle\, \mathcal{M} \,\rangle_{\mathcal{D}}\,, \langle\, \boldsymbol{g} \,\rangle_{\mathcal{D}}\Big)$ where the averaging procedure is not specified. Let us assume that the physical spacetime on small scales is a solution to Einstein's equations. The averaged Einstein equations in the form (2.5) then read

$$\langle\, G_{\mu\nu} \,\rangle = 8\pi G \,\langle\, T_{\mu\nu} \,\rangle, \tag{2.59}$$

where

$$\langle\, G_{\mu\nu} \,\rangle = \langle\, R_{\mu\nu} \,\rangle - \frac{1}{2}\,\langle\, R\, g_{\mu\nu} \,\rangle + \Lambda\,\langle\, g_{\mu\nu} \,\rangle.$$

Let us then decompose the 'physical metric' as a fluctuation or *perturbation* from the average to model inhomogeneities:

$$g_{\mu\nu} = g^{a}_{\mu\nu} + \delta\, g_{\mu\nu}\,, \tag{2.60}$$

where $g^{a}_{\mu\nu} = \langle\, g_{\mu\nu} \,\rangle$.

The averaged Einstein equation due to the inhomogeneities, therefore, can be reformulated by following [149]:

$$\langle\, G_{\mu\nu} \,\rangle = G^{a}_{\mu\nu} + \Delta\, G_{\mu\nu} = 8\pi G\,\langle\, T_{\mu\nu} \,\rangle. \tag{2.61}$$

Thus, the averaging process and the construction of the Einstein tensor do not commute — the averaged dynamics of spacetime is not equal to the dynamics of the averaged spacetime. This can perhaps be better understood by the statement:

$$G_{\mu\nu}\,(\langle\, g_{\mu\nu} \,\rangle) \neq \langle\, G_{\mu\nu}\,(g_{\mu\nu}) \,\rangle = 8\pi G \langle\, T_{\mu\nu} \,\rangle. \tag{2.62}$$

However, this is precisely what the standard model assumes;

$$G^{a}_{\mu\nu} = 8\pi G \langle\, T_{\mu\nu} \,\rangle. \tag{2.63}$$

The $\Delta\, G_{\mu\nu}$ term is the so-called 'backreaction' term and will be non-zero as long as inhomogeneities are present and can act on the dynamics of the averaged spacetime. By neglecting this term, the standard model assumes that the dynamics of the structures at small scales do not influence global dynamics. The open question is to understand if the backreaction term is large enough to account for dark energy and dark matter.

It should be noted that the fundamental issue with this approach, is that there exists no unique approach to the mathematically complex problem of averaging tensors. There are a handful of approaches in the literature which often involve extra mathematical structure [150–153]. Buchert averaging, on the other hand, considered in Chapter 5 is constructed from scalar variables, such as the intrinsic Ricci scalar, extrinsic curvature scalar, and stress-energy scalars.

Chapter 3

3+1 Formalism in General Relativity

The 3+1 formalism is an approach to general relativity that splits spacetime into space + time. This is done by splitting the four-dimensional manifold of spacetime, $\mathcal{M}$, equipped with a Lorentzian metric, i.e., the signature is $(-,+,+,+)$, into three-dimensional hypersurfaces that evolve with some notion of time. These hypersurfaces are required to be spacelike so the metric induced on the hypersurfaces is Riemannian, i.e., has signature $(+,+,+)$. Furthermore, the requirement for these hypersurfaces to spacelike means that we will also have a globally hyperbolic spacetime, which is a fundamental assumption for any physical theory[1].

The 3+1 formalism has become the basis for calculations in general relativity that do not presuppose some particular background. It is useful when one wishes to rewrite the Einstein field equations as an initial value problem, a Cauchy problem. In particular, a Cauchy problem which has a local unique solution as was shown by Yvonne Choquet-Bruhat in 1952 [154]. One can use an initial hypersurface as the Cauchy surface from which the Universe or parts of the Universe evolve. Note that the space + time splitting is not an *a priori* structure of general relativity, but rather somewhat depends on a choice of time coordinate. We should also make clear that the $3+1$ formalism is not the same as the $1+3$ formalism. These two formalisms differ in their basic structures, in the $3+1$ formalism, the basic structure is a family of three-dimensional hypersurfaces. In the $1+3$ formalism, the basic structure is a congruence of one-dimensional curves such as worldlines. We will discuss the $1+3$ formalism will be discussed in section 3.5.

The formalism that exists today originated from work done by Georges Darmois in the 1920s [155], André Lichnerowiez in the 1930s [156–158], and the aforementioned Yvonne Coquet-Bruhat in the 1950s. In the late 1950s and

[1]Globally hyperbolic spacetimes are used in 'physical' theories has they have no closed time-like curves and, therefore, causality is not violated.

early 1960s, Richard Arnowitt, Stanley Deser, and Chales W. Misner (ADM) used the $3+1$ splitting as a foundation for the Hamiltonian formulation of general relativity[2] [161]. In the 1970s, the 3+1 formalism became the backbone for numerical relativity, largely due to the work by James W. York who formed the 3+1 equations that were used in this community [162, 163]. Numerical relativity, in modern times is an essential tool to interpret astrophysical data. A strong motivation for further improvements in numerical techniques is the development of a completely new field of gravitational wave astronomy. This began with the first detections by LIGO [9] and will continue for decades with projects such as LISA [164].

3.1 Hypersurfaces

The hypersurfaces we discuss are 3-dimensional surfaces. These surfaces evolve dynamically to generate a 4-dimensional manifold, $\mathcal{M}$, via the Einstein equations. Hypersurfaces in the framework of the 3+1 formalism are introduced as surfaces of 'local simultaneity' for certain observers in a full spacetime. We will, therefore, in this section present the mathematical tools to make a 3+1 split of spacetime. Our discussion here will first deal with general embeddings as maps on manifolds without considering the Einstein equations.

3.1.1 Embedding Hypersurfaces in Spacetime

We define a hypersurface as a 3-dimensional manifold which we shall label, $\hat{\Sigma}$. The image of $\hat{\Sigma}$ by an embedding $\Phi : \hat{\Sigma} \to \mathcal{M}$ is a hypersurface, Σ of $\mathcal{M}$ (for a visual interpretation, see Figure 3.1). This is defined as:

$$\Sigma = \Phi(\hat{\Sigma}), \tag{3.1}$$

the embedding, $\Phi : \hat{\Sigma} \to \Sigma$ is a homeomorphism. A homeomorphism more generally, is a continuous function between topological spaces that has a continuous inverse function. Homeomorphisms are isomorphisms (i.e., one-to-one *and* onto) that preserve the topological properties of a given space. The one-to-one nature of the embedding map guarantees that Σ in $\mathcal{M}$ does not self-intersect. We can define a hypersurface locally as the set of all points, p such that a scalar field on $\mathcal{M}$ is constant:

$$\forall p \in \mathcal{M}, \quad p \in \Sigma \iff t(p) = 0, \tag{3.2}$$

where t is the scalar field on[3] $\mathcal{M}$.

[2]It should be noted that an earlier version of this was formulated by Paul Dirac [159, 160].

[3]We can see this explicitly with an example. Let us introduce a local coordinate system of $\mathcal{M}$, $x^\mu = (t, x, y, z)$. If we then have Σ, a submanifold of $\mathcal{M}$ then we define Σ by the

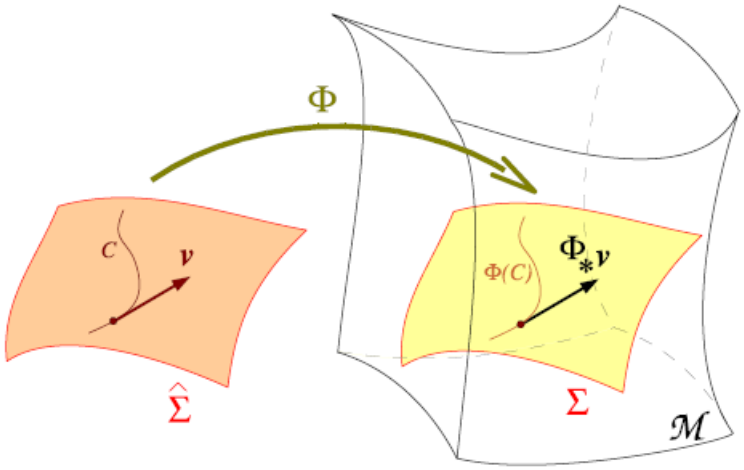

Figure 3.1: A visual representation of embedding from [165]. The embedding Φ can be seen carrying the hypersurface $\hat{\Sigma}$ into $\mathcal{M}$, thereby defining the hypersurface, $\Sigma \in \mathcal{M}$. The push-forward of the tangent vectors, $\Phi_* \boldsymbol{v}$, to curves, C become tangent vectors the curves $\Phi(C)$ in $\mathcal{M}$.

The embedding Φ also transports curves in $\hat{\Sigma}$ to curves in $\mathcal{M}$. Therefore, it also transports tangent vectors to these curves on $\hat{\Sigma}$ to vectors on $\mathcal{M}$. This can be seen in Figure 3.1 where the curve is C and the tangent vector is $\boldsymbol{v}$. One can thus relate the tangent spaces of $\hat{\Sigma}$, $\mathcal{T}_p(\hat{\Sigma})$ to the tangent spaces in $\mathcal{M}$, $\mathcal{T}_p(\mathcal{M})$. To do this, we use the push-forward mapping, Φ_*:

$$\begin{array}{rccc} \Phi_* : & \mathcal{T}_p(\hat{\Sigma}) & \longrightarrow & \mathcal{T}_p(\mathcal{M}) \\ & v^i & \longmapsto & \Phi_*(0, v^i), \end{array} \tag{3.4}$$

where $v^i = (v^x, v^y, v^z)$ are the components of a vector, $\boldsymbol{v}$ with respect to the basis of $\mathcal{T}_p(\Sigma)$ associated with the coordinate system, $x^\mu = (t, x, y, z)$. Similarly, the pull-back of Φ, Φ^*, relates the cotangent spaces of $\hat{\Sigma}$, $\mathcal{T}_p^*(\hat{\Sigma})$ to the cotangent spaces of $\mathcal{M}$, $\mathcal{T}_p^*(\mathcal{M})$:

$$\begin{array}{rccc} \Phi^* : & \mathcal{T}_p^*(\mathcal{M}) & \longrightarrow & \mathcal{T}_p(\hat{\Sigma}) \\ & \omega_\mu & \longmapsto & \Phi^* \omega_\mu = \omega_i, \end{array} \tag{3.5}$$

recalling that one-forms, ω_μ are the components of the 1-form, ω with respect to the dual coordinate basis, $\mathrm{d}x^\mu$ associated with the coordinates, x^μ. The idea of pull-backs of the embedding map can be generalised to multilinear functions of vectors, therefore, the bilinear form, $\boldsymbol{g}$ (the spacetime metric). We define the induced metric on Σ as:

$$\boldsymbol{h} := \Phi^*(\boldsymbol{g}). \tag{3.6}$$

coordinate condition, $t = 0$. We can, therefore, obtain an explicit for of Φ defined:

$$\begin{array}{rccc} \Phi : & \hat{\Sigma} & \longrightarrow & \mathcal{M} \\ & (x, y, z) & \longmapsto & (0, x, y, z). \end{array} \tag{3.3}$$

$\boldsymbol{h}$ is usually referred to as the 'first fundamental for of Σ' or the '3-metric'. In terms of the coordinates, x^i, introduced before, we have

$$h_{ij} = g_{ij}. \tag{3.7}$$

We wish to have the hypersurfaces be spacelike, and thus the metric, h is definite positive, i.e., has signature $(+,+,+)$. Note that we will only deal with vectors in $\mathcal{M}$ that have been identified with vectors in $\hat{\Sigma}$, that is, we will use the push-forward of vectors in $\hat{\Sigma}$ in $\mathcal{M}$. We will, therefore, use $\boldsymbol{v}$ instead of always using $\Phi_* \boldsymbol{v}$ – thereby, keeping the knowledge of the structure implicit.

3.1.2 Normal Vector

We wish to define a normal vector to Σ in $\mathcal{M}$. This can be done by considering a scalar field t and defining Σ as a level surface of t (such as one defined in (3.2)). The gradient[4], $\vec{\boldsymbol{\nabla}} t$ is a vector normal to the surface Σ in the sense that,

$$\boldsymbol{v} \cdot \vec{\boldsymbol{\nabla}} t = g_{\mu\nu}\, v^\nu\, \nabla^\mu t = 0, \quad v \in \mathcal{T}_q(\Sigma). \tag{3.8}$$

The vector $\vec{\boldsymbol{\nabla}} t$, furthermore, defines a unique normal direction to Σ, meaning that any other vector, $\boldsymbol{k}$, normal to Σ will be collinear to $\vec{\boldsymbol{\nabla}} t$. We can further define a unit normal vector to Σ as

$$\boldsymbol{n} \equiv \frac{1}{\sqrt{-\vec{\boldsymbol{\nabla}} t \cdot \vec{\boldsymbol{\nabla}} t}} \vec{\boldsymbol{\nabla}} t, \tag{3.9}$$

or in component form

$$n^\mu = \frac{1}{\sqrt{-g_{\alpha\beta} \nabla^\alpha t\, \nabla^\beta t}}\, \nabla^\mu t. \tag{3.10}$$

Note: the condition that the hypersurface, Σ, is spacelike restricts the normal vectors, $\vec{\boldsymbol{\nabla}} t$ and $\boldsymbol{n}$ to be timelike, implying

$$\boldsymbol{n} \cdot \boldsymbol{n} = n^\mu n_\mu = -1. \tag{3.11}$$

3.1.3 Curvature

In 1827, Gauss defined the notion of curvature in two ways for 2–dimensional surfaces embedded in $\mathbb{R}^3$. The first method was by considering a normal to a surface at a point, P and then drawing a plane containing this normal (a normal plane). The intersection of this plane with the surface is a curve on the surface. If the plane is rotated about the point, P, then amongst all the curves there will be one which has the maximum radius from P and one with a minimum. The *principal radii* at P are the reciprocal of the radii of the osculating circles of the curves at P. These radii are usually labelled κ_1 and κ_2.

[4]An arrow indicates the contravariant components, i.e., has components $\nabla^\mu t$.

The second notion of curvature was different. Consider, again, a point P which is associated with a point Q on a sphere in a way such that the normals are P and Q are parallel on the sphere. A circle of area, G in the neighbourhood of Q maps into a closed curve about P which encloses an area, F on the surface of the sphere. Gauss, thereby defined one number to characterise the curvature of this surface know as the *Gaussian curvature*:

$$|K_{Gauss}| = \lim_{F\to 0}(G/F). \tag{3.12}$$

The two concepts of curvature can be related by

$$K_{Gauss} = \kappa_1\kappa_2. \tag{3.13}$$

We also define the *mean curvature*:

$$K_{mean} = \kappa_1 + \kappa_2. \tag{3.14}$$

The two scalar curvature measurements are fundamentally different. For instance, K_{Gauss} can be measured from observations made from within the surface and without the knowledge of how the surface is embedded in a larger space[5]. K_{mean}, on the other hand is a property of the sheet within the context of the embedding space and may never be measured by observers on the surface[6]. It may not be surprising then that we refer to the Gaussian curvature as the *intrinsic curvature* (that we associate with the intrinsic Ricci scalar) and the mean curvature as the *extrinsic curvature*. We will, therefore, introduce the intrinsic and extrinsic curvature in the context of a $3+1$ splitting of spacetime.

Intrinsic Curvature

Intrinsic curvature of a surface was demonstrated by Gauss to be a curvature that could be determined by measurements made on the surface. This is the curvature we associate with gravity, the curvature of spacetime.

If the hypersurface, Σ is spacelike, then the induced metric, $\boldsymbol{h}$ is not degenerate. Therefore, we can conclude that there is a unique connection[7], $\boldsymbol{D}$ on the manifold, Σ. This connection is torsion-free and metric preserving ($\boldsymbol{Dh} = 0$). Here, $\boldsymbol{D}$ is the usual Levi-Civita connection used associated with the metric $\boldsymbol{h}$

[5]The Gauss–Bonnet theorem related the sum of the interior angles of a spherical triangle to the radius of the sphere. Gauss used this theorem to determine the radius of the Earth. Gauss used measurements of a triangle which had side lengths of $\sim$ 25km. This calculation, thereby consolidated the idea of being able to measure the curvature of a surface by making observations only *on the surface*, i.e., not requiring information of the 3-dimensional space in which it is embedded [166].

[6]One may note the different physical dimensions, K_{Gauss} has dimensions $[\,\mathrm{L}^{-2}\,]$ and K_{mean} has dimensions $[\,\mathrm{L}^{-1}\,]$.

[7]A degenerate metric is null and has signature $(0,+,+)$. To see details about how this relates to having a unique connection, see [167].

and restricted to Σ. The Riemann tensor that is associated to the connection, $\boldsymbol{D}$ represents the intrinsic curvature of $(\Sigma, \boldsymbol{h})$. We will denote this 3-dimensional Riemann tensor by $\boldsymbol{\mathcal{R}}$ to avoid confusion with the 4-dimensional intrinsic curvature of $(\mathcal{M}, \boldsymbol{g})$. As is the case of four dimensions, the 3-dimensional Riemann tensor can be expressed as the non-commutativity of two successive covariant derivatives:

$$\forall\, \boldsymbol{v} \in \mathcal{T}_p\,(\Sigma), \quad (D_i\, D_j - D_j\, D_i)\, v^k = \mathcal{R}^{\,k}{}_{pij}\, v^p. \tag{3.15}$$

The Ricci tensor, $\mathcal{R}_{ij}$, and the Ricci scalar, $\mathcal{R}$, are defined as:

$$\mathcal{R}_{ij} := \mathcal{R}^{\,k}{}_{ikj}, \quad \text{and} \quad \mathcal{R} := h^{ij}\, \mathcal{R}_{ij}. \tag{3.16}$$

Extrinsic Curvature

Previously, we had described the extrinsic curvature as a "mean curvature". For another geometric interpretation, one can consider the 'bending' of the manifold Σ, with respect to the manifold it is embedded within, $\mathcal{M}$. More precisely, the extrinsic curvature corresponds to the how the normal, $\boldsymbol{n}$ changes when one moves on Σ. We can formalise this notion of change by considering tangent vectors on Σ and moving the normal vector along them, then evaluating the variation in the normal vector. The variation will be evaluated via the spacetime connection, $\boldsymbol{\nabla}$:

$$\forall\, \boldsymbol{v} \in \mathcal{T}_p\,(\Sigma), \quad \boldsymbol{\chi} \,:\, \boldsymbol{v} \to \boldsymbol{\nabla}_{\boldsymbol{v}}\, \boldsymbol{n}, \tag{3.17}$$

where $\boldsymbol{\chi}(\boldsymbol{v})$ is the Weingarten map or shape-operator. Note that $\boldsymbol{\chi}(\boldsymbol{v}) \in \mathcal{T}_p\,(\Sigma)$ since[8]

$$\boldsymbol{n} \cdot \boldsymbol{\chi}(\boldsymbol{v}) = \boldsymbol{n} \cdot \boldsymbol{\nabla}_{\boldsymbol{v}}\, \boldsymbol{n} = n^\alpha\, v^\mu\, \nabla_\mu\, n_\alpha = 0. \tag{3.18}$$

The fundamental property of the Weingarten map is to be *self-adjoint* with respect to the induced metric, $\boldsymbol{h}$:

$$\forall\, (\boldsymbol{u}, \boldsymbol{v}) \in \mathcal{T}_p\,(\Sigma) \times \mathcal{T}_p\,(\Sigma), \quad \boldsymbol{u} \cdot \boldsymbol{\chi}(\boldsymbol{v}) = \boldsymbol{\chi}(\boldsymbol{u}) \cdot \boldsymbol{v}. \tag{3.19}$$

Here, the scalar product is with respect to $\boldsymbol{h}$ if the vectors, $\boldsymbol{u}$ and $\boldsymbol{v}$ are in $\mathcal{T}_p(\Sigma)$ or $\boldsymbol{g}$ if $\boldsymbol{u}$ and $\boldsymbol{v}$ are vectors[9] of $\mathcal{T}_p(\mathcal{M})$. Because $\boldsymbol{\chi}$ is self-adjoint, it implies that the bilinear form defined on the tangent bundle of Σ by

$$\begin{array}{rccc} \boldsymbol{\mathcal{K}} :\, \mathcal{T}_p\,(\Sigma) \times \mathcal{T}_p\,(\Sigma) & \longrightarrow & \mathbb{R} \\ (\boldsymbol{u}, \boldsymbol{v}) & \longmapsto & -\boldsymbol{u} \cdot \boldsymbol{\chi}(\boldsymbol{v}) \end{array} \tag{3.20}$$

[8]This shows that the normal and $\boldsymbol{\chi}(\boldsymbol{v})$ are orthogonal, hence, $\boldsymbol{\chi}(\boldsymbol{v})$ must live in $\mathcal{T}_p\,(\Sigma)$. This also means that the Weingarten map is well defined since $\boldsymbol{\chi} : \mathcal{T}_p\,(\Sigma) \to \mathcal{T}_p\,(\Sigma)$.

[9]In fact, for a 3–dimensional hypersurface, the eigenvalues of the Weingarten map are the principle curvatures (κ_1, κ_2, and κ_3) of the hypersurface, Σ. The mean curvature of Σ with these eigenvalues is defined as the arithmetic mean:

$$K_{Mean} := \frac{1}{3}(\kappa_1 + \kappa_2 + \kappa_3).$$

These eigenvalues are all strictly real numbers since $\boldsymbol{\chi}$ is self-adjoint.

is symmetric. This is called the *second fundamental form* of the hypersurface, Σ. It is also the extrinsic curvature tensor of Σ and contains the same information as the Weingarten map. Using the definition of $\boldsymbol{\chi}(\boldsymbol{v})$ in (3.17) we obtain

$$\forall(\boldsymbol{u},\boldsymbol{v}) \in \mathcal{T}_p(\Sigma) \times \mathcal{T}_p(\Sigma), \quad \boldsymbol{\mathcal{K}}(\boldsymbol{u},\boldsymbol{v}) = -\boldsymbol{u} \cdot \boldsymbol{\nabla}_{\boldsymbol{v}}\, \boldsymbol{n}. \tag{3.21}$$

3.1.4 Orthogonal Projector

At each point in spacetime, the tangent space of $\mathcal{M}$ can be decomposed as

$$\mathcal{T}_p(\mathcal{M}) = \mathcal{T}_p(\Sigma) \oplus \mathrm{Vect}(\boldsymbol{n}), \tag{3.22}$$

where Vect $\boldsymbol{n}$ is a 1-dimensional subspace of $\mathcal{T}_p(\mathcal{M})$ that is the span of $\boldsymbol{n}$. The *orthogonal projector* onto Σ associated with the decomposition above is the operator

$$\begin{array}{rccc} \vec{\boldsymbol{h}} & : & \mathcal{T}_p(\mathcal{M}) & \longrightarrow & \mathcal{T}_p(\Sigma) \\ & & \boldsymbol{v} & \longmapsto & \boldsymbol{v} + (\boldsymbol{n}\cdot\boldsymbol{v})\,\boldsymbol{n}. \end{array} \tag{3.23}$$

One would require that the orthogonal projector acts as the identity operator to any vectors tangent to Σ,

$$\forall\, \boldsymbol{v} \in \mathcal{T}_p(\Sigma), \quad \vec{\boldsymbol{h}}(\boldsymbol{v}) = \boldsymbol{v}. \tag{3.24}$$

We also have

$$\vec{\boldsymbol{h}}(\boldsymbol{n}) = 0, \tag{3.25}$$

as a consequence of $\boldsymbol{n}\cdot\boldsymbol{n} = -1$. According to (3.23), $\vec{\boldsymbol{h}}$ takes the form

$$h^{\mu}{}_{\nu} = \delta^{\mu}{}_{\nu} + n^{\mu}\, n_{\nu}. \tag{3.26}$$

We had previously noted that the embedding, Φ of Σ in $\mathcal{M}$ induces the push-forward, $\mathcal{T}_p(\Sigma) \to \mathcal{T}_p(\mathcal{M})$ and the pull-back, $\mathcal{T}_p{}^*(\mathcal{M}) \to \mathcal{T}_p{}^*(\Sigma)$. The embedding Φ, however, does not provide a mapping in the reverse direction. The orthogonal projector seems to provide a natural reverse mapping as by definition it maps from $\mathcal{T}_p(\mathcal{M}) \to \mathcal{T}_p(\Sigma)$. Using the orthogonal projector, we can construct a mapping from $\mathcal{T}_p{}^*(\Sigma) \to \mathcal{T}_p{}^*(\mathcal{M})$. For any linear form, $\boldsymbol{\omega} \in \mathcal{T}_p{}^*(\Sigma)$,

$$\begin{array}{rccc} \vec{\boldsymbol{h}}^{*} & : & \mathcal{T}_p{}^*(\Sigma) & \longrightarrow & \mathcal{T}_p{}^*(\mathcal{M}) \\ & & \boldsymbol{\omega} & \longmapsto & \boldsymbol{\omega} + \langle\, \boldsymbol{\omega}, \boldsymbol{n}\,\rangle\, \underline{\boldsymbol{n}}, \end{array} \tag{3.27}$$

where, $\underline{\boldsymbol{n}}$ is the dual to $\boldsymbol{n}$. One can obviously extend this notion further to multilinear forms. As the operator $\vec{\boldsymbol{h}}^{*}$ maps to the a cotangent space at $p \in \mathcal{M}$, we can naturally act on the induced metric, $\boldsymbol{h}$ and find a result that will still be in the cotangent space:

$$\boldsymbol{h} \equiv \vec{\boldsymbol{h}}^{*}\, \boldsymbol{h} = \boldsymbol{g} + \underline{\boldsymbol{n}} \otimes \underline{\boldsymbol{n}} \tag{3.28}$$

We use the same symbol as the induced metric because it is a bilinear form on[10] $\mathcal{M}$ and coincides with the induced metric if the two arguments are vectors tangent to[11] Σ. In component form, we write

$$h_{\mu\nu} = g_{\mu\nu} + n_\mu\, n_\nu. \tag{3.29}$$

Similarly, one could use $\vec{\boldsymbol{h}}^{\,*}$ to extend the extrinsic curvature to a bilinear form on $\mathcal{M}$ which is *a priori* defined as a bilinear form on Σ:

$$\boldsymbol{\mathcal{K}} := \vec{\boldsymbol{h}}^{\,*}\boldsymbol{\mathcal{K}}. \tag{3.30}$$

This process need not be restricted to bilinear forms of course, and can be extended to all tensors on $\mathcal{M}$. In addition to extending all 3-dimensional tensors to 4-dimensional tensors, we may use the orthogonal projection operation, $\vec{\boldsymbol{h}}$, to project all tensors on $\mathcal{M}$ "down to" Σ (or up from Σ to $\mathcal{M}$). In particular, this also applies to covariant derivative of a tensor. Given the covariant derivative of a tensor, $\boldsymbol{DT}$ on Σ, we can extend this to $\mathcal{M}$:

$$\boldsymbol{DT} = \vec{\boldsymbol{h}}^{\,*}\boldsymbol{\nabla T}, \tag{3.31}$$

or in component form,

$$D_\rho\, T^{\alpha_1\ldots\alpha_k}{}_{\beta_1\ldots\beta_l} = h^{\alpha_1}{}_{\mu_1}\ldots h^{\alpha_k}{}_{\mu_k} h^{\nu_1}{}_{\beta_1}\ldots h^{\nu_l}{}_{\beta_l}\, h^{\sigma}{}_{\rho}\, \nabla_\sigma T^{\mu_1\ldots\mu_k}{}_{\nu_1\ldots\nu_l}. \tag{3.32}$$

This idea will be of great use when trying to derive the 3-dimensional Riemann tensor from the definition of the 4-dimensional one.

3.1.5 The Relationship Between $\boldsymbol{\mathcal{K}}$ and $\boldsymbol{\nabla n}$

Recall that the unit normal vector, $\boldsymbol{n}$ has the property, $\boldsymbol{n}\cdot\boldsymbol{n} = -1$. Therefore, it would be reasonable to interpret it as a 4–velocity of some observer. We would, therefore, also have a 4-acceleration given by[12]

$$\boldsymbol{a} \equiv \boldsymbol{\nabla}_{\boldsymbol{n}}\, \boldsymbol{n}. \tag{3.33}$$

Using this information and the original definition of $\boldsymbol{\mathcal{K}}$ we may compute an explicit calculation for the extrinsic curvature:

$$\begin{aligned}
\boldsymbol{\mathcal{K}}(\boldsymbol{u},\boldsymbol{v}) &= \boldsymbol{\mathcal{K}}(\vec{\boldsymbol{h}}(\boldsymbol{u}),\vec{\boldsymbol{h}}(\boldsymbol{v})) \\
&= -\vec{\boldsymbol{h}}(\boldsymbol{u})\cdot\boldsymbol{\nabla}_{\vec{\boldsymbol{h}}(\boldsymbol{v})}\,\boldsymbol{n} \\
&= -(\,\boldsymbol{u} + (\,\boldsymbol{u}\cdot\boldsymbol{n})\,\boldsymbol{n}\,)\cdot(\boldsymbol{\nabla}_{\boldsymbol{v}}\,\boldsymbol{n} + (\boldsymbol{v}\cdot\boldsymbol{n})\,\boldsymbol{\nabla}_{\boldsymbol{n}}\,\boldsymbol{n}\,) \\
&= \boldsymbol{\nabla}\underline{\boldsymbol{n}}\,(\,\boldsymbol{u},\boldsymbol{v}\,) - \langle\,\boldsymbol{v},\underline{\boldsymbol{n}}\,\rangle\,\langle\,\boldsymbol{u},\underline{\boldsymbol{a}}\,\rangle.
\end{aligned} \tag{3.34}$$

[10] Put simply, we can use the same symbol as the induced metric as it is exactly the same as the induced metric when restricted to only acting on tangent vectors of Σ.

[11] $\vec{\boldsymbol{h}}$ can be thought of as the "extended" induced metric, $\boldsymbol{h}$ with the first index raised by the metric, $\boldsymbol{g}$.

[12] Note that $\boldsymbol{a} \in \mathcal{T}_p\,(\Sigma)$ since $\boldsymbol{n}\cdot\boldsymbol{a} = 0$.

Since this is true for any pair of vectors in $\mathcal{T}_p(\mathcal{M})$, we may conclude[13]

$$\boldsymbol{\nabla}\,\underline{\boldsymbol{n}} = -\boldsymbol{\mathcal{K}} - \underline{\boldsymbol{a}} \otimes \underline{\boldsymbol{n}}, \tag{3.35}$$

or in component form[14],

$$\nabla_\mu\, n_\nu = -\mathcal{K}_{\mu\nu} - a_\mu\, n_\nu. \tag{3.36}$$

If one takes the trace (with respect to $\boldsymbol{g}$) of the (3.35) we find the scalar extrinsic curvature to be

$$\mathcal{K} = -\nabla_\mu n^\mu. \tag{3.37}$$

3.2 Geometry of Foliations

In the previous section we introduced a hypersurface, Σ embedded in a spacetime, $(\mathcal{M}, \boldsymbol{g})$. We shall now consider a continuous set of such hypersurfaces, $(\Sigma_t)_{\,t\in\mathbb{R}}$. The entire set forms a cover for the entire manifold, $\mathcal{M}$. Such a foliation requires that $\mathcal{M}$ is globally hyperbolic. With this restriction, the results of this section apply generally, and in particular do not assume the Einstein equations.

3.2.1 Definition of a Foliation

Any spacetime $(\mathcal{M}, \boldsymbol{g})$ that is globally hyperbolic can be *foliated* by a family of spacelike hypersurfaces, Σ_t. We define a foliation or slicing by supposing there exists a scalar field, $\tilde{t}$ on $\mathcal{M}$ (which has non vanishing gradient), such that each hypersurface is a level surface of $\tilde{t}$.

$$\forall t \in \mathbb{R}, \quad \Sigma_t := \{p \in \mathcal{M},\, \tilde{t}(p) = t\}. \tag{3.38}$$

This is very similar to how we defined our chosen hypersurface in the previous section. Since the gradient of $\tilde{t}$ does not vanish, the Σ_t are non-intersecting:

$$\Sigma_t \cap \Sigma_{t'} = \varnothing \quad \text{for} \quad t \neq t'. \tag{3.39}$$

Each hypersurface, Σ_t is called a *slice* of the *foliation*. We will assume that hypersurfaces to be spacelike and thus the foliation covers $\mathcal{M}$:

$$\mathcal{M} = \bigcup_{t\,\in\,\mathbb{R}} \Sigma_t. \tag{3.40}$$

[13] We have made a sign choice here to be consistent with Gourgoulhon [165]. This sign choice differs from Carroll [64] for instance. This sign choice, however, will remain consistent in the derivations and does not change the final results, nor does it impact anything in Chapter 5.

[14] An alternative form of this equation is given by explicitly considering the acceleration for an Eulerian observer. One can show that $a_\mu = D_\mu \ln N$, and thus, we have

$$\nabla_\mu n_\nu = -\mathcal{K}_{\mu\nu} - (D_\mu \ln N)\, n_\nu$$

3.2.2 Foliation Kinematics

The kinematics of a foliation are determined by the 3-dimensional slices, Σ_t, the infinitesimal neighbouring slice, Σ_{t+dt} and the 4-dimensional space that fills the space between the slices. Misner, Thorne, and Wheeler, [168] and Alcubierre [169] discuss physical notions that are required to give the chosen foliation structure a sense of "rigidity". The physical notions are:

- A notion of how to measure proper distances given by the metric, h_{ij}.
- The *lapse* function which defines a notion of proper time between slices.
- The relative velocity of observers travelling normal to the slices (Eulerian observers) and the worldlines corresponding to constant spatial coordinates. This is given by the shift vector, $\boldsymbol{\beta}$.

Note that we use terms such as "velocity" and "observer". However, we do not need these notions to interpret the results in this section, even though this is their physical motivation.

Eulerian Observers

The idea of Eulerian observers is fundamental to the $3+1$ splitting of spacetime. We can regard $\boldsymbol{n}$ as the 4–velocity an Eulerian observer. The worldlines of Eulerian observers are obviously orthogonal to the hypersurfaces Σ_t. One may physically interpret this as meaning that the spacelike hypersurface, Σ_t, is *locally* is the surface of simultaneity of the Eulerian observers.

Lapse Function

Recall that the normal vector to Σ_t, $\boldsymbol{n}$, which is timelike and future-directed must be collinear to the vector $\vec{\boldsymbol{\nabla}} t$. Hence we will write

$$\boldsymbol{n} := -N\, \vec{\boldsymbol{\nabla}} t, \tag{3.41}$$

with

$$N := \left(\frac{-1}{\vec{\boldsymbol{\nabla}} t \cdot \vec{\boldsymbol{\nabla}} t} \right)^{1/2}. \tag{3.42}$$

The minus sign here is chosen so that $\boldsymbol{n}$ is future-oriented. Furthermore, the value of N ensures that $\boldsymbol{n}$ is a timelike unit vector with norm -1. The scalar field N is the *lapse function*, coined by Wheeler in 1964 [170]. By construction we also have $N > 0$, i.e., the lapse function never vanishes for a 'regular' foliation, or equivalently,

$$\underline{\boldsymbol{n}} = -N\, \mathbf{d}t. \tag{3.43}$$

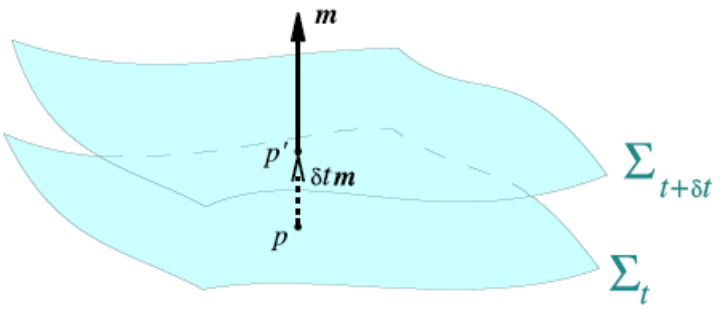

Figure 3.2: Diagram of a point in Σ_t and $\Sigma_{t+\delta t}$ from [165]. The hypersurface Σ_t evolves into $\Sigma_{t+\delta t}$ by the Lie derivative along $\boldsymbol{m}$. The point $p' \in \Sigma_{t+\delta t}$ is determined by $p \in \Sigma$ by the change in $\boldsymbol{m}$ over some time, δt i.e., by a displacement $\boldsymbol{m}\,\delta t$. The length of this displacement is the change in proper time, $\delta\tau$, for an Eulerian observer following the worldline connecting p and p'.

To properly understand the physical interpretation of the lapse function, let us introduce the normal evolution vector:

$$\boldsymbol{m} := N\boldsymbol{n}, \tag{3.44}$$

i.e., it has the properties

$$\boldsymbol{m}\cdot\boldsymbol{m} = -N^2 \quad \text{and} \quad \boldsymbol{\nabla}_{\boldsymbol{m}}\, t = m^\mu\, \nabla_\mu\, t = 1. \tag{3.45}$$

A consequence of this last property is that the hypersurface $\Sigma_{t+\delta t}$ can be obtained from the previous hypersurface, Σ_t by the 'small displacement' $\boldsymbol{m}\,\delta t$. In particular, one can show if p corresponds to a point with the coordinate position, $\boldsymbol{x}$, then

$$t(p') = t(\boldsymbol{x} + \boldsymbol{m}\,\delta t) = t(p) + \delta t\,. \tag{3.46}$$

'The last equality shows $p' \in \Sigma_{t+\delta t}$. Hence we say the vector $\boldsymbol{m}\,\delta t$ 'carries Σ_t into $\Sigma_{t+\delta t}$'. This notion is perfectly described by the *Lie derivative*[15] as the Lie derivative is associated directly with generating diffeomorphisms between manifolds (in this case, hypersurfaces). We describe the action of the Lie derivative of the curves and tangent vectors of Σ_t along $\boldsymbol{m}$ as 'evolving the hypersurface along the normal direction'. This justifies the name "normal evolution vector"[16].

Finally, to understand the role of the lapse function better, let us consider two events on a worldline of some Eulerian observer. Let t be the time coordinate of the event $p \in \Sigma_t$ and $t + \delta t$ the 'time' of $p' \in \Sigma_t$ (refer to Figure 3.2

[15] For an understanding of why the Lie derivative is natural for describing this scenario, the reader may refer to Appendix B of [64].

[16] Interestingly, if we consider the evolution of the 3-metric, $\boldsymbol{h}$, by taking the Lie derivative along $\boldsymbol{m}$ we find:

$$\mathcal{L}_{\boldsymbol{m}} h_{\mu\nu} = -2N\mathcal{K}_{\mu\nu}.$$

This relationship means that the extrinsic curvature can also be thought of as a measure of how the induced metric evolves in time.

for an illustration). We note that the proper time between these two events, $\delta\tau$ (measured by the Eulerian observer) is given by the metric length of the timelike vector linking these two events:

$$\begin{aligned}\delta\tau &= \sqrt{-\boldsymbol{g}(\boldsymbol{m},\boldsymbol{m})}\,\delta t \\ &= N\,\delta t.\end{aligned} \tag{3.47}$$

This justifies the name "lapse fucntion" given to N. N relates the time coordinate which labels the slices of the foliation to the physical time, τ measured by an Eulerian observer. Without the notion of observers, the lapse function is said to determine how far consecutive slices are from each other in the slice-orthogonal time direction at each point.

Shift Vector

To define a shift vector, $\boldsymbol{\beta}$, we require the notion of coordinates on our spacetime manifold. We introduce the natural basis, $\boldsymbol{\partial}_\mu = (\boldsymbol{\partial}_t, \boldsymbol{\partial}_i)$ of $\mathcal{T}_p(\mathcal{M})$ associated with the coordinates, x^μ. The vector which we usually refer to as the 'time vector', $\boldsymbol{\partial}_t$, has the same properties as[17] $\boldsymbol{m}$. In particular, the tangent vectors on $\mathcal{T}_p(\Sigma_t)$ can evolve along either $\boldsymbol{\partial}_t$ or $\boldsymbol{m}$ and the difference is given by a *shift* in reference coordinates. The two vectors only coincide if the spatial coordinates x^i are such that the x^i = constant lines are orthogonal to Σ_t. The difference between $\boldsymbol{\partial}_t$ and $\boldsymbol{m}$ is was also coined the *shift vector* by Wheeler in 1964 [170] and is denoted by β:

$$\boldsymbol{\beta} := \boldsymbol{\partial}_t - \boldsymbol{m} = \boldsymbol{\partial}_t - N\boldsymbol{n}. \tag{3.48}$$

For an illustration of this difference, one may refer to Figure 3.3. Note that the shift vector is tangent to the hypersurface as $\boldsymbol{n}\cdot\boldsymbol{\beta} = 0$. One can think of the shift vector as generating spatial diffeomorphisms relating points between successive slices [3].

3.3 3+1 Splitting of the Metric

The components of the metric tensor, $\boldsymbol{g}$, on $\mathcal{M}$ with respect to the coordinates x^μ are defined as

$$\boldsymbol{g} = g_{\mu\nu}\,\mathbf{d}x^\mu \otimes \mathbf{d}x^\nu. \tag{3.49}$$

We can therefore compute each component by using

$$g_{\mu\nu} = \boldsymbol{g}(\boldsymbol{\partial}_\mu, \boldsymbol{\partial}_\nu). \tag{3.50}$$

Using (3.48) we find

$$g_{00} = \boldsymbol{g}(\boldsymbol{\partial}_t, \boldsymbol{\partial}_t) = \boldsymbol{\partial}_t \cdot \boldsymbol{\partial}_t = -N^2 + \beta_i\,\beta^i. \tag{3.51}$$

[17] This is because $\langle\, \mathbf{d}t, \boldsymbol{\partial}_t \,\rangle = 1$ which was also the case for $\boldsymbol{m}$.

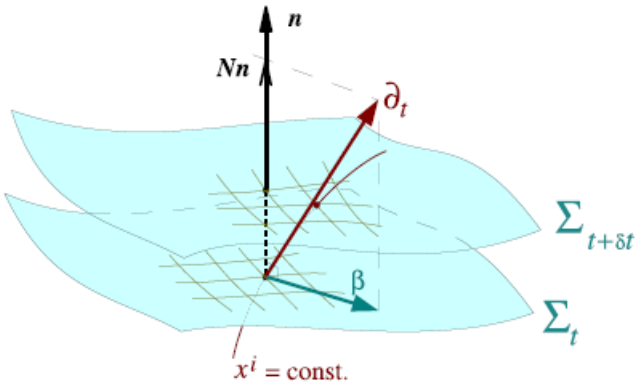

Figure 3.3: Illustration of the shift vector, $\boldsymbol{\beta}$ from [165]. The coordinates (x^i) on Σ_t define the 'time vector', $\boldsymbol{\partial}_t$ by the x^i = constant lines. The shift vector is the difference between the time vector and $\boldsymbol{m}$, therefore, the difference between the spacetime coordinates x^α, and the x^i = constant lines.

Note that we have used only Latin indices for the scalar product of the shift vector as it is tangent to the constant time hypersurfaces, meaning there is no time component. Similarly we have

$$g_{0i} = (\boldsymbol{m} + \boldsymbol{\beta}) \cdot \partial_i = \beta_i, \tag{3.52}$$

since $\boldsymbol{m} \cdot \boldsymbol{\partial}_i = 0$ by definition. Finally, the spatial part of the metric must be the induced metric,

$$g_{ij} = h_{ij}. \tag{3.53}$$

Collecting all of these components together we have

$$g_{\mu\nu} = \begin{pmatrix} -N^2 + \beta_k \beta^k & \beta_j \\ \beta_i & h_{ij} \end{pmatrix} \tag{3.54}$$

or,

$$\mathrm{d}s^2 = g_{\mu\nu}\, \mathrm{d}x^\mu\, \mathrm{d}x^\nu = -N^2\, \mathrm{d}t^2 + h_{ij}\, (\mathrm{d}x^i + \beta^i \mathrm{d}t)(\mathrm{d}x^j + \beta^j \mathrm{d}t). \tag{3.55}$$

The inverse metric in matrix form is[18]

$$g^{\mu\nu} = \frac{1}{N^2} \begin{pmatrix} -1 & \beta^j \\ \beta^i & N^2 h^{ij} - \beta^i \beta^j \end{pmatrix}. \tag{3.56}$$

3.4 3+1 Decomposition of the Einstein Equations

In the numerical relativity literature, the $3 + 1$ Einstein equations are often referred to as the "ADM equations" named after Arnowitt, Deser, and Misner

[18] One may notice that while $g_{ij} = h_{ij}$, $g^{ij} \neq h^{ij}$ in general. They are, however, equal in the case of vanishing shift.

[161]. For this reason, the splitting of spacetime we have discussed is often referred to as the "ADM gauge". The major contribution from ADM, however, was the Hamiltonian formulation of general relativity. Moreover, as stressed by York [171], the dynamical equations in the work of ADM involve projections of the Einstein tensor. Therefore, ADM use the Einstein equations in the form given by (2.5), whereas, other dynamical equations used — before ADM — involved the Einstein equation in the form (2.43).

Thus far we have only been interested in how the geometry of spacetime can be split into hypersurfaces, Σ_t that are 'foliated' along level surfaces of a of scalar field which we relate to some notion of time. We have also discussed how quantities that live on the tangent (and cotangent) planes of Σ_t and $\mathcal{M}$ can be related. We will now discuss the Einstein equations and how these can be decomposed in general. We will keep this decomposition general and will not discuss cosmological ideas until Chapter 5.

3.4.1 Gauss–Codazzi Equations

The first part of the Einstein equations we investigate is the Riemann tensor. We discussed the fact the Riemann tensor, Ricci tensor and Ricci scalar are intrinsic properties of a manifold and are inherently related to the notion of gravity. When using the $3+1$ formalism it is often useful to know the intrinsic curvature of the embedded hypersurface and understand its evolution.

Gauss' Equation

Let us consider the 3-dimensional Ricci identity (3.15). The 4-dimensional version of this is is

$$(D_\mu D_\nu - D_\nu D_\mu)\, v^\gamma = R^\gamma{}_{\kappa\mu\nu}\, v^\kappa. \tag{3.57}$$

This can be rewritten in terms of the ordinary 4-dimensional covariant derivative by using (3.32). We first write

$$D_\mu D_\nu v^\gamma = D_\mu(D_\nu v^\gamma) = h^\alpha{}_\mu\, h^\beta{}_\nu\, h^\gamma{}_\rho\, \nabla_\alpha (D_\beta v^\rho), \tag{3.58}$$

using (3.32) again, we obtain

$$D_\mu D_\nu v^\gamma = D_\mu(D_\nu v^\gamma) = h^\alpha{}_\mu\, h^\beta{}_\nu\, h^\gamma{}_\rho\, \nabla_\alpha (h^\sigma{}_\beta\, h^\rho{}_\lambda\, \nabla_\sigma v^\lambda). \tag{3.59}$$

By using $\nabla_\mu h^\sigma{}_\rho = \nabla_\mu (\delta^\sigma{}_\rho + n^\sigma n_\rho) = n_\rho \nabla_\mu n^\sigma + n^\sigma \nabla_\mu n_\rho$ and the fact that $h^\mu{}_\nu\, n_\mu = 0$ we find

$$D_\mu D_\nu v^\gamma = -\mathcal{K}_{\mu\nu}\, h^\gamma{}_\lambda\, n^\sigma \nabla_\sigma v^\lambda - \mathcal{K}^\gamma{}_\mu\, \mathcal{K}_{\nu\lambda}\, v^\lambda + h^\alpha{}_\mu\, h^\sigma{}_\nu\, h^\gamma{}_\lambda \nabla_\alpha \nabla_\sigma v^\lambda. \tag{3.60}$$

Swapping the indices on the 3-dimensional covariant derivatives and the corresponding ones on the right-hand side, we can rewrite (3.57) as

$$\begin{aligned}(D_\mu D_\nu - D_\nu D_\mu) v^\gamma = &(\mathcal{K}^\gamma{}_\nu \mathcal{K}_{\mu\lambda} - \mathcal{K}^\gamma{}_\mu \mathcal{K}_{\nu\lambda}) v^\lambda \\ &+ h^\alpha{}_\mu h^\sigma{}_\nu h^\gamma{}_\lambda \quad (\nabla_\alpha \nabla_\sigma - \nabla_\sigma \nabla_\alpha) v^\lambda.\end{aligned} \tag{3.61}$$

This can be simplified to[19]

$$h^\alpha{}_\mu h^\beta{}_\nu h^\gamma{}_\rho h^\sigma{}_\lambda R^\rho{}_{\sigma\alpha\beta} = \mathcal{R}^\gamma{}_{\lambda\mu\nu} + \mathcal{K}^\gamma{}_\mu \mathcal{K}_{\lambda\nu} - \mathcal{K}^\gamma{}_\nu \mathcal{K}_{\mu\lambda}, \tag{3.62}$$

which is Gauss' equation.

If we further contract on γ and μ and use $h^\mu{}_\alpha h^\alpha{}_\rho = \delta^\mu{}_\rho + n^\mu n_\rho$ then take the trace with respect to the induced metric we obtain the scalar Gauss equation

$$\mathcal{R} = R + 2 R_{\mu\nu} n^\mu n^\nu + \mathcal{K}^2 - \mathcal{K}_{ij} \mathcal{K}^{ij}, \tag{3.63}$$

where $\mathcal{K} = \mathcal{K}^\mu{}_\mu$ and $\mathcal{K}^{ij} \mathcal{K}_{ij} = \mathcal{K}^{\mu\nu} \mathcal{K}_{\mu\nu}$.

Codazzi Equation

The Codazzi equation can be manipulated into the momentum constraint equation and is just another decomposition of the Riemann tensor. We begin by contracting the Riemann tensor with the normal vector:

$$R^\gamma{}_{\mu\alpha\beta} n^\mu = (\nabla_\alpha \nabla_\beta - \nabla_\beta \nabla_\alpha) n^\gamma, \tag{3.64}$$

using the projection tensor to project the tensor quantities onto Σ_t we find,

$$h^\mu{}_\alpha h^\nu{}_\beta h^\gamma{}_\rho R^\rho{}_{\sigma\mu\nu} n^\nu = h^\mu{}_\alpha h^\nu{}_\beta h^\gamma{}_\rho (\nabla_\mu \nabla_\nu - \nabla_\nu \nabla_\mu) n^\mu \tag{3.65}$$

By using relations we used to derive Gauss' equation one can obtain the Codazzi equation,

$$h^\gamma{}_\rho n^\sigma h^\mu{}_\alpha h^\nu{}_\beta R^\rho{}_{\sigma\mu\nu} = D_\beta \mathcal{K}^\gamma{}_\alpha - D_\alpha \mathcal{K}^\gamma{}_\beta. \tag{3.66}$$

Contracting on γ and α we obtain the contracted Codazzi equation,

$$h^\gamma{}_\alpha n^\nu R_{\mu\nu} = D_\alpha \mathcal{K} - D_\mu \mathcal{K}^\mu{}_\alpha. \tag{3.67}$$

Last non-trivial projection of Riemann Tensor

Thus far we have found Gauss' equation which is a full projection of the Riemann tensor and the Codazzi equation by projecting three times with $\boldsymbol{h}$ and once along $\boldsymbol{n}$. Unlike these two projections which involve $\boldsymbol{h}$, $\boldsymbol{\mathcal{K}}$, $\mathcal{R}$, and $\boldsymbol{D}\,\boldsymbol{\mathcal{K}}$ the

[19]Note that usually the normal vector dual is of the form $n_\mu = (-N, 0, 0, 0)$ and therefore for computational purposes it can often be useful to use $R^{\mu\nu} n_\mu n_\nu$, allowing us to deal with only one term, $N^2 R^{00}$. This fact in general should also be used for the extrinsic curvature, reducing the computation time.

final projection will also involve derivatives normal to the hypersurfaces and not only on the tangent planes. This is important as we then have a notion of a dynamical equation — one the evolves in 'time'.

We begin with

$$h_{\alpha\mu}\, n^{\sigma} h^{\nu}{}_{\beta}\, (\nabla_{\nu}\nabla_{\sigma} - \nabla_{\sigma}\nabla_{\nu})\, n^{\mu} = h_{\alpha\mu}\, n^{\sigma} h^{\nu}{}_{\beta}\, R^{\mu}{}_{\rho\nu\sigma}\, n^{\rho}, \tag{3.68}$$

by use of[20] $\mathcal{K}^{\mu}{}_{\sigma} n^{\sigma} = 0$, $n^{\sigma}\nabla_{\nu}\, n_{\sigma} = 0$, $a_{\nu} = D_{\nu} \ln N$, and $h^{\nu}{}_{\beta} n_{\nu} = 0$ we find

$$h_{\alpha\mu} n^{\sigma} h^{\nu}{}_{\beta}\, R^{\mu}{}_{\rho\nu\sigma}\, n^{\rho} = -\mathcal{K}_{\alpha\sigma}\mathcal{K}^{\sigma}{}_{\beta} + h^{\mu}{}_{\alpha}\, h^{\nu}{}_{\beta}\, n^{\sigma}\, \nabla_{\sigma}\mathcal{K}_{\mu\nu} + D_{\beta}D_{\alpha} \ln N + D_{\alpha} \ln N D_{\beta} \ln N.$$

By use of the chain rule, we find

$$h_{\alpha\mu} n^{\sigma} h^{\nu}{}_{\beta}\, R^{\mu}{}_{\rho\nu\sigma}\, n^{\rho} = -\mathcal{K}_{\alpha\sigma}\mathcal{K}^{\sigma}{}_{\beta} + h^{\mu}{}_{\alpha}\, h^{\nu}{}_{\beta}\, n^{\sigma}\, \nabla_{\sigma}\mathcal{K}_{\mu\nu} + \frac{1}{N} D_{\beta}D_{\alpha}N. \tag{3.69}$$

Finally, we can relate $h^{\mu}{}_{\alpha}\, h^{\nu}{}_{\beta}\, n^{\sigma}\, \nabla_{\sigma}\mathcal{K}_{\mu\nu}$ to $\boldsymbol{\mathcal{L}_{m}}$. First, let us recall what this Lie derivative expands to

$$\mathcal{L}_{\boldsymbol{m}}\mathcal{K}_{\alpha\beta} = m^{\mu}\, \nabla_{\mu}\mathcal{K}_{\alpha\beta} + \mathcal{K}_{\mu\beta}\nabla_{\alpha}\, m^{\mu} + \mathcal{K}_{\alpha\mu}\nabla_{\beta}\, m^{\mu}. \tag{3.70}$$

Projecting this down onto Σ_t and by use of $\nabla_{\mu} m_{\nu} = \nabla_{\mu}(N n_{\nu})$ we find

$$\mathcal{L}_{\boldsymbol{m}}\mathcal{K}_{\alpha\beta} = N\, h^{\mu}{}_{\alpha}\, h^{\nu}{}_{\beta} n^{\sigma}\, \nabla_{\sigma}\, \mathcal{K}_{\mu\nu} - 2N\mathcal{K}_{\alpha\mu}\, \mathcal{K}^{\mu}{}_{\beta}. \tag{3.71}$$

Therefore, we can write our original decomposition as

$$h_{\alpha\mu} n^{\sigma} h^{\nu}{}_{\beta}\, R^{\mu}{}_{\rho\nu\sigma}\, n^{\rho} = \frac{1}{N}\mathcal{L}_{\boldsymbol{m}}\mathcal{K}_{\alpha\beta} + \frac{1}{N} D_{\alpha}D_{\beta}\, N + \mathcal{K}_{\alpha\mu}\mathcal{K}^{\mu}{}_{\beta}. \tag{3.72}$$

One can further use Gauss' equation to rewrite the above expression in terms of the spacetime Ricci tensor instead of the Riemann tensor, which is useful for the Einstein equations:

$$h^{\mu}{}_{\alpha}\, h^{\nu}{}_{\beta} R_{\mu\nu} = -\frac{1}{N}\mathcal{L}_{\boldsymbol{m}}\mathcal{K}_{\alpha\beta} - \frac{1}{N} D_{\alpha}D_{\beta}\, N + \mathcal{R}_{\alpha\beta} + \mathcal{K}\mathcal{K}_{\alpha\beta} - 2\,\mathcal{K}_{\alpha\mu}\mathcal{K}^{\mu}{}_{\beta}. \tag{3.73}$$

3.4.2 3+1 Decomposition of the Stress-Energy Tensor

In addition to a $3+1$ split of the geometric objects, it is natural to decompose tensors such as the stress-energy tensor, especially when discussing the Einstein equations. It does not make sense to discuss a stress-energy tensor without a source for this stress-energy. We can, therefore, think of a fluid as we do in cosmology, though we will not discuss general fluid variables until Chapter 5

[20] We have not derived the particular equality of a_{ν} here. One may, however find this derivation in many texts such as Gourgoulhon [165] (equation 3.17).

The $(0,0)$ component of the stress-energy tensor is defined to be the matter energy density measured by an Eulerian observer (i.e., in the normal frames). We write this in a 3+1 decomposition as

$$E := \boldsymbol{T}(\boldsymbol{n}, \boldsymbol{n}), \tag{3.74}$$

or in component form,

$$E = T_{\mu\nu}\, n^{\mu} n^{\nu}. \tag{3.75}$$

This follows from the fact that $\boldsymbol{n}$ is the 4-velocity for an Eulerian observer. Furthermore, if we write this equation as $T^{\mu\nu} n_{\mu} n_{\nu}$ then one can clearly see that $E = N^2\, T^{00}$.

Similarly, from the definition of the stress-energy tensor we also have the matter momentum density given by the $(0,i)$ components. In a $3+1$ split we write this as

$$\boldsymbol{J} := -\boldsymbol{T}(\boldsymbol{n}, \vec{\boldsymbol{h}}(.)), \tag{3.76}$$

and in component form we can write

$$J_{\alpha} = -T_{\mu\nu}\, n^{\mu} h^{\nu}{}_{\alpha}, \tag{3.77}$$

Note due to the projector, $\vec{\boldsymbol{h}}$, we find $\boldsymbol{J}$ is tangent to Σ_t.

Finally, the spatial components of the stress-energy tensor correspond to the matter stress tensor measured by an Eulerian observer. We express this as

$$\boldsymbol{S} := \vec{\boldsymbol{h}}^{*}\, \boldsymbol{T}, \tag{3.78}$$

and in component form:

$$S_{\alpha\beta} = T_{\mu\nu}\, h^{\mu}{}_{\alpha}\, h^{\nu}{}_{\beta}. \tag{3.79}$$

Just as was the case for the momentum, (3.76), $\boldsymbol{S}$ is a tensor field tangent to Σ_t. The trace of the stress tensor is

$$S := h^{ij} S_{ij} = g^{\mu\nu} S_{\mu\nu}. \tag{3.80}$$

With the parts of the stress-energy tensor we can reconstruct the tensor in the following way:

$$\boldsymbol{T} = \boldsymbol{S} + \underline{\boldsymbol{n}} \otimes \boldsymbol{J} + \boldsymbol{J} \otimes \underline{\boldsymbol{n}} + E\, \underline{\boldsymbol{n}} \otimes \underline{\boldsymbol{n}}. \tag{3.81}$$

We can take the trace of this equation with respect to $\boldsymbol{g}$ and find

$$\begin{aligned} T &= S + 2\,\langle \boldsymbol{p}, \boldsymbol{n} \rangle + E\,\langle \underline{\boldsymbol{n}}, \boldsymbol{n} \rangle \\ &= S - E, \end{aligned} \tag{3.82}$$

which follows from the fact that $\boldsymbol{p}$ and $\boldsymbol{n}$ are orthogonal.

3.4.3 Projection of the Einstein Equations and Dynamical Equations

With the various projections of the Riemann tensor and stress-energy tensor, we can project the Einstein equations onto Σ_t. There are three possibilities for projections and a fourth equation which is not a projection of the Einstein equations but rather a dynamical equation.

(1) Full projection onto Σ_t

A full projection implies that we apply the operator $\vec{\boldsymbol{h}}^*$ to the Einstein equations. In particular we will use the Einstein equations in the form (2.43):

$$\vec{\boldsymbol{h}}^* \boldsymbol{R} = 8\pi G \left(\vec{\boldsymbol{h}}^* \boldsymbol{T} - \frac{1}{2} T \vec{\boldsymbol{h}}^* \boldsymbol{g} \right). \tag{3.83}$$

The left-hand side of this is given by (3.73). For the right-hand side, by definition we have $\vec{\boldsymbol{h}}^* \boldsymbol{T} = \boldsymbol{S}$ and $T = S - E$ from (3.82). Therefore, we find the first dynamical equation to be

$$\mathcal{L}_{\boldsymbol{m}} \mathcal{K}_{\alpha\beta} = -D_\alpha D_\beta N + N \Big(\mathcal{R}_{\alpha\beta} + \mathcal{K}\mathcal{K}_{\alpha\beta} - 2\,\mathcal{K}_{\alpha\mu}\mathcal{K}^{\mu}{}_{\beta} + 4\pi G[\,(S-E)h_{\alpha\beta} - 2\,S_{\alpha\beta}\,] \Big). \tag{3.84}$$

Note that a fundamental property of the Lie derivative along $\boldsymbol{m}$ is that it is a map $\mathcal{T}^n(\Sigma_t) \longrightarrow \mathcal{T}^n(\Sigma_t)$. Furthermore, we know the quantities on the right-hand side to be tangent to Σ_t from previous discussions. Therefore, we can write (3.84) as

$$\mathcal{L}_{\boldsymbol{m}} \mathcal{K}_{ij} = -D_i D_j N + N \Big(\mathcal{R}_{ij} + \mathcal{K}\mathcal{K}_{ij} - 2\,\mathcal{K}_{ik}\mathcal{K}^{k}{}_{j} + 4\pi G[\,(S-E)\,h_{ij} - 2\,S_{ij}\,] \Big), \tag{3.85}$$

without loss of generality[21].

Note that we do not include the general case where the shift vector is non-zero. In fact, we can rewrite the left-hand side of this equation as we have $\boldsymbol{m} = \boldsymbol{\partial_t} - \boldsymbol{\beta}$. Because the Lie derivative is linear by definition we have

$$\left(\frac{\partial}{\partial t} - \mathcal{L}_{\boldsymbol{\beta}} \right) \mathcal{K}_{ij} = -D_i D_j N + N \Big(\mathcal{R}_{ij} + \mathcal{K}\mathcal{K}_{ij} - 2\,\mathcal{K}_{ik}\mathcal{K}^{k}{}_{j} + 4\pi G\,[\,(S-E)h_{ij} - 2\,S_{ij}\,] \Big). \tag{3.86}$$

[21] A cosmological constant can be included on the right-hand side of the (3.86). This is done by adding $-N\Lambda\, h_{ij}$.

(2) Full Projection Perpendicular to Σ_t

This projection amounts to contracting the Einstein equations in the form (2.5) with the normal vector. Since $\boldsymbol{g(n,n)} = -1$ we have

$$\boldsymbol{R(n,n)} + \frac{1}{4}R = 8\pi G\, \boldsymbol{T(n,n)}. \tag{3.87}$$

By use of the scalar Gauss equation (3.63) and $\boldsymbol{T(n,n)} = E$ we obtain[22]

$$\mathcal{R} + \mathcal{K}^2 - \mathcal{K}_{ij}\mathcal{K}^{ij} = 16\pi G\, E. \tag{3.88}$$

This equation is known as the *Hamiltonian constraint*.

(3) Mixed Projection

We project the Einstein equations in the form (2.5) once onto Σ_t and once along the normal vector:

$$\boldsymbol{R(n,\vec{h}(.))} - \frac{1}{2}R\, \boldsymbol{g(n,\vec{h}(.))} = 8\pi G\, \boldsymbol{T(n,\vec{h}(.))}. \tag{3.89}$$

Using the contracted Codazzi equation and the momentum projection for the stress-energy tensor we obtain

$$D_j\, \mathcal{K}^j{}_i - D_i K = 8\pi G J_i. \tag{3.90}$$

This equation is known as the *momentum constraint*.

(4) Final Dynamical Equation

We wish to have a set of dynamical equations that one can evolve forward in time. It turns out that the final equation that is usually considered is the evolution of the induced metric, $\partial_t h_{ij}$. In a foliation that has vanishing shift vector, we simply have

$$\partial_t\, h_{ij} = -2N\mathcal{K}_{ij}. \tag{3.91}$$

However, in the case that we do not have vanishing shift, we have

$$\partial_t\, h_{ij} = -2N\mathcal{K}_{ij} + D_j\, \beta_i + D_i\, \beta_j \tag{3.92}$$

Dynamics Discussion

4The Cauchy problem in general relativity involves specifying an initial hypersurface, Σ_0, and letting the initial data evolve in time. The initial data we refer to is the induced metric and the extrinsic curvature. We refer to the set of

[22] A cosmological constant can be added to the right-hand side of this equation by adding 2Λ.

equations (3.86) – (3.92) as the Einstein system, and as can be seen equations (3.85) and (3.92) describe the time evolution of the initial data. Equations (3.88) and (3.90) in the Einstein system are, therefore, suitably named the *constraint equations*. This is because we require the initial data, $(\boldsymbol{h}, \boldsymbol{\mathcal{K}})$ to obey the constraint equations as they evolve in time. In fact, because of the contracted Bianchi identity, one can show that the constraints are preserved by the dynamical evolution equations [165].

It should also be noted that the Einstein system does not contain time derivatives of the lapse function, N, nor the shift vector, $\boldsymbol{\beta}$. Consequently, N and $\boldsymbol{\beta}$ are not dynamic variables. This is related to the fact that they are are only associated with the choice of coordinates, (t, x^i). The general covariance of general relativity implies that we are free to choose the lapse and shift freely without changing the physical dynamics. However, an arbitrary choice of lapse and shift can lead to coordinate singularities.

3.5 1+3 formalism

In this section we will discuss a timelike congruence of curves that are the basic structure of the $1 + 3$ formalism as opposed to spacelike hypersurfaces of the $3 + 1$ formalism. Most of them formalism developed for the 3+1 splitting remains the same in the 1+3 formalism except, strictly speaking, we project onto *local* hypersurfaces in the neighbourhood of each timelike curve. This is because, in general we will have vorticity, meaning the timelike normals are *not hypersurface forming*.

Instead of considering the normal vector to a given hypersurface, we will consider the 4-velocity which is defined to be a tangent vector field to the timelike congruence. In general our 4-velocity will not be collinear to $\boldsymbol{n}$ — which was the case considered in the 3+1 split we discussed (in fact, in the previous chapter $\boldsymbol{n} = \boldsymbol{u}$). We will follow the 1+3 formalism as introduced by Carroll and Poisson [64, 172], except we will not assume that the timelike congruence is a geodesic congruence. (See Roy [173] for an in depth introduction to the 1+3 formalism.)

As before, we have a metric on the spatial frames that is related to the projection tensor. The projection tensor can be thought of as projecting onto a subspace of $\mathcal{T}_p(\mathcal{M})$ which are 'local hypersurfaces' with $\boldsymbol{u}$ as the normal vector. The induced metric is this case is

$$\boldsymbol{b} = \boldsymbol{g} + \underline{\boldsymbol{u}} \otimes \underline{\boldsymbol{u}}, \tag{3.93}$$

or in coordinate form,

$$b_{\mu\nu} = g_{\mu\nu} + u_\mu u_\nu. \tag{3.94}$$

One can interpret the timelike congruence as defining the trajectory of fluid particles and thus, the collection defines a fluid. With this interpretation, one

can think of the projection tensor as projecting onto the 'fluid rest frames'. In this sense, we can define a form of Gauss' equation (3.62) as well by simply replacing $\boldsymbol{n}$ with $\boldsymbol{u}$. However, one should be careful as in the case of nonzero vorticity there is no global hypersurface, and thus the intrinsic curvature does not hold the same physical intuition.

Furthermore, we can define the expansion of such a fluid. The expansion can be thought of as the neighbouring fluid worldlines *deviating*. Therefore, a natural way to define the expansion is by taking the covariant derivative of the 4-velocity:

$$\Theta_{\mu\nu} := \nabla_\nu u_\mu + u_\mu a_\nu, \tag{3.95}$$

where $a_\mu = u^\alpha \nabla_\alpha u_\mu$. One may observe the similarity between the expression for the expansion tensor and the extrinsic curvature. The two are not the same, however, because $\boldsymbol{u}$ is not necessarily collinear to $\boldsymbol{n}$ — this is usually expressed as "there is a tilt between $\boldsymbol{u}$ and $\boldsymbol{n}$. The idea of 'tilts' will be explored in Chapter 5. In the case that the 4-velocity is collinear, i.e., there is no 'tilt' we have,

$$\Theta_{\mu\nu} = -\mathcal{K}_{\mu\nu}. \tag{3.96}$$

We also define the expansion scalar,

$$\Theta := \nabla_\alpha u^\alpha, \tag{3.97}$$

which describes the change in volume of a sphere centred on one of the timelike worldlines. In the context of a spatially isotropic *and* homogeneous cosmology, we relate the Hubble parameter[23] to the expansion scalar by

$$H = \frac{1}{3}\Theta. \tag{3.98}$$

One can further define the *shear* tensor,

$$\begin{aligned} \sigma_{\mu\nu} &:= b^\alpha{}_\mu b^\beta{}_\nu \nabla_{(\alpha} u_{\beta)} - \frac{1}{3}\Theta\, b_{\mu\nu} \\ &= \nabla_{(\mu} u_{\nu)} + u_{(\mu} a_{\nu)} - \frac{1}{3}\Theta\, b_{\mu\nu}\,, \end{aligned} \tag{3.99}$$

which describes the distortion in the shape of the collection of test particles, from a sphere to an ellipsoid. The symmetric part is taken since the distortion will be the same in (for example) the x-direction and the $-x$-direction. For a geodesic congruence, the acceleration term would vanish. Finally, we define the vorticity tensor,

$$\begin{aligned} \omega_{\mu\nu} &:= b^\alpha{}_\mu b^\beta{}_\nu \nabla_{[\alpha} u_{\beta]} \\ &= \nabla_{[\mu} u_{\nu]} + u_{[\mu} a_{\nu]} \\ &= \partial_{[\mu} u_{\nu]} + u_{[\mu} a_{\nu]}\,, \end{aligned} \tag{3.100}$$

[23] Depending on if the expansion scalar depends on time or not, this could be the Hubble constant or the Hubble parameter. Here we will assume that the expansion scalar is varying.

which can be thought of as describing rotations and is antisymmetric. A fluid with zero vorticity is said to be *irrotational*, in this case $a^\mu = 0$ and the congruence is hypersurface forming

With all of the above decompositions of the expansion tensor, we can rewrite the expansion tensor as

$$\Theta_{\mu\nu} = \frac{1}{3}\Theta\, b_{\mu\nu} + \sigma_{\mu\nu} + \omega_{\mu\nu}. \tag{3.101}$$

The evolution of the expansion of these timelike curves is described by the covariant derivative of the expansion tensor along the path, $D/\mathrm{d}\tau = u^\mu \nabla_\mu$. We compute this for the expansion tensor to find:

$$\begin{aligned}\frac{D\,\Theta_{\mu\nu}}{\mathrm{d}\tau} &= u^\alpha \nabla_\alpha \nabla_\nu u_\mu \\ &= u^\alpha \nabla_\nu \nabla_\alpha u_\mu - u^\alpha R^\rho{}_{\mu\alpha\nu}\, u_\rho \\ &= \nabla_\nu (u^\alpha \nabla_\alpha u_\mu) - (\nabla_\nu u^\alpha)(\nabla_\alpha u_\mu) - R_{\rho\mu\alpha\nu}\, u^\alpha u^\rho \\ &= \nabla_\nu a_\mu - \Theta^\alpha{}_\nu\, \Theta_{\mu\alpha} - R_{\nu\alpha\mu\rho}\, u^\alpha u^\rho.\end{aligned} \tag{3.102}$$

Here we have used the Ricci identity for covectors, the Leibniz rule, and permuted the indices on the Riemann tensor. Note that $a_\mu = u^\alpha \nabla_\alpha u_\mu$ and if the congruence of curves are geodesics this term vanishes. Taking the trace of the above equation with respect to $\boldsymbol{g}$ we find

$$\frac{\mathrm{d}\Theta}{\mathrm{d}\tau} = -\frac{1}{3}\Theta^2 - \sigma_{\mu\nu}\,\sigma^{\mu\nu} + \omega_{\mu\nu}\,\omega^{\mu\nu} - R_{\mu\nu}\,u^\mu u^\nu + \nabla_\mu a^\mu. \tag{3.103}$$

This equation is known as *Raychaudhuri's equation* and is a fundamental result that describes the motion of neighbouring worldlines. Since the shear and vorticity are purely spatial we note that $\omega_{\mu\nu}\,\omega^{\mu\nu} \geq 0$ and $\sigma_{\mu\nu}\,\sigma^{\mu\nu} \geq 0$ with equality only holding if the tensors themselves are zero. There are various parts of Raychaudhuri's equation which can be thought of as promoting or opposing (re)-collapse of the worldlines. Collapse is opposed by nonzero vorticity and a positive divergence of the acceleration. It is promoted by nonzero shearing and a positive trace of the Ricci tensor, which is guaranteed by the strong energy condition.

In the case of an irrotational geodesic congruence Raychaudhuri's equation becomes

$$\frac{\mathrm{d}\Theta}{\mathrm{d}\tau} = -\frac{1}{3}\Theta^2 - \sigma_{\mu\nu}\,\sigma^{\mu\nu} - R_{\mu\nu}\,u^\mu u^\nu.$$

Consider geodesic congruences for matter obeying the timelike convergence condition $R_{\mu\nu}\,u^\mu u^\nu \geq 0$, or equivalently the strong energy condition on the stress-energy tensor, $T_{\mu\nu}\,u^\mu u^\nu \geq -(1/2)T$ (when $\Lambda = 0$). Under such conditions, all of the terms on the right-hand side are strictly positive, we see that if $\Theta < 0$ (i.e., the congruence is converging initially) the congruence will converge more rapidly as time passes. If, on the other hand, $\Theta > 0$ originally (congruence is

expanding) then we find that the congruence expansion will decrease as time passes. This is exactly what one expects from Newtonian gravity — that gravity is an "attractive" force. Conversely, fluids which violate the strong energy condition give rise to the possibility of a repulsive "levity".

Chapter 4

Perturbation Theory

The standard model of cosmology, ΛCDM is constructed on the assumption of the average expansion being that of an ideal spatially isotropic and homogeneous solution of Einstein's equations. The average expansion is observed to be isotropic in some statistical sense when averaged on a "suitably" large scale which we call the statistical scale of homogeneity (SSH). The SSH has been estimated to be around 70–120 h^{-1}Mpc [38] based on the 2–point galaxy correlation function. On scales smaller than this, observations indicate that the Universe is inhomogeneous with a hierarchy of scales ranging from planetesimals to galaxy clusters. The FLRW metric is not a good approximation on the scale of stellar systems or the neighbourhood of supermassive black holes. However, in the standard model it is implicitly assumed that cosmological observations made at any point with weak local gravitational fields can be exactly reduced to those of a FLRW model plus a local Lorentz boost. Once the local boost is removed from our CMB map, we observe temperature fluctuations associated with the density fluctuations which seeded the first structures to grow after recombination.

Understanding the primordial fluctuations/perturbations and how they grew over time to form the observed Universe today is one of the many goals of perturbation theory in cosmology, which was initially developed by Lifshitz [174]. Perturbation theory is an attempt to model a inhomogeneous Universe that is very close to homogeneous, i.e., very close to FLRW. Standard linear perturbation theory assumes a *background* cosmology which is an exact solution to the Einstein equations. In most cases, the background is FLRW, we then use the perturbed Einstein equations to describe how these perturbations evolve.

For an introduction to linear perturbation theory we will assume the background geometry to be FLRW with[1] $k = 0$ and denote this with a bar above the metric tensor, $\bar{g}_{\mu\nu}$ on a background manifold, $\bar{\mathcal{M}}$. We will also use conformal

[1]This is because the CMB suggests that the Universe was close to flat at the epoch of last scattering. Thus, if we wish to model the anisotropies of the CMB, we often perturb about a spatially flat Universe.

time and write the metric as:

$$\bar{g}_{\mu\nu}\mathrm{d}x^{\mu}\mathrm{d}x^{\nu} = a^2(\eta)(-\mathrm{d}\eta^2 + \delta_{ij}\mathrm{d}x^i\mathrm{d}x^j). \tag{4.1}$$

We often refer to the spacetime containing inhomogeneities as the *physical* spacetime or manifold, $\mathcal{M}$. This manifold is different to the background manifold with the metric $g_{\mu\nu}$. The perturbations are, therefore, the difference between the physical and background spacetime, and are defined as:

$$\delta g_{\mu\nu}(x) = g_{\mu\nu}(x) - \bar{g}_{\mu\nu}(x). \tag{4.2}$$

Note that we have specified a spacetime coordinate, x. This is an ill-posed statement because $g_{\mu\nu}$ and $\bar{g}_{\mu\nu}$ are tensors defined on different manifolds, and x is a coordinate defined through a different chart(s). Embedding these two distinct manifolds in one larger manifold would not solve the problem as evaluating the difference between two tensors at distinct points is poorly defined.

Therefore, a mapping which can map points of the background manifold to the physical manifold is required — for this purpose, we define a *gauge* [175–177]. A gauge is a one-to-one correspondence from $\bar{\mathcal{M}} \to \mathcal{M}$ and can be interpreted as a point-identification map which is generally arbitrary. If a coordinate system is introduced on the background manifold, $\bar{\mathcal{M}}$, then the gauge caries it to the physical manifold, $\mathcal{M}$. A change in the map from $\bar{\mathcal{M}} \to \mathcal{M}$, when keeping the background coordinates fixed is known as a gauge transformation. A gauge transformation introduces a coordinate transformation in the physical manifold, along with changes in an event in $\mathcal{M}$ which is associated with an event in $\bar{\mathcal{M}}$. Therefore, gauge transformations are different from coordinate transformations which are only a relabelling of events.

In general, while one can always perturb a given background spacetime, being able to recover a smooth metric from a given perturbed spacetime, however, is not a uniquely defined process. This can be problematic as one can always choose a different background and arrive at different perturbation values. Selecting an unperturbed spacetime from a given perturbed one is known as a *gauge choice*. Determining the best gauge is one version of the fitting problem — one that has no unique answer. The word "gauge", however, is more general and there have been tensions in the community because of these definitions. This, and the gauge problem will be discussed further in section 4.5.

We will now introduce the mechanics of linear perturbation theory and write perturbed Einstein equations. In standard perturbation theory, we have a condition of the form [65, 83, 174]:

$$|\bar{g}_{\mu\nu}| \gg |\delta g_{\mu\nu}| \sim \epsilon, \tag{4.3}$$

meaning, the perturbations are small, (characterised by an order of smallness, ϵ). We refer to such an expansion as a "weak-field" expansion[2]. We neglect

[2]Weak field here refers to expansions in cosmology when a geometry of space-time is close to a known exact solution — usually FLRW.

terms where perturbations are multiplied together, resulting in $\mathcal{O}(\epsilon^2)$ terms. The perturbation to the inverse of a general matrix, A is $\delta A^{-1} = -A^{-1}(\delta A)A^{-1}$. Therefore, the inverse of the metric perturbation is [65] (in a coordinate basis)

$$\delta g^{\mu\nu} = -\bar{g}^{\,\mu\rho}\delta g_{\rho\sigma}\bar{g}^{\,\nu\sigma}. \tag{4.4}$$

The components, therefore, will be:

$$\begin{aligned}
\delta g^{00} &= -\frac{1}{a^4}\delta g_{00}, \\
\delta g^{0i} &= \frac{1}{a^4}\delta^{ik}\delta g_{0k} = \frac{1}{a^4}\delta g_{0i}, \\
\delta g^{ij} &= -\frac{1}{a^4}\delta^{ik}\delta g_{km}\delta^{mj} = -\frac{1}{a^4}\delta g_{ij}.
\end{aligned} \tag{4.5}$$

Note that there is a negative sign in involved when computing the inverse perturbed metric. Finally, we may write the general 'full' line element as

$$g_{\,\mu\nu}\mathrm{d}x^\mu\mathrm{d}x^\nu = a^2(\eta)\left(-\mathrm{d}\eta^2 + \delta_{ij}\,\mathrm{d}x^i\,\mathrm{d}x^j\right) + a^2(\eta)\,\delta g_{\mu\nu}\mathrm{d}x^\mu\mathrm{d}x^\nu\,. \tag{4.6}$$

4.1 Perturbed Geometry Calculations

We are now in a position to compute the Christoffel symbols in a perturbed FLRW spacetime. Using linear perturbation theory and neglecting higher order terms, the full Christoffel symbols are:

$$\begin{aligned}
\Gamma^\mu{}_{\nu\rho} = \frac{1}{2}\bar{g}^{\,\mu\sigma}(\bar{g}_{\sigma\nu,\,\rho} + \bar{g}_{\sigma\rho,\,\nu} - \bar{g}_{\nu\rho,\,\sigma}) + \frac{1}{2}\bar{g}^{\,\mu\sigma}(\delta g_{\sigma\nu,\,\rho} + \delta g_{\sigma\rho,\,\nu} - \delta g_{\nu\rho,\,\sigma}) \\
+ \frac{1}{2}\delta g_{\mu\sigma}(\bar{g}_{\sigma\nu,\,\rho} + \bar{g}_{\sigma\rho,\,\nu} - \bar{g}_{\nu\rho,\,\sigma}) + \mathcal{O}(\delta g^2),
\end{aligned} \tag{4.7}$$

in particular, the perturbed part of the Christoffel symbols can be written as:

$$\delta\Gamma^\mu{}_{\nu\rho} = \frac{1}{2}\bar{g}^{\,\mu\sigma}(\delta g_{\sigma\nu,\,\rho} + \delta g_{\sigma\rho,\,\nu} - \delta g_{\nu\rho,\,\sigma} - 2\delta g_{\sigma\alpha}\bar{\Gamma}^\alpha{}_{\nu\rho}). \tag{4.8}$$

To use this equality, we first need the background Christoffel symbols. The only non-vanishing Christoffel symbols in the $k = 0$ FLRW spacetime are:

$$\begin{aligned}
\bar{\Gamma}^0{}_{00} &= \frac{a'}{a}, \\
\bar{\Gamma}^0{}_{ij} &= \frac{a'}{a}\delta_{ij}, \\
\bar{\Gamma}^i{}_{0j} &= \frac{a'}{a}\delta^i{}_j.
\end{aligned} \tag{4.9}$$

Therefore, we can now calculate the perturbed FLRW Christoffel symbols. These are found to be:

$$\begin{aligned}
\delta\Gamma^0{}_{00} &= -\frac{1}{2}\delta g'_{00}\,,\\
\delta\Gamma^0{}_{i0} &= -\frac{1}{2}(\delta g_{00,\,i} - 2\mathcal{H}\delta g_{0i})\,,\\
\delta\Gamma^i{}_{i0} &= \delta g'_{i0} + \mathcal{H}\delta g_{i0} - \frac{1}{2}\delta g_{00,\,i}\,,\\
\delta\Gamma^0{}_{ij} &= -\frac{1}{2}(\delta g_{0i,\,j} + \delta g_{0j,\,i} - \delta g'_{ij} - 2\mathcal{H}\delta g_{ij} - 2\mathcal{H}\delta_{ij}\delta g_{00})\,,\\
\delta\Gamma^i{}_{j0} &= \frac{1}{2}(\delta g'_{ij} + \delta g_{i0,\,j} - \delta g_{0j,\,i})\,,\\
\delta\Gamma^i{}_{jk} &= \frac{1}{2}(\delta g_{ij,\,k} + \delta g_{ik,\,j} - \delta g_{jk,\,i} - 2\mathcal{H}\delta_{jk}\delta g_{i0})\,,
\end{aligned} \tag{4.10}$$

recalling that primes represent derivatives with respect to conformal time, η and $\mathcal{H}$ is the Hubble parameter with respect to conformal time. One may note that indices do not always match in level. However, we have used the assumption that 3-tensors are raised and lowered by δ_{ij}, for example, $\delta g^i{}_0 = \delta g_{i0}$.

In order to compute the linearised Einstein equations, we will use the trace-reversed form, (2.43). This form of the field equations is used because one does not have to compute the Ricci scalar, and therefore, is economical. Note that some authors, such as Weinberg [65] choose to use the cosmic time coordinate, t instead of conformal time. To convert between the two, one can simply use the tensor transformation law:

$$A_{\mu\nu} = \tilde{A}_{\rho\sigma}\frac{\partial\tilde{x}^\rho}{\partial x^\mu}\frac{\partial\tilde{x}^\sigma}{\partial x^\nu}, \tag{4.11}$$

where tensors that use cosmic time are represented with tildes. Because changing from conformal time to cosmic time does not affect the spatial coordinates, we have[3]

$$A_{00} = a^2\tilde{A}_{00}\,, \quad A_{0i} = a\tilde{A}_{0i}\,, \quad A_{ij} = \tilde{A}_{ij}. \tag{4.12}$$

This rule will hold for perturbed quantities as well.

The Ricci tensor in a coordinate basis is:

$$R_{\mu\nu} = \partial_\rho\Gamma^\rho{}_{\mu\nu} - \partial_\nu\Gamma^\rho{}_{\mu\rho} + \Gamma^\rho{}_{\mu\nu}\Gamma^\sigma{}_{\rho\sigma} - \Gamma^\rho{}_{\mu\sigma}\Gamma^\sigma{}_{\nu\rho}. \tag{4.13}$$

Substituting the *full* Christoffel symbol,

$$\Gamma^\lambda{}_{\mu\nu} = \bar{\Gamma}^\lambda{}_{\mu\nu} + \delta\Gamma^\lambda{}_{\mu\nu}, \tag{4.14}$$

into the definition of the Ricci tensor, one obtains:

$$\begin{aligned}
R_{\mu\nu} = {}& \partial_\rho\bar{\Gamma}^\rho{}_{\mu\nu} - \partial_\nu\bar{\Gamma}^\rho{}_{\mu\rho} + \bar{\Gamma}^\rho{}_{\mu\nu}\bar{\Gamma}^\sigma{}_{\rho\sigma} - \bar{\Gamma}^\rho{}_{\mu\sigma}\bar{\Gamma}^\sigma{}_{\nu\rho}\\
&+ \partial_\rho\delta\Gamma^\rho{}_{\mu\nu} - \partial_\nu\delta\Gamma^\rho{}_{\mu\rho} + \bar{\Gamma}^\rho{}_{\mu\nu}\delta\Gamma^\sigma{}_{\rho\sigma} + \bar{\Gamma}^\sigma{}_{\rho\sigma}\delta\Gamma^\rho{}_{\mu\nu}\\
&- \bar{\Gamma}^\rho{}_{\mu\sigma}\delta\Gamma^\sigma{}_{\nu\rho} - \bar{\Gamma}^\sigma{}_{\nu\rho}\delta\Gamma^\rho{}_{\mu\sigma}.
\end{aligned} \tag{4.15}$$

[3]If there are derivatives with respect to time in the tensors, one must also convert these by the chain rule.

The first term in this expansion is the background Ricci tensor, and we label the second and third line as $\delta R_{\mu\nu}$ to linear order. Therefore, we write (4.15) as

$$R_{\mu\nu} = \bar{R}_{\mu\nu} + \delta R_{\mu\nu}, \tag{4.16}$$

with

$$\begin{aligned}\delta R_{\mu\nu} =& + \partial_\rho \delta\Gamma^\rho{}_{\mu\nu} - \partial_\nu \delta\Gamma^\rho{}_{\mu\rho} + \bar{\Gamma}^\rho{}_{\mu\nu}\delta\Gamma^\sigma{}_{\rho\sigma} + \bar{\Gamma}^\sigma{}_{\rho\sigma}\delta\Gamma^\rho{}_{\mu\nu} \\ & - \bar{\Gamma}^\rho{}_{\mu\sigma}\delta\Gamma^\sigma{}_{\nu\rho} - \bar{\Gamma}^\sigma{}_{\nu\rho}\delta\Gamma^\rho{}_{\mu\sigma}.\end{aligned} \tag{4.17}$$

Using this equality, the components of the Ricci tensor are found to be:

$$\begin{aligned}\delta R_{00} =& - \frac{1}{2}\nabla^2\delta g_{00} - \frac{3}{2}\mathcal{H}\partial_\eta \delta g_{00} + \partial_k\partial_\eta \delta g^k{}_0 \\ & + \mathcal{H}\partial_k \delta g^k{}_0 - \frac{1}{2}(\partial_\eta^2 \delta g^k{}_k + \mathcal{H}\partial_\eta \delta g^k{}_k),\end{aligned} \tag{4.18}$$

$$\begin{aligned}\delta R_{0i} =& - \mathcal{H}\partial_i \delta g_{00} - \frac{1}{2}(\nabla^2 \delta g_{0i} - \partial_i\partial_k \delta g^k{}_0) \\ & + \frac{\partial^2{}_\eta\, a}{a}\delta g_{0i} + \mathcal{H}^2 \delta g_{0i} - \frac{1}{2}(\partial_i\partial_\eta \delta g^k{}_k - \partial_k\partial_\eta \delta g^k{}_i),\end{aligned} \tag{4.19}$$

$$\begin{aligned}\delta R_{ij} =& \frac{1}{2}\partial_i\partial_j \delta g_{00} + \frac{1}{2}\mathcal{H}\partial_\eta \delta g_{00}\delta_{ij} + \left(\mathcal{H}^2 + \frac{\partial^2{}_\eta a}{a}\right)\delta g_{00}\delta_{ij} \\ & - \frac{1}{2}(\nabla^2 \delta g_{ij} - \partial_k\partial_j \delta g^k{}_i - \partial_k\partial_i \delta g^k{}_j + \partial_i\partial_j \delta g^k{}_k \\ & + \frac{1}{2}\partial^2{}_\eta \delta g_{ij} + \mathcal{H}\partial_\eta \delta g_{ij} + \left(\mathcal{H}^2 + \frac{\partial^2{}_\eta a}{a}\right)\delta g_{ij} \\ & + \frac{1}{2}\mathcal{H}\partial_\eta \delta g^k{}_k \delta_{ij} - \mathcal{H}\partial_k \delta g^k{}_0 \delta_{ij} - \frac{1}{2}(\partial_j\partial_\eta \delta g_{0i} + \partial_i\partial_\eta \delta g_{0j}) \\ & - \mathcal{H}(\partial_j \delta g_{0i} + \partial_i \delta g_{0j}),\end{aligned} \tag{4.20}$$

where $\nabla^2 = \delta^{ij}\partial_i\partial_j$ is the spatial Laplacian in comoving coordinates. Note if one were to use the original form of the field equations, (2.5), then we require the Einstein tensor. The Einstein tensor in linear perturbation theory is:

$$G_{\mu\nu} = \bar{G}_{\mu\nu} + \delta G_{\mu\nu}, \tag{4.21}$$

where

$$\begin{aligned}\delta G_{\mu\nu} &= \delta R_{\mu\nu} - \frac{1}{2}\delta\left(g_{\mu\nu}R\right) + \delta\Lambda \\ &= \delta R_{\mu\nu} - \frac{1}{2}(R\,\delta g_{\mu\nu} + g_{\mu\nu}\,\delta R) + 0,\end{aligned} \tag{4.22}$$

therefore, the perturbed Einstein tensor depends on both $g_{\mu\nu}$ *and* $\delta g_{\mu\nu}$. This information will be needed if one wishes to compute the perturbed Friedmann equations, as both forms of the Einstein equations are used.

4.2 Perturbed Stress-Energy Tensor

The right-hand side of the field equations in the trace reversed form can be labelled as a 'source' tensor,

$$S_{\mu\nu} := T_{\mu\nu} - \frac{1}{2} g_{\mu\nu} g^{\rho\sigma} T_{\rho\sigma}, \tag{4.23}$$

the perturbed source tensor is,

$$\begin{aligned} \delta S_{\mu\nu} &= \delta(\bar{T}_{\mu\nu} + \delta T_{\mu\nu}) - \frac{1}{2}\delta\Big((\bar{g}_{\mu\nu} + \delta g_{\mu\nu})(\bar{g}^{\,\rho\sigma} + \delta g^{\rho\sigma})(\bar{T}_{\rho\sigma} + \delta T_{\rho\sigma})\Big) \\ &= \delta T_{\mu\nu} - \frac{1}{2}\bar{g}_{\mu\nu}\delta T^{\rho}{}_{\rho} - \frac{1}{2}\delta g_{\mu\nu}\bar{T}^{\rho}{}_{\rho}. \end{aligned} \tag{4.24}$$

One can determine the trace of the background stress-energy tensor in terms of the scale factor and its derivatives (with respect to conformal time). To do this, we first find the trace in terms of the background pressure and background energy density:

$$\begin{aligned} \bar{T}^{\rho}{}_{\rho} &= \bar{g}^{\,\mu\rho}\bar{T}_{\mu\rho} = \bar{g}^{\,00}\bar{T}_{00} + \bar{g}^{\,11}\bar{T}_{11} + \bar{g}^{\,22}\bar{T}_{22} + \bar{g}^{\,33}\bar{T}_{33} \\ &= 3\bar{p} - \bar{\rho}. \end{aligned} \tag{4.25}$$

One could also simply take the trace of (2.42). We can also use the first Friedmann equation (2.48) (in conformal time) to obtain an equation for the background energy density:

$$\bar{\rho} = \frac{3}{8\pi G a^2}\left(\frac{a'^{\,2}}{a^2} - \frac{\Lambda a^2}{3}\right). \tag{4.26}$$

Using the above and the second Friedmann equation with respect to conformal time (2.49) we obtain an equation for the background pressure,

$$\bar{p} = -\frac{1}{8\pi G}\left(-\Lambda + \frac{2a''}{a} - \frac{a'^{\,2}}{a^2}\right). \tag{4.27}$$

Using (4.26) and (4.27) we can rewrite the trace of the background stress-energy tensor as[4]:

$$\bar{T}^{\rho}{}_{\rho} = -\frac{3}{8\pi G a^2}\left(2\frac{a''}{a} - \frac{4a^2}{3}\Lambda\right). \tag{4.28}$$

With the trace of the background stress-energy tensor, we can calculate the perturbed source tensor:

$$\begin{aligned} \delta S_{00} &= \delta T_{00} + \frac{1}{2}\delta T^{\rho}{}_{\rho} - \left[-\frac{3}{16\pi G a^2}\left(2\frac{a''}{a} - \frac{4a^2}{3}\Lambda\right)\right]\delta g_{00}\,, \\ \delta S_{0i} &= \delta T_{0i} - \left[-\frac{3}{16\pi G a^2}\left(2\frac{a''}{a} - \frac{4a^2}{3}\Lambda\right)\right]\delta g_{0i}\,, \\ \delta S_{ij} &= \delta T_{ij} - \frac{a^2}{2}\delta_{ij}\delta T^{\rho}{}_{\rho} - \left[-\frac{3}{16\pi G a^2}\left(2\frac{a''}{a} - \frac{4a^2}{3}\Lambda\right)\right]\delta g_{ij}\,. \end{aligned} \tag{4.29}$$

[4]One could alternatively take the trace of the background field equations. However, having these expressions for background density and pressure is useful in general.

To proceed further, we want to be able to write the remaining parts of $\delta S_{\mu\nu}$ in terms of the perturbed FLRW metric. Thus, we must write $\delta T_{\mu\nu}$ in terms of the metric perturbations. Let us begin with the standard FLRW stress-energy tensor and perturb it:

$$\begin{aligned}\delta T_{\mu\nu} = \delta\bar{T}_{\mu\nu} &= \delta\left(\bar{p}\bar{g}_{\mu\nu} + (\bar{\rho}+\bar{p})\bar{u}_\mu\bar{u}_\nu\right)\\ &= \delta p\,\bar{g}_{\mu\nu} + \bar{p}\,\delta g_{\mu\nu} + \bar{u}_\mu\bar{u}_\nu\,\delta\rho + \bar{u}_\mu\bar{u}_\nu\,\delta p\\ &\quad + \bar{u}_\mu(\bar{\rho}+\bar{p})\,\delta u_\nu + \bar{u}_\nu(\bar{\rho}+\bar{p})\,\delta u_\mu.\end{aligned} \tag{4.30}$$

To determine the form of δu_μ, we will choose the space part, i.e., δu_i to be a spatial velocity vector, v_i. For δu_0 let us use the normalisation condition,

$$\bar{g}^{\mu\nu}\bar{u}_\mu\bar{u}_\nu = -1, \tag{4.31}$$

where the background 4-velocity components (in conformal time) are

$$\bar{u}_\mu = -a(\eta)(1,0,0,0), \quad \text{and} \quad \bar{u}^\mu = \frac{1}{a(\eta)}(1,0,0,0). \tag{4.32}$$

We now perturb (4.31) to obtain:

$$\begin{aligned}0 &= \delta(\bar{g}^{\mu\nu}\bar{u}_\mu\bar{u}_\nu)\\ &= (\bar{u}_\mu\bar{u}_\nu)\,\delta g_{\mu\nu} + (\bar{g}_{\mu\nu}\bar{u}_\mu)\delta u_\nu + (\bar{g}_{\mu\nu}\bar{u}_\nu)\delta u_\mu\\ &= \delta g_{00} - 2a\delta u_0\\ &\implies \delta u_0 = \frac{\delta g_{00}}{2a},\end{aligned} \tag{4.33}$$

where we have used the fact that the only non zero component of the background 4-velocity is the time component, u_0. Because the normalisation condition (4.31) can be written with the indices inverted, we also have $\delta u^0 = \delta g_{00}/2a^3$.

Finally, we need to calculate u^i. To do this, we start with the covariant (or 1-form) form of the full 4-velocity and manipulate it is as follows:

$$\begin{aligned}\bar{u}_\mu + \delta u_\mu = u_\mu &= g_{\mu\nu}u^\nu = g_{\mu\nu}(\bar{u}^\nu + \delta u^\nu)\\ &= (\bar{g}_{\mu\nu} + \delta g_{\mu\nu})(\bar{u}^\nu + \delta u^\nu)\\ &= \bar{g}_{\mu\nu}\bar{u}^\nu + \bar{g}_{\mu\nu}\delta u^\nu + \delta g_{\mu\nu}\bar{u}^\nu \qquad \text{(expanded to first order)}\\ &\implies \delta u_\mu = \bar{g}_{\mu\nu}\delta u^\nu + \delta g_{\mu\nu}\bar{u}^\nu \qquad \text{(equating order by order)}\\ &\therefore\ \delta u^\mu = \bar{g}^{\,\mu\nu}\delta u_\nu - \bar{g}^{\,\mu\sigma}\delta g_{\sigma\nu}\bar{u}^\nu.\end{aligned} \tag{4.34}$$

This shows that the vector form of the 4-velocity has an extra part, $\delta g_{\mu\nu}\bar{u}^\nu$. This stems from the fact that $\bar{g}^{\,\mu\nu}$ raises indices on background quantities and $g^{\mu\nu}$ raises indices on full quantities (those in the physical manifold, $\mathcal{M}$) and δu_μ is neither. Therefore, the perturbed 4-velocity is:

$$u_\mu = a\left(-1 + \frac{\delta g_{00}}{2a^2}, v_i\right), \quad \text{and} \quad u^\mu = \frac{1}{a}\left(1 + \frac{\delta g_{00}}{2a^2}, v^i - \frac{1}{a^2}\delta g^i{}_0\right), \tag{4.35}$$

with (4.30)–(4.35) we can now calculate the components of the perturbed stress-energy tensor, they are:

$$\begin{aligned}
\delta T_{00} &= -\bar{\rho}\delta g_{00} + a^2\delta\rho \\
\delta T_{0i} &= \bar{p}\,\delta g_{0i} - a^2(\bar{\rho}+\bar{p})\,v_i \\
\delta T_{ij} &= \bar{p}\,\delta g_{ij} + a^2\delta_{ij}\,\delta p.
\end{aligned} \tag{4.36}$$

Finally we need the trace of the perturbed stress-energy tensor. We first need an equation that can relate the perturbed mixed index stress-energy tensor to what we already have. This can be found as follows:

$$\begin{aligned}
T^{\mu}{}_{\nu} = \bar{T}^{\mu}{}_{\nu} + \delta T^{\mu}{}_{\nu} &= g^{\mu\sigma}T_{\sigma\nu} \\
&= (\bar{g}^{\,\mu\sigma} + \delta g^{\mu\sigma})(\bar{T}_{\sigma\nu} + \delta T_{\sigma\nu}) \\
&= \bar{T}^{\mu}{}_{\nu} + \bar{g}^{\,\mu\sigma}\delta T_{\sigma\nu} + \delta g^{\mu\sigma}\bar{T}_{\sigma\nu} \\
&\therefore\ \delta T^{\mu}{}_{\nu} = \bar{g}^{\,\mu\sigma}\delta T_{\sigma\nu} + \delta g^{\mu\sigma}\bar{T}_{\sigma\nu}.
\end{aligned} \tag{4.37}$$

Using this, we can determine all of the mixed index components of the perturbed stress-energy tensor, these are:

$$\begin{aligned}
\delta T^{0}{}_{0} &= -\delta\rho, \\
\delta T^{0}{}_{i} &= (\bar{\rho}+\bar{p})\,v_i, \\
\delta T^{i}{}_{j} &= \delta p\,\delta^{i}{}_{j}, \\
\delta T^{\rho}{}_{\rho} &= 3\,\delta p - \delta\rho.
\end{aligned} \tag{4.38}$$

4.3 Perturbed Einstein Field Equations

We can now write expressions for the field equations in terms of the perturbed metric and perturbed fluid variables. For $\mu = \nu = 0$ we have

$$\begin{aligned}
&-\frac{1}{2}\nabla^2\delta g_{00} - \frac{3}{2}\mathcal{H}\partial_\eta\delta g_{00} + \partial_k\partial_\eta\delta g^{k}{}_{0} + \mathcal{H}\partial_k\delta g^{k}{}_{0} - \frac{1}{2}(\partial_\eta^2\delta g^{k}{}_{k} + \mathcal{H}\partial_\eta\delta g^{k}{}_{k}) \\
&-\frac{3}{16\pi G a^2}\left(2\frac{a''}{a} - \frac{4a^2}{3}\Lambda\right)\delta g_{00} + \bar{\rho}\delta g_{00} = \delta\rho + \frac{1}{2}\left(3\delta p - \delta\rho\right),
\end{aligned} \tag{4.39}$$

for $\mu = i$, $\nu = 0$ we have

$$\begin{aligned}
&-\mathcal{H}\partial_i\delta g_{00} - \frac{1}{2}(\nabla^2\delta g_{0i} - \partial_i\partial_k\delta g^{k}{}_{0}) + \frac{\partial^2{}_\eta a}{a}\delta g_{0i} + \mathcal{H}^2\delta g_{0i} - \frac{1}{2}\partial_i\partial_\eta\delta g^{k}{}_{k} \\
&-\frac{1}{2}\partial_k\partial_\eta\delta g^{k}{}_{i} - \frac{3}{16\pi G a^2}\left(2\frac{a''}{a} - \frac{4a^2}{3}\Lambda\right)\delta g_{0i} - \bar{p}\,\delta g_{0i} = -a^2(\bar{\rho}+\bar{p})\,v_i,
\end{aligned} \tag{4.40}$$

and finally for $\mu = i$, $\nu = j$ we have

$$\begin{aligned}
&\frac{1}{2}\partial_i\partial_j\delta g_{00} + \frac{1}{2}\mathcal{H}\partial_\eta\delta g_{00}\delta_{ij} + \left(\mathcal{H}^2 + \frac{\partial^2{}_\eta a}{a}\right)\delta g_{00}\delta_{ij} \\
&- \frac{1}{2}(\nabla^2\delta g_{ij} - \partial_k\partial_j\delta g^k{}_i - \partial_k\partial_i\delta g^k{}_j + \partial_i\partial_j\delta g^k{}_k \\
&+ \frac{1}{2}\partial^2{}_\eta\delta g_{ij} + \mathcal{H}\partial_\eta\delta g_{ij} + \left(\mathcal{H}^2 + \frac{\partial^2{}_\eta a}{a}\right)\delta g_{ij} \\
&+ \frac{1}{2}\mathcal{H}\partial_\eta\delta g^k{}_k\delta_{ij} - \mathcal{H}\partial_k\delta g^k{}_0\delta_{ij} - \frac{1}{2}(\partial_j\partial_\eta\delta g_{0i} + \partial_i\partial_\eta\delta g_{0j}) \\
&- \mathcal{H}(\partial_j\delta g_{0i} + \partial_i\delta g_{0j}) - \frac{3}{16\pi G a^2}\left(2\frac{a''}{a} - \frac{4a^2}{3}\Lambda\right)\delta g_{ij} - \bar{p}\,\delta g_{ij} \\
&\qquad = a^2\delta_{ij}\,\delta p - \frac{a^2}{2}\delta_{ij}\left(3\delta p - \delta\rho\right).
\end{aligned} \tag{4.41}$$

Beyond the problem of how complicated these equations look, we also have unphysical quantities that arise, i.e., those that have no significance to the 'real' nature of spacetime. We will, therefore, discuss how these problems are generally approached in cosmology with gauge freedoms.

4.4 Metric Decomposition

Before discussing different gauges and the problems behind selecting gauges we will introduce a useful decomposition of the perturbed metric. In general, one can perform a Helmholtz decomposition of the metric tensor [1, 65]. Since the metric is a symmetric rank 2 tensor, there should be 10 fluctuating degrees of freedom in the perturbed metric tensor, $\delta g_{\mu\nu}$.

There are four degrees of freedom corresponding to the scalar metric perturbations, i.e., there are only four ways to construct a metric from scalar functions [178]:

$$\delta g_{\mu\nu} = a^2\begin{pmatrix} -2\,\phi & \partial_i B \\ \partial_i B & 2\,(-\psi\,\delta_{ij} + \partial_i\partial_j E) \end{pmatrix}, \tag{4.42}$$

where the scalars are, ϕ, B, E, and ψ. Here ϕ is a generalisation of the Newtonian potential and ψ is the[5] 'curvature perturbation'. Scalar perturbations are the 'most important', as they couple with the density and pressure perturbations and exhibit gravitational instability. The scalar fluctuations are related to the temperature fluctuations we observe in the CMB via the Sachs-Wolfe effect. Density perturbations are primarily responsible for the structure we observe in the Universe.

[5]The curvature perturbation terminology derives from its common use in the longitudinal gauge, where it is the only perturbation involved in the scalar curvature.

There are four vector degrees of freedom of the metric perturbations,

$$\delta g_{\mu\nu} = a^2 \begin{pmatrix} 0 & -S_i \\ -S_i & \partial_i F_j + \partial_j F_i \end{pmatrix}, \tag{4.43}$$

where S_i and F_i are divergenceless[6] vectors, i.e.,

$$\frac{\partial S_i}{\partial x^i} = 0 \quad \text{and} \quad \frac{\partial F_i}{\partial x^i} = 0. \tag{4.44}$$

Vector perturbations couple to rotational velocity perturbations in the cosmic fluid. Since these decay in a expanding Universe, they are not usually examined in early Universe cosmology.

Finally, there are two tensor components. These two tensor components correspond to the two polarisation states of gravitational waves. We have,

$$\delta g_{\mu\nu} = a^2 \begin{pmatrix} 0 & 0 \\ 0 & D_{ij}, \end{pmatrix} \tag{4.45}$$

where D_{ij} is traceless and divergenceless,

$$D^i{}_i = \frac{\partial D_{ij}}{\partial x^i} = 0. \tag{4.46}$$

The three different types of fluctuations do not couple in linear perturbation theory and so the behaviour of each can be examined individually. Because of this, the field equations can be simplified by equating scalar, vector, and tensor perturbations for individual components of the field equations.

We summarise the metric components in the above decomposition as,

$$\begin{aligned} \delta g_{00} &= -2\, a^2 \phi \\ \delta g_{0i} &= a^2(\partial_i B - S_i) \\ \delta g_{ij} &= a^2(-2\,\psi\,\delta_{ij} + 2\,\partial_i\partial_j E + 2\,\partial_{(i}F_{j)} + D_{ij}), \end{aligned} \tag{4.47}$$

therefore, the full FLRW line element is written as:

$$\begin{aligned} g_{\mu\nu}\,\mathrm{d}x^\mu \mathrm{d}x^\nu = a^2(\eta)\Bigg(& -(1+2\phi)\,\mathrm{d}\eta^2 + 2\,(\partial_i B - S_i)\,\mathrm{d}\eta\,\mathrm{d}x^i \\ & + (-2\,\psi\,\delta_{ij} + 2\,\partial_i\partial_j E + 2\,\partial_{(i}F_{j)} + D_{ij})\,\mathrm{d}x^i \mathrm{d}x^j \Bigg). \end{aligned} \tag{4.48}$$

4.5 Gauges

The phrase gauge (Eich) transformation or gauge invariance was first introduced by Hermann Weyl in 1918 [179, 180]. Weyl was attempting to unify gravity and

[6] If one has vectors that do not have vanishing divergence, the divergence contributes to the scalar gravitational fluctuation modes [178].

electromagnetism and used the phrases *gauge transformation* and *gauge invariance* to mean change of length or calibration, i.e., Weyl wanted his theory to be invariant under changing of calibration or length. The concept of gauge invariance that the current generation of cosmologists has a very specific meaning. This is no doubt a consequence of a highly influential paper of Bardeen [176], titled "Gauge invariant cosmological perturbations", which is framed entirely in the FLRW setting.

There are, however, theorists in the community who still use a more general notion of "gauge". Researchers who use a 3+1 formalism in general relativity such as Buchert [3] attempt to define a cosmology without a reference background. Buchert makes choices of spatial hypersurfaces which are foliation or slicing choices [181]. Such choices could be deemed to be "gauge choices" in the broad sense as they fix a time coordinate for the normal vector. In the context of standard perturbation theory, however, we will follow the most common usage of "gauge". It is worth noting that when the Buchert formalism is introduced in Chapter 5, one does not have a background spacetime and the foliation choices or slicing choices do not correspond to the common phase 'gauge choice'.

A gauge choice in the standard model of cosmology attempts to distinguish between unphysical and physical quantities [83, 176]. While the decomposition of the metric in the previous section simplifies the perturbed field equations greatly, we have introduced unphysical scalar and vector modes. To see how this can occur, consider a choice of coordinates as a mapping between $\bar{\mathcal{M}}$ and $\mathcal{M}$, and label it $\mathcal{D}$. Let us then consider another mapping, $\mathcal{D}'$ which maps the same points (for example, the origin) in $\bar{\mathcal{M}}$ into different points in $\mathcal{M}$. Now consider a physical quantity, such as the Ricci scalar, R, on $\mathcal{M}$ with a corresponding quantity, $\bar{R}$ on $\bar{\mathcal{M}}$. Then in the first coordinate system defined by the map, $\mathcal{D}$, the perturbation δR of R at a point, $x \in \mathcal{M}$ can be expressed as:

$$\delta R(x) = R(x) - \bar{R}\,(\mathcal{D}^{-1}(x)), \tag{4.49}$$

where $\mathcal{D}^{-1}$ is the inverse to map $\mathcal{D}$. One can also define a similar perturbation with $\mathcal{D}'$:

$$\delta R'(x) = R(x) - \bar{R}\,(\mathcal{D}'^{-1}(x)). \tag{4.50}$$

The difference between these two perturbations is

$$\Delta R(x) = \delta R'(x) - \delta R(x). \tag{4.51}$$

This difference is referred to as a '*gauge artefact*' and carries no physical significance. This is the essence of the gauge problem in general relativity — physically meaningful quantities should not depend on a choice of coordinates.

Some of the perturbations in the perturbed Einstein in section 4.3 introduced these so-called gauge artefacts. To isolate these, we investigate how coordinate

transformations act on the metric. Consider an infinitesimal coordinate transformation:

$$x^\mu \mapsto \tilde{x}^\mu = x^\mu + \xi^\mu. \tag{4.52}$$

This coordinate transformation implies we have four independent gauge degrees of freedom. These correspond to one from the time component, ξ^0 and three from the spatial vector, ξ^i. One can decompose the spatial vector, ξ^i as

$$\xi^i = \zeta^i + \partial^i \zeta, \tag{4.53}$$

where ζ^i is the transverse, divergenceless part of ξ^i. Therefore, we note that there are two scalar *gauge modes*[7] given by ξ^0 and ζ, and two vector gauge modes from ζ^i. Furthermore, the tensor modes are gauge-invariant and, therefore, there are four physical perturbation or fluctuation modes[8].

We continue our investigation of how the metric transforms under (4.52):

$$\begin{aligned} \tilde{g}_{\mu\nu}(\tilde{x}) &= g_{\alpha\beta}\frac{\partial x^\alpha}{\partial \tilde{x}^\mu}\frac{\partial x^\beta}{\partial \tilde{x}^\nu} \\ &= g_{\alpha\beta}(\tilde{x}) - \mathcal{L}_\xi g_{\alpha\beta}(\tilde{x}), \end{aligned} \tag{4.54}$$

where $\mathcal{L}_\xi$ is the Lie derivative along the vector field, ξ^μ. If one defines the metrics in (4.54) as

$$\tilde{g}_{\mu\nu}(\tilde{x}) = \bar{g}_{\mu\nu}(\tilde{x}) + \delta\tilde{g}_{\mu\nu}(\tilde{x}) \quad \text{and} \quad g_{\mu\nu}(x) = \bar{g}_{\mu\nu}(x) + \delta g_{\mu\nu}(x), \tag{4.55}$$

then using (4.54) we find that the change in the perturbation of the metric due to coordinate transformation (4.52) is[9,10]

$$\delta\tilde{g}_{\mu\nu}(\tilde{x}) - \delta g_{\mu\nu}(\tilde{x}) = \Delta\,\delta g_{\mu\nu} = -\mathcal{L}_\xi \bar{g}_{\mu\nu} + \mathcal{O}(\delta g \xi). \tag{4.56}$$

Using this equation, we can find the transformations in the different components of the full metric by observing how the perturbed metric transforms.

The transformed perturbations are thus found by taking Lie derivatives of the unperturbed background FLRW metric,

$$\begin{aligned} -\Delta\,\delta g_{00} &= \mathcal{L}_\xi \bar{g}_{00} = \xi^\alpha \partial_\alpha \bar{g}_{00} + 2\bar{g}_{0\alpha}\partial_0 \xi^\alpha, \\ -\Delta\,\delta g_{0i} &= \mathcal{L}_\xi \bar{g}_{0i} = \xi^\alpha \partial_\alpha \bar{g}_{0i} + \bar{g}_{0\alpha}\partial_i \xi^\alpha + \bar{g}_{\alpha i}\partial_0 \xi^\alpha, \\ -\Delta\,\delta g_{ij} &= \mathcal{L}_\xi \bar{g}_{ij} = \xi^\alpha \partial_\alpha \bar{g}_{ij} + \bar{g}_{i\alpha}\partial_j \xi^\alpha + \bar{g}_{j\alpha}\partial_i \xi^\alpha. \end{aligned} \tag{4.57}$$

[7]The phrase gauge mode is simply to distinguish between scalar modes which come from the metric perturbations and scalar modes that arise from gauge transformations.

[8]More precisely, there are two that correspond to scalar perturbations and two that correspond to vector fluctuations.

[9]We have used the *active* gauge transformation here. Another way to obtain these results is to refer to the 'gauge group' of general relativity, the group of diffeomorphisms. To preserve the group structure associated to this active transformation, we use the exponential map: $A \mapsto \tilde{A} = e^{\mathcal{L}_\xi} A$, where A is any tensor field. Taylor expanding this result provides us with the result in (4.56) (up to a negative sign).

[10]Note that we have made a sign choice here, that is consistent with [65], this does not change anything significantly as it will propagate through trivially.

With the properties of the FLRW metric we find

$$\begin{aligned}
&-\Delta\,\delta g_{00} = 2\,a^2\Delta\,(\phi) = -2\,a'a\xi^0 - 2\,a^2\xi^{0\,\prime}\,,\\
&-\Delta\,\delta g_{0i} = -a^2\Delta(B_{,i} - S_i) = -a^2\xi^0_{,i} + a^2\xi_i'\,,\\
&-\Delta\,\delta g_{ij} = -a^2\Delta(-2\,\psi\,\delta_{ij} + 2\,E_{,ij} + 2\,F_{(i\,,j)} + D_{ij}) = 2a'a\xi^0\delta_{ij} + 2\,a^2\xi_{(i\,,j)}.
\end{aligned} \tag{4.58}$$

By using using the decomposition, $\xi^i = \zeta^i + \partial^i\zeta$ and equating scalars, vectors, and tensors on each side, we find

$$\begin{aligned}
\Delta\phi &= -\left(\frac{a'}{a}\xi^0 + \xi^{0\,\prime}\right),\\
\Delta B &= \xi^0 - \zeta'\,,\\
\Delta S_i &= \zeta_i{}'\,,\\
\Delta\psi &= \frac{a'}{a}\xi^0\,,\\
\Delta E &= -\zeta\,,\\
\Delta F_i &= -\zeta_i\,,\\
\Delta D_{ij} &= 0\,.
\end{aligned} \tag{4.59}$$

Therefore, the gauge transformed line element is

$$\begin{aligned}
\mathrm{d}s^2 = a^2(\eta)\Bigg\{ &-\left[1 + 2\,(\phi - \frac{a'}{a}\xi^0 - \xi^0)\right]\mathrm{d}\eta^2 + 2\,(B + \xi^0 - \zeta\,')_{,i}\,\mathrm{d}\eta\,\mathrm{d}\tilde{x}^i\\
&- 2\,(S_i + \zeta_i{}')\,\mathrm{d}\eta\,\mathrm{d}\tilde{x}^i + \Bigg[\Big(1 - 2(\psi + \mathcal{H}\xi^0)\Big)\delta_{ij} + 2\,(E - \zeta)_{,ij}\\
&\qquad + 2\,(F_i - \zeta_i)_{,j} + D_{ij}\Bigg]\,\mathrm{d}\tilde{x}^i\mathrm{d}\tilde{x}^j\Bigg\}.
\end{aligned} \tag{4.60}$$

To eliminate these gauge modes, there are two general approaches: the first is to fix a gauge, i.e., select a gauge by fixing coordinates by 'choosing' components of ξ^μ such that they do no appear in the field equations. The second is to use *gauge-invariant* quantities, first introduced by Bardeen [176]. We will investigate both of these in the context of standard perturbation theory.

4.5.1 Gauge Fixing

We will introduce a few of the common gauges in linear cosmological perturbation theory and the choice of the gauge generators that achieve these gauges.

- Synchronous gauge: We define the synchronous gauge by setting

$$\tilde{\phi} = \tilde{B} = \tilde{S}_i = 0. \tag{4.61}$$

This gauge was used widely for many calculations after it was introduced by Lifshitz in 1946 [174] but became unpopular in the 1980s. The use of the synchronous gauge decreased because of the fact that the condition (4.61) does not fix the gauge completely, i.e., there are still unphysical gauge modes. The time coordinate in the synchronous gauge is simply the proper time of comoving observers at fixed spatial coordinates. One may obtain this gauge by solving the differential equations $\phi = \xi^{0\,\prime} + \mathcal{H}\xi^0$ and $B_{,i} + S_i = \xi_i' - \xi^0{}_{,i}$. These differential equations are coupled, and one can see the equations imply

$$\begin{aligned} \xi^0 &= \frac{1}{a}\int a\phi\, d\eta + f(\mathbf{x}) \\ \zeta &= \int (\xi^0 + B)\, d\eta + g(\mathbf{x}) \\ A_i &= -\int S_i d\eta + h(\mathbf{x}). \end{aligned} \tag{4.62}$$

The integration variables, f, g, and h are purely spatial and give rise to *spurious* gauge modes. This problem can, however, be fixed if one chooses an initial gauge condition, such as a vanishing 3-velocity for perturbed dark matter which is 'natural' as dark matter is understood to be slow moving [182].

- Spatially flat gauge: We define the spatially flat gauge by choosing

$$\tilde{\psi} = \tilde{E} = \tilde{F}_i = 0. \tag{4.63}$$

This choice leaves the 3-metric on spatial hypersurfaces unperturbed, or "flat" as is the case of the $k = 0$ FLRW spacetime. In standard perturbation theory, one can fix this gauge by choosing $\xi^0 = -\psi/\mathcal{H}$, and $\xi_i = E_{,i} + F_i$.

- comoving orthogonal Gauge: This gauge is defined by choosing

$$\tilde{v}_i = 0 \quad \text{and} \quad \tilde{g}_{0i} = 0. \tag{4.64}$$

This gauge is, therefore, defined by the 3-velocity and 3-momentum of the fluid vanishing. The constant time hypersurfaces are orthogonal to the fluid 4-velocity in this gauge.

- Conformal Newtonian or longitudinal gauge: This gauge is defined by choosing

$$\tilde{B} = \tilde{E} = 0. \tag{4.65}$$

This gauge is also referred to as the "zero-shear" gauge because the scalar shear is given by $\sigma = E' - B$. This allows one to write the metric tensor in a diagonal form (for scalar perturbations). If one assumed anisotropic stresses to vanish then one finds $\psi = \phi$, allowing the field equations to be written in a form very close to the Newtonian equations for gravity. One can obtain this gauge by choosing $E = \zeta$ and $E' + B = -\xi^0$. This gauge is often used to model the CMB in simulations due to scalar perturbations being the simplest and most dominant perturbation. One can generalise this gauge to one which possesses all of the scalar perturbations.

- N-body gauge: The N-body gauge is defined when

$$\tilde{v} + \tilde{B} = 0. \tag{4.66}$$

However, there are still remaining gauge freedoms. These are used to set the "counting density" associated with N bodies. This is equal to the energy density at leading order. This condition requires the scalar deformation of the spatial volume to be zero. This can be expressed as:

$$\tilde{\psi} - \frac{1}{3}\nabla^2\tilde{E} = 0. \tag{4.67}$$

To fix this gauge completely, therefore, we require $v + B = -\xi^0$ and by solving $\nabla^2\zeta = (\nabla^2 E - 3\psi) + 3\mathcal{H}(v + B)$.

4.5.2 Gauge-Invariant Quantities

The second option one has is to work with *gauge-invariant* variables. As the name suggests, under gauge transformations of the form (4.59) these variables are invariant or remain unchanged. In general, the only perturbations of quantities that are gauge-invariant are ones that vanish or are constant in the background spacetime. This was formalised in the Stewart-Walker lemma [178]. The lemma states that a linear perturbation of a tensor field is gauge-invariant *if and only if* one of the following hold:

- $T_0 = 0$;
- T_0 is a constant scalar field;
- T_0 is a linear combination of products of delta functions, $\delta^\mu{}_\nu$,

where T_0 is the unperturbed tensor field.

Metric Invariants

One can define more than one scalar quantity that is invariant under the gauge transformations in (4.59). The first are the metric perturbations themselves introduced by Bardeen [176]. Examples of these are:

$$\Phi = \phi - \mathcal{H}\sigma - \sigma' \quad \text{and} \quad \Psi = \psi + \mathcal{H}\sigma, \tag{4.68}$$

where $\sigma = E' - B$ is the scalar shear. These scalars are gauge-invariant forms of the Newtonian potential and curvature perturbation. We can use (4.59) to show that these variables under such transformations. Let us first observe how σ transforms:

$$\begin{aligned} \sigma &= E' - B \\ &= \tilde{E}' + \zeta' - B' + \xi^0 - \zeta' \\ &= \tilde{\sigma} + \xi^0 \\ &\therefore \tilde{\sigma} - \sigma = \Delta\,\sigma = -\xi^0. \end{aligned} \tag{4.69}$$

From the transformation of σ we can determine

$$\begin{aligned} \Delta\Phi &= -\left(\mathcal{H}\xi^0 + \xi^{0\,\prime}\right) + \mathcal{H}\xi^0 + \xi^{0\,\prime}. \\ &= 0 \\ &\therefore \tilde{\Phi} = \Phi. \end{aligned} \tag{4.70}$$

Similarly,

$$\begin{aligned} \Delta\Psi &= \mathcal{H}\xi^0 - \mathcal{H}\xi^0 \\ &\therefore \tilde{\Psi} = \Psi. \end{aligned} \tag{4.71}$$

There are more gauge-invariant metric scalars that can be defined such as

$$\begin{aligned} \mathcal{A} &= \phi + \psi + \left(\frac{\psi}{\mathcal{H}}\right)', \\ \mathcal{B} &= -\sigma - \frac{\psi}{\mathcal{H}}, \\ \mathcal{Q} &= \phi + \frac{1}{2}(a(v+B))'. \end{aligned} \tag{4.72}$$

Because there are only two vector degrees of freedom (because there are two gauge modes) there will only be one gauge-invariant metric vector perturbation. This vector must be transverse (divergence-free), one choice for this is

$$\mathcal{P}_i = S_i + F_i{}'. \tag{4.73}$$

Curvature Invariants

The perturbed intrinsic Ricci scalar for a flat FLRW Universe is,

$$\delta\mathcal{R} = \frac{4}{a^2}\nabla^2\,\psi. \tag{4.74}$$

This is an invariant quantity as the intrinsic Ricci scalar vanishes in the background for a flat FLRW Universe. Therefore, by the Stewart-Walker lemma, it must be gauge-invariant. However, using Ψ is more useful because it is itself gauge-invariant and thus even for a $k \neq 0$ FLRW model, the intrinsic Ricci scalar will be gauge-invariant.

There are also other gauge-invariant curvature perturbations, such as:

$$\begin{aligned} \mathfrak{R} &= \psi - \mathcal{H}(v + B), \\ \mu &= -\psi - \mathcal{H}\frac{\delta\rho}{\rho'}. \end{aligned} \tag{4.75}$$

We note that $\mathfrak{R}$ coincides with the intrinsic Ricci perturbation in the comoving orthogonal gauge (where $v = B = 0$). While μ coincides with the intrinsic Ricci perturbation on 'uniform' density hypersurfaces[11]. It can further be shown that the perturbed $(0, i)$ field equation — in the gauge invariant form — gives an explicit gauge-invariant formula for $\mathfrak{R}$:

$$\mathfrak{R} = \Psi + \frac{2}{3}\frac{(\Psi' + \mathcal{H}\Phi)}{(1+w)\mathcal{H}}, \tag{4.76}$$

where w was defined in (2.50). This formula is useful as it relates the curvature perturbation to the metric potentials. In the case of vanishing anisotropic stress ($\Psi = \Phi$) we have

$$\mathfrak{R} = \Phi + \frac{2}{3}\frac{(\Phi' + \mathcal{H}\Phi)}{(1+w)\mathcal{H}}. \tag{4.77}$$

[11]This gauge is defined by setting the perturbation of the density to zero, $\delta\rho = 0$.

Chapter 5

Buchert Formalism

The widely accepted picture of the evolution of the Universe relates measurable quantities to the global cosmological parameters such as the mean matter density and the average global expansion rate. As demonstrated in Chapter 2 these parameters are derived from solutions of Einstein's equations[1] for spatially *homogeneous and isotropic* systems. The key argument that the standard model invokes is that the Universe *on average* should follow the evolution of simple FLRW models, without specifying a notion of averaging.

A viable cosmological model *should* provide an effective evolution history of the inhomogeneous Universe. Thomas Buchert's averaging formalism provides a procedure for spatially averaging the *scalar* characteristics of an inhomogeneous model of the Universe. In turn, this yields a system of scale-dependent 'Friedmann-like' equations with additional terms to the usual matter stress-energy. Backreaction may potentially replace the dark constituents of the Universe — which are fundamental puzzles in the standard model of cosmology.

Many debates have taken place in the last 20 years since the first formal introduction of Buchert's averaging scheme [4]. In considering such schemes, several researchers have questioned whether the apparent late time acceleration of cosmic expansion was due to the backreaction of inhomogeneities.

Some of the most notable arguments against this idea were made by Ishibashi and Wald [49] and Green and Wald [50–53] (see [184] for a review). In a series of papers, Green and Wald claimed that the effects of backreaction are negligible. However, this was only actually proven in a particular mathematical framework with simplifying assumptions about the nature of "backreaction". In particular, they assumed that average evolution is an exact solution of Einstein's equations on any scale of averaging. Buchert et al. [54] disagree about these mathematical assumptions. For example, the Buchert scheme [4, 34] does not assume that the average evolution is an exact solution of the Einstein equations. Therefore, any attempt to use Buchert averaging to create a cosmological

[1] One can also use Newton's equations for gravity in an ad hoc derivation of the Friedmann equations [183].

model must explain how and why average evolution is close to spatially homogeneous[2]. Wiltshire's timescape model [35, 36] is a phenomenological model which attempts to address these issues, via a *cosmological equivalence principle* [185] for average symmetries.

The averaged systems that are derived in [3, 4] which will be presented here are considered "background-free" approaches to relativistic cosmologies. One can alternatively, interpret spatial averages as a *general background cosmology* with a 'background' that is not fixed *a priori*, and instead evolves with the formation of structures. One may then investigate fluctuations with respect to these physical averages, thus eliminating the need for gauge transformations. The problem still remains, however, of being able to relate such statistical averages of structures to our own observations. Some preliminary attempts at developing "perturbation theory" about a 'general averaged' background have been made in [186].

5.1 Spacetime Foliation and Fluid Decomposition

We consider a model of the Universe that is sourced by a single general matter fluid — a fluid that is not assumed to be a perturbation of a background. We will use a general 3+1 splitting of spacetime and for the decomposition of the fluid flow and of its stress-energy tensor.

5.1.1 Geometry

Let us consider a globally hyperbolic four-dimensional manifold, $\mathcal{M}$, endowed with a pseudo-Riemannian metric tensor, $\boldsymbol{g}$ with a local coordinate system, x^μ. The fluid flow will be described by a timelike congruence with a unit, future-oriented, timelike tangent vector field, $\boldsymbol{u}$ which is the 4–velocity of the fluid[3].

We construct the spacetime manifold by foliating a family of spacelike hypersurfaces as Chapter 3, which has a unit vector $\boldsymbol{n}$. This unit vector is in general tilted with respect to the 4-velocity, $\boldsymbol{u}$. The normal vector is defined through (3.48) which in coordinate form gives

$$n^\mu = \frac{1}{N}\Big(1,\, -\beta^i\Big), \tag{5.1}$$

[2]Ishibashi and Wald [49] state 'the main point of their paper' is to stress that any new model of cosmology must show that all of the predictions of this new model are compatible with observation — a formalism for averaging does not suffice.

[3]There are many possible physical interpretations of the 4-velocity. For instance, it can be defined as the 'energy frame' for the fluid, or the barycentric velocity, or associated to another conserved current.

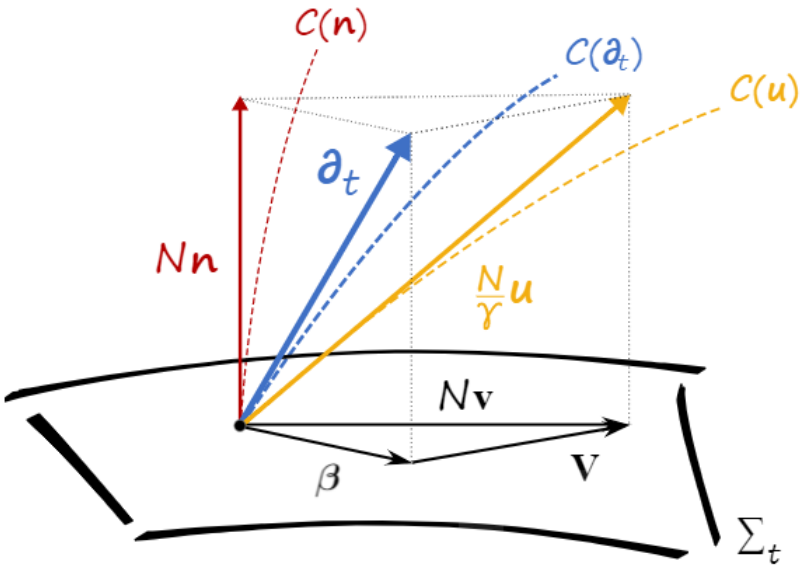

Figure 5.1: A spatial hypersurface, Σ_t is shown here with different congruences and corresponding tangent vectors from Buchert et al. [3]. The vector $N\boldsymbol{n}$ is the normal to the hypersurface scaled by the lapse (referred to as $\boldsymbol{m}$ in Chapter 3); it is tangent to the congruence $C(\boldsymbol{n})$. The time vector of the coordinate basis, $\boldsymbol{\partial}_t$ is tangent to the congruence of curves $C(\boldsymbol{\partial}_t)$, which have $x^i =$ constant. The 4–velocity of the fluid, $\boldsymbol{u}$, is tangent to the congruence of curves $C(\boldsymbol{u})$. The relationship between the various vectors is discussed in subsection 5.1.2. The difference between $C(\boldsymbol{n})$ and $C(\boldsymbol{\partial}_t)$ is characterised by the shift. The difference between $C(\boldsymbol{n})$ and $C(\boldsymbol{u})$ is characterised by the tilt. The difference between $C(\boldsymbol{\partial}_t)$ and $C(\boldsymbol{u})$ is characterised by the coordinate velocity. Notice that if $\boldsymbol{V} = 0$ then $\boldsymbol{\partial}_t = (N/\gamma)\boldsymbol{u}$ and thus the tilt is proportional to the shift. If $\boldsymbol{v} = 0$ then we have a fluid flow which is hypersurface orthogonal, $\boldsymbol{n} = \boldsymbol{u}$, hence $\boldsymbol{V} = -\boldsymbol{\beta}$.

with the dual vector components

$$n_\mu = -N\,(1, 0). \tag{5.2}$$

Recall that $\boldsymbol{\beta}$ is the shift vector, which in general, generates spatial diffeomorphisms between successive slices. We define the projection operator as follows with its various properties (in the coordinate description):

$$h_{\mu\nu} := g_{\mu\nu} + n_\mu n_\nu\,, \quad h_{\mu\nu}\,n^\mu = 0\,, \quad h^\mu{}_\alpha\, h^\alpha{}_\nu = h^\mu{}_\nu\,, \quad h^{\mu\nu}h_{\mu\nu} = 3, \tag{5.3}$$

where the restriction to the spacelike hypersurfaces defines the spatial metric. The four-dimensional line element can be written as

$$\mathrm{d}s^2 = g_{\mu\nu}\,\mathrm{d}x^\mu\,\mathrm{d}x^\nu = -\Big(N^2 - \beta^i\beta_i\Big)\,\mathrm{d}t^2 + 2\beta_i\,\mathrm{d}x^i\mathrm{d}t + h_{ij}\,\mathrm{d}x^i\mathrm{d}x^j\,. \tag{5.4}$$

The dynamic variables associated with the normal frames are the extrinsic curvature, $\boldsymbol{\mathcal{K}}$, and the acceleration which we shall refer to as $\boldsymbol{a}^{(n)}$.

5.1.2 Description of the Fluid

The general set up of the various congruences can be seen in Figure 5.1. The fluid 4-velocity, $\boldsymbol{u}$ can be decomposed as

$$\boldsymbol{u} = \gamma\,(\boldsymbol{n} + \boldsymbol{v}), \tag{5.5}$$

where,

$$\gamma = -n_\alpha\, u^\alpha = \frac{1}{\sqrt{1 - v^\alpha\, v_\alpha}} \tag{5.6}$$

is the Lorentz gamma factor. Here, $\boldsymbol{v}$ is the *Eulerian velocity* which is the spatial velocity of the fluid relative to the normal frames. It determines the tilt between the normal and fluid frames. For vanishing tilt we have $\boldsymbol{u} = \boldsymbol{n}$, therefore, $v = 0$ and $\gamma = 1$.

We also introduce the *coordinate velocity* of the fluid[4],

$$\boldsymbol{V} = \frac{\mathrm{d}\boldsymbol{x}}{\mathrm{d}t}, \tag{5.7}$$

where $\boldsymbol{x}$ is the spatial coordinate of the fluid element in the coordinate system (t, x^i) and $\mathrm{d}/\mathrm{d}t$ is the coordinate time derivative along the fluid flow lines. The Eulerian velocity can be written as

$$\boldsymbol{v} = \frac{1}{N}\,(\boldsymbol{\beta} + \boldsymbol{V}). \tag{5.8}$$

Using (5.5) and the above expression for the Eulerian velocity, we can rewrite the four velocity as

$$\boldsymbol{u} = \frac{\gamma}{N}\Big(N\boldsymbol{n} + \boldsymbol{\beta} + \boldsymbol{V}), \tag{5.9}$$

where

$$\frac{\gamma}{N} = \frac{1}{\sqrt{N^2 - (\beta^\mu + V^\mu)\,(\beta_\mu + V_\mu)}}. \tag{5.10}$$

Since, $\boldsymbol{V}$ depends on the shift, $\boldsymbol{\beta}$, for various coordinate systems we have different shift vectors. E.g., for a coordinate system comoving with the fluid we have $\boldsymbol{V} = 0$ and for a vanishing tilt, we have $\boldsymbol{V} = -\boldsymbol{\beta}$. A vanishing tilt indicates $\boldsymbol{v} = 0$, meaning $\boldsymbol{n} = \boldsymbol{u}$, and thus the fluid flow is 'hypersurface orthogonal'. This results in vanishing vorticity of the congruence.

In general, the fluid will possess vorticity, and not be hypersurface forming, unlike the normals, $\boldsymbol{n}$. In the actual Universe, as overdensities collapse, angular momentum perturbations grow. In general, particle geodesics will also cross in collapsing structures leading to a breakdown of our formalism: we cannot maintain a single fluid description for the entire evolution of the Universe.

Using (5.1) one can write the 4–velocity in a more intuitive way:

$$u^\mu = \frac{\gamma}{N}\Big(1,\, V^i\Big), \tag{5.11}$$

[4]As Figure 5.1 shows, both $\boldsymbol{v}$ and $\boldsymbol{V}$ are tangent to the spatial slices, Σ_t meaning $\boldsymbol{n}\cdot\boldsymbol{v} = 0$ and $\boldsymbol{n}\cdot\boldsymbol{V} = 0$.

with the dual

$$u_\mu = \frac{\gamma}{N}\Big(- N^2 + \beta^i\,(\beta_i + V_i)\,,\, \beta_i + V_i\Big). \tag{5.12}$$

Kinematic variables

Recall the projection operator, $\boldsymbol{b}$, that projects tensors onto the local rest frames of the fluid (those frames orthogonal to $\boldsymbol{u}$):

$$b_{\mu\nu} := g_{\mu\nu} + u_\mu u_\nu. \tag{5.13}$$

The properties of $\boldsymbol{b}$ are similar to the properties of $\boldsymbol{h}$,

$$b_{\mu\nu}\,u^\mu = 0\,, \quad b^\mu{}_\alpha\, b^\alpha{}_\nu = b^\mu{}_\nu\,, \quad b^{\mu\nu}\,b_{\mu\nu} = 3. \tag{5.14}$$

In the case where the fluid flow is hypersurface orthogonal, the projection operators $\boldsymbol{b}$ and $\boldsymbol{h}$ are the same. The kinematic variables are those introduced in section 3.5, namely, the expansion tensor, $\boldsymbol{\Theta}$, the expansion scalar, Θ, the shear, $\boldsymbol{\sigma}$, the vorticity, $\boldsymbol{\omega}$, and the acceleration, $\boldsymbol{a}$. Using $\boldsymbol{\sigma}$ and $\boldsymbol{\omega}$, one can also define the squared scalar shear,

$$\sigma^2 = \frac{1}{2}\,\sigma^{\mu\nu}\,\sigma_{\mu\nu}, \tag{5.15}$$

and the squared scalar vorticity,

$$\omega^2 = \frac{1}{2}\,\omega^{\mu\nu}\,\omega_{\mu\nu}. \tag{5.16}$$

Note that both are positive-definite.

Stress-Energy Tensor and Conservation Laws

One can decompose the stress-energy tensor as in (3.81), or one can decompose the tensor as follows:

$$\begin{aligned} T_{\mu\nu} &= \delta^\alpha{}_\mu\,\delta^\beta{}_\nu\,T_{\alpha\beta} = (b^\alpha{}_\mu - u^\alpha\,u_\mu)\,(b^\beta{}_\nu - u^\beta\,u_\nu)\,T_{\alpha\beta} \\ &= b^\alpha{}_\mu\,b^\beta{}_\nu\,T_{\alpha\beta} - 2\,u_{(\nu}b^\alpha{}_{\mu)}\,u^\beta\,T_{\alpha\beta} + u^\alpha u^\beta u_\mu u_\nu\,T_{\alpha\beta}\,, \end{aligned} \tag{5.17}$$

which we can written as

$$T_{\mu\nu} = \rho\,u_\mu\,u_\nu + 2\,q_{(\mu}\,u_{\nu)} + p\,b_{\mu\nu} + \pi_{\mu\nu}, \tag{5.18}$$

where

$$\rho := u^\mu u^\nu\,T_{\mu\nu}\,, \quad q_\mu := -b^\alpha{}_\mu\,u^\beta\,T_{\alpha\beta}\,, \quad p\,b_{\mu\nu} + \pi_{\mu\nu} := b^\mu{}_\alpha\,b^\nu{}_\beta\,T_{\mu\nu}\,, \quad b^{\mu\nu}\pi_{\mu\nu} = 0\,.$$

Here, ρ is the energy density of the fluid in the fluid rest frames, $\boldsymbol{q}$ is the spatial heat flux vector, p is the isotropic pressure, and $\boldsymbol{\pi}$ is the spatial and traceless anisotropic stress mentioned in chapter 1.

Decomposing the stress-energy tensor with respect to the normal frames, as done in (3.81), we find (in components)

$$T_{\mu\nu} = E\, n_\mu n_\nu + 2\, n_{(\mu}\, J_{\nu)} + S_{\mu\nu}. \tag{5.19}$$

By using (5.5) we relate the scalar quantities, E and $S \equiv S^{\mu}{}_{\mu}$, of both frames as

$$E = \gamma^2 \rho + (\gamma^2 - 1)\, p + 2\, \gamma\, v^\mu\, q_\mu + v^\mu\, v^\nu\, \pi_{\mu\nu}\,, \tag{5.20}$$

$$S = (\gamma^2 - 1)\, \rho + (\gamma^2 + 2)\, p + 2\, \gamma\, v^\mu\, q_\mu + v^\mu\, v^\nu\, \pi_{\mu\nu}\,. \tag{5.21}$$

Using the conservation of stress-energy equation, $\nabla_\nu\, T^{\mu\nu} = 0$, along with (5.18) and the kinematic variables, we find the energy conservation law[5]:

$$u_\mu \nabla_\nu\, T^{\mu\nu} = 0 \iff u^\alpha \nabla_\alpha\, \rho + \Theta\, (\rho + p) = -(\, a_\mu\, q^\mu + \nabla_\mu q^\mu + \pi^{\mu\nu} \sigma_{\mu\nu}\,)\,, \tag{5.22}$$

and the momentum conservation law:

$$\begin{aligned} &b_{\alpha\mu} \nabla_\nu\, T^{\mu\nu} = 0 \iff \\ &a_\alpha = -\frac{1}{\rho + p}\Big(b^{\alpha}{}_{\mu} \nabla_\alpha\, p + b_{\mu\alpha}\, u^\sigma \nabla_\sigma\, q^\alpha + \frac{4}{3}\, \Theta\, q_\mu \\ &\qquad\qquad + q^\alpha (\sigma_{\alpha\mu} + \omega_{\alpha\mu}) + b_{\mu\alpha} \nabla_\beta\, \pi^{\alpha\beta} \Big) \end{aligned} \tag{5.23}$$

These conservation laws are accompanied by the conservation of the *rest mass density*, μ, of the fluid in the fluid rest frame:

$$\nabla_\nu\, (\mu\, u^\nu) = 0, \quad \text{or,} \quad u^\nu \nabla_\nu\, \mu + \Theta\, \mu = 0. \tag{5.24}$$

Time derivatives

In the decomposition of spacetime so far, we have implied the existence of two times, in particular, the coordinate time, t and the fluid proper time, τ. Furthermore, as can be seen in Figure 5.1, there are three timelike congruences. This means there can be several definitions of time derivatives. The ones we shall use here are:

- The covariant derivative along the fluid flow lines; $u^\mu \nabla_\mu \boldsymbol{T}$, for any tensor field $\boldsymbol{T}$. We shall denote this with an overdot only using the comoving and Lagrangian description. This is because in the comoving description (as described below) this derivative aligns with the proper time derivative.

- The comoving derivative along the fluid flow lines according to the proper time, $\mathrm{d}/\mathrm{d}\tau$.

[5]When deriving this relation, the last term on the right-hand side comes from the fact that $\boldsymbol{\pi}$ is a symmetric tensor, it is orthogonal to $\boldsymbol{u}$.

- The comoving derivative along the fluid flow lines according to the coordinate time, t, $\mathrm{d}/\mathrm{d}t$.
- The partial coordinate time derivative along the vector $\boldsymbol{\partial_t}$. Note that these are the integral curves of constant x^i which we denote by $\partial_t\big|_{x^i}$.

For any tensor field, $\boldsymbol{T} = T^{\mu\nu\cdots}{}_{\alpha\beta\ldots}\,\boldsymbol{\partial}_\mu\otimes\boldsymbol{\partial}_\nu\otimes\cdots\otimes\mathbf{d}x^\alpha\otimes\mathbf{d}x^\beta\otimes\ldots$ as decomposed in the coordinates $(t,\, x^i)$, the last three time derivatives are related by

$$\frac{\mathrm{d}\,T^{\mu\nu\cdots}{}_{\alpha\beta\ldots}}{\mathrm{d}t} = \frac{\partial\,T^{\mu\nu\cdots}{}_{\alpha\beta\ldots}}{\partial t}\bigg|_{x^i} + V^i\,\frac{\partial\,T^{\mu\nu\cdots}{}_{\alpha\beta\ldots}}{\partial x^i}, \tag{5.25}$$

and

$$\frac{\mathrm{d}\,T^{\mu\nu\cdots}{}_{\alpha\beta\ldots}}{\mathrm{d}\tau} = \frac{\gamma}{N}\,\frac{\mathrm{d}\,T^{\mu\nu\cdots}{}_{\alpha\beta\ldots}}{\mathrm{d}t}. \tag{5.26}$$

We shall also introduce comoving (or Lagrangian) spatial coordinates, $\boldsymbol{X} = \{X^i\}$. These coordinates label the fluid elements in contrast to the Eulerian coordinates we have used thus far, $\boldsymbol{x} = \{x^i\}$ which are the positions of these elements at time t. These two coordinates coincide on the 'initial hypersurface' where $t = t_i$. For $t > t_i$, however, the comoving coordinates of each fluid element remain constant along the fluid flow line, whereas the reference coordinates, $\boldsymbol{x}$ do not. We relate the two sets of coordinates by a family of diffeomorphisms parameterized by coordinate time t,

$$\boldsymbol{X} \mapsto \boldsymbol{x} = \boldsymbol{f}(t, \boldsymbol{X}), \tag{5.27}$$

with $\boldsymbol{f}(t_i, \boldsymbol{X}) = X$. We also define the Jacobian associated with the diffeomorphism:

$$J\,(t, \boldsymbol{X}) := \det\frac{\partial\,\boldsymbol{f}(t, \boldsymbol{X})}{\partial \boldsymbol{X}}. \tag{5.28}$$

As an example, if one assumes isotropy and homogeneity then the function is a map from $\mathbb{R}^3 \to \mathbb{R}^3$, and we have $\boldsymbol{x} = a(t)\boldsymbol{X}$, where $a(t)$ is the Friedmann scale factor. The time derivative with respect to these comoving coordinates is related to the time derivative with respect to the reference coordinates by

$$\frac{\partial\,T^{\mu\nu\cdots}{}_{\alpha\beta\ldots}}{\partial t}\bigg|_{X^i} = \frac{\partial\,T^{\mu\nu\cdots}{}_{\alpha\beta\ldots}}{\partial t}\bigg|_{x^i} + V^i\,\frac{\partial\,T^{\mu\nu\cdots}{}_{\alpha\beta\ldots}}{\partial x^i}. \tag{5.29}$$

One should note, however, that this description is only possible before shell-crossing as there is no possible way for $\boldsymbol{f}$ to be a diffeomorphism once geodesics cross.

5.2 Comoving and Lagrangian Description

Comoving Description

We define the comoving description by setting the spatial part of $\boldsymbol{u}$ to zero. This corresponds to setting the shift as $\boldsymbol{\beta} = N\,\boldsymbol{v}$ and consequently, $\boldsymbol{V} = 0$. This

choice of foliation corresponds to the spatial coordinates propagating along the fluid flow lines, meaning the comoving or Lagrangian coordinates are a natural choice[6].

Using the coordinates, (t, X^i), of the comoving description, the 4–velocity of the fluid has the components

$$u^{\mu} = \frac{N}{\gamma}\,(1,\,0)\,, \tag{5.30}$$

and dual components

$$u_{\mu} = \Big(-\frac{N}{\gamma},\,\gamma v_i\Big). \tag{5.31}$$

The line element, (5.4) reduces to

$$\mathrm{d}s^2 = -\frac{N^2}{\gamma^2}\,\mathrm{d}t^2 + 2\,N v_i\,\mathrm{d}t\,\mathrm{d}X^i + h_{ij}\,\mathrm{d}X^i\mathrm{d}X^j\,. \tag{5.32}$$

Furthermore, in the comoving description, the projector $\boldsymbol{b}$ components are,

$$b_{00} = 0, \quad b_{0i} = 0, \quad b_{ij} = h_{ij} + \gamma^2\,v_i\,v_j. \tag{5.33}$$

Finally, we shall also introduce the kinematic quantities in this particular "gauge" or "foliation choice".

Firstly, in any coordinate system may rewrite the vorticity as

$$\omega_{\mu\nu} = u_{[\mu}\,a_{\nu]} + \nabla_{[\mu}\,u_{\nu]} = u_{[\mu}\,a_{\nu]} + \partial_{[\mu}\,u_{\nu]}. \tag{5.34}$$

From the orthogonality of the vorticity tensor and the fluid four velocity (in the comoving description) the following identity can be constructed:

$$0 = \omega_{\mu i}u^{\mu} = \frac{1}{2}\,(u_0\,a_i - u_i\,a_0) + \frac{1}{2}(\partial_0\,u_i - \partial_i\,u_0). \tag{5.35}$$

Furthermore, in any comoving description we have

$$a_0 = u^0\,\nabla_0\,u_0 + u^i\,\nabla_i\,u_0 = 0, \tag{5.36}$$

therefore, by rearranging (5.35) one can write the spatial components of the 4–acceleration as

$$a_i = \frac{\gamma}{N}\left(\frac{\mathrm{d}}{\mathrm{d}t}u_i + \frac{\gamma}{N}\,\partial_i\left(\frac{N}{\gamma}\right)\right). \tag{5.37}$$

We have used $\partial_t \equiv \partial_t\,|_{X^i} = \mathrm{d}/\mathrm{d}t$ which is true only in the a comoving description. Substituting this back into the equation for vorticity, the non-vanishing components of the vorticity are found to be

$$\omega_{ij} = \frac{\gamma}{N}\,u_{[i}\,\frac{\mathrm{d}}{\mathrm{d}t}u_{j]} + \frac{N}{\gamma}\,\partial_{[i}\left(\frac{\gamma}{N}\,u_{j]}\right). \tag{5.38}$$

[6]We refer to this as the "weak" Lagrangian description as there have been no constraints placed on the coordinate time.

The expansion tensor can be related to the Lie derivative of the projector[7], $\boldsymbol{b}$ along the fluid flow *in any coordinate system* according to

$$\begin{aligned}(\mathcal{L}_{\boldsymbol{u}}\boldsymbol{b})_{\mu\nu} &= u^{\alpha}\nabla_{\alpha}\, b_{\mu\nu} + b_{\alpha\nu}\nabla_{\mu}\, u^{\alpha} + b_{\mu\alpha}\nabla_{\nu}u^{\alpha} \\ &= 2\, u_{(\mu}\, a_{\nu)} + 2\,\nabla_{(\mu}\, u_{\nu)} = 2\,\Theta_{\mu\nu}.\end{aligned} \tag{5.39}$$

Therefore, in the comoving description, we can write the expansion tensor as

$$\Theta_{ij} = \frac{1}{2}u^{0}\,\partial_{0}\, b_{ij} = \frac{1}{2}\frac{\gamma}{N}\frac{\mathrm{d}}{\mathrm{d}t}b_{ij}. \tag{5.40}$$

The expansion scalar can thus be written as

$$\Theta = \frac{1}{2}\frac{\gamma}{N}\, b^{ij}\frac{\mathrm{d}}{\mathrm{d}t}\, b_{ij}. \tag{5.41}$$

Furthermore, by defining the 'representative length' l in the fluid rest frames, we can define a 'Hubble parameter'[8], $3\dot{l}/l := \Theta$. Thus we may write

$$\Theta = \frac{3}{l}\frac{\gamma}{N}\frac{\mathrm{d}l}{\mathrm{d}t}, \quad \text{and} \quad \sigma_{ij} = \frac{1}{2}\frac{\gamma}{N}\, l^{2}\frac{\mathrm{d}}{\mathrm{d}t}(l^{-2}\, b_{ij}). \tag{5.42}$$

Lagrangian Description

One may choose a foliation that allows the hypersurfaces to be labelled by the proper time τ of the fluid instead of the coordinate time, t. This class of foliations is referred to as the *fluid proper time foliations*. This choice of foliation may be realised by noting the evolution of the proper time relative to the coordinate time, $\mathrm{d}\tau/\mathrm{d}t = N/\gamma$. An obvious choice, therefore, would be to select[9] $N = \gamma$. For such foliations the hypersurfaces cannot be fluid orthogonal, in other words, a tilt must be present, except in the case of irrotational geodesic flow, which is the case for irrotational dust (for example as in the LTB model). In general, such a tilt may grow as time passes and become large. A large tilt may even cause the slices to not be spacelike everywhere. Therefore, for an analysis using the Lagrangian description we must restrict ourselves to the part of the whole spacetime where the hypersurfaces remain spacelike.

[7]Recall that the Lie derivative of the induced metric on the normal frames was related to the extrinsic curvature. Furthermore, recall that the expansion tensor and the extrinsic curvature are the same in the case of a hypersurface orthogonal flow.

[8]Recall that the expansion scalar is related to the Hubble parameter.

[9]In general, we define the proper time through

$$\tau(t, X^{i}) := \tau_{i} + \int_{t_{\Sigma_{i}}}^{t} \frac{N(\tilde{t}, X^{i})}{\gamma(\tilde{t}, X^{i})}\,\mathrm{d}\tilde{t}\,,$$

where Σ_{i} is the initial hypersurface parameterized by $t = t_{\Sigma_{i}}$ and τ_{i} is the value of τ on the initial hypersurface. Thus, by selecting $N = \gamma$ we find that the change in proper time from the initial hypersurface to another along the fluid flow is equal to the change in coordinate time.

In the coordinates (τ, X^i) the components of the 4–velocity vector are

$$u^{\mu} = (1,\, 0), \tag{5.43}$$

with corresponding dual components

$$u_{\mu} = (-1,\, \gamma v_i). \tag{5.44}$$

The line element (5.4) becomes

$$\mathrm{d}s^2 = -\mathrm{d}t^2 + 2\,\gamma v_i\,\mathrm{d}X^i\,\mathrm{d}t + h_{ij}\,\mathrm{d}X^i\mathrm{d}X^j\,. \tag{5.45}$$

5.3 Fluid-Extrinsic Scalar Averaging

Instead of assuming that the Universe expands according to the Friedmann scale factor $a(t)$ on any scale, we follow the Buchert averaging scheme. This results in a "effective scale factor" allowing inhomogeneities to develop in the evolution of the domain. We shall introduce Buchert averaging here, specifically, extrinsic averaging. We refer to this as extrinsic averaging as we are not performing the averaging in the rest-frame of the fluid. More precisely, these equations are also dubbed the "extrinsic" averaged equations because to derive them, we will use the Einstein equations projected along $\boldsymbol{n}$ instead of $\boldsymbol{u}$. That is, we will use the dynamical equations from Chapter 3 in a slightly different form:

$$\partial_t\,|_{x^i}\; h_{ij} = -2N\,\mathcal{K}_{ij} + D_j\beta_i + D_i\beta_j\,, \tag{5.46}$$

$$\begin{aligned}\partial_t\,|_{x^i}\; \mathcal{K}^i{}_j =& N\left(\mathcal{R}^i{}_j + \mathcal{K}\mathcal{K}^i{}_j + 4\pi G[(S-E)\,\delta^i{}_j - 2S^i{}_j] - \Lambda\,\delta^i{}_j\right)\\ &-D^iD_jN + \beta^kD_k\mathcal{K}^i{}_j + \mathcal{K}^i{}_kD_j\beta^k - \mathcal{K}^k{}_jD_k\beta^j,\end{aligned} \tag{5.47}$$

which are (effectively) equations[10] (3.92) and (3.86) respectively.

Buchert averaging is over a spatial (compact) domain lying in the hypersurfaces — this domain is transported along the congruence of the fluid. This form of transporting the domain ensures the domain encloses the same collection of fluid elements at all times. We denote the domain containing this collection with respect to the reference coordinates — at a given time — by $\mathcal{D}_{\boldsymbol{x}}$ and with respect to the comoving coordinates by $\mathcal{D}_{\boldsymbol{X}}$. This distinction is important as $\mathcal{D}_{\boldsymbol{x}}$ depends on time whereas $\mathcal{D}_{\boldsymbol{X}}$ by definition does not. For this analysis, we shall not use the Lagrangian description, nor the comoving description in order to preserve the all degrees of freedom in the splitting space and time.

[10]The second equation here is not exactly (3.86) as the indices are mixed. However, one may obtain this by considering the product rule for $\partial_t\,|_{x^i}\,(h^{ik}\,\mathcal{K}_{kj})$.

5.3.1 Volume of Domains and Their Time-Evolution

The Riemannian volume of a spatial domain $\mathcal{D}$ within the hypersurface is given by

$$\mathcal{V}_{\mathcal{D}}(t) = \int_{\mathcal{D}_{\boldsymbol{x}}} n^{\mu}\, \mathrm{d}\,\sigma_{\mu} = \int_{\mathcal{D}_{\boldsymbol{x}}} \sqrt{h\,(t, x^{i})}\, \mathrm{d}^{3}x, \tag{5.48}$$

where h is the determinant of the spatial metric, $h := \det(h_{ij})$, and $\mathrm{d}\,\sigma_{\mu}$ is the oriented volume element on the hypersurface, i.e., $\mathrm{d}\,\sigma_{\mu} := -n_{\mu}\sqrt{h}\,\mathrm{d}^{3}x$. Hence, $n^{\mu}\,\mathrm{d}\sigma_{\mu} = -n^{\mu}\,n_{\mu}\sqrt{h}\,\mathrm{d}^{3}x = \sqrt{h}\,\mathrm{d}^{3}x$. For an expanding Universe the volume of the domain in consideration will also increase, thus we wish to find an expression for the change in the Riemannian volume over time.

First let us examine

$$\frac{\mathrm{d}}{\mathrm{d}t}\,\mathcal{V}_{\mathcal{D}} = \frac{\mathrm{d}}{\mathrm{d}t}\int_{\mathcal{D}_{\boldsymbol{x}}} \sqrt{h}\,\mathrm{d}^{3}x. \tag{5.49}$$

To proceed beyond this step is complicated because the operators $\mathrm{d}/\mathrm{d}t$ and $\int_{\mathcal{D}_{\boldsymbol{x}}} \cdot\, \mathrm{d}^{3}x$ do not commute as the limits of integration which are determined by $\mathcal{D}_{\boldsymbol{x}}$ depend on (in general) t. A physical understanding of why these operators are not suitable follows from the fact that the fluid is moving with respect to the reference coordinates (t, x^{i}) and the domain moves *with* the fluid.

If we wish to have the coordinate time derivative and spatial volume integration operators to commute, we require the fluid to be 'not moving' with respect to the spatial coordinates, the natural choice then is to transform the integrand to Lagrangian coordinates to eliminate the time-dependence. We use

$$x^{i} = f^{\,i}\,(t, \boldsymbol{X})\,, \tag{5.50}$$

and

$$\mathrm{d}^{3}\,x = \det\left(\frac{\partial \boldsymbol{f}(t, \boldsymbol{X})}{\partial \boldsymbol{X}}\right)\mathrm{d}^{3}X = J\,(t, \boldsymbol{X})\,\mathrm{d}^{3}X,\,. \tag{5.51}$$

The domain transforms as $\mathcal{D}_{\boldsymbol{x}} \to \mathcal{D}_{\boldsymbol{X}} = \boldsymbol{f}^{-1}\,(\mathcal{D}_{\boldsymbol{x}})$. Inserting all of these transformations into (5.48) we obtain:

$$\mathcal{V}_{\mathcal{D}}(t) = \int_{\mathcal{D}_{\boldsymbol{X}}} \sqrt{h(\,t, f^{i}(\,t, \boldsymbol{X}\,))}\, J\,(t, \boldsymbol{X})\,\mathrm{d}^{3}\,X. \tag{5.52}$$

The boundaries are now fixed with respect to the fluid, therefore, we may now commute $\mathrm{d}/\mathrm{d}t$ and $\int_{\mathcal{D}_{\boldsymbol{X}}} \cdot\, \mathrm{d}^{3}X$:

$$\frac{\mathrm{d}}{\mathrm{d}t}\,\mathcal{V}_{\mathcal{D}}(t) = \int_{\mathcal{D}_{\boldsymbol{X}}} \frac{\mathrm{d}}{\mathrm{d}t}\left(\sqrt{h(\,t, f^{i}(\,t, \boldsymbol{X}\,))}\, J\,(t, \boldsymbol{X})\right)\mathrm{d}^{3}\,X. \tag{5.53}$$

We are now free to change back to the reference coordinates, x^{i} and obtain:

$$\frac{\mathrm{d}}{\mathrm{d}t}\,\mathcal{V}_{\mathcal{D}}(t) = \int_{\mathcal{D}_{\boldsymbol{x}}} \frac{\mathrm{d}}{\mathrm{d}t}\left(J\sqrt{h}\right)J^{-1}\,\mathrm{d}^{3}\,x = \int_{\mathcal{D}_{\boldsymbol{x}}} \left(J^{-1}\,\sqrt{h}\,\frac{\mathrm{d}}{\mathrm{d}t}J + \frac{\mathrm{d}}{\mathrm{d}t}\,\sqrt{h}\right)\mathrm{d}^{3}\,x, \tag{5.54}$$

where we have used $J^{-1}\,J = 1$.

To simplify this expression further, we require an expression for the Eulerian velocity in terms of the diffeomorphism, $\boldsymbol{f}$. To reformulate the Eulerian velocity consider the coordinate time derivative of the determinant of the Jacobian matrix ($\boldsymbol{J}$),

$$\partial_t\,|_{X^i}\,\det\!\left(\frac{\partial x^i}{\partial X^j}\right) = \partial_t\,|_{X^i}\,\det(J^{\,i}{}_{j}) = \partial_t\,|_{X^i}\,J. \tag{5.55}$$

Using the Jacobi identity we find

$$\begin{aligned}\partial_t\,|_{X^i}\,J &= \det\boldsymbol{J}\,\mathrm{tr}\left(\boldsymbol{J}^{-1}\,\partial_t\,|_{X^i}\,\boldsymbol{J}\right) = J\,\mathrm{tr}\left(\frac{\partial X^j}{\partial x^k}\frac{\partial}{\partial X^j}\left(\partial_t\,|_{X^i}\,f^i\right)\right)\\ &= J\,\frac{\partial}{\partial x^i}\left(\,\partial_t\,|_{X^i}\,f^i\right) = J\,\partial_i\,V^i.\end{aligned} \tag{5.56}$$

Furthermore, recalling (5.25), (5.54) simplifies to,

$$\begin{aligned}\frac{\mathrm{d}}{\mathrm{d}t}\,\mathcal{V}_{\mathcal{D}}\,(t) &= \int_{\mathcal{D}_{\boldsymbol{x}}}\left(\,\partial_t|_{x^i}\,\sqrt{h} + V^k\,\partial_k\sqrt{h} + \partial_k\,V^k\,\sqrt{h}\right)\mathrm{d}^3\,x\\ &= \int_{\mathcal{D}_{\boldsymbol{x}}}\left(\frac{1}{2}\,h^{ij}\,\partial_t|_{x^i}\,h_{ij} + \frac{1}{2}\,h^{ij}\,V^{\,k}\,\partial_k\,h_{ij} + \partial_k V^{\,k}\right)\sqrt{h}\,\mathrm{d}^3\,x,\end{aligned} \tag{5.57}$$

where we have used the Jacobi identity, as in (5.56) for the last equality – in order to differentiate $\sqrt{h}$. The last two terms can also be simplified by noting

$$\begin{aligned}D_k V^k &= \partial_k V^k + \Gamma^k{}_{kl}V^l\\ &= \partial_k V^k + \frac{1}{2}\,h^{ki}\left(h_{ik,l} + h_{il,k} - h_{kl,i}\right)V^l\\ &= \partial_k V^k + \frac{1}{2}\,h^{ij}\,V^k\,\partial_k\,h_{ij}.\end{aligned} \tag{5.58}$$

Finally, using the trace of (5.46) and (5.58), (5.57) can be simplified to:

$$\begin{aligned}\frac{\mathrm{d}}{\mathrm{d}t}\mathcal{V}_{\mathcal{D}} &= \int_{\mathcal{D}_{\boldsymbol{x}}}\left(\,-N\mathcal{K} + D_i\,V^{\,i} + D_i\,\beta^{\,i}\right)\sqrt{h}\,\mathrm{d}^3x\\ &= \int_{\mathcal{D}_{\boldsymbol{x}}}\left(\,-N\mathcal{K} + D_i\,(\,Nv^{\,i}\,)\right)\sqrt{h}\,\mathrm{d}^3x.\end{aligned} \tag{5.59}$$

5.3.2 Scalar Averaging and Commutation Rule

We define the extrinsic average of any scalar field[11] ψ on the compact comoving domain $\mathcal{D}$ as

$$\langle\,\psi\,\rangle_{\mathcal{D}}\,(t) := \frac{1}{\mathcal{V}_{\mathcal{D}}}\int_{\mathcal{D}}\psi\,n^{\mu}\,\mathrm{d}\sigma_{\,\mu} = \frac{1}{\mathcal{V}_{\mathcal{D}}}\int_{\mathcal{D}_{\boldsymbol{x}}}\psi\,(t,x^{\,i})\,\sqrt{h}\,\mathrm{d}^3x. \tag{5.60}$$

[11]This should not be confused with the curvature perturbation scalar from perturbation theory.

Noting that all of the terms in (5.59) are scalars, we can apply this definition to (5.59):

$$\frac{1}{\mathcal{V}_{\mathcal{D}}}\frac{\mathrm{d}}{\mathrm{d}t}\mathcal{V}_{\mathcal{D}} = \Big\langle -N\mathcal{K} + D_i\,(\,Nv^i\,)\Big\rangle_{\mathcal{D}}. \tag{5.61}$$

Using this we may find the coordinate-time derivative of an averaged scalar:

$$\begin{aligned}\frac{\mathrm{d}}{\mathrm{d}t}\langle\,\psi\,\rangle_{\mathcal{D}} &= -\left(\frac{1}{\mathcal{V}_{\mathcal{D}}}\int_{\mathcal{D}_{\boldsymbol{x}}}\psi\,\sqrt{h}\,\mathrm{d}^3x\right)\left(\frac{1}{\mathcal{V}_{\mathcal{D}}}\frac{\mathrm{d}}{\mathrm{d}t}\mathcal{V}_{\mathcal{D}}\right) + \frac{1}{\mathcal{V}_{\mathcal{D}}}\frac{\mathrm{d}}{\mathrm{d}t}\int_{\mathcal{D}_{\boldsymbol{x}}}\psi\,\sqrt{h}\,\mathrm{d}^3x \\ &= -\langle\,\psi\,\rangle_{\mathcal{D}}\,\Big\langle -N\mathcal{K} + D_i\,(\,Nv^i\,)\Big\rangle_{\mathcal{D}} + \frac{1}{\mathcal{V}_{\mathcal{D}}}\frac{\mathrm{d}}{\mathrm{d}t}\int_{\mathcal{D}_{\boldsymbol{x}}}\psi\,\sqrt{h}\,\mathrm{d}^3x.\end{aligned} \tag{5.62}$$

The second term on the right-hand side can be expanded and simplified further by taking similar steps to the derivation of the coordinate-time derivative of the Riemannian volume. We demonstrate the first step:

$$\begin{aligned}\frac{\mathrm{d}}{\mathrm{d}t}\int_{\mathcal{D}_{\boldsymbol{x}}}\psi\,\sqrt{h}\,\mathrm{d}^3x &= \frac{\mathrm{d}}{\mathrm{d}t}\int_{\mathcal{D}_{\boldsymbol{X}}}\psi\,(t,\boldsymbol{f})\,\sqrt{h}\,J\;\mathrm{d}^3X \\ &= \int_{\mathcal{D}_{\boldsymbol{X}}}\frac{\mathrm{d}}{\mathrm{d}t}\Big(\psi\,(t,\boldsymbol{f})\,\sqrt{h}\,J\Big)\;\mathrm{d}^3X.\end{aligned}$$

Using the product rule and the steps used previously, we find,

$$\frac{1}{\mathcal{V}_{\mathcal{D}}}\frac{\mathrm{d}}{\mathrm{d}t}\int_{\mathcal{D}_{\boldsymbol{x}}}\psi\,\sqrt{h}\,\mathrm{d}^3x = \Big\langle\frac{\mathrm{d}}{\mathrm{d}t}\,\psi\Big\rangle_{\mathcal{D}} + \Big\langle\Big(-N\mathcal{K} + D_i\,(\,Nv^i\,)\,\psi\Big)\Big\rangle_{\mathcal{D}}. \tag{5.63}$$

Inserting this back into (5.62) we obtain the commutation rule:

$$\begin{aligned}\frac{\mathrm{d}}{\mathrm{d}t}\langle\,\psi\,\rangle_{\mathcal{D}} - \Big\langle\frac{\mathrm{d}}{\mathrm{d}t}\,\psi\Big\rangle_{\mathcal{D}} &= -\langle\,\psi\,\rangle_{\mathcal{D}}\,\Big\langle -N\mathcal{K} + D_i\,(\,Nv^i\,)\Big\rangle_{\mathcal{D}} \\ &\quad + \Big\langle\Big(-N\mathcal{K} + D_i\,(\,Nv^i\,)\Big)\,\psi\Big\rangle_{\mathcal{D}}.\end{aligned} \tag{5.64}$$

This is referred to as the 'the commutation rule' because it is the difference of two operators, the time evolution and spatial averaging. This is valid for any 3+1 foliation of spacetime and any scalar ψ. One may note that this commutation rule does not depend on the shift vector, therefore, is also independent of the propagation of the spatial coordinates. It may seem as there is a dependence on the shift through the (Nv^i) term. However, this term is only equal to the shift vector in the weak Lagrangian description, and the whole derivation here has been fully general.

The commutation rule can also be formulated in terms of the kinematic variables. This is done by noting

$$\begin{aligned}D_i\,(\,Nv^i\,) &= v^i\,D_i\,N + ND_i\,v^i \\ &= N\,n^\alpha v^i\nabla_\alpha\,n_i + ND_i\,v^i \\ &= N\,n^\alpha(\nabla_\alpha(v^i n_i) - n_i\nabla_\alpha\,v^i) + ND_i\,v^i \\ &= 0 + ND_i\,v^i = N\nabla_\nu\,v^\nu,\end{aligned} \tag{5.65}$$

where we have used $D_i N = N a_i$ (introduced and used in (3.68)), the fact that $n_i = 0$, and $v^0 = 0$ for the last equality[12]. With the use of (5.65) and $\mathcal{K} = -\nabla_\nu n^\nu$, we obtain:

$$-N\mathcal{K} + D_i(Nv^i) = N\left(\nabla_\nu(n^\nu + v^\nu)\right) = \frac{N}{\gamma}\Theta - \frac{1}{\gamma}\frac{\mathrm{d}\gamma}{\mathrm{d}t}, \tag{5.66}$$

where we have used (5.5) for the last equality. Therefore, the commutation rule can be written as

$$\frac{\mathrm{d}}{\mathrm{d}t}\langle\psi\rangle_{\mathcal{D}} - \left\langle\frac{\mathrm{d}}{\mathrm{d}t}\psi\right\rangle_{\mathcal{D}} = -\langle\psi\rangle_{\mathcal{D}}\left\langle\frac{N}{\gamma}\Theta - \frac{1}{\gamma}\frac{\mathrm{d}\gamma}{\mathrm{d}t}\right\rangle_{\mathcal{D}} + \left\langle\left(\frac{N}{\gamma}\Theta - \frac{1}{\gamma}\frac{\mathrm{d}\gamma}{\mathrm{d}t}\right)\psi\right\rangle_{\mathcal{D}}. \tag{5.67}$$

5.3.3 Extrinsically Averaged Evolution Equations

To make a comparison with the standard evolution equations of the FLRW model, we define a scale factor. Buchert [3, 4] refers to this as the *extrinsic effective scale factor* $a_{\mathcal{D}}$ which is defined as

$$a_{\mathcal{D}}(t) := \left(\frac{\mathcal{V}_{\mathcal{D}}(t)}{\mathcal{V}_{\mathcal{D}_i}}\right)^{1/3}, \tag{5.68}$$

where $\mathcal{V}_{\mathcal{D}_i}$ refers to volume of the domain at the 'initial time' t_i. We may then reformulate the domain volume expansion rate as

$$\frac{1}{a_{\mathcal{D}}}\frac{\mathrm{d}a_{\mathcal{D}}}{\mathrm{d}t} = \frac{1}{3}\left\langle -N\mathcal{K} + D_i(Nv^i)\right\rangle_{\mathcal{D}}. \tag{5.69}$$

To derive the first effective evolution equation let us consider the Hamiltonian constraint (3.88):

$$\mathcal{R} + \mathcal{K}^2 - \mathcal{K}^{ij}\mathcal{K}_{ij} = 16\pi GE + 2\Lambda. \tag{5.70}$$

We can rearrange this equation and multiply through by N^2 to obtain

$$N^2\mathcal{R} + N^2(\mathcal{K}^2 - \mathcal{K}^{ij}\mathcal{K}_{ij}) - N^2 16\pi GE - 2N^2\Lambda = 0. \tag{5.71}$$

We can now "take an average" of this equation by using (5.60):

$$-\langle N^2\mathcal{R}\rangle_{\mathcal{D}} - \langle N^2(\mathcal{K}^2 - \mathcal{K}^{ij}\mathcal{K}_{ij})\rangle_{\mathcal{D}} + \langle N^2 16\pi GE\rangle_{\mathcal{D}} + \langle 2N^2\Lambda\rangle_{\mathcal{D}} = 0. \tag{5.72}$$

[12]One cannot immediately assume that $\nabla_0 v^0 = 0$. However, expanding this covariant derivative, we do in fact obtain zero as the result.

If we now square (5.69) and then combine it with (5.72) (effectively adding zero) we obtain

$$3\Big(\frac{1}{a_{\mathcal{D}}}\frac{\mathrm{d}a_{\mathcal{D}}}{\mathrm{d}t}\Big)^2 = \frac{1}{2}\Big(\frac{2}{3}\Big\langle N\mathcal{K} + D_i\,(\,Nv^i\,)\Big\rangle_{\mathcal{D}}^2 - \Big\langle N^2(\,\mathcal{K}^2 - \mathcal{K}^{ij}\mathcal{K}_{ij}\,)\Big\rangle_{\mathcal{D}}\Big) + 8\pi G\,\langle\, N^2 E\,\rangle_{\mathcal{D}} + \langle\, N^2\Lambda\,\rangle_{\mathcal{D}} - \frac{1}{2}\,\langle\, N^2\,\mathcal{R}\,\rangle_{\mathcal{D}}\,. \tag{5.73}$$

We define the kinematical backreaction as:

$$\mathcal{Q}_{\mathcal{D}} = -\frac{2}{3}\Big\langle N\mathcal{K} + D_i\,(\,Nv^i\,)\Big\rangle_{\mathcal{D}}^2 + \Big\langle N^2(\,\mathcal{K}^2 - \mathcal{K}^{ij}\mathcal{K}_{ij}\,)\Big\rangle_{\mathcal{D}}, \tag{5.74}$$

so that the first two terms in (5.73) are $\mathcal{Q}_{\mathcal{D}}$. Substituting the definition of energy (5.20) into (5.73) we find the first extrinsically averaged evolution equation,

$$3\Big(\frac{1}{a_{\mathcal{D}}}\frac{\mathrm{d}a_{\mathcal{D}}}{\mathrm{d}t}\Big)^2 = -\frac{1}{2}\mathcal{Q}_{\mathcal{D}} - \frac{1}{2}\langle\, N^2\,\mathcal{R}\,\rangle_{\mathcal{D}} + \langle\, N^2\,\rangle_{\mathcal{D}}\,\Lambda + 8\pi G\langle\, N^2\rho\,\rangle_{\mathcal{D}} - \frac{1}{2}\mathcal{T}_{\mathcal{D}}, \tag{5.75}$$

where $\mathcal{T}_{\mathcal{D}}$ is the stress-energy backreaction term, defined as

$$\mathcal{T}_{\mathcal{D}} := -16\pi G\left\langle N^2\Big((\gamma^2-1)\,(\rho+p) + 2\,\gamma v^{\alpha}q_{\alpha} + v^{\alpha}\,v^{\beta}\pi_{\alpha\beta}\Big)\right\rangle_{\mathcal{D}}. \tag{5.76}$$

In the literature, it is common to define

$$H_{\mathcal{D}} := \frac{1}{a_{\mathcal{D}}}\,\frac{\mathrm{d}a_{\mathcal{D}}}{\mathrm{d}t},$$

which is an *effective Hubble parameter*.

The second effective extrinsically averaged equation is the "acceleration" equation. The original form of this equation was introduced by Buchert [4] by averaging the Raychaudhuri equation for geodesic dust flow. Here we shall use the trace of (5.47) and the commutation rule, (5.64). First, note that by differentiating (5.69) with respect to coordinate time we have,

$$3\,\frac{1}{a_{\mathcal{D}}}\frac{\mathrm{d}^2a_{\mathcal{D}}}{\mathrm{d}t^2} = 3H_{\mathcal{D}}^2 + \frac{\mathrm{d}}{\mathrm{d}t}\Big\langle -N\mathcal{K} + D_i\,(\,Nv^i\,)\Big\rangle_{\mathcal{D}}. \tag{5.77}$$

By use of the commutation rule we can expand the second term

$$\frac{\mathrm{d}}{\mathrm{d}t}\left\langle -N\mathcal{K} + D_i\,(\,Nv^i\,)\right\rangle_{\mathcal{D}} = \left\langle -\mathcal{K}\,\frac{\mathrm{d}}{\mathrm{d}t}N - N\frac{\mathrm{d}}{\mathrm{d}t}\,\mathcal{K} + \frac{\mathrm{d}}{\mathrm{d}t}D_i\,(\,Nv^i\,)\right\rangle_{\mathcal{D}} - \Big\langle -N\mathcal{K} + D_i\,(\,Nv^i\,)\Big\rangle_{\mathcal{D}}^2 + \Big\langle(-N\mathcal{K} + D_i\,(\,Nv^i\,))^2\Big\rangle_{\mathcal{D}}. \tag{5.78}$$

To simplify this expression, we change the time derivative to a partial coordinate time derivative with respect to, x^i, according to $\mathrm{d}/\mathrm{d}t = \partial/\partial_t\,|_{x^i} + V^i\,\partial_i$. Using

the trace of (5.47), allows us to expand the $(\mathrm{d}\mathcal{K}/\mathrm{d}t)$ term in (5.78). The trace of (5.47) (multiplied by N) is

$$N\,\partial_t|_{x^i}\,\mathcal{K} = N^2\left(\mathcal{R}+\mathcal{K}^2+4\pi G\left[3\,(S-E)-2\,S\right]-3\,\Lambda\right) - D^iD_i\,N+\beta^i\,D_i\,\mathcal{K}. \quad (5.79)$$

Substituting this into (5.78) and then rearranging we find the second extrinsically averaged evolution equation:

$$3\,\frac{1}{a_{\mathcal{D}}}\frac{\mathrm{d}^2a_{\mathcal{D}}}{\mathrm{d}t^2} = -4\pi G\left\langle N^2\,(\rho+3p)\right\rangle_{\mathcal{D}} + \langle\,N^2\,\rangle_{\mathcal{D}}\;\Lambda + \mathcal{Q}_{\mathcal{D}} + \mathcal{P}_{\mathcal{D}} + \frac{1}{2}\,\mathcal{T}_{\mathcal{D}}, \quad (5.80)$$

where

$$\mathcal{P}_{\mathcal{D}} := \left\langle \Big(D_i(\,Nv^i\,)\Big)^2 + \frac{\mathrm{d}}{\mathrm{d}t}\Big(D_i\,(\,Nv^i\,)\Big) - 2N\mathcal{K}\,D_i\,(\,Nv^i) - N^2\,v^iD_i\,\mathcal{K}\right\rangle_{\mathcal{D}} + \left\langle N\,D^iD_iN - \mathcal{K}\,\frac{\mathrm{d}N}{\mathrm{d}t}\right\rangle_{\mathcal{D}}, \quad (5.81)$$

is the *extrinsic dynamical backreaction*.

There are two conditions for these equations to hold, namely, the integrability and energy balance conditions. The integrability condition is for the assurance that one can integrate (5.80) to obtain (5.75). This is obtained by taking the coordinate time derivative of (5.75) and then by substituting in the expressions for (5.75) and (5.80). The source part of this condition must also satisfy the averaged energy conservation law. The relevant expressions are given in section 3.4.2 of Buchert et al. [3].

5.4 Discussion

5.4.1 Backreaction Discussion

In subsection 2.6.1 we discussed how backreaction arises from the averaging of the Einstein equations. In the previous section we used the commutation rule for extrinsically averaged scalars and found that the Friedmann analogues have extra terms than one would obtain by averaging crudely. These extra terms are precisely the backreaction terms. We note that the backreaction terms are identically zero if one chooses to use periodic boundary conditions by Gauss' theorem. Therefore, one must be careful in simulations when attempting to determine backreaction effects:

The different types of backreaction are summarised as below.

- $\mathcal{Q}_{\mathcal{D}}$: *The kinematical backreaction term.* This term was the original 'type' of backreaction to be discussed by Buchert in[13] [4]. The kinematical backreaction is so named because it was originally introduced by averaging the Raychaudhuri equation (for a geodesic congruence) where the right-hand side is given in terms of the kinematic variables $\boldsymbol{\Theta}$, $\boldsymbol{\sigma}$, and $\boldsymbol{\omega}$. For this reason, the kinematical backreaction describes the impact of inhomogeneities on the average expansion related to the variance of the expansion as well as the averaged shear, and vorticity [4, 34]. We will also encounter the kinematic variables when we discuss the intrinsic averaging approach.

  The sign of the kinematical backreaction can change the dynamics of a domain. If $\mathcal{Q}_{\mathcal{D}} > 0$ then the kinematical backreaction contributes to the acceleration of the expansion of the domain we average over. If $\mathcal{Q}_{\mathcal{D}} < 0$ then the kinematical backreaction will 'slow down' the expansion of the domain we average over and will thus contribute to deceleration. If $\mathcal{Q}_{\mathcal{D}} = 0$ then there are no inhomogeneities present in the domain.

- $\mathcal{P}_{\mathcal{D}}$: *The dynamical backreaction term.* Dynamical backreaction was introduced in [34], where a congruence of general timelike curves was used — more precisely, not necessarily geodesics — without vorticity. This meant that an acceleration term was present in the Raychaudhuri equation. For this reason, the dynamical backreaction arises from non-vanishing pressure gradients in the spatial hypersurfaces [34]. As formulated in (5.81), the link to 4–acceleration is not entirely obvious, however. The sign of the dynamical backreaction also provides us with knowledge of the dynamics of a domain. If $\mathcal{P}_{\mathcal{D}} > 0$ then the dynamical backreaction behaves as an acceleration term to the domain averaged over. If $\mathcal{P}_{\mathcal{D}} < 0$ then the dynamical backreaction contributes a deceleration term to the domain averaged over.

- $\mathcal{T}_{\mathcal{D}}$: *The stress-energy back reaction term.* This backreaction term is purely due to the tilt of the fluid 4-velocity $\boldsymbol{u}$ relative to the hypersurface normal vector, $\boldsymbol{n}$. It can be interpreted in the following ways.

  1. $\mathcal{T}_{\mathcal{D}}$ measures the difference in the energy of the fluid as measured in its rest frames relative to the values measured in the normal frames. As such, it is an average measure of the kinetic energy of the fluid as measured in the normal frames. One can show this by expressing (5.20) as

$$\begin{aligned} E - \rho &= (\gamma^2 - 1)(\rho + p) + 2\gamma v^{\alpha} q_{\alpha} + v^{\alpha} v^{\beta} \pi_{\alpha\beta} \\ &= T_{\mu\nu} n^{\mu} n^{\nu} - T_{\mu\nu} u^{\mu} u^{\nu}, \end{aligned} \tag{5.82}$$

[13]Note that the original construction of Buchert averaging did not include vorticity as only a fluid-orthogonal approach was considered.

allowing us to write

$$\mathcal{T}_{\mathcal{D}} = -16\pi G \left\langle N^2 \left(T_{\mu\nu} n^\mu n^\nu - T_{\mu\nu} u^\mu u^\nu \right) \right\rangle_{\mathcal{D}}. \tag{5.83}$$

2. $\mathcal{T}_{\mathcal{D}}$ also expresses the difference between the isotropic pressure measured in the rest frames of the fluid and the normal frames. Using (5.21), we find

$$E - \rho = S - 3p = T_{\mu\nu} h^{\mu\nu} - T_{\mu\nu} b^{\mu\nu}, \tag{5.84}$$

and therefore,

$$\mathcal{T}_{\mathcal{D}} = -16\pi G \left\langle N^2 \left(T_{\mu\nu} h^{\mu\nu} - T_{\mu\nu} b^{\mu\nu} \right) \right\rangle_{\mathcal{D}}. \tag{5.85}$$

3. $\mathcal{T}_{\mathcal{D}}$ corresponds to a 'bulk' tilt contribution. This is because for a boundary-free domain, $\mathcal{T}_{\mathcal{D}}$ does not vanish whereas the tilt contributions (terms that contain $\boldsymbol{v}$) in $\mathcal{Q}_{\mathcal{D}}$ and $\mathcal{P}_{\mathcal{D}}$ vanish for such a domain[14].

The first two interpretations follow from the construction of the extrinsically averaged evolution equations, using the intrinsic variables — ρ and p. These equations are derived, however, from observations made in the normal frames which measure E and S.

The sign of $\mathcal{T}_{\mathcal{D}}$ will usually be constrained and remain negative [3], with the interpretation that $-\mathcal{T}_{\mathcal{D}}$ is a measure of the kinetic energy. This means that this particular type of backreaction will contribute a 'deceleration' term to the effective acceleration.

We have discussed the effects of the signs of each of the backreaction terms, however, the overall sign is the most important factor. If we combine all of the backreaction terms into one term, $\mathscr{Q}_{\mathcal{D}} = \mathcal{Q}_{\mathcal{D}} + \mathcal{P}_{\mathcal{D}} + \mathcal{T}_{\mathcal{D}}$, then in (5.80) a negative sign for $\mathscr{Q}_{\mathcal{D}}$ will contribute to a deceleration of the domain we average over. Conversely a positive sign will contribute to an acceleration of the domain we average over.

A negative sign for the overall backreaction, $\mathscr{Q}_{\mathcal{D}}$, can be thought of as being phenomenologically similar to dark matter since it increases the deceleration one would infer for a given fluid rest energy. By contrast, a positive overall backreaction has the same sign as the cosmological constant term in (5.80) and could, therefore, be phenomenologically similar to dark energy as it could contribute to an accelerated expansion. However, this analogy is not complete as the two backreaction terms, $\mathcal{Q}_{\mathcal{D}}$ and $\mathcal{T}_{\mathcal{D}}$ enter the analogue of the Friedmann equation (5.75) with the opposite sign to the cosmological constant.

[14]For more detail on this and a derivation of the effective equations for a boundary-free domain see section 3.5.3 of Buchert et al. [3].

Furthermore, we stress that care must be taken when interpreting (5.75) and (5.80) since they refer to statistical averages on extrinsic hypersurfaces with respect to an average time parameter, t, not to local observables. In Wiltshire's timescape model [35], using realistic initial conditions the backreaction never grows large enough to dominate the right-hand side of (5.75), and $3\,a_{\mathcal{D}}^{-1}(\mathrm{d}^2 a_{\mathcal{D}}/\mathrm{d}t^2)$ remains negative (decelerating). Nonetheless, the local proper time parameter, τ, of observers in 'bound structures' 'drifts' from the statistical extrinsic t parameter. This 'drift' is so extreme, that at late epochs the observers in 'bound structures' infer a positive acceleration at late epochs with respect to τ.

5.4.2 Extrinsic Conservation of the Fluid Rest Mass

The averaging approach discussed above is from the "extrinsic point of view", i.e., not in the rest frames of the fluid. In the literature, this has led to a concern with the conservation of the rest mass of the fluid. Buchert et al. [3] show that the averaging procedure we have followed does indeed result in a conserved fluid rest mass as shown below. Therefore, we follow the Buchert scheme of averaging rather than others. We discuss this in relation to three possible choices for picking how the domain propagates, corresponding to the three timelike congruences introduced.

The first choice is to assume the domain evolves along the congruence of coordinate frames $\boldsymbol{\partial}_t$, considered *implicitly* by Larena [187] and Brown et al. [188]. This choice has two problems: The first problem is that for a specific choice of shift, the vectors $\boldsymbol{\partial}_t$ and $\boldsymbol{u}$ will not be collinear. In general, this means that the fluid elements will flow across the boundary of the domain. One may question the use of averaged evolution equations for a domain that evolves according to $\boldsymbol{\partial}_t$, since the number of fluid elements at the one time cannot be guaranteed to be the number of fluid elements at a later time. The second problem is that the location of the averaging domain at a given time will depend of the choice of the shift vector. This results in the averaged system of equations depending on the choice of coordinates and how they propagate, which is 'unphysical'.

The second choice is to have the averaging domain to propagate along the integral curves of the normal vector associated to the normal frames, $\boldsymbol{n}$. This choice is distinct from $\boldsymbol{\partial}_t$ (characterised by the shift) and from the fluid 4–velocity (characterised by the tilt). This choice is considered by[15] Gasperini et al. [190]. Others such as Beltrán Jiménez et al. [191] and Smirnov [192] assume $\boldsymbol{n}$ to be geodesic and equivalent to the 4–velocity of the fluid (whereas Gasperini et al. assume $\boldsymbol{u}$ and $\boldsymbol{n}$ differ). These choices either restrict the degrees

[15] Gasperini et al. use a window function and have a covariant spacetime averaging formalism, rather than considering averages on spatial hypersurfaces [189].

of freedom in setting up the 3+1 splitting of space time, or more generally result in the fluid flowing over the boundary of the averaging domain.

The third choice is the one we have followed where the domain is comoving with the fluid — the boundaries follow $\boldsymbol{u}$ as shown in Figure 5.2. This ensures that the collection of fluid elements in the domain of averaging remains constant as the domain evolves in time. Such a choice, however, is only advantageous for one fluid. The two fluid or multi-fluid approach to cosmology has been investigated in recent years, see [193, 194]. The two-fluid approach, where one fluid is pressureless dark matter and the other is baryonic matter would be particularly interesting to investigate in future studies with the Buchert formalism. If one wishes to repeat this with even two fluids, however, we would have to choose the domain to propagate along the congruence of only one, thus only preserving one fluid rest mass.

We now show how the fluid rest mass is indeed conserved. We introduce the conserved fluid rest mass flux vector $\boldsymbol{M}$,

$$M^{\alpha} := \mu\, u^{\alpha}\,, \quad \nabla_{\alpha} M^{\alpha} = 0, \tag{5.86}$$

recalling that μ is the conserved rest mass density. We represent the rest mass of the fluid within the domain by the flow of $\boldsymbol{M}$ through $\mathcal{D}$ as

$$M_{\mathcal{D}} := \int_{\mathcal{D}} M^{\alpha}\, \mathrm{d}\sigma_{\alpha} = \int_{\mathcal{D}} -\mu\, u^{\alpha} n_{\alpha} \sqrt{h}\, \mathrm{d}^3x = \mathcal{V}_{\mathcal{D}} \left\langle \gamma\mu \right\rangle_{\mathcal{D}}\,, \tag{5.87}$$

where we have used the scalar averaging equation, (5.60) and $-u^{\alpha}n_{\alpha} = \gamma$.

We demonstrate that the rest mass of the fluid is conserved by integration of the conversation equation for $\boldsymbol{M}$ over the 'spacetime tube', $\mathscr{T}$, shown in Figure 5.2. This spacetime tube can be thought of as the portion of $\mathcal{M}$ swept out by the propagation of $\mathcal{D}$ between two hypersurfaces at times t_1 and t_2 where $t_2 > t_1$. We use Gauss' theorem to express this integration as

$$0 = \int_{\mathscr{T}} \nabla_{\alpha} M^{\alpha} \sqrt{g}\, \mathrm{d}^4\, x = \oint_{\partial\mathscr{T}} M^{\alpha}\, \mathrm{d}\eta_{\alpha}, \tag{5.88}$$

where $g := |\det(\, g_{\mu\nu}\,)|$ and $\mathrm{d}\eta_{\mu}$ is the outward-oriented volume element on the boundary of $\mathscr{T}$, which we represent with $\partial\mathscr{T}$. This equation can be decomposed into three parts, one for the rest mass of the fluid at t_1, one for the rest mass of the fluid at t_2, and one for the flux of the rest mass past the boundary of the domain. To perform this decomposition we introduce the timelike part of $\partial\mathscr{T}$, $\mathscr{A}$. This part of the boundary has an outward-oriented unit normal vector, $\boldsymbol{A}$ (see Figure 5.2 to visualise the various vectors). The timelike part, $\mathscr{A}$ also has an associated volume 3–form, $\mathrm{d}V_{\mathscr{A}}$. We can thus rewrite (5.88) as

$$\begin{aligned} 0 &= \int_{\mathcal{D}_{t_2}} \gamma\mu \sqrt{h}\, \mathrm{d}^3x - \int_{\mathcal{D}_{t_1}} \gamma\mu \sqrt{h}\, \mathrm{d}^3x + \int_{\mathscr{A}} M^{\alpha} A_{\alpha}\, \mathrm{d}V_{\mathscr{A}} \\ &= M_{\mathcal{D}_{t_2}} - M_{\mathcal{D}_{t_1}} + \int_{\mathscr{A}} \mu\, u^{\alpha} A_{\alpha}\, \mathrm{d}V_{\mathscr{A}}. \end{aligned} \tag{5.89}$$

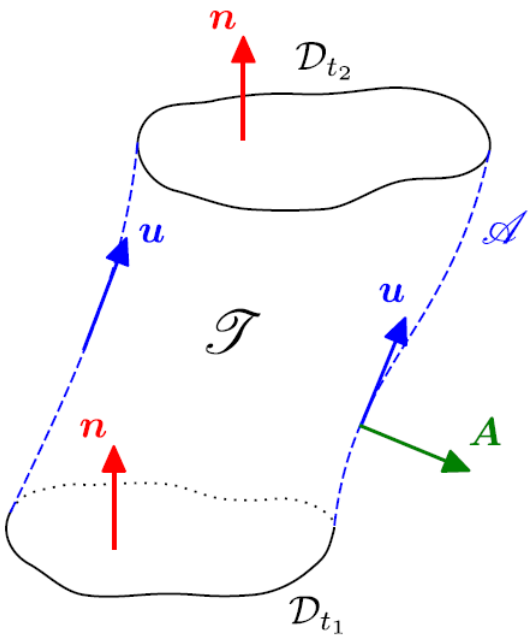

Figure 5.2: Representation of the spacetime tube, $\mathscr{T}$, from Buchert et al. [3]. The two domains at t_2 and t_1, and the various vectors used in the rest mass preserving proof are shown here. The vector $\boldsymbol{n}$ is orthogonal to the hypersurfaces at t_1 and t_2 and the 4–velocity is titled with respect to it. The vector $\boldsymbol{A}$ is orthogonal to the 4–velocity. Note the domain boundary is transported along the fluid congruence.

The last term on the right-hand side vanishes because the domain of the boundary is transported along $\boldsymbol{u}$. This implies that the outward-oriented normal vector $\boldsymbol{A}$ is everywhere orthogonal to $\boldsymbol{u}$, hence $u^\alpha A_\alpha = 0$. Therefore, we find, $M_{\mathcal{D}_{t_2}} = M_{\mathcal{D}_{t_1}}$, showing that the rest mass is preserved. In general, however, the last term will not be zero depending on which congruence the averaging domain is transported along — leading to the problem of rest mass now being conserved.

A proof of this can be constructed by considering the three congruences: Consider an outward-oriented vector for a domain (not the one we are averaging over) that is comoving along the congruence of curves with tangent vector $\boldsymbol{u}$, $\boldsymbol{A}_{(\boldsymbol{u})}$. We have shown that this corresponds to a conserved rest mass because $\boldsymbol{A}_{(\boldsymbol{u})}$ and $\boldsymbol{u}$ are orthogonal. Now consider our actual domain of averaging that moves along the congruences with tangent vector $\boldsymbol{\partial}_t$. This domain of averaging has an outward-oriented normal vector $\boldsymbol{A}_{(\boldsymbol{\partial}_t)}$. We relate the two vectors by

$$\boldsymbol{A}_{(\boldsymbol{\partial}_t)} = \boldsymbol{A}_{(\boldsymbol{u})} - \boldsymbol{V}. \tag{5.90}$$

Therefore, if we consider the integral above,

$$\int_{\mathscr{A}} \mu\, u_\alpha\, A^\alpha_{(\boldsymbol{\partial}_t)}\, \mathrm{d}V_{\mathscr{A}} = \int_{\mathscr{A}} \mu\, u_\alpha\, (\, A^\alpha_{(\boldsymbol{u})} - V^\alpha\,)\, \mathrm{d}V_{\mathscr{A}}, \tag{5.91}$$

then we notice there is an extra term which corresponds to the flux ($\mathscr{F}$) through

the averaging domain,

$$\mathscr{F} = -\int_{\mathscr{A}} \mu\, u_\alpha\, V^\alpha\, \mathrm{d}V_{\mathscr{A}}. \tag{5.92}$$

One could repeat this argument for an averaging domain that propagates along the congruence with tangent vector $\boldsymbol{n}$ by replacing $\boldsymbol{V}$ with $N\boldsymbol{v}$.

5.4.3 Time-Reparameterization Invariance of Extrinsically - Averaged Equations

In Chapter 6 we will develop the Buchert averaging formalism under the rules of the post-Newtonian expansion. The particular form of the post-Newtonian expansion we will follow by Clifton et al. [1] uses conformal time instead the coordinate (or 'cosmic') time. Furthermore, the conformal time, η is *dimensionful*, a point which is not discussed in depth in the literature. While we can show that the Buchert equations, (5.75) and (5.80), are invariant under a time reparameterization, this does not help us to understand what a 'dimensionful' conformal time means physically and following others in the literature we treat it simply as a mathematical construct.

A time reparameterization of the form $t \mapsto T(t)$ can be implemented by transforming the lapse function as:

$$N \mapsto \tilde{N} = N\,\frac{\mathrm{d}t}{\mathrm{d}T}. \tag{5.93}$$

In (5.75) this means that the left-hand side will gain a factor of $(\mathrm{d}t/\mathrm{d}T)^2$, and therefore the right-hand side must also gain the same factor in order for the entire equation to be invariant. Note that under the transformation (5.93) we then have

$$\begin{aligned} &-\frac{1}{2}\mathcal{Q}_{\mathcal{D}} - \frac{1}{2}\langle\, N^2\,\mathcal{R}\,\rangle_{\mathcal{D}} + \langle\, N^2\,\rangle_{\mathcal{D}}\,\Lambda + 8\pi G\langle\, N^2\rho\,\rangle_{\mathcal{D}} - \frac{1}{2}\mathcal{T}_{\mathcal{D}} \mapsto \\ &-\frac{1}{2}\Big(\frac{\mathrm{d}t}{\mathrm{d}T}\Big)^2\mathcal{Q}_{\mathcal{D}} - \frac{1}{2}\Big(\frac{\mathrm{d}t}{\mathrm{d}T}\Big)^2\langle\, N^2\,\mathcal{R}\,\rangle_{\mathcal{D}} + \Big(\frac{\mathrm{d}t}{\mathrm{d}T}\Big)^2\langle\, N^2\,\rangle_{\mathcal{D}}\,\Lambda + \\ &\qquad\qquad 8\pi G\Big(\frac{\mathrm{d}t}{\mathrm{d}T}\Big)^2\langle\, N^2\rho\,\rangle_{\mathcal{D}} - \Big(\frac{\mathrm{d}t}{\mathrm{d}T}\Big)^2\frac{1}{2}\mathcal{T}_{\mathcal{D}}. \end{aligned} \tag{5.94}$$

From the definition of the extrinsic kinematical backreaction (5.74) note that we have assumed that the reparameterization only impacts the lapse and not the 'doubly contracted' extrinsic curvature, the scalar extrinsic curvature, nor the 3–dimensional intrinsic curvature. This is the essential part of the argument since, the Buchert equations would otherwise not be invariant under the time reparameterization. Since these quantities are scalars, they will not change

under a time reparameterization and thus we find

$$\begin{aligned}\frac{3}{a_{\mathcal{D}}^2}\Big(\frac{\mathrm{d}t}{\mathrm{d}T}\Big)^2\Big(\frac{\mathrm{d}a_{\mathcal{D}}}{\mathrm{d}t}\Big)^2 &= -\frac{1}{2}\Big(\frac{\mathrm{d}t}{\mathrm{d}T}\Big)^2\mathcal{Q}_{\mathcal{D}} - \frac{1}{2}\Big(\frac{\mathrm{d}t}{\mathrm{d}T}\Big)^2\langle\, N^2\,\mathcal{R}\,\rangle_{\mathcal{D}} + \\ &\qquad \Big(\frac{\mathrm{d}t}{\mathrm{d}T}\Big)^2\langle\, N^2\,\rangle_{\mathcal{D}}\;\Lambda + 8\pi G\Big(\frac{\mathrm{d}t}{\mathrm{d}T}\Big)^2\langle\, N^2\rho\,\rangle_{\mathcal{D}} - \Big(\frac{\mathrm{d}t}{\mathrm{d}T}\Big)^2\frac{1}{2}\mathcal{T}_{\mathcal{D}} \mapsto \\ \frac{3}{a_{\mathcal{D}}^2}\Big(\frac{\mathrm{d}a_{\mathcal{D}}}{\mathrm{d}t}\Big)^2 &= -\frac{1}{2}\mathcal{Q}_{\mathcal{D}} - \frac{1}{2}\langle\, N^2\,\mathcal{R}\,\rangle_{\mathcal{D}} + \langle\, N^2\,\rangle_{\mathcal{D}}\;\Lambda + 8\pi G\langle\, N^2\rho\,\rangle_{\mathcal{D}} - \frac{1}{2}\mathcal{T}_{\mathcal{D}}.\end{aligned} \tag{5.95}$$

I.e., the equation is invariant under a time reparameterization.

The second averaged equation, (5.80) is slightly more complicated. While the discussion from above will still apply, i.e., we gain an extra factor of $(\mathrm{d}t/\mathrm{d}T)^2$, the dynamical backreaction, $\mathcal{P}_{\mathcal{D}}$, and $(3/a_{\mathcal{D}})\,(\mathrm{d}^2a_{\mathcal{D}}/\mathrm{d}t^2)$ will each undergo an affine transformation. This will be the same for both sides and thus the equation will remain invariant. To see this, first consider the effect of (5.93) on the left-hand side of (5.80):

$$\frac{3}{a_{\mathcal{D}}}\frac{\mathrm{d}t}{\mathrm{d}T}\frac{\mathrm{d}}{\mathrm{d}t}\left(\frac{\mathrm{d}t}{\mathrm{d}T}\frac{\mathrm{d}a_{\mathcal{D}}}{\mathrm{d}t}\right) = \frac{3}{a_{\mathcal{D}}}\left(\frac{\mathrm{d}a_{\mathcal{D}}}{\mathrm{d}t}\frac{\mathrm{d}^2t}{\mathrm{d}T^2} + \left(\frac{\mathrm{d}t}{\mathrm{d}T}\right)^2\frac{\mathrm{d}^2a_{\mathcal{D}}}{\mathrm{d}t^2}\right). \tag{5.96}$$

The first term on the right-hand side cancels exactly with a similar transformation in the $\mathcal{P}_{\mathcal{D}}$ term, namely $\Big\langle \mathrm{d}/\mathrm{d}t\Big(D_i(N\,v^i)\Big) - \mathcal{K}\,\mathrm{d}N/\mathrm{d}t\Big)\Big\rangle_{\mathcal{D}}$ term. Under the transformation (5.93) this becomes

$$\left\langle \frac{\mathrm{d}^2t}{\mathrm{d}T^2}\Big(D_i(N\,v^i) + \frac{\mathrm{d}}{\mathrm{d}t}(D_i(N\,v^i)\Big) + \frac{\mathrm{d}^2t}{\mathrm{d}T^2}\mathcal{K}\left(N + \frac{\mathrm{d}}{\mathrm{d}t}N\right)\right\rangle_{\mathcal{D}}. \tag{5.97}$$

Noting that by (5.69)

$$\frac{3}{a_{\mathcal{D}}}\left(\frac{\mathrm{d}a_{\mathcal{D}}}{\mathrm{d}t}\frac{\mathrm{d}^2t}{\mathrm{d}T^2}\right) = \frac{\mathrm{d}^2t}{\mathrm{d}T^2}\left\langle\Big(D_i\,(Nv^i) + \mathcal{K}N\Big)\right\rangle_{\mathcal{D}}, \tag{5.98}$$

we find

$$\begin{aligned}3\,\frac{1}{a_{\mathcal{D}}}\frac{\mathrm{d}^2a_{\mathcal{D}}}{\mathrm{d}t^2} &= -4\pi G\left\langle N^2\,(\rho+3p)\right\rangle_{\mathcal{D}} + \langle\, N^2\,\rangle_{\mathcal{D}}\;\Lambda + \mathcal{Q}_{\mathcal{D}} + \mathcal{P}_{\mathcal{D}} + \frac{1}{2}\,\mathcal{T}_{\mathcal{D}} \mapsto \\ \frac{3}{a_{\mathcal{D}}}\left(\left(\frac{\mathrm{d}t}{\mathrm{d}T}\right)^2\frac{\mathrm{d}^2a_{\mathcal{D}}}{\mathrm{d}t^2}\right) + \frac{\mathrm{d}^2t}{\mathrm{d}T^2}\left\langle\Big(D_i\,(Nv^i) + \mathcal{K}N\Big)\right\rangle_{\mathcal{D}} &= \\ &\qquad -4\pi G\left(\frac{\mathrm{d}t}{\mathrm{d}T}\right)^2\left\langle N^2\,(\rho+3p)\right\rangle_{\mathcal{D}} \\ &\quad + \left(\frac{\mathrm{d}t}{\mathrm{d}T}\right)^2\mathcal{P}_{\mathcal{D}} + \left\langle\frac{\mathrm{d}^2t}{\mathrm{d}T^2}\Big(D_i(N\,v^i)\Big) + \frac{\mathrm{d}^2t}{\mathrm{d}T^2}\mathcal{K}\,N\right\rangle_{\mathcal{D}} \\ &\quad + \left(\frac{\mathrm{d}t}{\mathrm{d}T}\right)^2\langle\, N^2\,\rangle_{\mathcal{D}}\;\Lambda + \left(\frac{\mathrm{d}t}{\mathrm{d}T}\right)^2\mathcal{Q}_{\mathcal{D}} + \frac{1}{2}\left(\frac{\mathrm{d}t}{\mathrm{d}T}\right)^2\mathcal{T}_{\mathcal{D}},\end{aligned} \tag{5.99}$$

and therefore, under (5.93)

$$
\begin{aligned}
3\,\frac{1}{a_{\mathcal{D}}}\frac{\mathrm{d}^2 a_{\mathcal{D}}}{\mathrm{d}t^2} &= -4\pi G\left\langle N^2\left(\rho+3p\right)\right\rangle_{\mathcal{D}} + \langle\, N^2\,\rangle_{\mathcal{D}}\;\Lambda + \mathcal{Q}_{\mathcal{D}} + \mathcal{P}_{\mathcal{D}} + \frac{1}{2}\,\mathcal{T}_{\mathcal{D}} \mapsto \\
3\,\frac{1}{a_{\mathcal{D}}}\frac{\mathrm{d}^2 a_{\mathcal{D}}}{\mathrm{d}t^2} &= -4\pi G\left\langle N^2\left(\rho+3p\right)\right\rangle_{\mathcal{D}} + \langle\, N^2\,\rangle_{\mathcal{D}}\;\Lambda + \mathcal{Q}_{\mathcal{D}} + \mathcal{P}_{\mathcal{D}} + \frac{1}{2}\,\mathcal{T}_{\mathcal{D}},
\end{aligned}
\tag{5.100}
$$

i.e., the equation is invariant under a time reparameterization.

5.5 Fluid-Intrinsic Scalar Averaging

The various results in the literature discussed in subsection 5.4.2 adopt the extrinsic fluid averaging approach. This was not the approach originally taken by Buchert 20 years ago [4, 34]. Extrinsic averaging procedures are built from averaging domains that evolve along the normal congruence or along the coordinate congruence associated with $\boldsymbol{\partial}_t$. As we showed, these approaches face challenges with not being able to preserve the rest mass of the fluid, and suffer from a potential coordinate dependence.

The averaging procedure of subsection 5.3.3 does not suffer from these problems. Nevertheless, Buchert et al. [3] argue that the intrinsic properties of the fluid such as Θ, σ^2, and ω^2 are 'more relevant' for characterising an effective cosmological model. The extrinsic approach, however, can be used to be a 'measure' of the deviations from the dynamics of an isotropic and homogeneous model of the Universe.

There are, however, limitations to the intrinsic approach which we will also discuss. Recall that the kinematic variables introduced in section 3.5, these variables were introduced in the context of a $1+3$ formalism. As discussed, the basic structure in the 1+3 formalism is a congruence of timelike curves and *not* a hypersurface, which is required for the averaging operations. Therefore, intrinsic averaging can be interpreted as a 1+3 formalism jointly with a 3+1 formalism. The limitation here is that the fluid rest frames of a fluid with vorticity are not hypersurface-forming. Thus, while we may be able to mathematically describe the intrinsically averaged equations using only the comoving description introduced in section 5.2, we still require extra mathematical structure to be rigorous — for instance, the Lagrangian description.

5.5.1 Intrinsic Averaging Operator

For the "fluid intrinsic" averaging, we shall use the fluid intrinsic metric, $\boldsymbol{b}$ instead of the induced metric on the normal frames, $\boldsymbol{h}$. Firstly, let us determine the relation between the determinants of $\boldsymbol{b}$ and $\boldsymbol{h}$,

$$
\begin{aligned}
b &= \det\left(g_{ij}+u_i u_j\right) = \det\left(h_{ij}+u_i u_j\right) = h\,\det\left(\delta^i{}_j + h^{ij}u_k u_j\right) \\
&= h\left(1+h^{ij}u_i u_j\right) = h\left(1+h^{\mu\nu}u_\mu u_\nu\right) = h\gamma^2,
\end{aligned}
\tag{5.101}
$$

and therefore, $\sqrt{b}\,\mathrm{d}^3x = \gamma\sqrt{h}\,\mathrm{d}^3x$. Thus, we see that the two volume measures coincide when the fluid flow is hypersurface orthogonal, as expected. We also claim that since the volume measured with respect to the fluid rest frames is the 'proper' volume, this is the 'more natural' averaging scheme. We define the total proper volume of the fluid elements within a domain $\mathcal{D}$:

$$\mathcal{V}^b_{\mathcal{D}}(t) := \int_{\mathcal{D}} u^\mu \,\mathrm{d}\sigma_\mu = \int_{\mathcal{D}} \gamma\sqrt{h}\,\mathrm{d}^3x = \int_{\mathcal{D}} \sqrt{b}\,\mathrm{d}^3x. \tag{5.102}$$

The superscript b indicates that the volume is evaluated with respect to the metric $\boldsymbol{b}$. Indeed if one compares the expression for the rest mass of the fluid using $\sqrt{b}\,\mathrm{d}^3x$ we find

$$M_{\mathcal{D}} = \int_{\mathcal{D}} \gamma\mu\sqrt{h}\,\mathrm{d}^3x = \int_{\mathcal{D}} \mu\sqrt{b}\,\mathrm{d}^3x, \tag{5.103}$$

which is what one would expect when defining the rest mass. The difference between this definition and (5.87) is due to the fact that the rest mass density, μ, is a quantity in the rest frame of the fluid.

We further define the *intrinsic* scalar average over $\mathcal{D}$ for any scalar, ψ in $\mathcal{D}$ as:

$$\begin{aligned} \langle\,\psi\,\rangle^b_{\mathcal{D}} &:= \frac{1}{\mathcal{V}^b_{\mathcal{D}}}\int_{\mathcal{D}} \psi\, u^\mu \,\mathrm{d}\sigma_\mu = \frac{1}{\mathcal{V}^b_{\mathcal{D}}}\int_{\mathcal{D}} \psi\,\gamma\sqrt{h}\,\mathrm{d}^3x \\ &= \frac{1}{\mathcal{V}^b_{\mathcal{D}}}\int_{\mathcal{D}} \psi\sqrt{b}\,\mathrm{d}^3x. \end{aligned} \tag{5.104}$$

The expressions for the volume and the scalar averaging only differ from the fact that the volume 3–form used is now built from $\boldsymbol{u}$ instead of $\boldsymbol{n}$. However, the coordinate time derivative of the volume and the intrinsic evolution equations will differ in more ways as we are using the comoving description. The two averaging schemes are related as follows:

$$\mathcal{V}^b_{\mathcal{D}} = \mathcal{V}^h_{\mathcal{D}}\,\langle\,\gamma\,\rangle^h_{\mathcal{D}}\,, \quad \text{and} \quad \langle\,\psi\,\rangle^b_{\mathcal{D}} = \frac{1}{\langle\,\gamma\,\rangle^h_{\mathcal{D}}}\,\langle\,\gamma\,\psi\,\rangle^h_{\mathcal{D}}\,, \tag{5.105}$$

where we have used the superscript h to indicate volumes and averages with respect to the induced metric on the normal frames, $\boldsymbol{h}$. We notice again that the volumes with respect to the different metrics and scalar averages coincide in the absence of tilt, i.e., when $\gamma = 1$. We also have an approximate equivalence in the case of small tilts which corresponds to non-relativistic Eulerian velocities. Furthermore, we note that in general, $\mathcal{V}^b_{\mathcal{D}} > \mathcal{V}^h_{\mathcal{D}}$, this can be seen as a Lorentz contraction of the volume of each fluid element because the tilt corresponds to a boost.

5.5.2 Fluid-Intrinsic Time Evolution

To determine the time evolution of the intrinsic fluid volume $\mathcal{V}^b_{\mathcal{D}}$ we follow the same procedure as in the extrinsic case. We change the spatial coordinates

to comoving ones in order to determine the commutation rule between time evolution and spatial volume integration. The distinction here is that we are explicitly using the comoving description (hence the coordinate velocity, $\boldsymbol{V} = 0$). Therefore, we have the following:

$$\frac{1}{\mathcal{V}^b_{\mathcal{D}}}\frac{\mathrm{d}}{\mathrm{d}t}\mathcal{V}^b_{\mathcal{D}} = \frac{1}{\mathcal{V}^b_{\mathcal{D}}}\int_{\mathcal{D}_{\boldsymbol{x}}}\left(\frac{1}{2}\,b^{ij}\frac{\mathrm{d}}{\mathrm{d}t}b_{ij}\right)\sqrt{b}\,\mathrm{d}^3x, \tag{5.106}$$

which may be simplified by using (5.41), to obtain

$$\frac{1}{\mathcal{V}^b_{\mathcal{D}}}\frac{\mathrm{d}}{\mathrm{d}t}\mathcal{V}^b_{\mathcal{D}} = \left\langle\frac{N}{\gamma}\,\Theta\right\rangle^b_{\mathcal{D}} = \left\langle\tilde{\Theta}\right\rangle^b_{\mathcal{D}}. \tag{5.107}$$

Here, we have introduced the 'rescaled scalar expansion', $\tilde{\Theta} := (N/\gamma)\,\Theta$, which may be interpreted as the fluid's 'local expansion' with respect to the coordinate time t. One the other hand, Θ, describes the local expansion with respect to the proper time, τ, because $N/\gamma = \mathrm{d}\tau/\mathrm{d}t$.

In terms of evolution by the coordinate time, t, and intrinsic spatial averages, we arrive at the commutation rule,

$$\frac{\mathrm{d}}{\mathrm{d}t}\left\langle\psi\right\rangle^b_{\mathcal{D}} - \left\langle\frac{\mathrm{d}}{\mathrm{d}t}\,\psi\right\rangle^b_{\mathcal{D}} = -\left\langle\tilde{\Theta}\right\rangle^b_{\mathcal{D}}\left\langle\psi\right\rangle^b_{\mathcal{D}} + \left\langle\tilde{\Theta}\,\psi\right\rangle^b_{\mathcal{D}}. \tag{5.108}$$

This commutation rule is, again, independent of the shift due to the coordinate independent definition of the domain propagation. However, there is still a dependence on the tilt through the factor N/γ in the rescaled expansion factor. Furthermore, given the local continuity equation, $\mathrm{d}\mu/\mathrm{d}t + \tilde{\Theta}\mu = 0$ we see that substituting $\psi = \mu$ in (5.108) gives

$$\frac{\mathrm{d}}{\mathrm{d}t}\left\langle\mu\right\rangle^b_{\mathcal{D}} - \left\langle\tilde{\Theta}\right\rangle^b_{\mathcal{D}}\left\langle\mu\right\rangle^b_{\mathcal{D}} = 0, \tag{5.109}$$

which is equivalent to the rest mass conservation equation, where $M_{\mathcal{D}} = \mathcal{V}^b_{\mathcal{D}}\,\langle\,\mu\,\rangle^b_{\mathcal{D}}$.

5.5.3 Fluid-Intrinsic Averaged Evolution Equations

We define the intrinsic effective scale factor in the domain $\mathcal{D}$ similarly to before, except we use the intrinsic volume domain:

$$a^b_{\mathcal{D}}(t) := \left(\frac{\mathcal{V}^b_{\mathcal{D}}(t)}{\mathcal{V}_{\mathcal{D}_i}}\right)^{1/3}. \tag{5.110}$$

The rate of change of the scale factor defines the averaged fluid expansion rate in coordinate time[16]:

$$H^b_{\mathcal{D}} := \frac{1}{a^b_{\mathcal{D}}}\frac{\mathrm{d}a^b_{\mathcal{D}}}{\mathrm{d}t} = \frac{1}{3}\left\langle\tilde{\Theta}\right\rangle^b_{\mathcal{D}}. \tag{5.111}$$

[16]Note the similarity between this expression and the definition of the Hubble parameter and the expansion scalar we introduced in (3.98). The difference here is that we are using a local Hubble parameter valid only for the domain we average over.

Instead of using the Einstein equations projected along $\boldsymbol{n}$ as we did in section 5.3, we express the local dynamics of the fluid by a projection of Einstein's equations along $\boldsymbol{u}$. This projection yields Raychaudhuri's equation, expressed slightly differently from section 3.5:

$$\dot{\Theta} = -\frac{1}{3}\Theta^2 - 2\,\sigma^2 + 2\,\omega^2 + \mathcal{A} - 4\pi G\,(\rho + 3p) + \Lambda, \tag{5.112}$$

where $\mathcal{A} = \nabla_\mu\, a^\mu$. Raychaudhuri's equations can be complemented by an analogue to Gauss' equation (3.63). We define a 'fluid rest frame 3–curvature' scalar, $\mathscr{R}$ from the 4–Ricci tensor and scalar:

$$\mathscr{R} := \nabla_\mu\, u^\nu \nabla_\nu\, u^\mu - \nabla_\mu\, u^\mu \nabla_\nu\, u^\nu + R + 2\,R_{\mu\nu}\, u^\mu u^\nu. \tag{5.113}$$

The scalar Gauss equation (3.63), however, is only valid when there exist $\boldsymbol{u}$-orthogonal hypersurfaces, and this is only the case when there is zero vorticity. In the case of vanishing vorticity, $\mathscr{R}$ does coincide with the scalar intrinsic curvature of the $\boldsymbol{u}$-orthogonal hypersurfaces. For non-zero vorticity, however, we cannot interpret $\mathscr{R}$ as the intrinsic scalar curvature. We emphasise that in general $\mathscr{R}$ is not equal to the scalar curvature $\mathcal{R}$ of the $\boldsymbol{n}$-orthogonal hypersurfaces.

We may form a constraint equation by substituting the Einstein equations directly projected along $\boldsymbol{u}$ into (5.113):

$$\frac{2}{3}\Theta^2 - 2\,\sigma^2 + 2\,\omega^2 + \mathscr{R} = 16\pi G\rho + 2\Lambda, \tag{5.114}$$

where the covariant derivative of $\boldsymbol{u}$ have been decomposed into its kinematic parts. This equation allows us to relate $\mathscr{R}$ to the fluid rest frame energy density. Following the derivation of the extrinsically averaged evolution equations, we multiply (5.114) and (5.112) by $(N/\gamma)^2$ and then use the evolution of the intrinsic volume and scalar averaging formulae to determine the intrinsically averaged evolution equations. Let us first introduce the rescaled variables of interest:

$$\begin{aligned}
&\tilde{\sigma}^2 := \left(\frac{N}{\gamma}\right)^2 \sigma^2, \quad \tilde{\omega}^2 := \left(\frac{N}{\gamma}\right)^2 \omega^2, \quad \tilde{\rho} := \left(\frac{N}{\gamma}\right)^2 \rho, \quad \tilde{p} := \left(\frac{N}{\gamma}\right)^2 p, \\
&\tilde{\mathcal{A}} := \left(\frac{N}{\gamma}\right)^2 \mathcal{A}, \quad \text{and} \quad \tilde{\mathscr{R}} := \left(\frac{N}{\gamma}\right)^2 \mathscr{R}.
\end{aligned} \tag{5.115}$$

By squaring (5.111) and rearranging the rescaled version of (5.114) such that we add zero to the squared effective Hubble parameter, we obtain the first intrinsically averaged evolution equation:

$$3\,(H^b_{\mathcal{D}})^2 = 8\pi G\langle\,\tilde{\rho}\,\rangle^b_{\mathcal{D}} - \frac{1}{2}\,\langle\,\tilde{\mathscr{R}}\,\rangle^b_{\mathcal{D}} + \tilde{\Lambda}^b_{\mathcal{D}} - \frac{1}{2}\,\tilde{\mathcal{Q}}^b_{\mathcal{D}}, \tag{5.116}$$

where,

$$\tilde{\Lambda}^{b}_{\mathcal{D}} := \Lambda \left\langle \frac{N^{2}}{\gamma^{2}} \right\rangle^{b}_{\mathcal{D}}, \tag{5.117}$$

and

$$\tilde{\mathcal{Q}}^{b}_{\mathcal{D}} := \frac{2}{3}\left(\left\langle \tilde{\Theta}^{2} \right\rangle^{b}_{\mathcal{D}} - \left\langle \tilde{\Theta} \right\rangle^{b}_{\mathcal{D}}{}^{2} \right) - 2\left\langle \tilde{\sigma}^{2} \right\rangle^{b}_{\mathcal{D}} + 2\left\langle \tilde{\omega}^{2} \right\rangle^{b}_{\mathcal{D}}, \tag{5.118}$$

which is the intrinsic kinematical backreaction. Furthermore, by differentiating (5.111) with respect to coordinate time, using the intrinsic commutation rule (5.108), rewriting (5.112) in terms of coordinate time, and substituting in (5.116) we obtain the second intrinsically averaged evolution equation:

$$3\,\frac{1}{a^{b}_{\mathcal{D}}}\,\frac{\mathrm{d}^{2}a^{b}_{\mathcal{D}}}{\mathrm{d}t} = -4\pi G\,\langle\,\tilde{\rho} + 3\tilde{p}\,\rangle^{b}_{\mathcal{D}} + \tilde{\Lambda}^{b}_{\mathcal{D}} + \tilde{\mathcal{Q}}^{b}_{\mathcal{D}} + \tilde{\mathcal{P}}^{b}_{\mathcal{D}}, \tag{5.119}$$

where

$$\tilde{\mathcal{P}}^{b}_{\mathcal{D}} := \left\langle \tilde{\mathcal{A}} \right\rangle^{b}_{\mathcal{D}} + \left\langle \tilde{\Theta}\,\frac{\gamma}{N}\,\frac{\mathrm{d}}{\mathrm{d}t}\left(\frac{N}{\gamma}\right) \right\rangle^{b}_{\mathcal{D}}, \tag{5.120}$$

is the intrinsic dynamical backreaction. Once again, there are completeness conditions, such as an integrability condition that ensures one can obtain (5.116) from (5.119): these can be found in section 4.2.2 of [3].

Note that the backreaction terms in this intrinsic formalism, $\tilde{\mathcal{Q}}^{b}_{\mathcal{D}}$ and $\tilde{\mathcal{P}}^{b}_{\mathcal{D}}$ are not in general the same as the backreaction terms we have formulated in subsection 5.3.3. They do coincide, however, in the case of a hypersurface orthogonal flow. In that case, we have $\mathcal{K}_{ij} = -\Theta_{ij}$, $\omega^{2} = 0$, and $\tilde{\mathcal{A}} = ND^{i}D_{i}\,N$, so that the two definitions of backreaction terms will be the same.

There is no stress-energy backreaction in the intrinsic averaging case, nor is there a stress-energy backreaction in the fluid-orthogonal extrinsic averaging case. We had previously stated that $\mathcal{T}_{\mathcal{D}}$ was due to the tilt characterised by $N\boldsymbol{v}$. However, there is still a remnant of the tilt in the intrinsic averaging scheme due to the comoving description. Therefore, perhaps, a more precise statement is that a stress-energy backreaction will manifest whenever one attempts to average over a domain which has a normal vector that is not collinear to the fluid 4–velocity.

5.5.4 Effective Friedmannian Form

In the interest of making a correspondence with the standard Friedmann equations, we can reparameterize quantities in (5.116) and (5.119). We shall make this correspondence by rewriting these equations as if they are sourced by an *effective stress-energy tensor* [3, 4]. We define the corresponding effective, time-

dependent energy density and pressure:

$$\rho^b_{\rm eff}(t) := \langle\,\tilde{\rho}\,\rangle^b_{\mathcal{D}} - \frac{1}{16\pi G}\tilde{\mathcal{Q}}^b_{\mathcal{D}} - \frac{1}{16\pi G}\tilde{\mathcal{W}}_{\mathcal{D}} + \frac{1}{8\pi G}\tilde{\mathcal{L}}_{\mathcal{D}}\,; \tag{5.121}$$

$$p^b_{\rm eff} := \langle\,\tilde{p}\,\rangle^b_{\mathcal{D}} - \frac{1}{16\pi G}\tilde{\mathcal{Q}}^b_{\mathcal{D}} + \frac{1}{48\pi G}\tilde{\mathcal{W}}_{\mathcal{D}} - \frac{1}{8\pi G}\tilde{\mathcal{L}}_{\mathcal{D}} - \frac{1}{12\pi G}\tilde{\mathcal{P}}^b_{\mathcal{D}}, \tag{5.122}$$

where we have new backreaction terms $\tilde{\mathcal{W}}_{\mathcal{D}}$ and $\tilde{\mathcal{L}}_{\mathcal{D}}$. Here (5.121) describes the deviation of the averaged fluid 3–curvature, $\langle\,\tilde{\mathscr{R}}\,\rangle^b_{\mathcal{D}}$ from a constant curvature 'behaviour'. While (5.122) describes the deviation of[17] $\tilde{\Lambda^b_{\mathcal{D}}}$ from the cosmological constant, they are defined as:

$$\tilde{\mathcal{W}}_{\mathcal{D}} := \langle\,\tilde{\mathscr{R}}\,\rangle^b_{\mathcal{D}} - 6\frac{1}{(a^b_{\mathcal{D}})^2}\,k_{D_i}, \quad \text{and} \quad \tilde{\mathcal{L}}_{\mathcal{D}} := \tilde{\Lambda}^b_{\mathcal{D}} - \Lambda, \tag{5.123}$$

where $k_{\mathcal{D}_i}$ is a domain-dependent constant. With the effective sources, (5.116) and (5.119) may be rewritten as the respective Friedmann-like equations:

$$\begin{aligned} 3\,(H^b_{\mathcal{D}})^{\,2} &= 8\pi G\,\rho^b_{\rm eff} - 3\frac{1}{(a^b_{\mathcal{D}})^2}\,k_{D_i} + \Lambda \\ 3\,\frac{1}{a^b_{\mathcal{D}}}\,\frac{{\rm d}^2 a^b_{\mathcal{D}}}{{\rm d}t} &= -4\pi G\Big(\rho^b_{\rm eff} + 3p^b_{\rm eff}\Big) + \Lambda\,. \end{aligned} \tag{5.124}$$

5.5.5 Lagrangian Description

In the Lagrangian description, one sets the coordinate time equal to the proper time by specifying the choice of lapse, $N = \gamma$. In the case of the LTB and Szekeres models that we shall discuss in Chapter 7, we will use a Lagrangian description[18]. With this choice, the commutation rule takes the form[19]:

$$\frac{\rm d}{{\rm d}\tau}\Big\langle\psi\Big\rangle^b_{\mathcal{D}} = \left\langle\frac{\rm d}{{\rm d}\tau}\,\psi\right\rangle^b_{\mathcal{D}} - \Big\langle\Theta\Big\rangle^b_{\mathcal{D}}\Big\langle\psi\Big\rangle^b_{\mathcal{D}} + \Big\langle\Theta\,\psi\Big\rangle^b_{\mathcal{D}}, \tag{5.125}$$

and the scale factor evolution equation takes the form:

$$\frac{1}{a^b_{\mathcal{D}}}\frac{\rm d}{{\rm d}\tau}a^b_{\mathcal{D}} = \frac{1}{3}\langle\,\Theta\,\rangle^b_{\mathcal{D}}\,. \tag{5.126}$$

The intrinsically averaged evolution equations, (5.116) and (5.119) in the Lagrangian picture respectively read:

$$3\,(\,H^b_{\mathcal{D}}\,)^2 = 8\pi G\langle\,\rho\,\rangle^b_{\mathcal{D}} + \Lambda - \frac{1}{2}\langle\,\mathscr{R}\,\rangle^b_{\mathcal{D}} - \frac{1}{2}\mathcal{Q}^b_{\mathcal{D}}\,; \tag{5.127}$$

$$3\,\frac{1}{a^b_{\mathcal{D}}}\,\frac{{\rm d}^2 a^b_{\mathcal{D}}}{{\rm d}\tau^2} = -4\pi G\,\langle\,\rho + 3p\,\rangle^b_{\mathcal{D}} + \Lambda + \mathcal{Q}^b_{\mathcal{D}} + \mathcal{P}^b_{\mathcal{D}}\,, \tag{5.128}$$

[17] If one assumes the existence of a cosmological constant representing dark energy then the averaged equations we have shown above suggest we must also account for a *dark energy backreaction*.

[18] We will actually specify coordinates with $N = 1$ instead of setting $N = \gamma$. This is simply because there will be no tilt considered, hence $N\boldsymbol{v} = 0$.

[19] Note that overdot (the derivative with respect to coordinate time in the comoving description for a scalar) is the same as ${\rm d}/{\rm d}t$ in the Lagrangian picture. Also note that in this description tilde scalars are the same as normal ones because $N/\gamma = 1$

with the backreaction terms being reduced to:

$$\begin{aligned}\mathcal{Q}^b_{\mathcal{D}} &:= \frac{2}{3}\left(\left\langle \Theta^{\,2}\right\rangle^b_{\mathcal{D}} - \left\langle \Theta\right\rangle^{b\ 2}_{\mathcal{D}}\right) - 2\left\langle \sigma^{\,2}\right\rangle^b_{\mathcal{D}} + 2\left\langle \omega^{\,2}\right\rangle^b_{\mathcal{D}}\,; \\ \mathcal{P}^b_{\mathcal{D}} &= \left\langle \mathcal{A}\right\rangle^b_{\mathcal{D}}\,.\end{aligned} \tag{5.129}$$

Chapter 6

Post-Newtonian Cosmology and Viable Gauges

In Chapter 4, we introduced standard linear perturbation theory, which is widely used in cosmology to understand the formation of structure and model inhomogeneities. Standard perturbation theory is a weak-field and slow-motion approximation which assumes that all perturbed quantities are small. The order of smallness is characterised by a parameter, ϵ, and any terms of order ϵ^2 are neglected. Post-Newtonian cosmology is also a slow-motion and weak-field expansion. However, unlike standard perturbation theory, it remains valid when density contrasts are large. The post-Newtonian formalism does not assume the same order of magnitude for all perturbed quantities and furthermore, assumes orders of smallness for time derivatives as well. We follow the treatment of post-Newtonian theory from Clifton et al. [1] with the aim of determining viable gauge choices in this formalism. It should be noted, however, that this work builds on earlier paper, such as [195, 196].

When considering the applicability of different approaches to weak-field gravity, an important factor we must consider is the volume of the domain. On spatial domains that are "small" and on which matter is moving slowly (relative to c) one finds the dynamics of gravity can be well approximated by the Poisson equation. This is the case for the post-Newtonian theory — we change the structure of the perturbative expansion by reducing partial differential equations to only spatial variables. In general, however, this simplification is not valid on large scales.

The key idea that we use in post-Newtonian theory is the domains we consider are 'sufficiently small'— see Figure 6.1. This restriction is placed so that a change in the background geometry, over time, is negligible relative to the time that information of this change will take to propagate from one side of the system to another. We may express this statement more precisely as follows[1].

[1]In this part of the discussion, for clarity we will not set $c = 1$. Later on we shall suppress c again.

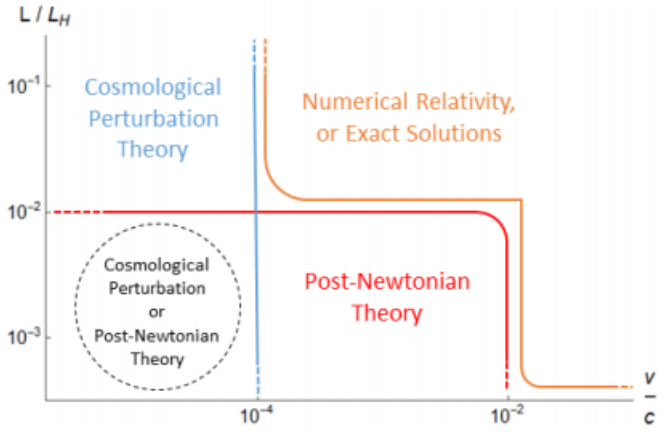

Figure 6.1: The domains in which post-Newtonian theory and cosmological perturbation theory are shown here. Standard perturbation theory applies left of the blue line. Post-Newtonian theory applies under the red line. Both formalisms apply on small scales when velocities are small. The characteristic spatial scale of the system under consideration is denoted by L and the Hubble scale is denoted L_H. This figure is from Clifton et al. [1]

Consider a 'characteristic time-scale' for variations in the background geometry of a system, η_c, in conformal time[2]. Since gravitational waves propagate at the speed of light, we may define a characteristic length scale which light travels in the time the variations of the background occur as

$$\lambda_c = c\,\eta_c. \tag{6.1}$$

In the post-Newtonian approximation λ_c will be large compared to the scale of the system we are considering, denoted by r_c. The matter in the systems we consider will generally have a velocity of magnitude $v_c = r_c/\eta_c$. Therefore, the slow-motion condition, $v_c \ll c$, is equivalent to the condition $r_c \ll \lambda_c$. This is precisely the statement above: the slow-motion systems we consider must exist on spatial scales much smaller than those over which gravitational information can travel in some time-scale.

It must be noted that the definition (6.1) presupposes that conformal time is dimensionful — choice II discussed in subsection 2.3.1. I.e., we take $\mathrm{d}\eta = \mathrm{d}t/a$ with $a(\eta)$ dimensionless rather than $\mathrm{d}\eta = c\,\mathrm{d}t/a$ with $a(t)$ dimensionful which is the alternative choice. Treating conformal time as dimensionful has become a common practice in cosmology and is generally considered to be a mathematical convenience. This choice, however, may have fundamental implications which have not been fully considered.

When studying the evolution of the Universe we are often interested in structures that grow over time-scales comparable to the age of the Universe.

[2]This may, for instance, correspond to the orbital period in close proximity, or the time-scale for a large body to assemble itself gravitationally.

We therefore have[3], $\eta_c \sim \mathcal{H}^{-1}$, implying, $\lambda_c \sim c\mathcal{H}^{-1}$. Note since this is a heuristic calculation, Clifton et al. in fact assume $\eta_c \sim 3.3h\mathcal{H}^{-1}$. From the virial relation we note that the Newtonian potential, $\phi \sim v^2/c^2$, and furthermore from "empirical observations" [1] we know $\phi \sim 10^{-4}$, implying,

$$\frac{r_c}{\lambda_c} \sim \frac{v_c}{c} \sim 10^{-2}\,. \tag{6.2}$$

We note from (6.1) and the discussion above that λ_c is the size of the observable Universe, $\lambda_c \sim 10^4\,\mathrm{Mpc}$, implying $r_c \sim 100\mathrm{Mpc}$. This means that size of the systems we are restricted to when using a slow-motion *and* weak-field expansion are ~ 100 Mpc or smaller. We characterise an order of smallness in this expansion, related to the slow-motion condition:

$$\chi := \frac{v_c}{c} \ll 1. \tag{6.3}$$

Furthermore, we note that the slow-motion condition also has consequences for the order-of-smallness of derivatives. It follows that if the parts of a system 'move slowly' then the time-variation of state variables (here, S) must also vary slowly. Therefore, we say

$$\frac{\partial S}{\partial \eta} \sim \chi, \tag{6.4}$$

that is, conformal-time derivatives "add an extra order of smalless". This implies the background Friedmann equations — which contain two conformal-time derivatives (or one conformal-time derivative squared) — are of order χ^2. Other post-Newtonian attempts to model large density contrasts are similar to this approach, except they use an 'order of largeness'. This is done by making spatial derivatives large based solely on the Poisson equation [195].

Following Clifton et al. [1], we will hereafter adopt the units $c = 1$. However, we will not set $G = 1$ as they do. Clifton et al. also make the choice of $r_c = 1$, which results in statements such as $\chi \sim 1/\eta_c \sim \mathcal{H}$. These statements are consistent with χ being dimensionless, however, we stress that when using this formalism for practical purposes, we would strictly have $\chi \sim r_c/c\eta_c \sim r_c\mathcal{H}/c$.

6.1 Perturbations and their Orders of Magnitude

We use the same expansion of the metric that we used in section 4.4. The 4–velocity, however, is specified slightly differently, the components are:

$$u^\mu = \frac{1}{a}\left(1 - \phi + \frac{1}{2}v^2, v^i\right). \tag{6.5}$$

[3]Recall that $\mathcal{H}$ is the Hubble parameter in conformal time which is directly associated to the horizon.

Interestingly, if one specifies the lapse according to the g_{00} component then we obtain exactly this 4–velocity following the Buchert formalism. With this 4–velocity and (2.39) we compute the components of the 'full' stress-energy tensor[4]:

$$\begin{aligned} T^{0}{}_{0} &\simeq -G\rho\,(1+v^2) + \mathcal{O}(\chi^5), \\ T^{0}{}_{i} &\simeq G\rho\, v^i + \mathcal{O}(\chi^4), \\ T^{i}{}_{j} &\simeq G\rho\, v^i v_j + Gp\,\delta^{i}{}_{j} + \mathcal{O}(\chi^5), \end{aligned} \tag{6.6}$$

where ρ is the energy density of the fluid and p is the isotropic pressure. The order of magnitudes are found by realising that to leading order, ρ is order $\mathcal{O}(\chi^2)$, if the background Friedmann equations are to hold.

We may use the 'full' Einstein tensor to determine the magnitude of the perturbed metric components (see Appendix A) by equating the Einstein equations order-by-order. By noting the background Friedmann equations are $\mathcal{O}(\chi^2)$, $\phi \sim v^2 = \mathcal{O}(\chi^2)$, and conformal-time derivatives add a factor of χ we determine:

$$\delta\, g_{00} \sim \chi^2, \quad \delta\, g_{0i} \sim \chi^3, \quad \delta\, g_{ij} \sim \chi^2, \tag{6.7}$$

which implies

$$\begin{aligned} &\phi \sim \psi \sim F_{i,j} \sim E_{,ij} \sim D_{ij} \sim \rho \sim \chi^2, \\ &S_i \sim B_{,i} \sim \chi^3, \\ &p \sim \chi^4\,. \end{aligned} \tag{6.8}$$

This all stems from[5],

$$\begin{aligned} \delta\, G^{0}{}_{0} &\sim \chi^4 \\ \delta\, G^{0}{}_{i} &\sim \chi^3 \\ \delta\, G^{i}{}_{j} &\sim \chi^4, \end{aligned} \tag{6.9}$$

which matches the orders of magnitude for the perturbed stress-energy tensor. One should note, however, that *because* the background Einstein equations for the $(0,i)$ components are zero, we have this difference in orders of magnitude. If a 'physical' background spacetime model existed for which this was not the case, we would find all of the perturbed metric components would be of the same order. This obviously differs from standard perturbation theory which assumes all perturbations are of the same order, ϵ.

Perhaps the most useful aspect of the post-Newtonian expansion is that these orders of magnitude are related to a physically 'sensible' condition — the slow-moving condition. The slow-motion condition implies that on scales $r < r_c$ we approximate the entire past light cone of a point by some constant

[4]This is not how one would strictly compute the perturbed stress-energy tensor in linear perturbation theory. Here we simply define the perturbation of the stress-energy tensor as the difference between the full and the background.

[5]Really, we should state the $T^0{}_i$ component is a perturbation. This is why the order of $G^0{}_i$ is lower than the others, because this is really the first time a $(0,i)$ component appears. Conversely, the perturbed $(0,0)$ and (i,j) components are the second time these components appear in the expansion.

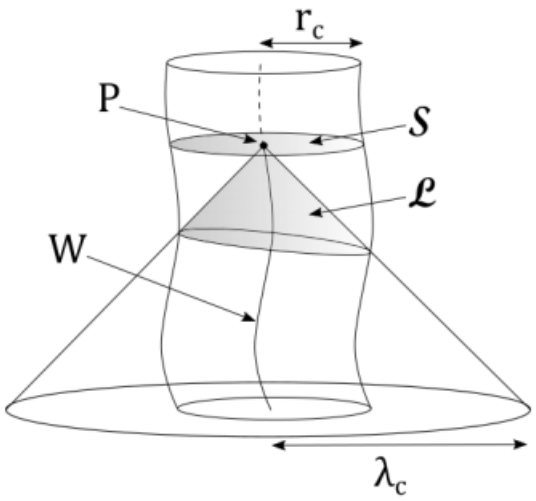

Figure 6.2: The past lightcone, $\mathcal{L}$ of a point P which is on a worldline W. Support of the metric perturbations at the point P can be approximated locally on the spacelike hypersurface, S under the assumption $r_c \ll \lambda_c$. This figure was obtained from Clifton et al. [1].

η-hypersurface, S (see Figure 6.2). This is because the time it takes gravitational information to propagate from one side of the domain is negligible when compared to η_c. Therefore, we simplify the integrals involved in determining the gravitational field. For instance, consider the perturbed constraint and evolution equation:

$$\mathcal{H}^2 + \frac{2}{3}\nabla^2\psi = \frac{8\pi G}{3}\rho a^2 + \frac{\Lambda}{3}a^2 + \mathcal{O}(\chi^4), \tag{6.10}$$

and

$$\dot{\mathcal{H}} - \frac{1}{3}\nabla^2\phi = -\frac{4\pi G}{3}(\rho + 3\bar{p})\,a^2 + \frac{\Lambda}{3}a^2 + \mathcal{O}(\chi^4), \tag{6.11}$$

where $\nabla \equiv \bar{g}^{ij}\,\partial_i\partial_j$. Note that we have included background pressure here. This is normally taken to be zero except in the early Universe. The slow-motion condition allows us to physically restrict the perturbed equations showing its use when attempting to solve equations for the gravitational field. One may note that these equations are simply a combination of the background Friedmann equations and the Newton-Poisson equations for ϕ and ψ. Furthermore, they occur at the same order of magnitude here, which is not the case in standard perturbation theory.

6.2 Gauge Choices in the Post-Newtonian Expansion

Due to the different orders of magnitude associated with the different perturbed metric components, Clifton et al. [1] find that there are many standard cosmological gauges that are *not viable*. These gauges are not viable in the sense

that many of the physical quantities that are set to zero in standard perturbation theory are gauge invariant in the post-Newtonian expansion. We will demonstrate that this is the case and test the uniform Hubble expansion gauge as well. Before starting a detailed analysis, one may crudely understand how certain quantities such as ϕ will be gauge invariant as they are $\mathcal{O}(\chi^2)$, as are the background field equations[6]. More precisely, to select a gauge we must specify coordinates by a *choice* of the gauge generators as done in subsection 4.5.1. However, in post-Newtonian cosmology sometimes no such choice can be made.

Recall the gauge transformations we performed in (4.57) and (4.58). We must analyse the order of magnitude of these equations to determine the order of magnitude of the gauge generators. Let us begin with the $(0,0)$ components

$$-\Delta\,\delta g_{00} = \mathcal{O}(\xi^0\,\partial_\eta\,a) - \mathcal{O}(\partial_\eta\,\xi^0) = \mathcal{O}(\chi\,\xi^0) - \mathcal{O}(\chi\,\xi^0). \tag{6.12}$$

This puts the minimum restriction on ξ^0 to be $\mathcal{O}(\chi)$ in order to obtain the correct orders of magnitude on both sides of the equation as δg_{00} is $\mathcal{O}(\chi^2)$. For the $(0,i)$ components we have

$$-\Delta\,\delta g_{0i} = \mathcal{O}(\xi^0) + \mathcal{O}(\chi\,\xi^i), \tag{6.13}$$

This puts the minimum restriction on ξ^0 to be $\mathcal{O}(\chi^3)$ and ξ^i to be $\mathcal{O}(\chi^2)$ as δg_{0i} is $\mathcal{O}(\chi^3)$. Finally, for the (i,j) components we have

$$\Delta\delta g_{ij} = \mathcal{O}(\chi\,\xi^0) + \mathcal{O}(\xi^i), \tag{6.14}$$

from which we see that no new restrictions have been added on either gauge generator. Therefore, we conclude that

$$\xi^0 = \mathcal{O}(\chi^3), \quad \text{and} \quad \xi^i = \mathcal{O}(\chi^2)\,. \tag{6.15}$$

This differs from the assumption standard cosmological perturbation theory which assumes $\xi^\mu \sim \epsilon$.

It is important to note that the $\mathcal{O}(\delta g\,\xi)$ terms in (4.56) cannot be neglected as some of these appear at the same order as $\mathcal{L}_\xi \bar{g}_{\mu\nu}$. Therefore, we must use

$$\Delta\,\delta g_{\mu\nu} = -\mathcal{L}_\xi g_{\mu\nu}, \tag{6.16}$$

instead of $\mathcal{L}_\xi \bar{g}_{\mu\nu}$, resulting in the following transformations:

$$\begin{aligned}
&\Delta\phi = -\Big(\mathcal{H}\,\xi^0 + \xi^{0\,\prime} + \phi_{\,,i}\,\xi^i\Big),\\
&\Delta B = \xi^0 - \zeta^{\,\prime}\\
&\Delta S_i = \zeta_i{}^{\prime},\\
&\Delta\psi = \mathcal{H}\,\xi^0\,,\\
&\Delta E = -\zeta\,,\\
&\Delta F_i = -\zeta_i\,,\\
&\Delta D_{ij} = 0\,.
\end{aligned} \tag{6.17}$$

[6]As we will show, this does not mean that all quantities that are $\mathcal{O}(\chi^2)$ are gauge invariant.

Performing the same gauge transformation on the stress-energy tensor with components given in (6.6) we find,

$$\begin{aligned} &\Delta\,\mu = 0 \\ &\Delta\,\Pi = \xi^i\,(\ln\mu)_{,i} \quad \Delta\,P = 0, \\ &\Delta\,v^i = 0\,. \end{aligned} \tag{6.18}$$

Here we have decomposed the energy density, ρ into two parts of order $\mathcal{O}(\chi^2)$, μ and Π, such that $\rho = \mu\,(1+\Pi)$ where μ is the rest mass density and Π is the specific energy density.

With all of the gauge transformations of the various metric components and the stress-energy components, we may investigate which components are gauge-invariant. Notice that the right-hand side of the transformations for ϕ, ψ, p, $\boldsymbol{v}$, μ, Π, and D_{ij} are either zero or of a higher order in χ than the left-hand sides — meaning they are all required to be gauge-invariant. This is because we cannot set any choice of $\boldsymbol{\xi}$ to generate a change that is the same order of magnitude as the quantity we wish to change. The only quantities that are not gauge-invariant are B, S_i, E, and F_i as the right-hand sides are the same order of magnitude in χ as the left-hand sides. Notice that the only quantities that are order $\mathcal{O}(\chi^2)$ and not gauge-invariant are E and F_i.

We now investigate the viability of the gauges investigated in section subsection 4.5.1 with the information above

- **Synchronous gauge**: The synchronous gauge is defined by setting

  $$\tilde{\phi} = \tilde{B} = \tilde{S}_i = 0.$$

  This was achievable in standard perturbation theory but is not viable in the post-Newtonian expansion. This is because ϕ is gauge invariant at leading order — meaning it cannot be set to 0. The other requirements ($\tilde{B} = \tilde{S}_i = 0$) are still achievable in the post-Newtonian expansion by solving the differential equations (4.62).

- **Spatially flat gauge**: This gauge is defined by setting

  $$\tilde{\psi} = \tilde{E} = \tilde{F}_i = 0.$$

  This was achievable in standard perturbation theory, but not in post-Newtonian perturbation theory because ψ is gauge-invariant. Thus we cannot make it vanish, though we can set $\tilde{E}$ and $\tilde{F}_i$ to zero.

- **Comoving orthogonal gauge**: We choose

  $$\tilde{v}_i = 0 \quad \text{and} \quad g_{0i} = 0\,.$$

  We cannot achieve this gauge in the post-Newtonian expansion as $\boldsymbol{v}$ is gauge-invariant at leading order. This means that we *must* have a tilt between the normal frames and the fluid rest frames.

- **Conformal Newtonian or longitudinal gauge**: One defines this gauge by choosing
$$\tilde{B} = \tilde{E} = 0.$$
This gauge is the only standard gauge in cosmology investigated by Clifton et al. [1] that is achievable in both standard perturbation theory and the post-Newtonian expansion. This allows most standard approaches to modelling the evolution of the Universe from the CMB as an initial hypersurface viable in post-Newtonian perturbation theory.

- **N-Body gauge**: Recall that the first condition to define the N-body gauge is
$$\tilde{v} + \tilde{B} = 0.$$
This condition is obviously not achievable in post-Newtonian theory as v and B are $\mathcal{O}(\chi)$ and $\mathcal{O}(\chi^3)$ respectively. The second condition for the N-body gauge is[7]
$$\tilde{\psi} - \frac{1}{3}\nabla^2 \tilde{E} = 0,$$
which can be achieved by picking ζ such that is solves $\nabla^2\zeta = -(3\psi + -\nabla^2 E)$. Interestingly, this condition can be satisfied in the post-Newtonian expansion. This opens up the opportunity to modify the first condition to have a modified version of this gauge that is viable, which has been investigated by [196, 197].

6.2.1 Uniform Hubble Expansion Gauge

This gauge has also been called the Mach 1 gauge by Bičák et al. [2] who determine three alternative gauges, Mach 1 to Mach 3 using Mach's principle as a guide[8]. Bičák, Katz and Lynden-Bell describe these gauges as follows: "*In these gauges, the local inertial frames can be determined instantaneously from the perturbed Einstein field equations from the distribution of energy and momentum in the Universe*". We shall only investigate the Mach 1 gauge here.

The uniform Hubble expansion gauge is defined by two conditions:

$$\delta\Theta = 0\,, \tag{6.19}$$

and the minimal-shift distortion condition which is equivalent to

$$\nabla_i {}^T h^i{}_k. \tag{6.20}$$

[7]There is a sign error in the corresponding equation presented by Clifton et al. [1]. This sign propagates through trivially.

[8]Mach's principle states "*Local inertial frames are determined through the distributions of energy and momentum in the universe by some weighted average of the apparent motions*". There are actually many different principles that are referred to as "Mach's principle" — Bondi and Samuel list 10 [198].

Here ${}^{T}h^{i}{}_{k}$ is the traceless part of the induced metric on the normal hypersurfaces, h_{ij}. The condition (6.19) was introduced by Bardeen [176] and implies that the expansion of the fluid on a hypersurface is the same as the expansion of the background manifold — in this case, the FLRW background. The latter condition (6.20) was introduced by Smarr and York in 1978 [199] because it allows kinematic and dynamical effects to be separated in order to study the kinematics of the worldlines that create a hypersurface. In perturbation theory the traceless part of $\boldsymbol{h}$ is

$$ {}^{T}h^{i}{}_{k} = 2\,F_{i,j} + D_{ij}, \tag{6.21} $$

meaning the minimal-shift distortion condition becomes

$$ \nabla_{i}\,{}^{T}h^{i}{}_{k} = 2\,\nabla_{i}\,F^{i}{}_{,k} + \nabla_{i}\,D^{i}{}_{k} = 0. \tag{6.22} $$

Since $\boldsymbol{F}$ and $\boldsymbol{D}$ are divergenceless the condition is automatically satisfied in both standard and post-Newtonian perturbation theory.

Recall that in the case of non-vanishing tilt, we do not have $\mathcal{K} = \Theta$. This is exactly the case we deal with in the post-Newtonian expansion as the 3–velocity of the fluid cannot be set to zero. This means we cannot exactly follow Bičák et al. [2] who use a fluid velocity that is hypersurface orthogonal[9]. Instead we must compute

$$ \nabla_{\mu}u^{\mu} =: \Theta\,, \tag{6.23} $$

where we use $\boldsymbol{u}$ as defined in (6.5). Carrying out this calculation we find (in a general gauge)

$$ \Theta = \frac{1}{a}\,3\mathcal{H} + \frac{1}{a}\Bigg[\partial_{i}\,v^{i} + 3\mathcal{H}\left(-\phi + \frac{v^{2}}{2}\right) - v^{i}\,\partial_{i}\left(\,3\psi - \nabla^{2}E + \nabla^{2}\zeta\,\right) \\ + \partial_{\eta}\left(\,3\psi - \nabla^{2}E + \nabla^{2}\zeta\,\right) + v^{i}\partial_{i}\,\phi + v^{i}\,{v_{i}}'\Bigg] + \mathcal{O}(\chi^{5})\,. \tag{6.24} $$

Note the background expansion scalar is $\bar{\Theta} = 3\mathcal{H}/a$, thus, the perturbed part of Θ is everything after the first term. Interestingly, there is one term of order $\mathcal{O}(\chi)$, namely[10], $1/a\,\partial_{i}v^{i}$ which is the same order as the background term, and the other terms are all $\mathcal{O}(\chi^{3})$. We see the only gauge generator we have present is ζ which is order $\mathcal{O}(\chi^{2})$, while the leading order term in $\delta\Theta$ is order $\mathcal{O}(\chi)$. This implies that we cannot set $\delta\Theta$ to zero and, therefore, the gauge is not viable in the post-Newtonian expansion.

We may, however, construct a 'weaker' condition that sets all of the χ^{3} terms to zero. We then obtain

$$ \Theta = \bar{\Theta} + \frac{1}{a}\,\partial_{i}v^{i}, \tag{6.25} $$

[9] In the case of a fluid velocity that is hypersurface orthogonal, this gauge is also referred to as the *constant mean extrinsic curvature* gauge as $\mathcal{K} = \Theta$.

[10] This is similar to the perturbed equations (6.10) and (6.11) which involve the background Friedmann equations and the perturbations, ϕ and ψ.

which means the expansion is simply the background expansion with the addition of the spatial divergence of the 3–velocity of the fluid. This condition or gauge choice expresses that the observed expansion (through the Hubble parameter) will be uniform regardless of how we split the background expansion to be and the spatial divergence of the velocity field. It accords with there being no observational distinction between the divergence of the spatial velocity of "the fluid" and an isotropic component of the local expansion.

To determine whether or not this gauge choice is viable, we collect the various $\mathcal{O}(\chi^3)$ terms in (6.24). Let

$$A = \nabla^2\zeta, \quad B = 3\psi - \nabla^2 E, \quad C = -3\phi\,\frac{\mathcal{H}}{a} + 3\,\mathcal{H}\frac{v^2}{a^2}, \quad \text{and} \quad Z = \phi_{,i} + v_i'\,, \tag{6.26}$$

and therefore the condition of setting all of the $\mathcal{O}(\chi^3)$ terms in (6.24) to zero becomes

$$v^i\,(-\partial_i\,(A+B) + Z) + \partial_\eta\,(A+B) + C = 0. \tag{6.27}$$

This requires us to solve the following set of coupled differential equations:

$$\begin{aligned} \partial_\eta\,(A+B) + C &= 0\,, \\ -\,\partial_i\,(A+B) + Z &= 0. \end{aligned} \tag{6.28}$$

Taking the derivative of the first equation with respect to spatial coordinates, and taking the derivative of the second equation with respect to conformal time, we find

$$\begin{aligned} \partial_i\partial_\eta\,(A+B) + \partial_i C &= 0\,, \\ -\,\partial_i\partial_\eta\,(A+B) + \partial_\eta Z &= 0. \end{aligned} \tag{6.29}$$

To solve this system of equations, we obviously require $\partial_i C = -\partial_\eta Z$, i.e.,

$$-\,\partial_\eta\,(\,\phi_{,i} + v_i'\,) = \partial_i\Big(-3\phi\,\frac{\mathcal{H}}{a} + 3\,\mathcal{H}\,\frac{v^2}{2a}\Big), \tag{6.30}$$

which cannot be set by choice of *gauge*, or in other words, by choice of $\boldsymbol{\xi}$. Thus, this gauge in not viable in the post-Newtonian expansion.

6.3 Construction of Buchert Averaging in the Post-Newtonian Formalism

Our aim here is to construct Buchert averages in the post-Newtonian expansion. This should be possible due to all the freedom the extrinsic approach to averaging allows. One has a total 4 degrees of freedom in the time-time and space-time components and all 6 (if required) in the space-space components of the metric tensor (as well as three timelike congruences).

Let us first summarise the restrictions imposed on us by the post-Newtonian expansion:

- Different degrees of freedom in the metric have different orders of magnitude in χ.
- We are not allowed to have vanishing tilt as $\boldsymbol{v}$, the Eulerian velocity is gauge-invariant at leading order.
- We must work with conformal time which must be dimensionful, while the scale factor must, therefore, be dimensionless.

To make contact between the two formalisms, we must first consider the line elements. The four degrees of freedom in the 3+1 formalism which are given by the lapse, N, and shift, $\boldsymbol{\beta}$, can be specified as follows

$$N^2 = a^2(\eta)\,(\,1 + 2\,\phi\,), \tag{6.31}$$

and,

$$\beta_i = a(\eta)\,(\,B_{,i} - S_i\,). \tag{6.32}$$

We note that the standard set of spatial coordinates in the standard model of cosmology are the comoving coordinates. With the knowledge that[11] $\boldsymbol{x} = a\boldsymbol{X}$ we may write the following

$$\begin{aligned} \mathrm{d}s^2 &= g_{\mu\nu}\,\mathrm{d}x^\mu\mathrm{d}x^\nu = -N^2\,\mathrm{d}\eta^2 + 2\beta_i\,\mathrm{d}x^i\mathrm{d}\eta + h_{ij}\,\mathrm{d}x^i\mathrm{d}x^j \\ &= a^2(\eta)\Big(-(1+2\phi)\,\mathrm{d}\eta^2 + 2\,(\,B_{,i} - S_i\,)\,\mathrm{d}X^i\,\mathrm{d}\eta + h_{ij}\,\mathrm{d}X^i\mathrm{d}X^j\Big)\,, \end{aligned} \tag{6.33}$$

where

$$h_{ij} = ((1 - 2\,\psi)\,\delta_{ij} + 2\,E_{,ij} + 2\,\partial_{(i}F_{j)} + D_{ij}). \tag{6.34}$$

The perturbed FLRW line element here is exactly the same as (4.48) except we have now used a different symbol for the spatial coordinates to match the Buchert formalism. We have also transformed the time coordinate that Buchert uses to the conformal time, which we are allowed to do by the argument in subsection 5.4.3. Therefore, we find that the lapse is $1 + \mathcal{O}(\chi^2)$, and the shift is $\mathcal{O}(\chi^3)$. Due to this, we have neglected the $\beta^i\beta_i$ term in the g_{00} component of the line element in (5.4) as this would be order $\mathcal{O}(\chi^6)$.

Let us now turn our attention to the three congruences shown in Figure 5.1. Up to a negative sign, we may relate the vectors $\boldsymbol{\beta}$, $N\boldsymbol{v}$, an $\boldsymbol{V}$ by

$$\begin{aligned} \boldsymbol{\beta} &= N\boldsymbol{v} - \boldsymbol{V} \\ &\approx a\,(\,1 + \phi\,)\,\boldsymbol{v} + \boldsymbol{V}. \end{aligned} \tag{6.35}$$

The left-hand side of this equation, the shift vector is $\mathcal{O}(\chi^3)$, implying the right-hand side must be $\mathcal{O}(\chi^3)$. To achieve this, we require that the coordinate velocity cancels the Eulerian velocity (multiplied by a) which is $\mathcal{O}(\chi)$. Therefore,

$$\boldsymbol{V} = a\boldsymbol{v}, \quad \text{and} \quad \boldsymbol{\beta} = a\,\phi\,\boldsymbol{v}, \tag{6.36}$$

[11] Recall that in the Buchert formalism, $\{x^i\}$ are the reference coordinates or *Eulerian coordinates* and $\{X^i\}$ are comoving coordinates.

which satisfy the post-Newtonian expansion constraints. It may seem odd that $\boldsymbol{\beta}$, which is not gauge-invariant is constructed from two quantities that are gauge-invariant. This, however, does not matter as the gauge transformations that we consider are applied to the metric and stress-energy tensor, (not individual scalars/vectors). This means that if a component is gauge invariant, it will remain gauge invariant as long as the order of magnitude remains the same.

We have fixed the lapse and shift vectors in the Buchert formalism to ensure that the post-Newtonian formalism is not violated. Therefore, we can now extend the Buchert averaging scheme. Let us begin with the time evolution of the volume, which becomes

$$\frac{\mathrm{d}}{\mathrm{d}t}\mathcal{V}_{\mathcal{D}} = \int_{\mathcal{D}_{\boldsymbol{x}}} \Big(-a(1+\phi)\mathcal{K} + a D_i \Big((1+\phi)(v^i) \Big) \Big) \sqrt{h}\, \mathrm{d}^3x. \tag{6.37}$$

Furthermore, the commutation rule (5.64), and the extrinsically averaged evolution equations (5.75), (5.80), change by the replacement $N = a(\,1+\phi\,)$. Further changes will come from the fact that the induced metric determinant, h, is now perturbed as well. This allows us to determine the order of magnitude of various terms in the averaged evolution equations, for instance, the backreaction terms.

6.3.1 Longitudinal Gauge and Backreaction Magnitudes

If one wishes to simulate the evolution of the Universe from some initial Cauchy surface using the post-Newtonian expansion with Buchert averaging then the only viable standard gauge is the longitudinal gauge. The line element in the longitudinal gauge takes the form

$$\mathrm{d}s^2 = a^2(\eta)\Big(-(1+2\phi)\,\mathrm{d}\eta^2 + (\,1+\psi\,)\,\delta_{ij}\,\mathrm{d}X^i\mathrm{d}X^j \Big). \tag{6.38}$$

Thus, the shift vanishes in this gauge.

Recall that in the extrinsic averaging formalism, we must compute the backreaction in terms of the extrinsic curvature. In the longitudinal gauge, the scalar extrinsic curvature is

$$\mathcal{K} = \frac{1}{a}\Big(3\mathcal{H} - 3\phi\mathcal{H} + \frac{3}{2}\,\psi' \Big), \tag{6.39}$$

and the contracted extrinsic curvature tensor scalar is

$$\mathcal{K}^{ij}\mathcal{K}_{ij} = \frac{1}{a^2}\Big(3\mathcal{H}^2 - 6\phi\mathcal{H}^2 - 3\mathcal{H}\psi' \Big). \tag{6.40}$$

We must also determine the intrinsic curvature of the hypersurface, which in the longitudinal gauge is

$$\mathcal{R} = \frac{4}{a^2}\,\nabla^2\,\psi. \tag{6.41}$$

Finally, to average, we need the determinant of the spatial metric, $\boldsymbol{h}$:

$$h = \det(h_{ij}) = a^6(\,1-6\psi\,) \implies \sqrt{h} = a^3\sqrt{1-6\psi} \approx a^3(\,1-3\psi\,). \tag{6.42}$$

Before writing down the expressions for the backreaction terms in terms of a post-Newtonian expansion, let us examine the volume operator. The volume of our domain is written (in comoving coordinates) as

$$\mathcal{V}_{\mathcal{D}} = \int_{\mathcal{D}_{\boldsymbol{X}}} a^6(\,1-3\psi\,)\,\mathrm{d}^3X, \tag{6.43}$$

where the extra powers of a come from the Jacobian that transforms from $\boldsymbol{x} \to \boldsymbol{X}$. The relative size of the volume is determined by the integration domain chosen. When averaging scalars, we will therefore have a leading order part multiplied by a^6 and decrease the order by χ^2 when multiplying by the $3\psi\,a^6$ term.

The kinematical backreaction in the post-Newtonian formalism is, therefore, determined to be[12]:

$$\begin{aligned}\mathcal{Q}_{\mathcal{D}} &= \frac{2}{3}\Big\langle N\mathcal{K} + D_i(\,Nv^i\,)\Big\rangle_{\mathcal{D}}^2 - \Big\langle N^2(\,\mathcal{K}^2 - \mathcal{K}^{ij}\mathcal{K}_{ij}\,)\Big\rangle_{\mathcal{D}} \\ &= \frac{2}{3}\Big\langle 3\mathcal{H} + \frac{3}{2}\,\psi' + D_i(\,a(1+\phi)(v^i)\,)\Big\rangle_{\mathcal{D}}^2 - \Big\langle 6\mathcal{H}^2 - 6\,\mathcal{H}\psi'\Big\rangle_{\mathcal{D}} + \langle\,\mathcal{O}(\chi^5)\,\rangle_{\mathcal{D}}\,.\end{aligned} \tag{6.44}$$

We see that the leading order terms will be $\mathcal{O}(\chi^2)$, which will not change due to the averaging procedure by the argument above[13]. Therefore, one can say that "backreaction" is, at leading order, $\mathcal{O}(\chi^2)$. We find

$$\begin{aligned}\mathcal{P}_{\mathcal{D}} := \Bigg\langle &\Big(D_i(\,a(1+\phi)v^i\,)\Big)^2 + \frac{1}{a}\frac{\mathrm{d}}{\mathrm{d}\eta}\Big(D_i(\,a(1+\phi)\,v^i\,)\Big) \\ &- (\,3\mathcal{H} + \frac{3}{2}\,\psi'\,)\,D_i(\,a(1+\phi)(v^i)\,) + a(\,1+2\phi\,)\,v^i D_i\,3\phi\mathcal{H}\Bigg\rangle_{\mathcal{D}} \\ + \Bigg\langle &a^2(\,1+\phi\,)\,D^iD_i(\,1+\phi\,) - \frac{3\mathcal{H}}{a^2}\,\frac{\mathrm{d}}{\mathrm{d}\eta}\,a(\,1+\phi\,)\Bigg\rangle_{\mathcal{D}} + \langle\,\mathcal{O}(\chi^5)\,\rangle_{\mathcal{D}}\,,\end{aligned} \tag{6.45}$$

where the leading order terms are the same order as the leading order terms in the kinematical backreaction expression. Finally, we may express the stress-energy backreaction as

$$\mathcal{T}_{\mathcal{D}} = -16\pi G\Big\langle a(\,1+2\phi\,)(E-\rho)\Big\rangle_{\mathcal{D}}, \tag{6.46}$$

[12]This is only the case if we *do not* have periodic boundary conditions. As mentioned in subsection 5.4.1, all averages will vanish if one assumes periodic boundary conditions.

[13]More precisely, the square root of the determinant of the metric does not change (to leading order). Thus it does not increase the order of smallness of any of the terms inside the angle brackets.

where we assume E to be $\mathcal{O}(\chi^2)$ as it is essentially the same order as ρ, only measured in a different frame. Therefore, the stress-energy backreaction is also $\mathcal{O}(\chi^2)$ at leading order.

We now write the extrinsically averaged evolution equations as:

$$3\left(\frac{1}{a_{\mathcal{D}}}\frac{\mathrm{d}a_{\mathcal{D}}}{\mathrm{d}\eta}\right)^2 = 8\pi G\left\langle a^2(1+2\phi)\rho\right\rangle_{\mathcal{D}} + \left\langle a^2(1+2\phi)\right\rangle_{\mathcal{D}}\Lambda - \frac{1}{2}\left\langle a^2(1+2\phi)\frac{4}{a^2}\nabla^2\psi\right\rangle_{\mathcal{D}} - \frac{1}{2}\mathcal{Q}_{\mathcal{D}} - \frac{1}{2}\mathcal{T}_{\mathcal{D}} + \langle\,\mathcal{O}(\chi^5)\,\rangle_{\mathcal{D}}\ , \quad (6.47)$$

$$3\frac{1}{a_{\mathcal{D}}}\frac{\mathrm{d}^2a_{\mathcal{D}}}{\mathrm{d}\eta^2} = -4\pi G\left\langle a^2(\rho+2\phi\rho+3p)\right\rangle_{\mathcal{D}} + \left\langle a^2(1+2\phi)\right\rangle_{\mathcal{D}}\Lambda + \mathcal{Q}_{\mathcal{D}} + \mathcal{P}_{\mathcal{D}} + \frac{1}{2}\mathcal{T}_{\mathcal{D}} + \langle\,\mathcal{O}(\chi^5)\,\rangle_{\mathcal{D}}\ . \quad (6.48)$$

We note from the previous discussion that like the backreaction terms, the leading order parts in these equations are also $\mathcal{O}(\chi^2)$.

Finally let us consider the fluid-intrinsic averaging scheme introduced in section 5.2. The comoving description or the 'weak Lagrangian description' restricts the freedoms in the general 3+1 splitting of spacetime. This is done by setting the coordinate velocity, $\boldsymbol{V}$, to zero and thereby setting the shift vector to $N\boldsymbol{v}$. This can be thought of as a non-viable gauge choice in the post-Newtonian expansion which requires the coordinate velocity to be gauge-invariant. Furthermore, the Lagrangian description restricts the freedom even further by fixing the lapse such that $\phi = 0$, which we know is not a 'viable gauge choice' either. Therefore, only extrinsic Buchert averaging is possible in the post-Newtonian expansion as the tilt cannot be set to zero.

The fact that the backreaction terms appear at the same order, $\mathcal{O}(\chi^2)$, as the other terms in the averaged equations (6.47)–(6.48) may appear surprising. However, we are dealing with regional averages on small scales, not a global averaged Friedmann background. Our result, therefore, has no bearing on the debate about the magnitude of backreaction [50–54]. That debate concerns assumptions about how one constructs the global averages, which we do not consider here. Since $\chi \sim r_c/c\eta_c \sim r_c\mathcal{H}/c$, our slow-motion restriction limits us to scales $r_c \sim c\chi/\mathcal{H}$.

We see explicitly that the post-Newtonian framework can be readily applied to small scale Buchert averages. In particular, in (6.38) $a(\eta)$ can be identified as a spatially homogeneous part of a generic lapse function, rather than necessarily the scale factor of a FLRW background. Issues about global averages require additional assumptions. It was already noted by Clifton et al. that their formalism could allow for the inclusion of nontrivial backreaction — however, they chose not to consider the possibility, and only worked with a perturbed FLRW background.

This possibility of a background–free post–Newtonian approach could be investigated in future by not restricting quantities such as ϕ and ψ to be "small". Rather we would simply take these scalars to characterise the deviations from spatial homogeneity. This would mean steps such as (6.42) where we Taylor expand the volume form $\sqrt{h}$ would remain exact. Obviously this would increase the complexity of the equations as neither the extrinsic curvature nor intrinsic Ricci scalar would be truncated at $\mathcal{O}(\chi^2)$. This is similar to the approach the in Lagrangian perturbation theory of Buchert [44] where perturbations are not necessarily small. Clearly, there are many open avenues for future research.

Chapter 7

The Szekeres Model and Backreaction

In Chapter 4, we reviewed the standard approach to modelling inhomogeneities in the Universe using linear cosmological perturbation theory. In Chapter 6, we discussed a relatively new approach to modelling non-linear structure evolution in the Universe. Both of these approaches (in general) perturb about an FLRW background. Linear perturbation theory in particular is known to poorly explain the late epoch Universe on small scales, thus we seek alternatives.

Perturbation theory about the FLRW model implicitly neglects backreaction. We, therefore, will step away from perturbation theory and use an exact inhomogeneous solution to the Einstein equations — the Szekeres model — in order to investigate the magnitude of backreaction on small scales $\leq 100\,h^{-1}$ Mpc. A similar investigation has been undertaken by Bolejko in 2017 [5] with different parameters and different analysis techniques.

The Szekeres model was introduced in 1975 [200] and is the most general known exact solution of the Einstein equations for an inhomogeneous dust source. The Szekeres solution is a generalisation of the spherically symmetric Lemaître-Tolman-Bondi (LTB) [201–203] solution. The LTB models were an earlier inhomogeneous exact solution to the Einstein equations which are sourced by dust[1]. The subclass of quasispherical Szekeres solutions adds a mass dipole and possible shell rotation [204] to the LTB model. In appropriate limits the Szekeres model reduces to the LTB model and the LTB model further reduces to the FLRW model when $\rho(t,r) \to \rho(t)$. The Szekeres model has been used numerically in ray-tracing investigations to determine to effects of inhomogeneities below the statistical scale of homogeneity [134, 205].

The quasispherical Szekeres solutions represent a family of concentric but asymmetric radial shells, with areal radius, $R(t,r)$. In general, these shells are displaced from each other according to the functions P, Q, and S in the line element. The line element of the quasispherical Szekeres model in spherical

[1] In fact, Lemaître originally studied fluids with pressure as well [201].

coordinates is [200, 206]

$$
\begin{aligned}
\mathrm{d}s^2 = &-\mathrm{d}t^2 + \frac{1}{1+2E}\left[R_{,r} + \frac{R}{S}(S_{,r}\,\cos(\theta) + N\,\sin(\theta)\right]^2 \mathrm{d}r^2 \\
&+ \left(\frac{R}{S}\right)^2 \Big[S_{,r}\,\sin\theta + N\,(1-\cos\theta)\Big]^2 \mathrm{d}r^2 + \left(\frac{R}{S}\right)^2 \Big[(N_{,\phi}(1-\cos\theta)\Big]^2 \mathrm{d}r^2 \\
&- 2\left(\frac{R}{S}\right)^2 \Big[SS_{,r}\,\sin\theta + SN\,(1-\cos\theta)\Big]\,\mathrm{d}r\,\mathrm{d}\theta \\
&+ 2\left(\frac{R}{S}\right)^2 \Big[S(N_{,\phi}\sin\theta(1-\cos\theta)\Big]\,\mathrm{d}r\,\mathrm{d}\phi + R^2\left(\mathrm{d}\theta^2 + \sin^2\theta\,\mathrm{d}\phi^2\right),
\end{aligned}
\tag{7.1}
$$

where $E = E(r) \geq -1/2$, $S = S(r)$, and $N(r,\phi) \equiv (P_{,r}\cos\phi + Q_{,r}\sin\phi)$. Here $Q = Q(r)$ and $P = P(r)$.

The Einstein equations with nonzero cosmological constant and dust source with density, ρ, can be written as

$$
G_{\mu\nu} = 8\pi G\rho\, u_\mu u_\nu + \Lambda g_{\mu\nu}. \tag{7.2}
$$

They can be reduced to the evolution equation and the mass distribution equation [207]. The evolution equation takes the form

$$
(\partial_t R(t,r))^2 = -k(r) + \frac{2M(r)}{R} + \frac{1}{3}\Lambda R^2, \tag{7.3}
$$

where $k(r) = -2E(r)$, and $M(r)$ is related to the mass density via

$$
8\pi G\rho = 2\frac{M_{,r} - 3M\mathcal{E}_{,r}/\mathcal{E}}{R^2(R_{,r} - R\mathcal{E}_{,r}/\mathcal{E})}. \tag{7.4}
$$

Here

$$
\frac{\mathcal{E}_{,r}}{\mathcal{E}} = -\frac{1}{S}\Big[S_{,r}\cos\theta + N\,\sin\theta\Big], \tag{7.5}
$$

which describes the departure from spherical symmetry. Notice that the only function that depends on time in (7.3) is $R(t,r)$, thus we may integrate this equation to give

$$
t - t_B(r) = \int_0^R \frac{\mathrm{d}\tilde{R}}{\sqrt{2M/\tilde{R} - k + (1/3)\Lambda\tilde{R}^2}}, \tag{7.6}
$$

where $t_B(r)$ is the *bang time* function. This encodes the fact that the age of the Universe can be *position dependent*.

The Szekeres model becomes homogeneous in the limit

$$\begin{aligned} &R(t,r) \to r\,a(t), \\ &M(r) \to \frac{1}{2} {H_0}^2 \Omega_m r^3, \\ &k(r) \to H_0^2(\Omega_m + \Omega_\Lambda - 1), \\ &S(r) \to \text{constant}, \\ &P(r) \to \text{constant}, \\ &Q(r) \to \text{constant}, \end{aligned} \tag{7.7}$$

when we recover the FLRW model. Here we will investigate a particular example of the Szekeres model studied by Nazer, Bolejko, and Wiltshire [134]. It is chosen to asymptote to the standard FLRW model with the limits (7.7) on spatial scales $> 100\,h^{-1}\,\text{Mpc}$, with parameters chosen to match the best fit values (2.57) for the fit to the Planck data. Notice that in the homogeneous limit, we clearly see that r is a comoving coordinate, as introduced in (5.27).

The departure from homogeneity can be modelled by using the following profile for the mass function [134, 205, 208],

$$M(r) = \frac{1}{2} {H_0}^2 \Omega_m r^3 (1 + \delta(r)), \tag{7.8}$$

where[2] $\delta(r)$ specifies the departure from homogeneity. Bolejko et al. [134] chose the $\delta(r)$ according to (7.9) to model a sharp gradient in density contrast at a void/wall boundary,

$$\delta(r) = \frac{1}{2}\delta_0\Big(1 - \tanh\frac{r - r_0}{2\Delta r}\Big), \tag{7.9}$$

as can be seen in Figure 7.1. Here $\delta_0 \in [-1, 0]$, r_0, and Δr are constants. The constant r_0 is the 'characteristic size of the void', while Δr determines the 'steepness' of the density profile.

The function $k(r)$ is only dependent on the radial coordinate and thus we may choose conditions for R at a given time to solve (7.6) for $k(r)$. Therefore, we make the following assumptions: firstly, the age of the Universe is the same everywhere for comoving observers, i.e., $t_B = 0$. Secondly, $R(t_0, r) = r$, where t_0 is the age of the Universe in the spatially flat FLRW model. Under these assumptions we may solve (7.6) numerically for $k(r)$.

Furthermore, we will not use the full Szekeres metric in our analysis, but rather only the axially symmetric case. This is specified by choosing S, P, and Q to be

$$\begin{aligned} &S(r) = r\left(\frac{r}{1\,\text{Mpc}}\right)^{\alpha-1}, \\ &P(r) = 0, \\ &Q(r) = 0. \end{aligned} \tag{7.10}$$

[2]Note that $\delta(r)$ is designed to take numerical values similar to the density contrast though it is not defined in exactly the same way.

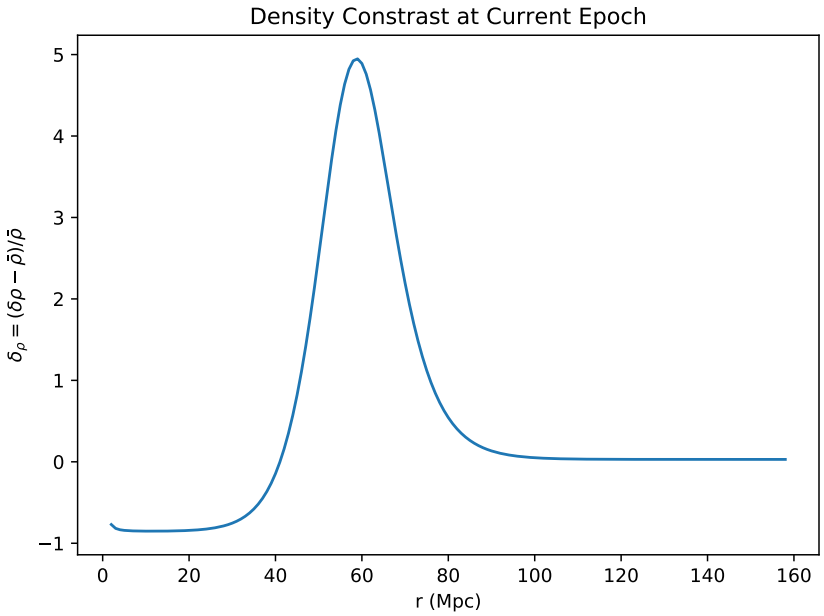

Figure 7.1: The density contrast $\delta_\rho = (\rho - \bar{\rho})/\bar{\rho}$ at $t = 0$ in the plane $\theta = \pi$. A sharp increase from void to wall is shown when density contrast grows from ~ -1 to ~ 5. Another steep transition from the wall region to asymptotic spatial homogeneity can be seen as the density contrast approaches zero.

Here α is a free parameter and in the limit that $\alpha \to 0$, we recover an LTB model. Finally, with the solution to $k(r)$ the "full" $R(t, r)$ is determined by solving[3] (7.3) for all r and t with the condition $R(t_0, r) = r$. The free parameters are selected to be

$$r_0 = 38.5\, h^{-1}\,\text{Mpc}, \quad \delta_0 = -0.86, \quad \text{and} \quad \alpha = 0.86. \tag{7.11}$$

7.1 Backreaction in the Szekeres Model

The Szekeres solution is described by irrotational dust and the coordinates (7.1) correspond to a fluid orthogonal comoving slicing, so that

$$n^\mu = u^\mu = (1, 0, 0, 0).$$

Consequently we use the Lagrangian form of the Buchert equations introduced in subsection 5.5.5. Furthermore, the dynamical backreaction vanishes, because the 4–acceleration is zero, leaving us only with the kinematical backreaction, $\mathcal{Q}_\mathcal{D}$.

[3]Note that we have not actually fully specified all of the functions in (7.3) as the parameters r_0 and δ_0 are still unspecified. These parameters are determined via a 5-dimensional parameter space search constrained by ray tracing and being able to realistically model the dipole and quadrupole of the CMB and the Hubble expansion anisotropy.

In order to carry out the averaging procedures (5.127)–(5.129), we require the expansion scalar, Θ, the shear scalar, σ^2, the intrinsic Ricci scalar[4], $\mathscr{R}$, and the determinant of the spatial metric, h. These are found to be

$$\begin{aligned}
\Theta &= \frac{\dot{R}_{,r} + 2\dot{R}R_{,r}/R - 3\dot{R}\mathcal{E}_{,r}/\mathcal{E}}{R_{,r} - R\mathcal{E}_{,r}/\mathcal{E}}, \\
\sigma^2 &= \frac{1}{3}\frac{3\dot{R}_{,r} - \dot{R}R_{,r}/R}{R_{,r} - R\mathcal{E}_{,r}/\mathcal{E}}, \\
\mathscr{R} &= 2\frac{k}{R^2}\left(1 + \frac{Rk_{,r}/k - 2R\mathcal{E}_{,r}/\mathcal{E}}{R_{,r} - R\mathcal{E}_{,r}/\mathcal{E}}\right), \\
\sqrt{h} &= \sin\theta\left(\frac{R^2R_{,r} - R^3\mathcal{E}_{,r}/\mathcal{E}}{\sqrt{1-k}}\right).
\end{aligned} \tag{7.12}$$

In order to make a comparison between the various functions describing the average evolution we use the dimensionless density parameters, Ω_i. Using the Buchert formalism, these are dubbed the *cosmic quartet* [62] of averaged parameters and are defined as

$$\begin{aligned}
\Omega_m^{\mathcal{D}} &:= \frac{8\pi G}{3(H_{\mathcal{D}}^b)^2}\langle\rho\rangle_{\mathcal{D}}^b, \\
\Omega_\Lambda^{\mathcal{D}} &:= \frac{1}{3(H_{\mathcal{D}}^b)^2}\Lambda, \\
\Omega_{\mathscr{R}}^{\mathcal{D}} &:= -\frac{1}{6(H_{\mathcal{D}}^b)^2}\langle\mathscr{R}\rangle_{\mathcal{D}}^b, \\
\Omega_{\mathcal{Q}}^{\mathcal{D}} &:= -\frac{1}{6(H_{\mathcal{D}}^b)^2}\mathcal{Q}_{\mathcal{D}}^b.
\end{aligned} \tag{7.13}$$

The averaged Hamiltonian constraint (5.127) then is equivalent to the sum rule

$$\Omega_m^{\mathcal{D}} + \Omega_\Lambda^{\mathcal{D}} + \Omega_{\mathscr{R}}^{\mathcal{D}} + \Omega_{\mathcal{Q}}^{\mathcal{D}} = 1\,. \tag{7.14}$$

The new density parameters, $\Omega_{\mathcal{Q}}^{\mathcal{D}}$ and $\Omega_{\mathscr{R}}^{\mathcal{D}}$ correspond to the kinematical back-reaction and intrinsic Ricci scalar averaged in a domain, $\mathcal{D}$, respectively.

To calculate the averages of the functions (7.12), we used the python integration routine, `scipy.integrate.nquad`. We choose to integrate over separate shells with different density contrasts which can be seen in Figure 7.1. The first shell is within the void region (underdense), $\{10 < r < 20\,\text{Mpc}\}$. The second shell is within the wall (overdense) region, $\{55 < r < 65\,\text{Mpc}\}$. The final shell is within the asymptotically FLRW region, $\{140 < r < 150\,\text{Mpc}\}$. I.e., every shell is chosen with a radius of 10 Mpc. These averages are then iterated over time in steps of $1\,\text{Mpc} \sim 3.29\text{Myr}$ back to $1 \times 10^3\text{Mpc} \sim 3.29\text{Gyr}$. The integrals

[4]We refer to this as the intrinsic Ricci scalar here despite our discussion in subsection 5.5.3 because the vorticity vanishes and the congruence is hypersurface forming.

in the various domains take the form

$$2\pi \int_{\theta=0}^{\theta=\pi} \int_{r=r_i}^{r=r_f} \psi \sin\theta \left(\frac{R^2 R_{,r} - R^3 \mathcal{E}_{,r}/\mathcal{E}}{\sqrt{1-k}} \right) \mathrm{d}r \, \mathrm{d}\theta, \tag{7.15}$$

where r_i and r_f are the radii at the beginning of the domain and the end of the domain respectively, and ψ is the scalar we will average. On account of axial symmetry, we gain a factor of 2π in the ϕ integral. Note that as time passes, the volume of these averaging shells increase due to $\sqrt{h}$ being time dependent and increasing over time (stemming from the fact that r is a comoving coordinate).

7.2 Results and Discussion

We present the cosmic quartet for the three different regions — the void, wall, and FLRW limit. A similar analysis was undertaken by Bolejko [5] who uses different function choices for (7.8). Furthermore, Bolejko uses a different value for the parameter α, Bolejko uses $\alpha = 0.52$, whereas we use $\alpha = 0.86$, and as can be seen from (7.4), this changes the density dramatically.

In addition we also plot 'pseudo-averaged density parameters', defined as

$$\begin{aligned}
\bar{\Omega}_m^{\mathcal{D}} &:= \frac{8\pi G}{3\bar{H}^2} \langle \rho \rangle_{\mathcal{D}}^b \,, \\
\bar{\Omega}_\Lambda^{\mathcal{D}} &:= \frac{1}{3\bar{H}^2} \Lambda, \\
\bar{\Omega}_{\mathscr{R}}^{\mathcal{D}} &:= -\frac{1}{6\bar{H}^2} \langle \mathscr{R} \rangle_{\mathcal{D}}^b \,, \\
\bar{\Omega}_{\mathcal{Q}}^{\mathcal{D}} &:= -\frac{1}{6\bar{H}^2} \mathcal{Q}_{\mathcal{D}},
\end{aligned} \tag{7.16}$$

where $\bar{H}(t)$ is the background or FLRW Hubble parameter. These parameters do not obey the sum rule (7.14). These parameters are introduced for visualisation purposes since values of the parameters (7.13) depend strongly on the values of $H_{\mathcal{D}}$ which varies significantly from shell to shell. This can be seen in Figure 7.2, where we plot the relative expansion rate $\Theta(t, r, \pi)/(3\bar{H}(t))$ as a function of r for three time slices.

7.2.1 Asymptotic FLRW shell

In Figure 7.3 we first display the parameters of the cosmic quartet for averages in the asymptotic region outer shell, as a check on our numerical procedures. As expected, these are indeed found to match those of the spatially flat ΛCDM model with the Planck normalised parameters, $\Omega_{m0} \simeq 0.31$, $\Omega_{\Lambda 0} = 0.69$. The only significant parameters are the decreasing matter density parameter $\Omega_m^{\mathcal{D}}$ (top right panel) and the increasing cosmological constant density parameter $\Omega_\Lambda^{\mathcal{D}}$ (bottom right panel). There is a tiny positive spatial curvature, corresponding

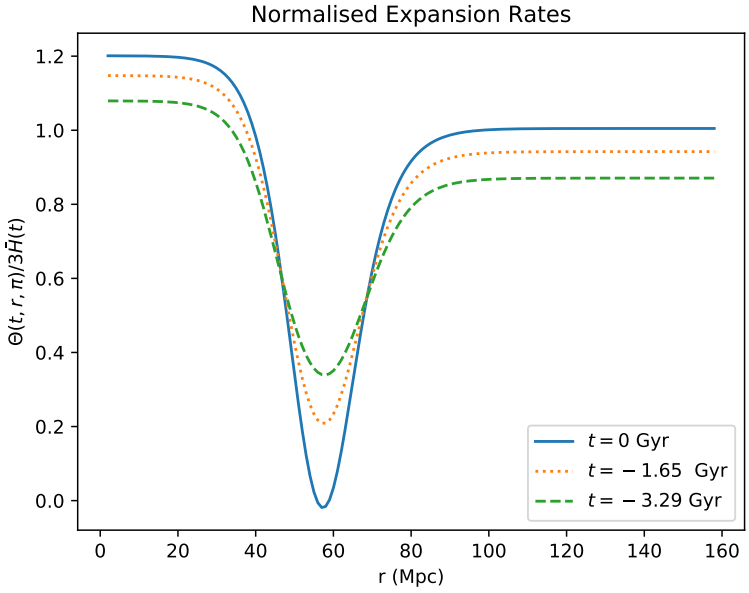

Figure 7.2: Relative expansion rate(s) in the plane $\theta = \pi$ at the present and two past epochs. Regional expansion of the inhomogeneities relative to the asymptotic FLRW shell grows more extreme as t increases.

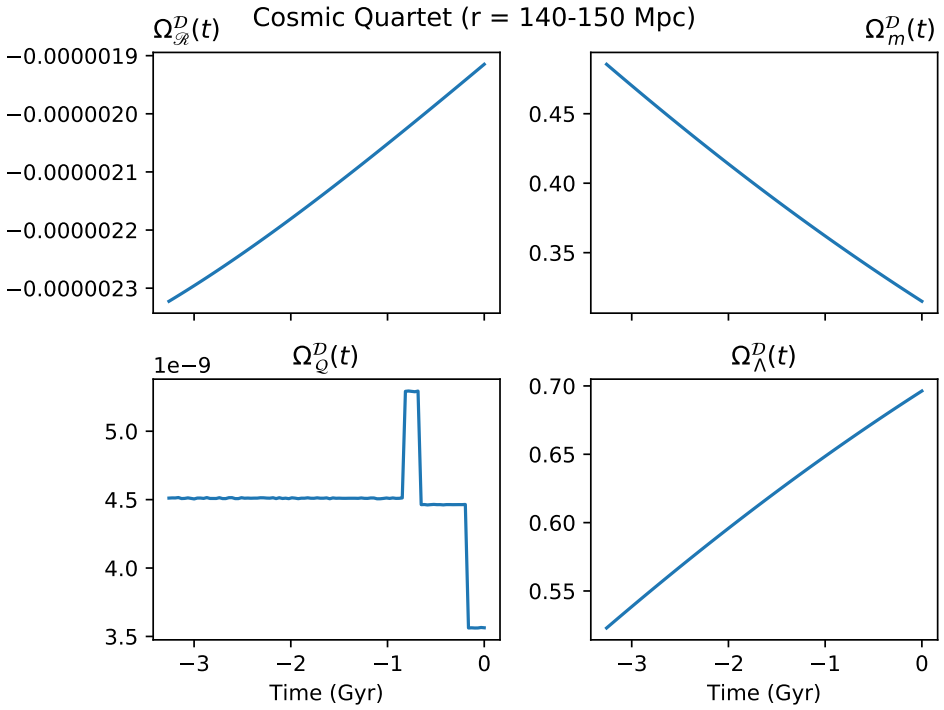

Figure 7.3: The cosmic quartet, in the outer shell $140\,\mathrm{Mpc} < r < 150\,\mathrm{Mpc}$, averaged over time from 3.29 Gyr in the past to the present epoch. (For this shell the corresponding pseudo-averaged density parameters are identical.)

to a negative $\Omega^{\mathcal{D}}_{\mathscr{R}}$, with a magnitude decreasing to $|\Omega^{\mathcal{D}}_{\mathscr{R}}| \sim 1.9 \times 10^{-6}$ at the present epoch. The backreaction density parameter $\bar{\Omega}^{\mathcal{D}}_{\mathcal{Q}} \sim 4.5 \times 10^{-9}$ is even

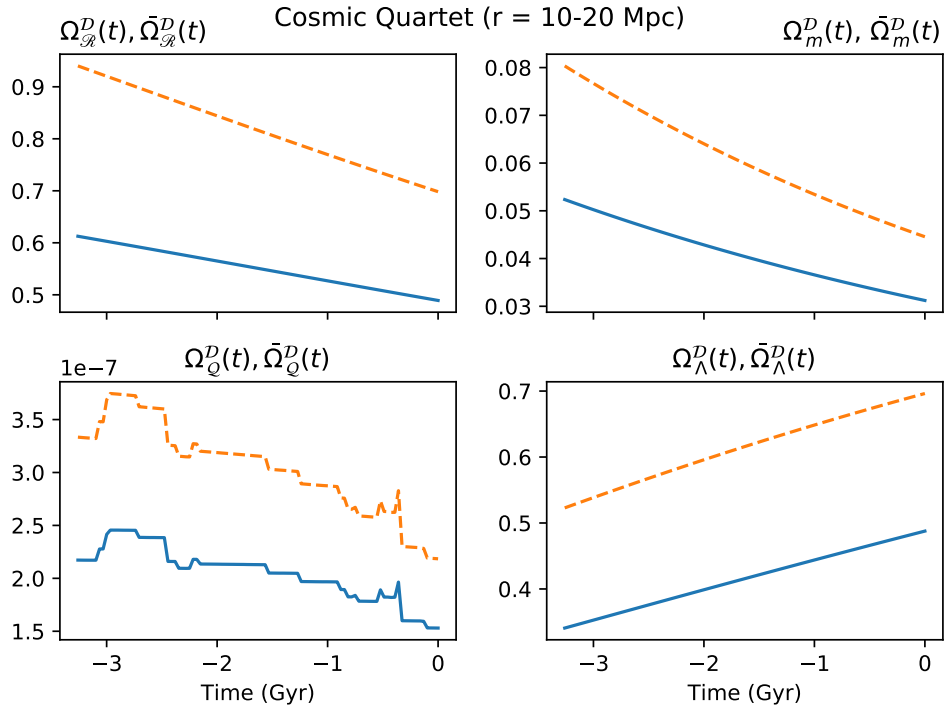

Figure 7.4: The cosmic quartet (full line) and the pseudo cosmic quartet (dashed line), in the shell $10 < r < 20\,\mathrm{Mpc}$, averaged over time from 3.29 Gyr in the past to the present epoch.

smaller, with fluctuations that are characteristic of numerical noise.

7.2.2 Void and wall shells

Next we present the cosmic quartet for both the void and wall shells in Figure 7.4 and Figure 7.5 respectively. In each case we plot the pseudo-averaged parameters as well, indicated by dotted lines.

Averaged cosmological constant parameters

The (pseudo)-averaged parameters ($\bar{\Omega}^{\mathcal{D}}_{\Lambda}$, $\Omega^{\mathcal{D}}_{\Lambda}$) are shown in the bottom right panels. Since Λ is constant, $\bar{\Omega}^{\mathcal{D}}_{\Lambda}$ is by definition the same in both void and wall and equal to the FLRW region case in Figure 7.3. In the void region we have $\Omega^{\mathcal{D}}_{\Lambda} < \bar{\Omega}^{\mathcal{D}}_{\Lambda}$, while in the wall region region $\Omega^{\mathcal{D}}_{\Lambda} > \bar{\Omega}^{\mathcal{D}}_{\Lambda}$. This is a consequence of the definitions (7.13) combined with the fact that $\Theta_{\mathcal{D}\,\mathrm{wall}} < 3\bar{H} < \Theta_{\mathcal{D}\,\mathrm{void}}$.

Averaged matter density parameters

The averaged matter parameter, $\Omega^{\mathcal{D}}_{m}$, and pseudo averaged matter parameter, $\bar{\Omega}_{m}$, are shown for the void and wall are seen in the top right panels. As compared to the FLRW case Figure 7.3 the void is underdense, and the wall is overdense, as we expect. Furthermore, both the underdensity and overdensity are more extreme in terms of the domain dependent averages:

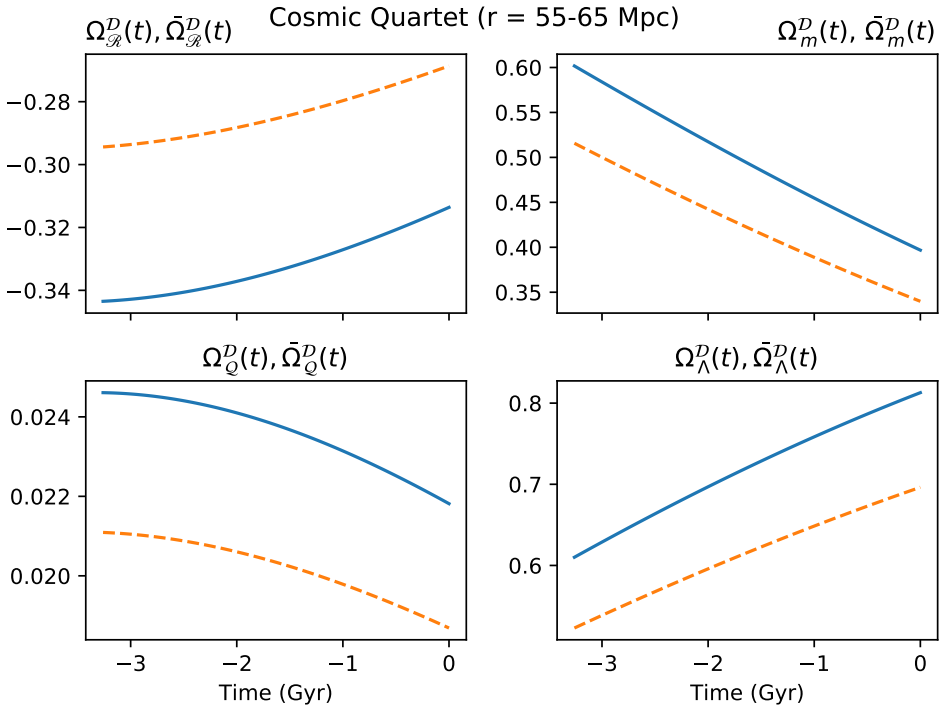

Figure 7.5: The cosmic quartet (full line) and the pseudo cosmic quartet (dashed line), in the shell $55 < r < 65\,\mathrm{Mpc}$, averaged over time from 3.29 Gyr in the past to the present epoch.

$\Omega^{\mathcal{D}}_{m\,\mathrm{void}} < \bar{\Omega}_{m\,\mathrm{void}} < \bar{\Omega}_m$, and $\Omega^{\mathcal{D}}_{m\,\mathrm{wall}} > \bar{\Omega}_{m\,\mathrm{wall}} > \bar{\Omega}_m$, where $\bar{\Omega}_m$ is the FLRW parameter. In each case, the averaged matter density parameters decrease over time since each region is expanding.

Averaged backreaction density parameters

The averaged backreaction parameter, $\Omega^{\mathcal{D}}_{\mathcal{Q}}$, and pseudo-averaged backreaction parameter, $\bar{\Omega}^{\mathcal{D}}_{\mathcal{Q}}$, are shown for the void and wall regions in the bottom left panels. There is significant backreaction, with $\Omega^{\mathcal{D}}_{\mathcal{Q}}\,\mathrm{wall} \sim 0.022$–$0.024$ (around 2.3 %) in the wall region, but not in the void region. The principal parameter which determines this is the spatial gradient of the density. Within the void, the backreaction is negligible, with $\Omega^{\mathcal{D}}_{\mathcal{Q}}\,\mathrm{void} \sim 1.5$–$2.5 \times 10^{-7}$. Nonetheless this small value is still two orders of magnitude larger than the numerical noise level of the FLRW region, with a discernible decrease over time. In Figure 7.6 we plot the magnitude of the density gradient $|\partial_r \rho|$ at the present epoch on a logarithmic scale. This illustrates how the two orders of magnitude difference between the void and FLRW shells correlates with the two orders of magnitude in the small backreaction density parameter.

The backreaction term is largest in the wall region where the density gradients are largest. Moreover, it is interesting that the magnitude of this term, at the 2.3% level, is comparable to the level found at the present epoch in the timescape model [36], as is the decreasing trend. In the present case, this order

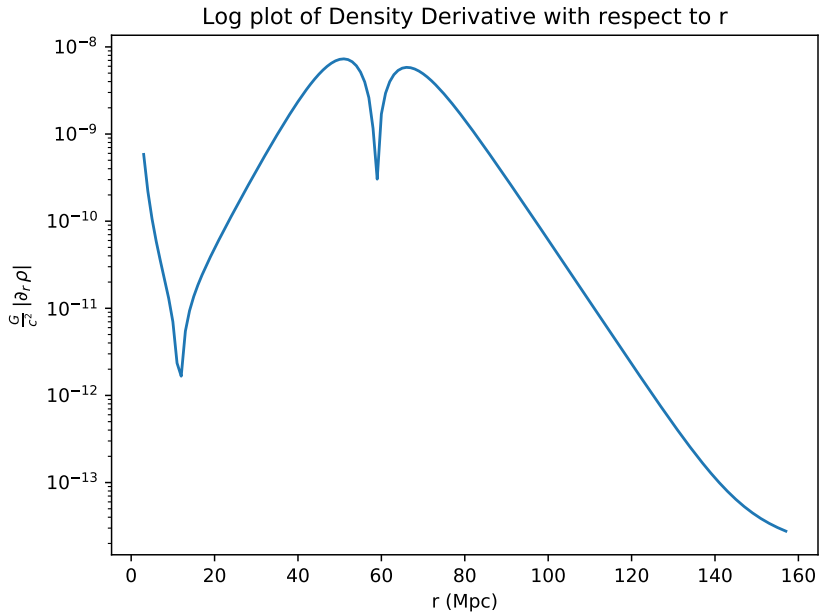

Figure 7.6: Log plot of the absolute value of the density derivative with respect to r is shown, at $t = 0$, in the plane $\theta = \pi$. This is to illustrate the order of magnitude differences in density gradients in the various shells we average in.

of magnitude arises from an empirical Szekeres model for small scale density contrasts with parameters constrained via realistic ray-tracing.

Averaged curvature density parameters

Finally the (pseudo)-averaged curvature parameters ($\bar{\Omega}^{\mathcal{D}}_{\mathscr{R}}$, $\Omega^{\mathcal{D}}_{\mathscr{R}}$) are shown for the void and wall the top left panels. The positive density parameters in the void region represent negative averaged intrinsic Ricci scalar curvature, while the negative parameters in the wall correspond to positive averaged intrinsic Ricci scalar curvature there. This is exactly as we would expect. Similar to the matter density parameters we have $\Omega^{\mathcal{D}}_{\mathscr{R}\,\mathrm{void}} < \bar{\Omega}_{\mathscr{R}\,\mathrm{void}}$ and $|\Omega^{\mathcal{D}}_{\mathscr{R}\,\mathrm{wall}}| > |\bar{\Omega}_{\mathscr{R}\,\mathrm{wall}}|$.

In both the void and wall regions the magnitude of both curvature parameters is decreasing with time *for the range of epochs shown* over 3.29 Gyr to the present. In fact, the magnitudes of the curvature parameters increase until shortly before the earliest epoch shown[5] in Figure 7.4 and Figure 7.5. Furthermore, the maximum backreaction in the wall region occurs when $|\Omega^{\mathcal{D}}_{\mathscr{R}\,\mathrm{wall}}|$ reaches its maximum.

The fact that the magnitudes of the curvature density parameters are ultimately decreasing with time is a consequence the cosmological constant. This must ultimately dominate the energy density: $\mathscr{R}$ decays as $\sim 1/R^2$ as $R(t, r)$ increases, whereas Λ remains constant. This is the basic difference from models

[5]Unfortunately, we encountered a numerical singularity with our code at the epoch when curvature parameters reached their maximum magnitude. We have not had time to hunt down the origin of the bug, but have checked that it does not affect our other conclusions.

with backreaction with $\Lambda = 0$, where spatial curvature is the largest contribution to the energy density. In those cases, the far future limit is one in which voids dominate, becoming emptier and emptier and closer to an empty (negatively curved) Milne universe.

7.2.3 Comparison with other studies

Bolejko [5] has performed a similar analysis to ours, with somewhat different Λ–Szekeres models. Qualitatively, his results are very similar to ours. Furthermore, he explicitly demonstrates the growth of $|\Omega^{\mathcal{D}}_{\mathscr{R}}|$ in the walls and voids before these parameters turn around and then decrease when the cosmological term eventually dominates. However, we find somewhat lower backreaction and spatial curvature in our results. This most likely due to Bolejko's use of a density profile that leads to a much greater density contrast in the wall region, with a maximum $\delta_\rho \sim 8$ as compared to our maximum $\delta_\rho \sim 5$. The greater density contrast would imply a sharper density gradient, and this appears to drive the magnitude of the backreaction term. Within the wall region, Bolejko finds $\Omega^{\mathcal{D}}_{\mathcal{Q}}$ to be $\sim$4–7 %, as compared to our $\sim 2.3\,\%$. Furthermore, Bolejko determines $\Omega^{\mathcal{D}}_{\mathscr{R}} \simeq -0.8$ in the same region, as compared to our value of $\Omega^{\mathcal{D}}_{\mathscr{R}} \simeq -0.33$. This illustrates the effects of having a density contrast which is near double our maximal value.

Bolejko's typical values of $\Omega^{\mathcal{D}}_{\mathscr{R}}$ in the void region are similar to ours, which is to be expected since in both cases the density contrast of the void is close to the minimum possible value $\delta_\rho \sim -1$. Bolejko finds the same trend in $\Omega^{\mathcal{D}}_{\mathscr{R}\,\mathrm{void}}$ as we do, and determines the present day value to be[6] $\Omega^{\mathcal{D}}_{\mathscr{R}\,\mathrm{void}} \sim 0.45$, as compared to our $\Omega^{\mathcal{D}}_{\mathscr{R}\,\mathrm{void}} \sim 0.5$ (or $\bar{\Omega}^{\mathcal{D}}_{\mathscr{R}\,\mathrm{void}} \sim 0.72$ for the pseudo-averaged parameter).

It should be noted that both Bolejko's analysis and our analysis contain an asymptotic homogeneous limit given by a FLRW model with standard ΛCDM parameters. Consequently we find similar results for evolution in this limit.

It is clear that in the void and wall regions spatial curvature significantly affects the dynamics of the domain. This is true whether we examine the averaged cosmic quartet or the pseudo-averaged cosmic quartet. Furthermore, even when in the wall region where the sharp density gradients lead to the largest backreaction this term is only of the order of a few percent. This means we should consider the kinematical backreaction, $Q_{\mathcal{D}}$, as only part of the "backreaction phenomenon" of regions with non-linear growth as there is a larger contribution that is often overlooked — the spatial curvature. Furthermore, it has been shown that $\Omega^{\mathcal{D}}_{\mathcal{Q}}$ only needs to be of the level of a few percent to obtain evolution that is non-Friedmannian [36, 209].

Repeating this investigation without a cosmological constant could prove

[6] Bolejko only gave the regional averages, rather than values for the pseudo averaged cosmic quartet.

to be interesting. This is because when it is present, a cosmological constant will always dominate as $t \to \infty$. With $\Lambda = 0$ the spatial curvature due to voids, $\Omega^{\mathcal{D}}_{\mathscr{R}\,\mathrm{void}}$ will dominate the cosmic quartet at later times, resulting in very different average dynamics.

Chapter 8

Conclusion

The aim of this thesis was to investigate theories that go beyond the standard model of cosmology in order to explain what we observe in the Universe today. To do so, we firstly discussed the ΛCDM model and its observational status, along with fundamental questions that are mostly ignored.

The standard model of cosmology, ΛCDM, is predicated on the cosmological principle, the idea that the Universe is isotropic and homogeneous and it uses the FLRW metric to model the Universe. While observations support an average isotropic and homogeneous expansion law on scales larger than the 'statistical scale of homogeneity', there is no reason the FLRW metric should apply for all scales of averaging, nor is it clear if or how smoothing over small-scale structure impacts the large-scale dynamics we observe.

Over the last two decades, since the discovery of the accelerated expansion of the Universe from the evidence of type Ia supernovae, the ΛCDM model has pointed to the existence of "dark energy". This dark energy is a mysterious repulsive vacuum energy with negative pressure that drives this accelerated expansion at late epochs. Some theorists including Buchert [4] argue that this accelerated expansion is in fact due to the small-scale dynamics. This is because the average evolution of spacetime is not equal to the evolution of a completely averaged spacetime — which gives rise to backreaction. Wiltshire [35, 99] further argues that while the backreaction terms themselves may only make a contribution of $1 - 4\%$ to the averaged energy density, the inference of cosmic acceleration depends crucially on how statistical averages are calibrated relative to local clocks and rulers. In particular, cumulative effects can be large. While these models are still contested by the community at large, the growing tensions in the standard model such as the Hubble tension may lead other researchers to explore such alternatives in the coming decade.

We introduced the 3+1 and 1+3 formalisms in general relativity in order to properly understand the averaging procedures used by Buchert in [3]. We discussed the notion of embedding a 3–dimensional spacelike hypersurface in a 4–dimensional spacetime manifold. This process can be made more specific by

introducing foliation kinematics which are motivated by physical choices. We characterised the foliation kinematics by the lapse, N, shift vector, $\boldsymbol{\beta}$, and the induced metric, $\boldsymbol{h}$.

To formulate the various projections of the Einstein equations, one also requires the projections of the stress-energy tensor, discussed in subsection 3.4.2. With these expressions, we formulated projections of the Einstein equations onto the embedded hypersurfaces, which are widely used in the numerical relativity community and by theorists who use the 3+1 decomposition. We further introduced the 1+3 formalism which gives rise the Raychaudhuri equation, a fundamental equation describing the evolution of a congruence of curves.

We investigated how inhomogeneities in the early Universe are approached in the standard model — by use of linear perturbation theory about a FLRW background. This method of modelling inhomogeneities gives rise to complicated (perturbed) Einstein equations which have "unphysical" quantities associated with "gauge artefacts". To obtain a faithful set of Einstein equations — ones that do not have unphysical quantities — one is required to make *gauge choices* that eliminate the unphysical quantities. Certain gauge choices, however, give rise to *spurious gauge modes*, such is the case for the synchronous gauge. The alternative to making gauge choices is to use gauge invariant quantities, such as those introduced by Bardeen in 1980 [176], and those explored in subsection 4.5.2. There are still deficiencies with this approach to "inhomogeneous cosmology": firstly, we still assume a background cosmology *a priori*. Secondly, this is still a linear approach to a fundamentally non-linear theory. Lastly, this approach still points to exotic physics in the late Universe.

We proceeded by investigating the recent and most developed version of the Buchert formalism from Buchert et al. [3]. This approach to averaging is a background free approach that does not assume the average evolution of spacetime is equal to the evolution of some averaged spacetime. The construction we investigated first is the "extrinsic approach". By performing averages with respect to the Einstein equations projected along the normal to 3–dimensional spacelike hypersurfaces, we formulated Friedmann equation analogues — the "extrinsically averaged evolution equations" — that included extra terms, the backreaction terms. Due to a tilt (or local boost) between the 4–velocity of the fluid and the normal to the hypersurfaces, an extra backreaction term not in Buchert's original formulation [4, 34] — The stress-energy backreaction. Furthermore, because the averaging domain was propagated along the fluid congruence we found the fluid rest-mass was conserved, which is a problem in other constructions of this averaging formalism. We showed explicitly the flux of the fluid rest-mass across the boundary of the domain in the case where the averaging domain did not propagate along the fluid congruence.

While the extrinsic averaging procedure is useful in the case where a "tilt" is present, Buchert et al. [3] argue that the"natural" way to define the char-

acteristics of a fluid is in its own rest frame, or the "intrinsic frame". This is particularly useful when considering cosmological models where the 4–velocity has vanishing spatial components, i.e., the fluid is hypersurface orthogonal. However, this fluid intrinsic approach is still not the same as taken by Buchert in his earlier papers [4, 34] as the tilt still manifests through the scaling parameter, N/γ. The fluid intrinsic approach allows us to rewrite the "intrinsically averaged equations" in an effective Friedmann form where we rewrite the usual pressure and energy density as an *effective* pressure and energy density containing the backreaction terms. Finally, we repeat this analysis using the Lagrangian description by setting $N = \gamma$, meaning there is now no dependence on the original tilt. The Lagrangian description is effectively the synchronous gauge which, became unpopular when using standard perturbation theory. However, because Buchert's approach is "background free", the standard problems of the synchronous gauge do not apply here.

This does not mean that the Buchert approach is without problems, however. As we discussed in subsection 5.4.1, backreaction is a phenomenological replacement for dark matter and dark energy — dependent on the relative signs of the various backreaction terms with respect to the cosmological constant. By itself, the Buchert formalism also does not explain why average evolution is in fact close to homogeneous, something the timescape model attempts to reconcile via the *cosmological equivalence principle*. Furthermore, in the timescape model, backreaction never grows large enough to dominate the right-hand side of the effective Friedmann equations for a given energy density. Therefore, these domains will continue to decelerate without a cosmological constant, thus the analogy is not complete.

Following the approach of Clifton et al. [1], we investigated the post-Newtonian expansion and tested if various gauges used in the standard model were viable in this expansion or not. We found that all gauges tested, except the longitudinal gauge were not viable. This is fundamentally because the post-Newtonian expansion does not consider all perturbations to be of the same order of smallness as in linear perturbation theory.

Clifton et al. state that their assumption of perturbing about a Friedmann background results in a vanishing backreaction. This is actually because of their assumption of periodic boundary conditions *and* because they are perturbing about a FLRW background. Not assuming these boundary conditions and following the 'expansion rules' of Clifton et al. we showed that the Buchert averaging scheme could be constructed in the post-Newtonian expansion. However, this can only be constructed using the extrinsic averaging approach as we cannot set the tilt to zero in the post-Newtonian expansion.

We derived the extrinsically averaged Friedmann-like equations in the post-Newtonian expansion and estimated the orders of magnitude of the components of these equations. These equations revealed the leading order parts of backre-

action appear at the same order as the background Friedmann equations, $\mathcal{O}(\chi^2)$. This only applied to regional averages on small scales, however. We concluded that this order-of-magnitude estimate had no bearing on the debate concerning the magnitude of backreaction which is about constructing *global averages*.

Finally, we investigated the magnitude of backreaction in the Szekeres model. We found that the backreaction parameter, $\Omega_{\mathcal{Q}}^{\mathcal{D}}$, is correlated strongly with the density gradient, being negligible except in the overdense region where the density gradients is sharpest, leading to the $\Omega_{\mathcal{Q}}^{\mathcal{D}} \sim 2.3\%$ at late epochs. Our results are similar to those of Bolejko [5], the differences being attributable to a somewhat larger late epoch density contrast in his case.

This research has led to several question related to how one may use the Buchert equations to model the real Universe. For instance, the extrinsic approach to averaging seems to lay a natural path to take if considering two (or more) fluids for the early Universe where one is pressureless dark matter and the other is ordinary baryonic matter. This is because of the three timelike congruences in the general setup allowing one to prescribe a fluid velocity to each of these congruences. By itself, this does not seem difficult, however, the interesting problem to investigate here would be how one would overcome no longer having conversation of rest mass.

Furthermore, it would be interesting to extend the investigation in Chapter 7 to models without the cosmological constant and with an ensemble of different density profiles to represent the statistical variety of different cosmic web structures that we observe in the low redshift universe. This could provide insight into how curvature and backreaction effects change the evolution of the domains, and the important question of whether realistic models can be obtained in the absence of dark energy. It is interesting that the order of magnitude of $\Omega_{\mathcal{Q}}^{\mathcal{D}}$ that we found in Chapter 7 for structures that had been constrained by realistic ray tracing [134] in Λ–Szekeres models is comparable to that found in the timescape cosmology [36] without dark energy. The big challenge is how one constructs an ensemble of structures with a suitable average to replace the asymptotic FLRW region of our toy models.

In the end, we are left with many avenues for future research, and only time will tell if any of the theories we investigated in this thesis will aid in the development of a new standard model of cosmology.

Bibliography

[1] T. Clifton, C. S. Gallagher, S. Goldberg, and K. A. Malik, "*Viable gauge choices in cosmologies with nonlinear structures*", Physical Review D **101**, 063530 (2020).

[2] J. Bičák, J. Katz, and D. Lynden-Bell, "*Cosmological perturbation theory, instantaneous gauges, and local inertial frames*", Physical Review D **76**, 063501 (2007).

[3] T. Buchert, P. Mourier, and X. Roy, "*On average properties of inhomogeneous fluids in general relativity III: general fluid cosmologies*", General Relativity and Gravitation **52**, 1–73 (2020).

[4] T. Buchert, "*On average properties of inhomogeneous fluids in general relativity: dust cosmologies*", General Relativity and Gravitation **32**, 105–125 (2000).

[5] K. Bolejko, "*Cosmological backreaction within the Szekeres model and emergence of spatial curvature*", Journal of Cosmology and Astroparticle Physics **06**, 025 (2017).

[6] A. Einstein, "*Zur Allgemeinen Relativitätstheorie*", Sitzungsberichte der Preussischen Akadamie der Wissenschaften **1915**, 778–786 (1915).

[7] A. des Sciences (Paris), *Comptes rendus hebdomadaires des séances de l'Académie des sciences* (Gauthier-Villars, 1869), pp. 379–383.

[8] F. W. Dyson, A. S. Eddington, and C. Davidson, "*IX. A determination of the deflection of light by the Sun's gravitational field, from observations made at the total eclipse of May 29, 1919*", Philosophical Transactions of the Royal Society of London. **220**, 291–333 (1920).

[9] B. P. Abbott et al. (LIGO Scientific Collaboration and Virgo Collaboration), "*Observation of Gravitational Waves from a Binary Black Hole Merger*", Physical Review Letters **116**, 061102 (2016).

[10] A. Einstein, "*Kosmologische Betrachtungen zur allgemeinen Relativitäts theorie*", Sitzungsberichte der Preussischen Akadamie der Wissenschaften, 142–152 (1917).

[11] A. Friedmann, "*Über die Krümmung des Raumes*", Zeitschrift für Physik **10**, 377–386 (1922).

[12] A. Friedmann, "*Über die Möglichkeit einer Welt mit konstanter negativer Krümmung des Raumes*", Zeitschrift für Physik **21**, 326–332 (1924).

[13] G. Lemaître, "*Un Univers homogène de masse constante et de rayon croissant rendant compte de la vitesse radiale des nébuleuses extra-galactiques*", Annales de la Société scientifique de Bruxelles **47**, 49–59 (1927).

[14] E. Hubble, "*A relation between distance and radial velocity among extra-galactic nebulae*", Proceedings of the National Academy of Sciences **15**, 168–173 (1929).

[15] A. Einstein, "*Zum kosmologischen Problem der allgemeinen Relativitäts theorie*", Sitzungsberichte der Preussischen Akademie der Wissenschaften 1914–1932, 361–364 (2005).

[16] A. Einstein and W. De Sitter, "*On the Relation between the Expansion and the Mean Density of the Universe*", Proceedings of the National Academy of Sciences of the United States of America **18**, 213 (1932).

[17] N. Straumann, "*The history of the cosmological constant problem*", arXiv:gr-qc/0208027 (2002).

[18] A. G. Riess et al., "*Observational evidence from supernovae for an accelerating universe and a cosmological constant*", Astronomical Journal **116**, 1009 (1998).

[19] S. Perlmutter et al., "*Measurements of* Ω *and* Λ *from 42 high-redshift supernovae*", Astrophysical Journal **517**, 565 (1999).

[20] A. H. Jaffe et al., "*Cosmology from MAXIMA-1, BOOMERANG, and COBE DMR Cosmic Microwave Background Observations*", Physical Review Letters **86**, 3475–3479 (2001).

[21] L. Verde et al., "*First-Year Wilkinson Microwave Anisotropy Probe (WMAP)* Observations: Parameter Estimation Methodology*", Astrophysical Journal Supplement Series **148**, 195 (2003).

[22] W. T. B. Kelvin, *Baltimore lectures on molecular dynamics and the wave theory of light* (CJ Clay and Sons, 1904).

[23] K. C. Freeman, "*On the Disks of Spiral and S0 Galaxies*", Astrophysical Journal **160**, 811 (1970).

[24] V. C. Rubin and J. Ford W. Kent, "*Rotation of the Andromeda Nebula from a Spectroscopic Survey of Emission Regions*", Astrophysical Journal **159**, 379 (1970).

[25] V. C. Rubin, J. Ford W. K., and N. Thonnard, "*Rotational properties of 21 SC galaxies with a large range of luminosities and radii, from NGC 4605 (R=4kpc) to UGC 2885 (R=122kpc).*", Astrophysical Journal **238**, 471–487 (1980).

[26] D. J. Bacon, A. R. Refregier, and R. S. Ellis, "*Detection of weak gravitational lensing by large-scale structure*", Monthly Notices of the Royal Astronomical Society **318**, 625–640 (2000).

[27] G. Hinshaw et al., "*Nine-year Wilkinson Microwave Anisotropy Probe (WMAP) observations: cosmological parameter results*", Astrophysical Journal Supplement Series **208**, 19 (2013).

[28] G. Bertone and D. Hooper, "*History of dark matter*", Reviews of Modern Physics **90**, 045002 (2018).

[29] N. Aghanim et al. (Planck), "*Planck 2018 results. VI. Cosmological parameters*", Astronomy & Astrophysics **641**, A6 (2020).

[30] C. Blake et al., "*The WiggleZ Dark Energy Survey: mapping the distance–redshift relation with baryon acoustic oscillations*", Monthly Notices of the Royal Astronomical Society **418**, 1707–1724 (2011).

[31] L. Anderson et al., "*The clustering of galaxies in the SDSS-III Baryon Oscillation Spectroscopic Survey: baryon acoustic oscillations in the Data Releases 10 and 11 Galaxy samples*", Monthly Notices of the Royal Astronomical Society **441**, 24–62 (2014).

[32] A. G. Riess et al., "*Milky Way Cepheid standards for measuring cosmic distances and application to Gaia DR2: implications for the Hubble constant*", Astrophysical Journal **861**, 126 (2018).

[33] A. G. Riess et al., "*New parallaxes of galactic cepheids from spatially scanning the hubble space telescope: Implications for the hubble constant*", Astrophysical Journal **855**, 136 (2018).

[34] T. Buchert, "*On average properties of inhomogeneous fluids in general relativity: perfect fluid cosmologies*", General Relativity and Gravitation **33**, 1381–1405 (2001).

[35] D. L. Wiltshire, "*Cosmic clocks, cosmic variance and cosmic averages*", New Journal of Physics **9**, 377 (2007).

[36] D. L. Wiltshire, "*Average observational quantities in the timescape cosmology*", Physical Review D **80**, 123512 (2009).

[37] K. Bolejko, "*Relativistic numerical cosmology with silent universes*", Classical and Quantum Gravity **35**, 024003 (2017).

[38] D. W. Hogg, D. J. Eisenstein, M. R. Blanton, N. A. Bahcall, J. Brinkmann, J. E. Gunn, and D. P. Schneider, "*Cosmic homogeneity demonstrated with luminous red galaxies*", Astrophysical Journal **624**, 54 (2005).

[39] F. S. Labini, N. L. Vasilyev, L. Pietronero, and Y. V. Baryshev, "*Absence of self-averaging and of homogeneity in the large-scale galaxy distribution*", Europhysics Letters **86**, 49001 (2009).

[40] M. I. Scrimgeour et al., "*The WiggleZ Dark Energy Survey: the transition to large-scale cosmic homogeneity*", Monthly Notices of the Royal Astronomical Society **425**, 116–134 (2012).

[41] B. F. Roukema, T. Buchert, H. Fujii, and J. J. Ostrowski, "*Is the baryon acoustic oscillation peak a cosmological standard ruler?*", Monthly Notices of the Royal Astronomical Society: Letters **456**, L45–L48 (2015).

[42] S. Genel, M. Vogelsberger, V. Springel, D. Sijacki, D. Nelson, G. Snyder, V. Rodriguez-Gomez, P. Torrey, and L. Hernquist, "*Introducing the Illustris project: the evolution of galaxy populations across cosmic time*", Monthly Notices of the Royal Astronomical Society **445**, 175–200 (2014).

[43] D. Potter, J. Stadel, and R. Teyssier, "*PKDGRAV3: beyond trillion particle cosmological simulations for the next era of galaxy surveys*", Computational Astrophysics and Cosmology **4**, 1–13 (2017).

[44] T. Buchert and M. Ostermann, "*Lagrangian theory of structure formation in relativistic cosmology: Lagrangian framework and definition of a nonperturbative approximation*", Physical Review D **86**, 023520 (2012).

[45] T. Buchert, C. Nayet, and A. Wiegand, "*Lagrangian theory of structure formation in relativistic cosmology. II. Average properties of a generic evolution model*", Physical Review D **87**, 123503 (2013).

[46] A. Alles, T. Buchert, F. Al Roumi, and A. Wiegand, "*Lagrangian theory of structure formation in relativistic cosmology. III. Gravitoelectric perturbation and solution schemes at any order*", Physical Review D **92**, 023512 (2015).

[47] F. Al Roumi, T. Buchert, and A. Wiegand, "*Lagrangian theory of structure formation in relativistic cosmology. IV. Lagrangian approach to gravitational waves*", Physical Review D **96**, 123538 (2017).

[48] Y.-Z. Li, P. Mourier, T. Buchert, and D. L. Wiltshire, "*Lagrangian theory of structure formation in relativistic cosmology. V. Irrotational fluids*", Physical Review D **98**, 043507 (2018).

[49] A. Ishibashi and R. M. Wald, "*Can the acceleration of our universe be explained by the effects of inhomogeneities?*", Classical and Quantum Gravity **23**, 235 (2005).

[50] S. R. Green and R. M. Wald, "*New framework for analyzing the effects of small scale inhomogeneities in cosmology*", Physical Review D **83**, 084020 (2011).

[51] S. R. Green and R. M. Wald, "*Newtonian and relativistic cosmologies*", Physical Review D **85**, 063512 (2012).

[52] S. R. Green and R. M. Wald, "*Examples of backreaction of small-scale inhomogeneities in cosmology*", Physical Review D **87**, 124037 (2013).

[53] S. R. Green and R. M. Wald, "*How well is our universe described by an FLRW model?*", Classical and Quantum Gravity **31**, 234003 (2014).

[54] T. Buchert et al., "*Is there proof that backreaction of inhomogeneities is irrelevant in cosmology?*", Classical and Quantum Gravity **32**, 215021 (2015).

[55] Ž. Ivezić et al., "*LSST: from science drivers to reference design and anticipated data products*", Astrophysical Journal **873**, 111 (2019).

[56] R. Maartens, F. B. Abdalla, M. Jarvis, and M. G. Santos, "*Overview of Cosmology with the SKA*", Proceedings of Science (2014).

[57] C. Clarkson, B. Bassett, and T. H.-C. Lu, "*A general test of the Copernican Principle*", Physical Review Letters **101**, 011301 (2008).

[58] D. Sapone, E. Majerotto, and S. Nesseris, "*Curvature versus distances: Testing the FLRW cosmology*", Physical Review D **90**, 023012 (2014).

[59] H. J. Macpherson, P. D. Lasky, and D. J. Price, "*Inhomogeneous cosmology with numerical relativity*", Physical Review D **95**, 064028 (2017).

[60] H. J. Macpherson, "*Inhomogeneous cosmology in an anisotropic Universe*", PhD thesis (Monash University, 2019).

[61] J. Adamek, C. Barrera-Hinojosa, M. Bruni, B. Li, H. J. Macpherson, and J. B. Mertens, "*Numerical solutions to Einstein's equations in a shearing-dust universe: a code comparison*", Classical and Quantum Gravity **37**, 154001 (2020).

[62] T. Buchert, M. Kerscher, and C. Sicka, "*Back reaction of inhomogeneities on the expansion: The evolution of cosmological parameters*", Physical Review D **62**, 043525 (2000).

[63] J. D. Jackson, *Classical Electrodynamics*, 1999.

[64] S. M. Carroll, *Spacetime and Geometry* (Cambridge University Press, 2019).

[65] S. Weinberg, *Cosmology* (Oxford University Press, 2008).

[66] S. Weinberg, *Gravitation and Cosmology: Principles and Applications of the General Theory of Relativity* (John Wiley and Sons, New York, 1972).

[67] S. Dodelson, *Modern Cosmology* (Elsevier, 2003).

[68] S. Weinberg, "*The cosmological constant problem*", Reviews of Modern Physics **61**, 1 (1989).

[69] P. A. Ade et al., "*Planck 2015 results-xiii. cosmological parameters*", Astronomy & Astrophysics **594**, A13 (2016).

[70] G. Efstathiou, W. J. Sutherland, and S. Maddox, "*The cosmological constant and cold dark matter*", Nature **348**, 705–707 (1990).

[71] G. Efstathiou, J. Bond, and S. White, "*COBE background radiation anisotropies and large-scale structure in the universe*", Monthly Notices of the Royal Astronomical Society **258**, 1P–6P (1992).

[72] L. A. Kofman, N. Y. Gnedin, and N. A. Bahcall, "*Cosmological constant, COBE cosmic microwave background anisotropy, and large-scale clustering*", Astrophysical Journal **413**, 1–9 (1993).

[73] J. P. Ostriker and P. J. Steinhardt, "*The observational case for a low-density Universe with a non-zero cosmological constant*", Nature **377**, 600–602 (1995).

[74] A. A. Penzias and R. W. Wilson, "*A measurement of excess antenna temperature at 4080 Mc/s.*", Astrophysical Journal **142**, 419–421 (1965).

[75] R. H. Dicke, P. J. E. Peebles, P. G. Roll, and D. T. Wilkinson, "*Cosmic black-body radiation.*", Astrophysical Journal **142**, 414–419 (1965).

[76] G. F. Smoot et al., "*Structure in the COBE differential microwave radiometer first-year maps*", Astrophysical Journal **396**, L1–L5 (1992).

[77] E. K. Conklin, "*Velocity of the Earth with respect to the cosmic background radiation*", Nature **222**, 971–972 (1969).

[78] P. S. Henry, "*Isotropy of the 3 K Background*", Nature **231**, 516–518 (1971).

[79] G. F. Smoot et al., "*First results of the COBE satellite measurement of the anisotropy of the cosmic microwave background radiation*", Advances in Space Research **11**, 193–205 (1991).

[80] N. W. Boggess et al., "*The COBE mission-Its design and performance two years after launch*", Astrophysical Journal **397**, 420–429 (1992).

[81] E. Komatsu et al., "*Five-Year Wilkinson Microwave Anisotropy Probe Observations: Cosmological Interpretation*", Astrophysical Journal Supplement Series **180**, 330–376 (2009).

[82] W. Hu, "*Wandering in the background: a CMB explorer*", PhD thesis (Chicago University, 1995).

[83] G. F. Ellis, R. Maartens, and M. A. MacCallum, *Relativistic cosmology* (Cambridge University Press, 2012).

[84] G. Jungman, M. Kamionkowski, A. Kosowsky, and D. N. Spergel, "*Cosmological-parameter determination with microwave background maps*", Physical Review D **54**, 1332 (1996).

[85] D. J. Eisenstein et al., "*Detection of the baryon acoustic peak in the large-scale correlation function of SDSS luminous red galaxies*", Astrophysical Journal **633**, 560 (2005).

[86] S. Cole et al., "*The 2dF Galaxy Redshift Survey: power-spectrum analysis of the final data set and cosmological implications*", Monthly Notices of the Royal Astronomical Society **362**, 505–534 (2005).

[87] M. M. Phillips, "*The absolute magnitudes of Type IA supernovae*", Astrophysical Journal **413**, L105–L108 (1993).

[88] B. P. Schmidt et al., "*The high-Z supernova search: measuring cosmic deceleration and global curvature of the universe using type Ia supernovae*", Astrophysical Journal **507**, 46 (1998).

[89] A. G. Riess et al., "*The farthest known supernova: support for an accelerating universe and a glimpse of the epoch of deceleration*", Astrophysical Journal **560**, 49 (2001).

[90] A. G. Riess et al., "*Type Ia supernova discoveries at $z > 1$ from the Hubble Space Telescope: Evidence for past deceleration and constraints on dark energy evolution*", Astrophysical Journal **607**, 665 (2004).

[91] A. G. Riess et al., "*New Hubble space telescope discoveries of type Ia supernovae at $z \geq 1$: narrowing constraints on the early behavior of dark energy*", Astrophysical Journal **659**, 98 (2007).

[92] B. P. Abbott et al. (LIGO Scientific Collaboration and Virgo Collaboration), "*Observation of Gravitational Waves from a Binary Black Hole Merger*", Physical Review Letters **116**, 061102 (2016).

[93] R. B. Tully, E. J. Shaya, I. D. Karachentsev, H. M. Courtois, D. D. Kocevski, L. Rizzi, and A. Peel, "*Our peculiar motion away from the local void*", Astrophysical Journal **676**, 184 (2008).

[94] F. Hoyle and M. S. Vogeley, "*Voids in the PSCz Survey and the Updated Zwicky Catalog*", Astrophyiscal Journal **566**, 641–651 (2002).

[95] F. Hoyle and M. S. Vogeley, "*Voids in the two-degree field galaxy redshift survey*", Astrophysical Journal **607**, 751 (2004).

[96] D. L. Wiltshire, "*What is dust?—Physical foundations of the averaging problem in cosmology*", Classical and Quantum Gravity **28**, 164006 (2011).

[97] L. B. Szabados, "*Quasi-local energy-momentum and angular momentum in general relativity*", Living Reviews in Relativity **12**, 1–163 (2009).

[98] G. F. Ellis and W. Stoeger, "*The'fitting problem'in cosmology*", Classical and Quantum Gravity **4**, 1697 (1987).

[99] D. L. Wiltshire, "*Dark energy without dark energy*", 6th International Heidelberg Conference on Dark Matter in Astro and Particle Physics (2007).

[100] G. Ellis, "*General Relativity and Gravitation*", ed B Bertotti F de Felice and A Pascolini (Dordrecht: Reidel) pp, 215–88 (1984).

[101] G. Ellis and W. Stoeger, "*The evolution of our local cosmic domain: effective causal limits*", Monthly Notices of the Royal Astronomical Society **398**, 1527–1536 (2009).

[102] T. Buchert, A. A. Coley, H. Kleinert, B. F. Roukema, and D. L. Wiltshire, "*Observational challenges for the standard FLRW model*", International Journal of Modern Physics D **25**, 1630007 (2016).

[103] E. Di Valentino, O. Mena, S. Pan, L. Visinelli, W. Yang, A. Melchiorri, D. F. Mota, A. G. Riess, and J. Silk, "*In the realm of the Hubble tension − a review of solutions*", arXiv: 2103.01183 (2021).

[104] A. G. Riess, S. Casertano, W. Yuan, J. B. Bowers, L. Macri, J. C. Zinn, and D. Scolnic, "*Cosmic distances calibrated to 1% precision with Gaia EDR3 parallaxes and Hubble Space Telescope photometry of 75 Milky Way Cepheids confirm tension with* ΛCDM", Astrophysical Journal Letters **908**, L6 (2021).

[105] B. P. Abbott et al. (LIGO Scientific, Virgo, 1M2H, Dark Energy Camera GW-E, DES, DLT40, Las Cumbres Observatory, VINROUGE, MASTER), "*A gravitational-wave standard siren measurement of the Hubble constant*", Nature **551**, 85–88 (2017).

[106] A. Heinesen and T. Buchert, "*Solving the curvature and Hubble parameter inconsistencies through structure formation-induced curvature*", Classical and Quantum Gravity **37**, [Erratum: Class. Quant. Grav.37,no.22,229601(2020)], 164001 (2020).

[107] I. Ben-Dayan, R. Durrer, G. Marozzi, and D. J. Schwarz, "*Value of H 0 in the inhomogeneous Universe*", Physical Review Letters **112**, 221301 (2014).

[108] D. Camarena and V. Marra, "*Impact of the cosmic variance on H 0 on cosmological analyses*", Physical Review D **98**, 023537 (2018).

[109] R. Gaur, "*Understanding The Universe's Accelerated Expansion by Probing Type Ia Supernovae Light-Curves*", Internship Report Phys391, University of Canterbury, 2019.

[110] M. Betoule et al., "*Improved cosmological constraints from a joint analysis of the SDSS-II and SNLS supernova samples*", Astronomy & Astrophysics **568**, A22 (2014).

[111] D. M. Scolnic et al., "*The complete light-curve sample of spectroscopically confirmed SNe Ia from Pan-STARRS1 and cosmological constraints from the combined pantheon sample*", Astrophysical Journal **859**, 101 (2018).

[112] L. H. Dam, A. Heinesen, and D. L. Wiltshire, "*Apparent cosmic acceleration from type Ia supernovae*", Monthly Notices of the Royal Astronomical Society **472**, 835–851 (2017).

[113] M. Rameez, "*Concerns about the reliability of publicly available SNe Ia data*", arXiv:1905.00221 (2019).

[114] M. Rameez and S. Sarkar, "*Is there really a 'Hubble tension'?*", arXiv: 1911.06456 (2019).

[115] D. J. Schwarz, C. J. Copi, D. Huterer, and G. D. Starkman, "*CMB Anomalies after Planck*", Classical and Quantum Gravity **33**, 184001 (2016).

[116] M. Tegmark, A. de Oliveira-Costa, and A. Hamilton, "*A high resolution foreground cleaned CMB map from WMAP*", Physical Review D **68**, 123523 (2003).

[117] H. K. Eriksen, F. K. Hansen, A. J. Banday, K. M. Gorski, and P. B. Lilje, "*Asymmetries in the Cosmic Microwave Background anisotropy field*", Astrophysical Journal **605**, [Erratum: Astrophys. J.609,1198(2004)], 14–20 (2004).

[118] H. K. Eriksen, A. J. Banday, K. M. Gorski, F. K. Hansen, and P. B. Lilje, "*Hemispherical power asymmetry in the three-year Wilkinson Microwave Anisotropy Probe sky maps*", Astrophysical Journal Letters **660**, L81–L84 (2007).

[119] J. Hoftuft, H. K. Eriksen, A. J. Banday, K. M. Gorski, F. K. Hansen, and P. B. Lilje, "*Increasing evidence for hemispherical power asymmetry in the five-year WMAP data*", Astrophysical Journal **699**, 985–989 (2009).

[120] C. J. Copi, D. Huterer, D. J. Schwarz, and G. D. Starkman, "*Lack of large-angle TT correlations persists in WMAP and Planck*", Monthly Notices of the Royal Astronomical Society **451**, 2978–2985 (2015).

[121] A. de Oliveira-Costa, M. Tegmark, M. Zaldarriaga, and A. Hamilton, "*The Significance of the largest scale CMB fluctuations in WMAP*", Physical Review D **69**, 063516 (2004).

[122] D. J. Schwarz, G. D. Starkman, D. Huterer, and C. J. Copi, "*Is the low-l microwave background cosmic?*", Physical Review Letters **93**, 221301 (2004).

[123] K. Land and J. Magueijo, "*The Axis of evil*", Phys. Rev. Lett. **95**, 071301 (2005).

[124] C. J. Copi, D. Huterer, D. J. Schwarz, and G. D. Starkman, "*On the large-angle anomalies of the microwave sky*", Monthly Notices of the Royal Astronomical Society **367**, 79–102 (2006).

[125] J. Kim and P. Naselsky, "*Anomalous parity asymmetry of the Wilkinson Microwave Anisotropy Probe power spectrum data at low multipoles*", Astrophysical Journal Letters **714**, L265–L267 (2010).

[126] P. Vielva, E. Martinez-Gonzalez, R. B. Barreiro, J. L. Sanz, and L. Cayon, "*Detection of non-Gaussianity in the WMAP 1 - year data using spherical wavelets*", Astrophys. J. **609**, 22–34 (2004).

[127] P. Vielva, "*A Comprehensive overview of the Cold Spot*", Advances in Astronomy **2010**, 592094 (2010).

[128] P. A. R. Ade et al. (Planck), "*Planck 2013 results. XXIII. Isotropy and statistics of the CMB*", Astronomy & Astrophysics **571**, A23 (2014).

[129] P. A. R. Ade et al. (Planck), "*Planck 2015 results. XVI. Isotropy and statistics of the CMB*", Astronomy & Astrophysics **594**, A16 (2016).

[130] Y. Akrami et al. (Planck), "*Planck 2018 results. VII. Isotropy and Statistics of the CMB*", Astronomy & Astrophysics **641**, A7 (2020).

[131] D. J. Fixsen, E. S. Cheng, J. M. Gales, J. C. Mather, R. A. Shafer, and E. L. Wright, "*The cosmic microwave background spectrum from the full COBE/FIRAS data set*", Astrophysical Journal **473**, 576 (1996).

[132] C. L. Bennett et al. (WMAP), "*First year Wilkinson Microwave Anisotropy Probe (WMAP) observations: Preliminary maps and basic results*", Astrophysical Journal Supplement Series **148**, 1–27 (2003).

[133] D. L. Wiltshire, P. R. Smale, T. Mattsson, and R. Watkins, "*Hubble flow variance and the cosmic rest frame*", Physical Review D **88**, 083529 (2013).

[134] K. Bolejko, M. A. Nazer, and D. L. Wiltshire, "*Differential cosmic expansion and the Hubble flow anisotropy*", Journal of Cosmology and Astroparticle Physics, 035 (2016).

[135] N. Aghanim et al. (Planck), "*Planck 2013 results. XXVII. Doppler boosting of the CMB: Eppur si muove*", Astronomy & Astrophysics **571**, A27 (2014).

[136] Y. Akrami et al. (Planck), "*Planck intermediate results. LVI. Detection of the CMB dipole through modulation of the thermal Sunyaev-Zeldovich effect: Eppur si muove II*", Astronomy & Astrophysics **644**, A100 (2020).

[137] A. K. Singal, "*Large peculiar motion of the solar system from the dipole anisotropy in sky brightness due to distant radio sources*", Astrophysical Journal Letters **742**, L23 (2011).

[138] M. Rubart and D. J. Schwarz, "*Cosmic radio dipole from NVSS and WENSS*", Astronomy & Astrophysics **555**, A117 (2013).

[139] A. K. Singal, "*Peculiar motion of the solar system derived from a dipole anisotropy in the redshift distribution of distant quasars*", Monthly Notices of the Royal Astronomical Society **488**, L104–L108 (2019).

[140] A. K. Singal, "*Large disparity in cosmic reference frames determined from the sky distributions of radio sources and the microwave background radiation*", Physical Review D **100**, 063501 (2019).

[141] N. J. Secrest, S. von Hausegger, M. Rameez, R. Mohayaee, S. Sarkar, and J. Colin, "*A test of the cosmological principle with quasars*", Astrophysical Journal Letters **908**, L51 (2021).

[142] T. M. Siewert, M. Schmidt-Rubart, and D. J. Schwarz, "*The Cosmic Radio Dipole: Estimators and Frequency Dependence*", arXiv:2010.08366 (2020).

[143] A. K. Singal, "*Our peculiar motion inferred from number counts of mid infra red AGNs and the discordance seen with the cosmological principle*", arXiv:2102.12084 (2021).

[144] D. Tytler, J. M. O'Meara, N. Suzuki, and D. Lubin, "*Review of Big Bang nucleosynthesis and primordial abundances*", Physica Scripta **T85**, 12 (2000).

[145] G. Steigman, "*Primordial nucleosynthesis: successes and challenges*", International Journal of Modern Physics E **15**, 1–36 (2006).

[146] R. H. Cyburt, B. D. Fields, and K. A. Olive, "*An update on the big bang nucleosynthesis prediction for 7Li: the problem worsens*", Journal of Cosmology and Astroparticle Physics **2008**, 012 (2008).

[147] R. H. Cyburt, J. Ellis, B. D. Fields, F. Luo, K. A. Olive, and V. C. Spanos, "*Gravitino decays and the cosmological lithium problem in light of the LHC Higgs and supersymmetry searches*", Journal of Cosmology and Astroparticle Physics **2013**, 014 (2013).

[148] K. Jedamzik, "*Did something decay, evaporate, or annihilate during big bang nucleosynthesis?*", Physical Review D **70**, 063524 (2004).

[149] G. F. Ellis, "*Inhomogeneity effects in cosmology*", Classical and Quantum Gravity **28**, 164001 (2011).

[150] R. M. Zalaletdinov, "*Averaging problem in general relativity, macroscopic gravity and using Einstein's equations in cosmology*", Bulletin of the Astronomical Society of India **25**, 401–416 (1997).

[151] R. Zalaletdinov, "*Towards a theory of macroscopic gravity*", General Relativity and Gravitation **25**, 673–695 (1993).

[152] R. M. Zalaletdinov, "*Averaging out the Einstein equations and macroscopic space-time geometry*", General Relativity and Gravitation **24**, 1015–1031 (1992).

[153] M. Korzyński, "*Covariant coarse graining of inhomogeneous dust flow in general relativity*", Classical and quantum gravity **27**, 105015 (2010).

[154] Y. Foures-Bruhat, "*Théorème d'existence pour certains systèmes d'équations aux dérivées partielles non linéaires*", Acta mathematica **88**, 141–225 (1952).

[155] G. Darmois, *Les équations de la gravitation Einsteinienne* (Gauthier-Villars, Paris, 1927).

[156] A. Lichnérowicz, "*Sur certains problèmes globaux relatifs au système des équations d'Einstein*", PhD thesis (Paris, 1939).

[157] A. Lichnerowicz, *L'intégration des équations de la gravitation relativiste et le problème des N-corps* (Gauthier-Villars, Paris, 1944).

[158] A. Lichnerowicz, "*Sur les équations relativistes de la gravitation*", Bulletin de la Société Mathématique de France **80**, 237–251 (1952).

[159] P. A. M. Dirac, "*The theory of gravitation in Hamiltonian form*", Proceedings of the Royal Society of London. **246**, 333–343 (1958).

[160] P. Dirac, "*Fixation of coordinates in the Hamiltonian theory of gravitation*", Physical Review **114**, 924 (1959).

[161] R. Arnowitt, S. Deser, and C. W. Misner, "*Dynamical structure and definition of energy in general relativity*", Physical Review **116**, 1322 (1959).

[162] J. W. York Jr, "*Kinematics and dynamics of general relativity*", Sources of gravitational radiation, 83–126 (1979).

[163] J. W. York Jr, "*Conformally invariant orthogonal decomposition of symmetric tensors on Riemannian manifolds and the initial-value problem of general relativity*", Journal of Mathematical Physics **14**, 456–464 (1973).

[164] P. Amaro-Seoane et al., *Laser Interferometer Space Antenna*, 2017.

[165] E. Gourgoulhon, *3+ 1 formalism in general relativity: bases of numerical relativity* (Springer Science, Heidelberg, 2012).

[166] P. Monaco, "*Approximate methods for the generation of dark matter halo catalogs in the age of precision cosmology*", Galaxies **4**, 53 (2016).

[167] O. C. Stoica, "*Cartan's structural equations for singular manifolds*", arXiv:1111.0646 (2011).

[168] C. W. Misner, K. S. Thorne, and J. A. Wheeler, *Gravitation* (W. H. Freeman, San Francisco, 1973).

[169] M. Alcubierre, *Introduction to 3+ 1 numerical relativity* (Oxford University Press, 2008).

[170] J. Wheeler, *Geometrodynamics and the issue of the final state Relativity, Groups and Topology edited by DeWitt CM and DeWitt BS*, 1964.

[171] J. W. York, "*Velocities and momenta in an extended elliptic form of the initial-value conditions*", Nuovo Cimento B **119**, 823 (2004).

[172] E. Poisson, *A relativist's toolkit: the mathematics of black-hole mechanics* (Cambridge University Press, 2004).

[173] X. Roy, *On the 1+3 Formalism in General Relativity*, arXiv:1405.6319, 2014.

[174] E. M. Lifshitz, "*On the gravitational stability of the expanding universe*", Zhurnal Eksperimentalnoi i Teoreticheskoi Fiziki **16**, 587–602 (1946).

[175] E. M. Lifshitz and I. M. Khalatnikov, "*Investigations in relativistic cosmology*", Advances in Physics **12**, 185–249 (1963).

[176] J. M. Bardeen, "*Gauge-invariant cosmological perturbations*", Physical Review D **22**, 1882 (1980).

[177] G. F. Ellis and M. Bruni, "*Covariant and gauge-invariant approach to cosmological density fluctuations*", Physical Review D **40**, 1804 (1989).

[178] R. H. Brandenberger, "*Lectures on the theory of cosmological perturbations*", arXiv:hep-th/0306071 (2004).

[179] H. Weyl, "*Gravitation und Elektrizität*", Sitzungsberichte der Preussischen Akademie der Wissenschaften (Berlin, 465–478 (1918).

[180] H. Weyl, "*Gravitation and the electron*", Proceedings of the National Academy of Sciences of the United States of America **15**, 323 (1929).

[181] T. Buchert, P. Mourier, and X. Roy, "*Cosmological backreaction and its dependence on spacetime foliation*", Classical and Quantum Gravity **35**, 24LT02 (2018).

[182] O. F. Piattella, *Lecture Notes in Cosmology* (Springer, Switzerland, 2018).

[183] H. Bondi and I. W. Roxburgh, *Cosmology* (Courier Corporation, 2010).

[184] T. Clifton and R. A. Sussman, "*Cosmological backreaction in spherical and plane symmetric dust-filled space-times*", Classical and Quantum Gravity **36**, 205004 (2019).

[185] D. L. Wiltshire, "*Cosmological equivalence principle and the weak-field limit*", Physical Review D **78**, 084032 (2008).

[186] X. Roy and T. Buchert, "*Relativistic cosmological perturbation scheme on a general background: scalar perturbations for irrotational dust*", Classical and Quantum Gravity **29**, 115004 (2012).

[187] J. Larena, "*Spatially averaged cosmology in an arbitrary coordinate system*", Physical Review D **79**, 084006 (2009).

[188] I. A. Brown, J. Behrend, and K. A. Malik, "*Gauges and cosmological backreaction*", Journal of Cosmology and Astroparticle Physics **2009**, 027 (2009).

[189] M. Gasperini, G. Marozzi, and G. Veneziano, "*Gauge invariant averages for the cosmological backreaction*", Journal of Cosmology and Astroparticle Physics **2009**, 011 (2009).

[190] M. Gasperini, G. Marozzi, and G. Veneziano, "*A covariant and gauge invariant formulation of the cosmological "backreaction"*", Journal of Cosmology and Astroparticle Physics **2010**, 009 (2010).

[191] J. B. Jimenez, A. de la Cruz-Dombriz, P. K. Dunsby, and D. Sáez-Gómez, "*Backreaction mechanism in multifluid and extended cosmologies*", Journal of Cosmology and Astroparticle Physics **2014**, 031 (2014).

[192] J. Smirnov, "*Gauge-invariant average of Einstein equations for finite volumes*", arXiv:1410.6480 (2014).

[193] C. Rampf, C. Uhlemann, and O. Hahn, "*Cosmological perturbations for two cold fluids in ΛCDM*", Monthly Notices of the Royal Astronomical Society **503**, 406–425 (2021).

[194] S. Nájera and R. A. Sussman, *Non-comoving Cold Dark Matter in a ΛCDM background*, arXiv:2011.11192, 2020.

[195] C. Fidler, T. Tram, C. Rampf, R. Crittenden, K. Koyama, and D. Wands, "*General relativistic weak-field limit and Newtonian N-body simulations*", Journal of Cosmology and Astroparticle Physics **2017**, 022 (2017).

[196] C. Fidler, A. Kleinjohann, T. Tram, C. Rampf, and K. Koyama, "*A new approach to cosmological structure formation with massive neutrinos*", Journal of Cosmology and Astroparticle Physics **2019**, 025 (2019).

[197] N. E. Chisari and M. Zaldarriaga, "*Connection between Newtonian simulations and general relativity*", Physical Review D **83**, 123505 (2011).

[198] H. Bondi and J. Samuel, "*The Lense-Thirring effect and Mach's principle*", Physics Letters A **228**, 121–126 (1997).

[199] L. Smarr and J. W. York, "*Kinematical conditions in the construction of spacetime*", Physical Review D **17**, 2529–2551 (1978).

[200] P. Szekeres, "*A class of inhomogeneous cosmological models*", Communications in Mathematical Physics **41**, 55–64 (1975).

[201] G. Lemaître, "*L'univers en expansion*", Annales de la Société scientifique de Bruxelles **53**, 51 (1933).

[202] R. C. Tolman, "*Effect of inhomogeneity on cosmological models*", Proceedings of the national academy of sciences of the United States of America **20**, 169 (1934).

[203] H. Bondi, "*Spherically symmetrical models in general relativity*", Monthly Notices of the Royal Astronomical Society **107**, 410–425 (1947).

[204] R. G. Buckley and E. M. Schlegel, "*Physical geometry of the quasispherical Szekeres models*", Phys. Rev. **D101**, 023511 (2020).

[205] L. Dam, "*Inhomogeneous Cosmological Models and the Cosmic Microwave Background*", MSc Thesis, University of Canterbury, 2016.

[206] P. Szekeres, "*Quasispherical gravitational collapse*", Physical Review D **12**, 2941 (1975).

[207] K. Bolejko, A. Krasiński, C. Hellaby, and M.-N. Célérier, *Structures in the Universe by exact methods: formation, evolution, interactions* (Cambridge University Press, 2010).

[208] K. Bolejko, "*Evolution of cosmic structures in different environments in the quasispherical Szekeres model*", Physical Review D **75**, 043508 (2007).

[209] T. Buchert, J. Larena, and J.-M. Alimi, "*Correspondence between kinematical backreaction and scalar field cosmologies—the 'morphon field'*", Classical and Quantum Gravity **23**, 6379 (2006).

Appendix A

Perturbed Einstein Tensor Components

We will list the components of the perturbed Einstein tensor (to first order) with respect to the metric (4.6) in this Appendix. This is useful mainly for post-Newtonian theory as we can directly determine what order of magnitude the various metric perturbations should be. This is done by matching the orders of magnitude of the left-hand and right-hand sides of Einstein's equations. We compute the components of the Einstein tensor both from the various ingredients listed in Chapter 4, and the use of a computer algebra package, `sagemath` to check our results.

The $(0,0)$ component of the perturbed Einstein tensor is

$$2a^2\delta G^0{}_0 = -6\mathcal{H}^2\,\delta g_{00} + 4\mathcal{H}\,\delta g_{k0,k} - 2\mathcal{H}\,\delta g'_{kk} + \nabla^2\delta g_{kk} - \delta g_{kl,kl}\,, \tag{A.1}$$

the $(0,i)$ component is

$$2a^2\delta G^0{}_i = 2\mathcal{H}\,\delta g_{00,i} + \nabla^2\delta g_{0i} - \delta g_{k0,ki} + \delta g'_{kk,i} - \delta g'_{ki,k}\,, \tag{A.2}$$

and finally, the (i,j) component is

$$\begin{aligned} 2a^2\delta G^i{}_j = \Bigg[& -4\frac{a''}{a}\,\delta g_{00} - 2\mathcal{H}\,\delta g'_{00} - \nabla^2\delta g_{00} - 2\mathcal{H}\delta g'_{kk} \\ & + \nabla^2\delta g_{kk} - \delta g_{kl,kl} + 2\delta g'_{k0,k} + 4\mathcal{H}\,\delta g_{0k,k} - \delta g''_{kk} \Bigg]\delta^i{}_j \\ & + \delta g_{ki,kj} + \delta g_{kj,ki} - \delta g_{kk,ij}\delta g''_{ij} + 2\mathcal{H}\delta g'_{ij} \\ & - \delta g'_{0i,j} - \delta g'_{0j,i} - 2\mathcal{H}\,(\delta g_{0i,j} + \delta g_{0j,i}). \end{aligned} \tag{A.3}$$

Upon examination, we note that $G^0{}_0$ is $\mathcal{O}(\chi^2) + \mathcal{O}(\chi^4)$, under the assumption that $\delta g_{00} \sim \chi^2$, $\delta g_{0k} \sim \chi^3$, and $\delta g_{ij} \sim \chi^2$. This is consistent with the right-hand side of the stress-energy tensor under the post-Newtonian expansion. Assuming that the above orders of magnitudes are an ansatz for now, let us continue examining the other components. Under the assumptions we have made for

the order of magnitude of the perturbed metric components, we note that $G^0{}_i$ is $\mathcal{O}(\chi^3)$, and $G^i{}_j$ is $\mathcal{O}(\chi^2) + \mathcal{O}(\chi^4)$. We find that these orders of magnitude match the right-hand side of Einstein's equations given in (6.6), and thus we can safely assume the ansatz to be correct.